

Spatial variations in snow stability on uniform slopes : implications for extrapolation to surrounding terrain
by Christopher Cameron Landry

A thesis submitted in partial fulfillment of the requirements for the degree of Master of Science in Earth Sciences
Montana State University
© Copyright by Christopher Cameron Landry (2002)

Abstract:
Avalanche forecasters frequently perform field tests at study plots or other representative sites to reduce uncertainty regarding snowpack stability. This research investigated whether single snowpits represented stability throughout a carefully selected plot. The study utilized seven relatively uniform 900 m2 plots, three each in the Bridger and Madison Ranges of Southwest Montana, and one in the Columbia Mountains near Rogers Pass, British Columbia. Teams collected systematic samples from five snowpits, each containing ten 0.25 m2 stability-sampling cells, at each plot. Quantified loaded column stability tests measured strength in a single weak layer. Collection of in-situ slab shear stress data enabled the calculation of a stability ratio. Altogether, eleven stabilitysampling trials were performed during 2000/2001 and 2001/2002, testing several weak layer types exhibiting a wide range of strengths. Of the 54 valid snowpit results, 28 (51.9%) represented plot-wide stability, 16 did not, and the remaining 10 pits were empirically unrepresentative of their plot. Three of the eleven plots sampled contained full complements of five representative snowpits. As an additional component of this study, a GIS-based model extrapolated Bridger Range plot stability data onto avalanche starting zones, with poor results. The results of this study provide sufficient evidence of local spatial variation in snowpack stability within relatively uniform plots to reject the hypothesis that stability at a single snowpit will reliably represent a plot. However, these results do not suggest that information from snowpits is not important. Experienced forecasters interpret study plot stability data conservatively and are capable of utilizing “targeted sampling” and a variety of other data to effectively reduce uncertainty about slope stability.

SPATIAL VARIATIONS IN SNOW STABILITY ON UNIFORM SLOPES: IMPLICATIONS FOR EXTRAPOLATION TO SURROUNDING TERRAIN

by

Christopher Cameron Landry

A thesis submitted in partial fulfillment
of the requirements for the degree

of

Master of Science

in

Earth Sciences

MONTANA STATE UNIVERSITY
Bozeman, Montana

April 2002

© COPYRIGHT

by

Christopher Cameron Landry

2002

All Rights Reserved

N378
L2379

APPROVAL

of a thesis submitted by

Christopher Cameron Landry

This thesis has been read by each member of the thesis committee and has been found to be satisfactory regarding content, English usage, format, citations, bibliographic style, and consistency, and is ready for submission to the College of Graduate Studies.

Katherine J. Hansen, Co-chair — Katherine J. Hansen (Signature) 3-29-02 (Date)

Karl W. Birkeland, Co-chair — (Signature) 3/25/02 (Date)

Approved for the Department of Earth Sciences

James G. Schmitt, Dept. Head — (Signature) 3-29-02 (Date)

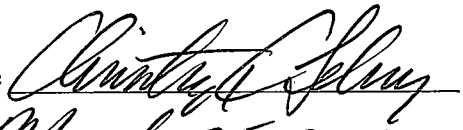
Approved for the College of Graduate Studies

Bruce R. McLeod, Dean — Bruce R. McLeod (Signature) 4-1-02 (Date)

STATEMENT OF PERMISSION TO USE

In presenting this thesis in partial fulfillment of the requirements for a master's degree at Montana State University – Bozeman, I agree that the Library shall make it available to borrowers under rules of the Library.

If I have indicated my intention to copyright this thesis by including a copyright notice page, copying is allowable only for scholarly purposes, consistent with "fair use" as prescribed in the U.S. Copyright Law. Requests for permission for extended quotation from or reproduction of this thesis in whole or in parts may be granted only by the copyright holder.

Signature 

Date March 25, 2002

ACKNOWLEDGEMENTS

It has been my good fortune to have enjoyed the guidance and encouragement of my esteemed graduate committee, Katherine Hansen, Karl Birkeland, John Borkowski, Robert Brown, and Richard Aspinall. Each was indispensable to this research

I wish to gratefully acknowledge support of my research by the Department of Earth Sciences, the Barry C. Bishop Scholarship for Mountain Research, and EPSCoR MONTS. Contributions by the American Avalanche Association and the Canadian Avalanche Association were particularly meaningful. The Mazamas, the American Alpine Club, and the Geological Society of America Foundation's John Montagne Fund all provided vital resources. And, Bridger Bowl Ski Area, the Parks Canada avalanche control program at Glacier National Park, Life Link International, and Snowmetrics each contributed access to research sites, in-kind products, and services. For his moral support, thanks to Hal Hartman. For technical support, thanks to Karin Kirk. Finally, and especially, my thanks go to Jeff Deems, Ron Johnson, and Karl Birkeland for leading data collection teams, and to assistants Chuck Lindsay, Doug Chabot, Stuart Dominick, Lance Riek, Chas Day, Aleph Johnston-Bloom, Zach Matthews, Mark Schaffer, Jim Rasmussen, John Kelly, Johann Schleiss, Dan Miller, Michael Cooperstein, Jeanette Romig, Blase Reardon, and Reid Sanders for their undaunted enthusiasm for snow science, despite sometimes miserable conditions. It was my pleasure to work with you all.

TABLE OF CONTENTS

	Page
1. INTRODUCTION	1
2. RESEARCH HYPOTHESES	6
3. LITERATURE REVIEW	8
Avalanche Forecasting Principles and Data Collection	8
Snowpack Stability Testing and Indices	10
Spatial Variation of Snowpack Properties	13
Modeling Snowpack Stability	15
Modeling Snowpack Accumulation	17
4. STUDY AREA	22
5. METHODS	25
Selection of Study Plot Sites	25
Avalanche Cycle Capture	31
Quantified Loaded Column Stability Test	33
Study Plot Stability Sampling Design	35
Study Plot Stability Sampling Sessions	37
Winter of 1999/2000	37
Winters of 2000/2001 and 2001/2002	38
Avalanche Starting Zones Atlas	40
Avalanche Observations	44
GIS "BASEDAT" Preparation	45
Stability Modeling	50
Storm Weather Data Collection	59

TABLE OF CONTENTS – CONTINUED

Page

5. METHODS continued .....

Data Analysis 60
Inter-Study-Plot Variability 60
Coefficients of Variation 60
Z Score of Strength 61
Stability Ratio S_{QLCT} 61
Z Score of Stability S_{QLCT} 62
Two-Sample *t*-Tests 62
Intra-Study-Plot Stability Variability 64
Stability Model Evaluation 65

6. RESULTS AND DISCUSSION 66

Winter of 2000/2001 66
Weather and Snowpack 66
Inter-Study-Plot Variability 70
Bacon Rind Study Plot Trials – 1/3/01 70
Bradley Meadow Study Plot Trials – 1/27/01 77
Round Hill Trials – 2/4/01 85
Baldy Mountain Study Plot Trials – 2/18/01 91
Saddle Peak Study Plot Trials – 2/18/01 98
Bradley Meadow Study Plot Trials – 2/18/01. 107
Bradley Meadow Study Plot Trials – 3/17/01. 112
Intra-Study-Plot Variability 119
Bridger Range Study Plot Trials – 2/18/01 119
Summary 123
Winter of 2001/2002 125
Weather and Snowpack 125
Inter-Study-Plot Variability 127
Middle Basin Trials – 12/7/01 127
Lionhead Mountain Plot Trials – 1/9/02 139
Lionhead Mountain Plot Trials – 1/15/02 147
Lionhead Mountain Plot Trials – 1/26/02 156
Bridger Range Stability Model 164

TABLE OF CONTENTS – CONTINUED

Page

7. CONCLUSIONS 168

Sampling Method 168
Study Plot Stability and Hypothesis #1 171
Extrapolation of Study Plot Stability and
Stability Modeling 182
Implications for Conventional Avalanche Forecasting 184
Scales of Spatial Variation in Stability and
Suggestions for Future Research 186

8. REFERENCES CITED 189

9. APPENDICES 195

Appendix A: Southern Bridger Range SWE Transect 196

Appendix B: 2000/2001 Study Plot Trials QLCT Results 198
Bacon Rind Study Plot 1/3/01 Trials 199
Bradley Meadow Study Plot 1/27/01 Trials 200
Round Hill 2/4/01 Trials 201
Baldy Mountain Study Plot 2/18/01 Trials 202
Saddle Peak Study Plot 2/18/01 Trials 203
Bradley Meadow Study Plot 2/18/01 Trials 204
Bradley Meadow Study Plot 3/17/01 Trials 205

Appendix C: 2001/2002 Study Plot Trials QLCT Results 206
Middle Basin Plot 12/7/01 Trials 207
Lionhead Mountain Plot 1/09/02 Trials 208
Lionhead Mountain Plot 1/15/02 Trials 209
Lionhead Mountain Plot 1/26/02 Trials 210

Appendix D: *t*-Tests of Strength 2000/2001 Trials 211
Bacon Rind Study Plot 1/3/01 Trials 212
Bradley Meadow Study Plot 1/27/01 Trials 212
Round Hill 2/4/01 Trials 213
Baldy Mountain Study Plot 2/18/01 Trials 213
Saddle Peak Study Plot 2/18/01 Trials 214
Bradley Meadow Study Plot 2/18/01 Trials 214
Bradley Meadow Study Plot 3/17/01 Trials 215
Plot-to-Plot 2/18/01 Trials 215

TABLE OF CONTENTS – CONTINUED

Page

Appendix E: *t*-Tests of Strength 2001/2002 Trials 216
Middle Basin Plot 12/7/01 Trials,
Pooled Weak Layers A & B (no "NR" results) 217
Middle Basin Plot 12/7/01 Trials,
Pooled Weak Layers A & B (inc. est. "NR" results) 217
Lionhead Mountain Plot 1/9/02 Trials 218
Lionhead Mountain Plot 1/15/02 Trials 218
Lionhead Mountain Plot 1/26/02 Trials 219

Appendix F: *t*-Tests of Stability 2000/2001 Trials 220
Bacon Rind Study Plot 1/3/01 Trials 221
Bradley Meadow Study Plot 1/27/01 Trials 221
Round Hill 2/4/01 Trials 222
Baldy Mountain Study Plot 2/18/01 Trials 222
Saddle Peak Study Plot 2/18/01 Trials 223
Bradley Meadow Study Plot 2/18/01 Trials 223
Bradley Meadow Study Plot 3/17/01 Trials 224
Plot-to-Plot 2/18/01 Trials 224

Appendix G: *t*-Tests of Stability 2001/2002 Trials 225
Middle Basin Plot 12/7/01Trials,
Pooled Weak Layers A & B (no "NR" results) 226
Middle Basin Plot 12/7/01 Trials,
Pooled Weak Layers A & B (inc. est. "NR" results) 226
Lionhead Mountain Plot 1/9/02 Trials 227
Lionhead Mountain Plot 1/15/02 Trials 227
Lionhead Mountain Plot 1/26/02 Trials 228

TABLE OF CONTENTS – CONTINUED

Page

Appendix H: 2000/2001 Snow Profiles 229
Profile #1 230
Profile #2 231
Profile #4 232
Profile #7 233
Profile #9 234
Profile #12. 235
Profile #14. 236
Profile #15. 237
Profile #16. 238
Profile #17. 239
Profile #18. 240
Profile #19. 241

Appendix I: 2001/2002 Snow Profiles 242
Profile #2 243
Profile #7 244
Profile #9 245
Profile #10 246
Profile #11 247
Profile #12 248

LIST OF TABLES

Table — Page

1. Avalanche Forecasting "Contributory Factor" Data Classification 9
2. Bridger Bowl Ski Area Climate Data 24
3. Study Plot Stability-Sampling Trials Summary 39
4. Canadian Snow Avalanche Size Classification System 41
5. GIS "BASEDAT" Theme Variables 50
6. Stability Model Data and Variables 51
7. Bacon Rind Study Plot (BRSP) 1/3/01 Trials: QLCT Results 71
8. Bacon Rind Study Plot (BRSP) 1/3/01 Trials: Shear Stress 74
9. Bacon Rind Study Plot (BRSP) 1/3/01 Trials: Stability 74
10. Bacon Rind Study Plot (BRSP) 1/3/01 Trials: *t*-Tests of Strength 75
11. Bacon Rind Study Plot (BRSP) 1/3/01 Trials: *t*-Tests of Stability 76
12. Bradley Meadow Study Plot (BMSP) 1/27/01 Trials: QLCT Results 78

LIST OF TABLES - CONTINUED

Table Page

13. Bradley Meadow Study Plot (BMSP) 1/27/01 Trials: Shear Stress 80

14. Bradley Meadow Study Plot (BMSP) 1/27/01 Trials: Stability 81

15. Bradley Meadow Study Plot (BMSP) 1/27/01 Trials: *t*-Tests of Strength 84

16. Bradley Meadow Study Plot (BMSP) 1/27/01 Trials: *t*-Tests of Stability 85

17. Round Hill (RH) 2/4/01 Trials: QLCT Results 86

18. Round Hill (RH) 2/4/01 Trials: Shear Stress 88

19. Round Hill (RH) 2/4/01 Trials: Stability 88

20. Round Hill (RH) 2/4/01 Trials: *t*-Tests of Strength 90

21. Round Hill (RH) 2/4/01 Trials: *t*-Tests of Stability 90

22. Baldy Mountain Study Plot (BLSP) 2/18/01 Trials: QLCT Results 92

23. Baldy Mountain Study Plot (BLSP) 2/18/01 Trials: Shear Stress 94

24. Baldy Mountain Study Plot (BLSP) 2/18/01 Trials: Stability 95

LIST OF TABLES - CONTINUED

Table Page

25. Baldy Mountain Study Plot (BLSP) 2/18/01 Trials: *t*-Tests of Strength 96

26. Baldy Mountain Study Plot (BLSP) 2/18/01 Trials: *t*-Tests of Stability 97

27. Saddle Peak Study Plot (SPSP) 2/18/01 Trials: QLCT Results 99

28. Saddle Peak Study Plot (SPSP) 2/18/01 Trials: Shear Stress 101

29. Saddle Peak Study Plot (SPSP) 2/18/01 Trials: Stability 102

30. Saddle Peak Study Plot (SPSP) 2/18/01 Trials: *t*-Tests of Strength 104

31. Saddle Peak Study Plot (SPSP) 2/18/01 Trials: *t*-Tests of Stability 105

32. Bradley Meadow Study Plot (BMSP) 2/18/01 Trials: QLCT Results 108

33. Bradley Meadow Study Plot (BMSP) 2/18/01 Trials: Shear Stress 110

34. Bradley Meadow Study Plot (BMSP) 2/18/01 Trials: Stability 111

35. Bradley Meadow Study Plot (BMSP) 2/18/01 Trials: *t*-Tests of Strength 111

LIST OF TABLES - CONTINUED

Table Page

36. Bradley Meadow Study Plot (BMSP) 3/17/01 Trials: QLCT Results 113

37. Bradley Meadow Study Plot (BMSP) 3/17/01 Trials: Shear Stress 115

38. Bradley Meadow Study Plot (BMSP) 3/17/01 Trials: Stability 116

39. Bradley Meadow Study Plot (BMSP) 3/17/01 Trials: *t*-Tests of Strength 117

40. Bradley Meadow Study Plot (BMSP) 3/17/01 Trials: *t*-Tests of Stability 118

41. Bridger Range Study Plots 2/18/01Trials: Plots Mean Strength 120

42. Bridger Range Study Plots 2/18/01 Trials: Plots Mean Shear Stress 120

43. Bridger Range Study Plots 2/18/01 Trials: Plots' Mean Stability 121

44. Bridger Range Study Plots 2/18/01 Trials: *t*-Tests of Strength 122

45. Bridger Range Study Plots 2/18/01 Trials: *t*-Tests of Stability 122

46. Middle Basin Plot (MBP) 12/7/01 Trials: QLCT Results for Pooled A and B Weak Layers 128

47. Middle Basin Plot (MBP) 12/7/01 Trials: Shear Stress for Pooled A and B Weak Layers 132

LIST OF TABLES - CONTINUED

Table		Page
48.	Middle Basin Plot (MBP) 12/7/01 Trials: Stability for Pooled A and B Weak Layers	133
49.	Middle Basin Plot (MBP) 12/7/01 Trials: *t*-Tests of Strength for Pooled A and B Weak Layers	135
50.	Middle Basin Plot (MBP) 12/7/01 Trials: *t*-Tests of Stability for Pooled A and B Weak Layers	136
51.	Lionhead Mountain Plot (LMP) 1/9/02 Trials: QLCT Results	141
52.	Lionhead Mountain Plot (LMP) 1/9/02 Trials: Shear Stress	143
53.	Lionhead Mountain Plot (LMP) 1/9/02 Trials: Stability	143
54.	Lionhead Mountain Plot (LMP) 1/9/02 Trials: *t*-Tests of Strength	145
55.	Lionhead Mountain Plot (LMP) 1/9/02 Trials: *t*-Tests of Stability	145
56.	Lionhead Mountain Plot (LMP) 1/15/02 Trials: QLCT Results	148
57.	Lionhead Mountain Plot (LMP) 1/15/02 Trials: Shear Stress	150
58.	Lionhead Mountain Plot (LMP) 1/15/02 Trials: Stability	151

LIST OF TABLES - CONTINUED

Table Page

59. Lionhead Mountain Plot (LMP) 1/15/02 Trials: *t*-Tests of Strength 153

60. Lionhead Mountain Plot (LMP) 1/15/02 Trials: *t*-Tests of Stability 153

61. Lionhead Mountain Plot (LMP) 1/21/02 Trials: QLCT Results 157

62. Lionhead Mountain Plot (LMP) 1/21/02 Trials: Shear Stress 159

63. Lionhead Mountain Plot (LMP) 1/21/02 Trials: Stability 159

64. Lionhead Mountain Plot (LMP) 1/21/02 Trials: *t*-Tests of Strength 160

65. Lionhead Mountain Plot (LMP) 1/21/02 Trials: *t*-Tests of Stability 161

66. QLCT vs. Shear Frame Trials 166

67. Stability-Sampling Trials Summary 173

68. Stability-Sampling Trials' Weak Layer And Slab Characteristics. 176

LIST OF FIGURES

Figure — Page

1. Bridger Range Study Area Map 23
2. Bridger Range Study Plots Map 27
3. Madison Range Study Sites Map 29
4. Round Hill Study Site Map 30
5. Standard Snowpit Layout 34
6. Study Plot Stability-Sampling Trials Layout, Pits #1 through #5 36
7. Extrapolated Study Plot Stability Model 52
8. Bridger Range SWE Transects, January 2001 56
9. Bacon Rind Study Plot 1/3/01 Trials: Z Scores of Strength τ_∞ 72
10. Bradley Meadow Study 1/27/01 Trials: Z Scores of Strength τ_∞ 79
11. Bradley Meadow Study Plot 1/27/01 Trials: Z Scores of Stability S_{QLCT} 82
12. Round Hill 2/4/01 Trials: Z Scores of Strength τ_∞ 87
13. Round Hill 2/4/01 Trials: Z Scores of Stability S_{QLCT} 89
14. Baldy Mountain Study Plot 2/18/01 Trials: Z Scores of Strength τ_∞ 93
15. Baldy Mountain Study Plot 2/18/01 Trials: Z Scores of Stability S_{QLCT} 95

LIST OF FIGURES – CONTINUED

Figure Page

16. Saddle Peak Study Plot 2/18/01 Trials: Z Scores of Strength τ_∞ 100

17. Saddle Peak Study Plot 2/18/01 Trials: Z Scores of Stability S_{QLCT} 103

18. Bradley Meadow Study Plot 2/18/01 Trials: Z Scores of Strength τ_∞ 109

19. Bradley Meadow Study Plot 3/17/01 Trials: Z Scores of Strength τ_∞ 114

20. Bradley Meadow Study Plot 3/17/01 Trials: Z Scores of Stability S_{QLCT} 116

21. Middle Basin Plot 12/7/01 Trials: Z Scores of Strength $\overline{\tau}_\infty$ 130

22. Middle Basin Plot 12/7/01 Trials: Z Scores of Stability S_{QLCT} 134

23. Lionhead Mountain Plot 1/9/02 Trials: Z Scores of Strength $\overline{\tau}_\infty$ 142

24. Lionhead Mountain Plot 1/9/02 Trials: Z Scores of Stability S_{QLCT} 144

25. Lionhead Mountain Plot 1/15/02 Trials: Z Scores of Strength $\overline{\tau}_\infty$ 150

26. Lionhead Mountain Plot 1/15/02 Trials: Z Scores of Stability S_{QLCT} 152

LIST OF FIGURES – CONTINUED

Figure Page

27. Lionhead Mountain Plot 1/21/02 Trials: Z Scores of Strength $\bar{\tau}_{\infty}$ 158

28. Lionhead Mountain Plot 1/21/02 Trials: Z Scores of Stability S_{QLCT} 160

29. Comparisons of Coefficients of Variation (*CV*) in Stress and Strength 175

30. Weak Layer Age vs. Measures of Pit Strength 178

31. Lionhead Plot Trials Weak Layer Age vs. Measures of Pit Strength 180

ABSTRACT

Avalanche forecasters frequently perform field tests at study plots or other representative sites to reduce uncertainty regarding snowpack stability. This research investigated whether single snowpits represented stability throughout a carefully selected plot. The study utilized seven relatively uniform 900 m^2 plots, three each in the Bridger and Madison Ranges of Southwest Montana, and one in the Columbia Mountains near Rogers Pass, British Columbia. Teams collected systematic samples from five snowpits, each containing ten 0.25 m^2 stability-sampling cells, at each plot. Quantified loaded column stability tests measured strength in a single weak layer. Collection of in-situ slab shear stress data enabled the calculation of a stability ratio. Altogether, eleven stability-sampling trials were performed during 2000/2001 and 2001/2002, testing several weak layer types exhibiting a wide range of strengths. Of the 54 valid snowpit results, 28 (51.9%) represented plot-wide stability, 16 did not, and the remaining 10 pits were empirically unrepresentative of their plot. Three of the eleven plots sampled contained full complements of five representative snowpits. As an additional component of this study, a GIS-based model extrapolated Bridger Range plot stability data onto avalanche starting zones, with poor results. The results of this study provide sufficient evidence of local spatial variation in snowpack stability within relatively uniform plots to reject the hypothesis that stability at a single snowpit will reliably represent a plot. However, these results do not suggest that information from snowpits is not important. Experienced forecasters interpret study plot stability data conservatively and are capable of utilizing "targeted sampling" and a variety of other data to effectively reduce uncertainty about slope stability.

INTRODUCTION

Snow avalanches fall harmlessly by the hundreds of thousands throughout the uninhabited and unvisited mountains of the world each winter season (Armstrong and Williams, 1986). However, these otherwise harmless avalanches become potential hazards whenever and wherever people do enter the mountain realm (McClung and Schaerer, 1993), and lives and property are lost. Between 1970 and 1995, 365 people died in avalanche incidents in the United States (Logan and Atkins, 1996) and another 220 people were killed in Canada (Jamieson and Geldsetzer, 1996). Although those statistics reflect a wide variety of incidents, it has been persuasively argued that, " ... a major source of [avalanche] fatalities and accidents is failure in human perception; people perceived the state of instability of the snow cover to be something other than it was" (McClung, 2000). This study evaluates the perceived value, and underlying reliability, of field measurements of snow cover instability performed by avalanche experts.

World-wide, public and private sector avalanche forecasters are employed to evaluate avalanche conditions and apprise recreationists, transportation corridor managers, local government public safety officials, and other mountain enterprise operators of current and future danger (Williams, 1998). Their work spans avalanche hazards ranging in spatial scale from a few avalanche paths encompassing one or two square kilometers to several mountain ranges consisting of thousands of square kilometers of terrain and hundreds of avalanche paths. Similarly, their "products" range in temporal specificity from "now"

forecasts triggering specific operational responses, implemented within minutes or hours, to multi-day forecasts anticipating changing conditions and future risk mitigation actions.

McClung (2000) defined the practice of avalanche forecasting as, "... the prediction of current and future snow instability in space and time relative to a given triggering (deformation energy) level". It follows, then, that the goal of a forecaster is to "... minimize the uncertainty about instability introduced by the temporal and spatial variability of the snow cover, [by] incremental changes in snow and weather conditions, [and by] variations in human perception and estimation" (McClung, 2000). The process of preparing an avalanche forecast is sometimes supported by historic avalanche records retrieved by a computer program, or by the modeling of snowpack conditions across large areas, or by an "expert system" that combines both of those elements. However, even where those technologies are applied, so-called "conventional" avalanche forecasting remains the dominant forecasting methodology, an iterative and inductive mental exercise in the repeated collection and interpretation of data spanning a wide range of "informational entropy", or ease of interpretation and relevance (LaChapelle, 1980; McClung, 2000). The human capacity of skilled and experienced avalanche forecasters to grasp, appropriately weight, synthesize, and extrapolate such wide-ranging data has yet to be matched by computers (Schweizer and Föhn, 1996). Still, at least some uncertainty exists in every avalanche forecast.

Since avalanche forecasters seek to minimize uncertainty regarding instability, evidence of instability obtained from the observation of actual avalanches is customarily considered unambiguous, "low entropy", "scaled" information of the utmost relevance

and, as such, given the highest weighting (LaChapelle, 1980). In the absence of actual avalanche observations, or to corroborate the evidence they present, field measurements of snowpack stability obtained from in-situ "stability tests" are also considered relevant, low entropy data. In-situ stability tests measure the critical "triggering" load, or deformation energy required, for snowpack rupture in a limited number of samples. However, it is rarely safe to conduct in-situ stability tests within avalanche starting zones, particularly when conditions approach the threshold of avalanching (CAA/NRCC and Schleiss, 1995; Föhn, 1987; Föhn, 1988). Further, it is infeasible to obtain stability test data from every starting zone of interest, given the magnitude of terrain that most forecasters evaluate (Armstrong, 1991). Finally, some starting zones may simply be inaccessible.

For these reasons, avalanche forecasters routinely perform stability tests at proxy "study plots" carefully selected to reveal conditions presumed to be "representative" of nearby avalanche terrain but without the hazards associated with entering that terrain (McClung and Schaerer, 1993; Fredston and Fesler, 1994). Consequently, unlike the more easily interpreted meaning of actual avalanche observations, study plot stability test data interpretation does contain informational ambiguity due to unknown spatial variations in snowpack characteristics between the study site and avalanche starting zones (Birkeland, 1997). Linking stability measured at the scale of sampling performed at a study plot to the relevant scales of prediction – single starting zones, an array of starting zones, or regions within a mountain range – requires extrapolation. Improved understanding of the reliability of stability test results, and of the spatial relationships

between study plot stability and stability in adjoining and distant terrain, could significantly improve forecasters' perception of the meaning of stability test results and, thereby, reduce uncertainty.

As an avalanche forecaster working from 1990 through 1998 on a quarry access road near Marble, Colorado, I was confronted with the challenge of extrapolating snowpack stability information from study plots onto some eight square kilometers of "uncontrolled" and active avalanche terrain located inside the federally designated Raggeds Wilderness Area (Landry, 1994). In seven winter seasons over 700 natural avalanches (U.S. Class 2 size or larger) fell in the subject terrain and some 72 avalanches from 94 starting zones reached the quarry road (Landry, 1998), with only one minor incident. To evaluate the sensitivity of the snowpack to additional precipitation loading, traditional "collapse" stability tests (McClung and Schaerer, 1993) were utilized and the development of a quantified loaded column stability test was begun (Landry, 1998 and 1999). Two specific case studies during that period provide the impetus for the proposed research.

In the first instance, traditional collapse stability tests at a study plot adjoining the quarry road produced consistent shear fracturing results in a 40 cm slab under the equivalent of 37-50 mm of precipitation water equivalent of additional load. The next day, with a storm in progress, an adjoining avalanche path some 500 meters northwest of and 200 meters higher than the study plot produced a U.S. Class 3 size avalanche that hit and buried the road as the storm HNW reached 41-43 mm. Several adjoining paths also produced significant events within hours of the first event and within the range of 37-50

mm HNW of new loading, and all events appeared to have run in the same weak layer tested at the study plot.

A second case was documented involving the same study plot and adjoining avalanche path during the winter of 1998/99. Following a significant storm and avalanche cycle I conducted an analysis of the precipitation loading responsible for a deep slab avalanche to the road and cracking and collapse of the study plot snowpack. It revealed that the snowpack in both locations had failed under very similar levels of additional shear stress (aprox. 340 N/m^2). While no loaded column stability tests had been performed before the storm, the post-storm analysis suggested that the study plot snowpack and the avalanche path would have presented very similar pre-storm stability conditions. Several more adjoining starting zones had also produced U.S. Class 3-4 avalanches running in the same basal depth hoar weak layer.

Surprisingly little research has evaluated this widespread practice of extrapolation of stability/instability data from study plots to avalanche terrain. This is a matter of substantial interest to field practitioners who, in the absence of "better" (lower entropy) information, must often make significant assumptions based on study plot stability data. Avalanche researchers modeling snowpack characteristics and instability based on study plot meteorological data are also concerned with scaling the output of their modeling "up" to the sub-region or regional spatial scale. My experience while working in Colorado as a consulting avalanche forecaster suggests that correlations between study plot instability and instability in adjoining terrain sometimes *seem* to exist but at other times clearly do not, and those observations instigated this research.

RESEARCH HYPOTHESES

This study's objectives are to evaluate the reliability of snowpack stability test results obtained at carefully selected study plots and, then, to develop and evaluate a spatial model of avalanche starting zone stability which deterministically extrapolates measurements of Bridger Range study plot stability onto adjoining avalanche terrain. I investigated three hypotheses regarding study plot stability, at three spatial scales:

1. Stability measured at a randomly selected snowpit location within a carefully selected study plot will demonstrate a significant probability of predicting the mean stability of the entire study plot.
2. Stability measured at a study plot will reliably predict avalanche starting zone stability within 1-2 km of the study plot when adjusted for spatial variations in snowpack characteristics caused by elevation, aspect, slope angle, and redistribution of snow by wind.
3. Stability measured at a study plot will exhibit systematically decreasing correlation to stability in increasingly distant avalanche terrain and, therefore, will not predict stability throughout an avalanche region.

If stability testing at randomly selected sites within carefully selected study plots does not reliably indicate mean stability throughout a study plot (hypothesis #1), this will constitute an important finding regarding the measurement of stability at a very small spatial scale and compel avalanche forecasters to reconsider the weighting they give to

study plot stability tests. Rejecting hypothesis #1 would also nullify hypotheses #2 and #3. If hypothesis #1 is not rejected, and snowpit stability tests reliably measure study plot stability, analysis of hypothesis #2 could reveal the absence of a significant relationship between stability at a study plot and stability in nearby terrain. This finding would nullify both hypotheses #2 and #3 and cause avalanche forecasters to seek other, more reliable sources of starting zone stability information. Conversely, strong region-wide correlation of stability measured at single or multiple study plots with starting zone stability would be a very important finding. Alternatively, it is possible that closely spaced study plots will present overlapping zones of high-confidence correlation between study plot stability and starting zone stability, but "gaps" of low-confidence correlation will be found between more widely spaced plots.

LITERATURE REVIEW

Several relevant themes are reviewed within the snow avalanche research literature. These include 1) avalanche forecasting principles and data collection, 2) snowpack stability testing and indices, 3) spatial variation of snowpack properties, 4) modeling snowpack stability and 5) modeling snowpack accumulation.

Avalanche Forecasting Principles and Data Collection

Most operational avalanche forecasting programs in the United States rely on "conventional" methods (Williams, 1998). Conventional avalanche forecasting is an iterative and inductive integration of at least three categories of contributory factor information. The objective of the iterative, inductive process is to minimize uncertainty by repeatedly seeking "low entropy", easily interpreted and relevant information (LaChapelle, 1980; McClung, 2000). Contributory factor information categories have been defined by McClung and Schaerer (1993) as Class III (meteorological), Class II (snowpack stratigraphy and state) and Class I (stability) information (listed in order from high- to low-entropy). Birkeland (1997) has proposed adding a fourth Class of data to the scheme, representing terrain. A synthesis of these data classes, and examples of the data they represent, is presented in Table 1.

Class I stability information includes the stability test data collected during this research. Such data have been considered especially important when forecasting slab avalanches originating in older layers within the snowpack (Armstrong and LaChapelle, 1976). McClung (1998) also describes the importance of objective Class I snowpack stability information during periods of "conditional stability", when conditions are not obvious and human perception of the spatial distribution of (in)stability, and the probability of directly measuring (in)stability, are poorest.

Table 1. Avalanche Forecasting "Contributory Factor" Data Classification.

Class	*Information*	*Examples of data*
I	Stability	Stability test results, avalanche observations, explosive testing …
II	Snowpack	Weak layer type, slab thickness, slab density, snowpack height …
III	Meteorological	New snow water equivalence, wind speed and direction, air temperature …
IV	Terrain	Slope angle, elevation, aspect, slope curvature, vegetation, substrate …

Although Class I stability data are vital to conventional forecasters, collecting the data is problematic. Identifying data collection sites that balance the need for reliable Class I snowpack stability information indicative of avalanche starting zone conditions against the risk and practicality of obtaining that information requires skill and experience (Föhn, 1988; CAA/NRCC and Schleiss, 1995). Also, some avalanche starting zones may simply be inaccessible, and as the geographic scale of the stability forecast area grows, it is increasingly difficult to obtain data at an ideal (low entropy) spatial resolution (Armstrong, 1991).

Consequently, forecasters identify safe and accessible study plots that seem likely to exhibit snowpack conditions representative of (at least) the adjoining avalanche terrain. There they collect stability data which are then integrated with other contributory factors and extrapolated, inductively, to the surrounding terrain using their understanding of snowpack processes and their forecasting experience to spatially modify the study plot results. Interestingly, individual forecasters may apply different weightings to the same set of contributory factor data to develop equally accurate forecasts, demonstrating that, "there is more than one way to forecast an avalanche" (LaChapelle, 1980). This study evaluates the underlying reliability of study plot stability measurements and analyzes the practice of spatially extrapolating stability test result data using a spatial modeling approach not previously described in the literature.

Snowpack Stability Testing and Indices

McClung and Schaerer (1993) described stability as "the ratio of the resistance to failure versus the forces acting toward a failure". While the avalanche forecasting literature initially concentrated on tensile stress/strength relationships (LaChapelle, 1966), shear fracture is now generally accepted as the primary mechanism in slab avalanche release (McClung, 1977; McClung and Schaerer, 1993). Consequently, researchers and field practitioners have developed a number of in-situ field tests measuring shear fracture strength.

The shear frame test produces a quantified, continuous measurement of shear strength. Researchers have refined the shear frame test procedure by evaluating the

effects of frame size, load rates, and normal loads on tests results, and by developing stability indices based on shear strength measurements (Perla and Beck, 1983; Föhn, 1987b; Föhn, 1988; Jamieson, 1995). Shear frame tests are typically conducted at approximately level study sites (CAA/NRCC, 1995). Shear stress is introduced to a snow sample using a single rapid load parallel to and immediately above the suspect weak layer being tested. The shear frame procedure is more difficult to perform on a slope, does not necessarily identify the weakest layer in the snowpack, requires removal of the snowpack above the layer being measured, and is particularly difficult to perform when a relatively harder layer directly overlies the weak layer of interest. These shortcomings caused Perla and Beck (1983, p. 490) to advocate that, "the shear frame be replaced by a device that measures a more fundamental index of *gleitschict* [potential zone of shear fracture within the snowpack] strength".

The shear frame test quantifies shear strength in units of force but requires a certain degree of skill and painstaking preparation. Other stability tests have been developed which are less time intensive and more intuitively interpreted by recreationists. The Rutschblock test developed by the Swiss Army (Föhn, 1987a) yields an ordinal rating of the snowpack's vulnerability to skier-triggered shear fracture. In this test, shear stress is generated in an isolated column of snow with a surface area of 3 m^2 by the dynamic vertical load of a skier in a succession of increasing loads. Birkeland and Johnson (1999) introduced a "stuffblock" test that utilizes the same testing approach as the Rutschblock – successively increasing dynamic loading of an isolated column of snow – but at a smaller sample size of 0.09 m^2. Efforts to evaluate and calibrate the two tests with other

tests have yielded significant correlations between the shear frame and Rutschblock (Föhn, 1987a; Jamieson and Johnston, 1992; Jamieson 1995) and the stuffblock and Rutschblock (Birkeland and Johnson, 1999). Backcountry recreationists and professional avalanche forecasters have adopted the Rutschblock and stuffblock tests as relatively simple, quick, and efficient techniques for testing current snowpack stability, given prudent and skilled interpretation.

Other field stability tests include the "compression" (tap) test (CAA/NRCC, 1995) and the "collapse" (loaded column) test (McClung and Schaerer, 1993). Jamieson and Johnston (1997) have evaluated the compression test and correlated its results with Rutschblock results and skier-triggered avalanching. Like the stuffblock, the compression test employs a successive series of dynamic loads upon a 0.09 m^2 isolated column of snow, and can be performed on sloping or level terrain. The collapse (loaded column) test also employs an isolated column of snow but, rather than using repeated dynamic loads, blocks of snow are gently added to the top of the column until the column fractures in shear or collapses. If desired, the water content of the added blocks of snow can be estimated.

The Rutschblock, stuffblock and compression tests all differ from the shear frame test in that they are typically conducted on slopes and the normal load produced by the snowpack above the weak layer being tested is left largely intact. However, unknown effects produced by cumulative compression of the snow during the test procedures, and their ordinal results, make the Rutschblock, stuffblock, and compression test difficult to interpret or verify in terms of quantities of precipitation loading or shear stress. The

collapse test, on the other hand, can yield results in terms of quantities of precipitation loading and Schaerer (1991) called for additional development of the collapse (loaded column) test. This study employs a more rigorous "quantified loaded column test" (Landry et al., 2000) designed to produce continuous measurements of shear strength as well as express test results in terms of precipitation loading.

Stability indices have historically summarized shear frame test data by relating measured shear strength with shear stress introduced by the gravitational load of the in-situ snowpack above the tested weak layer (Föhn, 1987b and 1988). Other stability indices based on shear frame test results incorporate the effects of sample size and normal pressure, and account for human-trigger loads (Föhn, 1987b; Conway and Abrahamson, 1984; Jamieson, 1995). However, McClung and Schweizer (1999) cast doubt on the premises underlying stability indices (ratios) through an analysis of the mechanics of slab failure, size-effects related to stability tests, and the effects of slab properties on stability tests and skier-triggering. Further, none of the indices contain information about the spatial distribution of stability.

Spatial Variation of Snowpack Properties

Variation in stability on the scale of a particular, single slope has been investigated as a manifestation of so-called "deficit zones" (Föhn, 1988). Deficit zones, or "super-weak areas", are pre-requisites to natural avalanching (Bader and Salm, 1990; Schweizer, 1998). Conway and Abrahamson (1988) utilized shear strength measurements and a 'stationary random process' statistical technique to model stability variations on a single

slope caused by hypothesized deficit zones. Jamieson (1992) measured distributions of Rutschblock test scores on single, uniform slopes, identifying the probability of a test falling within one 'degree' (one step in the rank order) of the slope's median score.

At the larger spatial scale of adjoining slopes, Bradley (1970) investigated the link between spatial and temporal patterns in "deep slab" avalanches. Dexter (1986) documented systematic variations in snowpack depth and strength due to variations in slope aspect and elevation over an area of 10 km^2. Substantial spatial variations between similar slopes in stability-related snowpack characteristics has been documented (Birkeland et al., 1995). Föhn (1988) suggests that many snowpack parameters vary to the same extent, including shear strength. Stability variation within avalanche starting zones is well known but does not easily lend itself to field measurement (Föhn, 1988).

Spatial variation research at the scale of many public-safety avalanche forecasting programs is limited. Such programs typically evaluate conditions over hundreds, even thousands of square kilometers (Williams, 1998). Jamieson and Johnston (1992, 1994) conducted extensive field trials in several ranges of British Columbia to develop a stability index for skier-triggered avalanching using the shear frame. The index was evaluated on a single slope scale and used to monitor the stabilization of a significant weak layer associated with numerous skier-triggered avalanches over areas within a 10-15 km radius of the study sites. While their index values were consistent with the gradual decline in skier/human triggered events in at least one region, triggered events did continue and were attributed to terrain- or weather-related "anomalies" in the snowpack.

They did not discuss or elaborate on any spatial patterns of avalanche activity or snowpack characteristics they observed during the study.

Birkeland (1997, 2001) advanced a geographic approach to stability research with his Bridger Range study in southwest Montana. The study deployed teams of field observers to 70 data collection sites spanning a distance of almost 40 kilometers. Data collected by the teams was analyzed to reveal linkages between stability and a set of variables measuring terrain, snowpack, and snow strength parameters. His thesis that the Bridger Range comprised a single "avalanche region" with similar avalanche conditions was generally supported by his findings that terrain parameters roughly determined stability patterns, rather than location within the Range. However, Birkeland did not correlate his findings with stability test results from study plots.

Modeling Snowpack Stability

Class III (meteorological) and Class II (snowpack stratigraphy and state) study plot data have been utilized by researchers pursuing a wide variety of statistical avalanche forecasting strategies at the regional and local scale (Good and Amman, 1994). Expert systems that model regional snowpack characteristics from point meteorological inputs (Giraud et al., 1994; Durand et al., 1999) or that combine meteorological, snowpack, geographic, topographic and field observations of avalanche activity (Bolognesi, 1988), are under continued development. Rink (1987) used discriminant and cluster analyses to identify key groups of geographical parameters (termed "geosystems") influencing avalanche formation including the definition of "slope climates" characterizing terrain at

a local or regional scale. Buisson and Charlier (1989) developed an "expert system" combining a GIS digital terrain model composed from an irregular triangulated net with meteorological inputs and "specialist reasoning" to model stability and avalanche dynamics in a single path. The model required considerable avalanche experience to specify numerous boundary condition parameters. Chernouss and Federenko (1998) evaluated the spatial distribution of avalanche release probability at a local, single-slope scale, modeling slab characteristics and verifying the model with slab thickness measurements. However, Class I stability data have generally not been incorporated in these statistical methods or models, frequently citing the difficulty of estimating the spatial variation of snowpack stability and, hence, implying the difficulty in extrapolating stability measurements from study plots.

Process-oriented studies incorporating measured or modeled snowpack characteristics and processes from study plot (or point) data sources are of particular relevance to this thesis research. Judson et al. (1980) developed a deterministic, process-oriented approach to modeling snowpack stability at a local scale. They modeled snowpack processes for a "theoretical avalanche" designed to replicate the behavior of an array of 13 avalanche paths. The model proved effective in identifying artificially triggered avalanche days but poor at identifying non-avalanche days, perhaps because it employed no measured Class I stability test data due to problems with quantification.

In British Columbia, Canada, the Ministry of Highways presently employs a promising methodology at Kootenay Pass. It combines a "nearest neighbor" module (which matches current contributory factor conditions to an historic avalanche occurrence

and weather database) with a rule-based computerized snow profile evaluation module (McClung, 1994). The nearest neighbor module requires forecasters to evaluate their "degree of belief" in the analysis before generating its final output. The snow profile evaluation module includes a "certainty factor" ranking the avalanche potential of individual snowpack elements according to forecaster-defined rules incorporating conventional data. Forecasters presently employ these two modules at a large local scale (within 10-15 km of the study plot) and their success "approaches human [conventional forecasting] capability in forecasting accuracy"(McClung, 1994, p. 424). Those results suggest that the inclusion of Class I stability information is critical for the success of process-oriented numeric forecasting systems.

Modeling Snowpack Accumulation

Investigations of mountain precipitation by snow hydrologists and others have described the influence of elevation and geographic location, relative to nearby terrain, on snow water equivalence (SWE) accumulation in mountainous terrain (Farnes, 1995; Sommerfeld and Smith, 1998; Balk et al., 1998). Complex interactions between terrain, air mass characteristics, microphysical processes in clouds, and atmospheric wind fields control the vertical distribution of precipitation in the mountains. In mid-latitude mountain ranges snow precipitation increases with elevation to a certain point (Barry, 1992). Further, Caine (1975) used snow course data from the San Juan Mountains of southwest Colorado to demonstrate that variation in distribution of SWE was also

inversely related to elevation, meaning that high-elevation SWE is less variable than low elevation SWE.

Studies in and near the Bridger Range of southwest Montana confirm the relationship between precipitation and elevation. McPartland (1971) tracked snow precipitation for two winter seasons at 66 sites representing a variety of spatial attributes in the Bangtail Range located approximately 10 km east of the southern Bridger Range. After evaluating a number of spatial variables, including wind exposure, he concluded that elevation was the parameter that best predicted snowpack depth. Birkeland's (1997) study of elevation and aspect influences on snowpack conditions and stability in the Bridger Range found that snow depth generally increased with elevation, although slope aspect complicated the relationship. Birkeland (personal communication, 2000) considers elevation and easting (distance downwind from barrier) to be spatially autocorrelated in the Bridger Range and, in effect, a single variable (partially) determining SWE at a given location. Pipp and Locke (1998, page 34) also found, using a set of three snow/elevation and easting gradient transects at sub-alpine sites in the Ross Pass area of the Bridger Range, that both elevation and easting were "equally competent, linear predictors of snowfall [SWE]". Their linear function for the influence of elevation on SWE at all fifteen sampling points in their study area is:

$$SWE(mm) = -887 + 628\left[Elev(km)\right] \qquad r^2 = 0.62,\ p < 0.001 \qquad (1)$$

Snow hydrologists, charged with predicting snowmelt runoff from mountain watersheds, are interested in modeling SWE, and predicting snow-melt runoff, at spatial scales ranging from a single mountain basin to an entire mountain range. A network of

instrument arrays operating throughout the western United States by the National Resource Conservation Service (NRCS), called SnoTel, measures snow precipitation and other weather parameters at wind-sheltered sites below treeline. Often, pairs of high/low-elevation SnoTel sites are used to measure elevation differences in precipitation within a basin. Water management agencies, including NRCS, have developed numerous algorithms which are reasonably successful in modeling snowpack distribution below treeline from this network of SnoTel point data.

Modeling snowpack distribution (and SWE) in alpine terrain above treeline, however, has been found to be particularly problematic due to the redistribution of snow by wind. At the basin scale, Ingersoll (1996) empirically evaluated SWE in the Andrews Creek basin of the Front Range in Colorado, but the processes controlling distribution were not modeled. Winstral and Elder (1998) adapted a "fetch" algorithm originally developed for predicting snow drift in the Canadian prairies incorporating curvature and wind-exposure indices derived from a 30 m digital elevation model (re-sampled at 400m for deriving curvature). They found their empirical method was roughly twice as effective in explaining snowpack distribution at the 406 points measured above treeline as using a combination of elevation, radiation, and slope parameters. The single-basin scale of this and other SWE modeling efforts offers insights into snowpack distribution processes to avalanche scientists modeling stability in individual avalanche starting zones within basins.

Building on the numerous investigations during the 1970's and 80's of the physical laws governing snow drift conducted by Schmidt, Tabler, and others, increasingly

complex physical models of snow drift in alpine terrain are emerging. Among the more recent, three-dimensional models is the work by Liston and Sturm (1998), in which a numerical snow transport model for complex terrain was developed. SnowTran-3D was tested during the 1997/98 winter by Greene et al. (1999) on an alpine ridge near Cameron Pass, Colorado. This limited trial produced an adequate simulation of the actual drifting at the site. Additionally, Gauer (1999) modeled snow scouring and deposition on the Gaudergrat ridge near Davos, Switzerland, using a physically based numerical method with a spatial resolution of 5 m^2.

Preceding these three-dimensional models are the earlier works by Föhn (1980) and Föhn and Meister (1983), that describe two-dimensional physical models of wind drift over mountain ridges. In the first of those studies, Föhn (1980) evaluated the snow mass flux produced by "wind power" from windward to leeward slopes of an alpine ridge. Fohn's (1980) empirically derived equation for the increase in snow depth produced by wind-power induced drift is:

$$H_{NS} = k\bar{u}^3 \left\{ m/d \right\} \qquad (2)$$

where H_{NS} represents the increase in snowpack depth, in meters per day, u is the 24-hour mean wind speed (meters/second), and k is an empirically derived coefficient $k = 8 \times 10^{-5} s^3 d^{-1} m^{-2}$.

This model was further refined (Föhn and Meister, 1983) by describing three general patterns of snow drift, related to ridge crest apex angles: 1) the formation of a snow cornice at the ridge crest, with an area of scouring just below the cornice (on the leeward slope), and a secondary area of enhanced deposition some distance further down the lee

slope, grading into the 'normal' snowpack for that elevation, 2) enhanced deposition, without a cornice, immediately leeward of and attached to the crest, grading into the normal snowpack, and 3) scouring in the immediate lee of the ridge crest, with enhanced deposition down-slope and detached from the crest, grading into the normal snowpack. Föhn and Meister explain these patterns of drift using the combined effects of "plume" and "potential flow" models. The potential flow model was applied to precipitating snow while the plume model was applied to the erosion of a snowpack lying on the windward slope; both models assumed a wind flow perpendicular to an elongated ridge [such as occurs at the Bridger Range] and incorporate wind speed and terrain ("hump") shape. Föhn and Meister acknowledge that, in more severe terrain, the exact positioning of deposition elements, such as a cornice, may not be accurately estimated by the models.

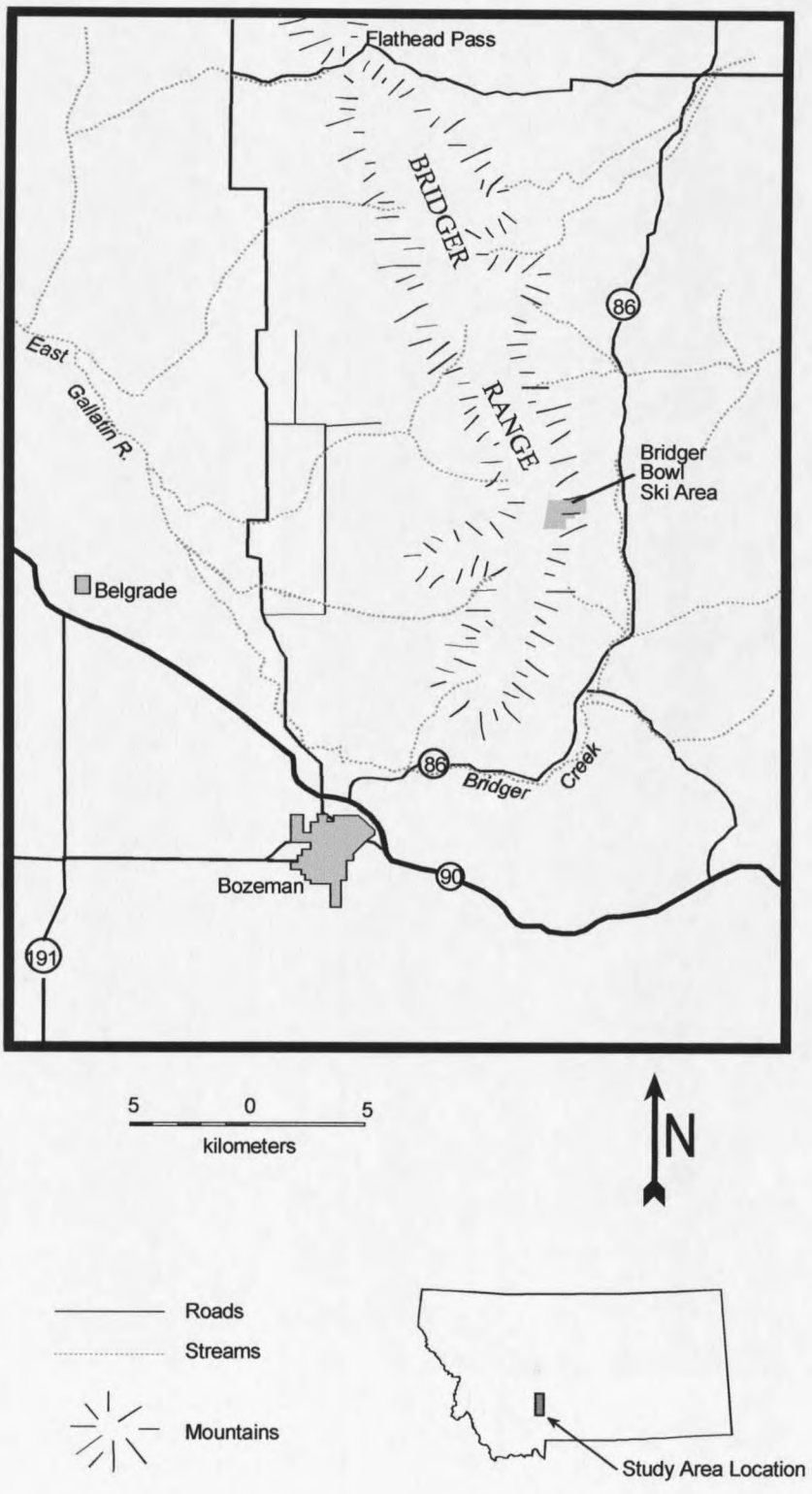
STUDY AREA

The Bridger Range of southwest Montana, from Baldy Mountain to Flathead Pass (Figure 1), was chosen as the primary study area for this research because:

1) the topography of the Bridger Range is relatively consistent, with a single, generally north-south ridge axis and a long array of generally east-facing terrain, facilitating the identification of numerous potential study plot sites with similar characteristics,
2) steep, generally east-facing slopes, sparse vegetation near the ridgeline, and frequent precipitation events, with intervening periods of weather conducive to the formation of weaknesses within the snowpack, combine to create active avalanche terrain,
3) safe access to the potential study plot sites is possible
4) Bridger Bowl ski area and other researchers are collecting high quality meteorological data at a central location within the study area.

The Bridger Range lies within the Intermountain avalanche region of the United States (Armstrong and Armstrong, 1988; Mock and Birkeland, 2000). The snow climate of this area is also described as "transitional" (McClung and Schaerer, 1993) wherein characteristics of both continental and maritime snowpacks and weather are found. Winter weather in the Bridgers consists of low temperatures, long duration and strong wind events, and varying amounts of precipitation. Year-to-year snowpack depths in the

Figure 1: Bridger Range Study Area Map



Bridger Range vary widely from shallow and weak snowpacks resembling continental climate conditions and dominated by depth hoar, to deep and strong coverage resembling maritime snow climate snowpacks (Birkeland, 1997). Frequently, attributes of both continental and maritime snowpacks are mixed in the same season. Climate data collected at the Bridger Bowl Ski Area including snowfall, precipitation, and air temperatures (Table 2). Over the winters of 1984/85 through 2000/2001, mean seasonal total snow-water equivalent precipitation (SWE), from November through March, was 500.3 mm. Northwesterly flow aloft generally produces the largest precipitation events at Bridger Bowl (Birkeland and Mock, 1996) along with westerly winds, windloading the east-facing aspects of the Range and building large, east-facing cornices at the ridgeline.

Table 2: Bridger Bowl Ski Area Climate Data. Temperature Data for Period 1969-1994 (WAN, 1995). Snow and Precipitation (SWE) Data for Period 1984/85 through 2000/2001 (Bridger Bowl Ski Patrol, 2001).

	1969-1994 Average Daily Maximum Air Temp °C	1969-1994 Average Daily Minimum Air Temp °C	1984/85 – 2000/2001 Average Monthly Snowfall (m)	1984/85 – 2000/2001 Average Monthly Precipitation (SWE) (mm)
November[1]	0.0	-8.4	1.18	100.3
December	-2.6	-10.7	1.28	94.0
January	-3.2	-11.0	1.42	106.4
February	-1.3	-10.1	1.04	80.0
March	1.3	-8.0	1.50	119.6
		Season Total	6.42	500.3

[1] November temperature data for period 1984-1994 only.

METHODS

Selection of Study Plot Sites

During the summer of 1999 I identified nine potential study plots on the east-facing slopes of the Bridger Range study area using USGS 1:24,000 scale topographic maps, visual scouting from the valley, and field inspections. I selected the nine prospective study plot sites using the following criteria:

1) comparable topography:
    - elevation of 2,250 m ± 60 m elevation, and within 1 km east of the Range's north/south primary ridgeline
    - slope aspect of east to northeast
    - slope terrain generally smooth and planar, without trees or large scree or rock outcrops
2) minimal human activity that might alter natural conditions
    - study plot site unlikely to be disturbed by skiers, snowmobilers, or other recreationists
    - nearby avalanche terrain is generally uninfluenced by human activity
3) minimum surface area of 900 m^2 (typical of a study plot large enough for a season-long time series of single snowpits without repeating observations at a point)

4) accessible enough to complete the full set of observations in a single day

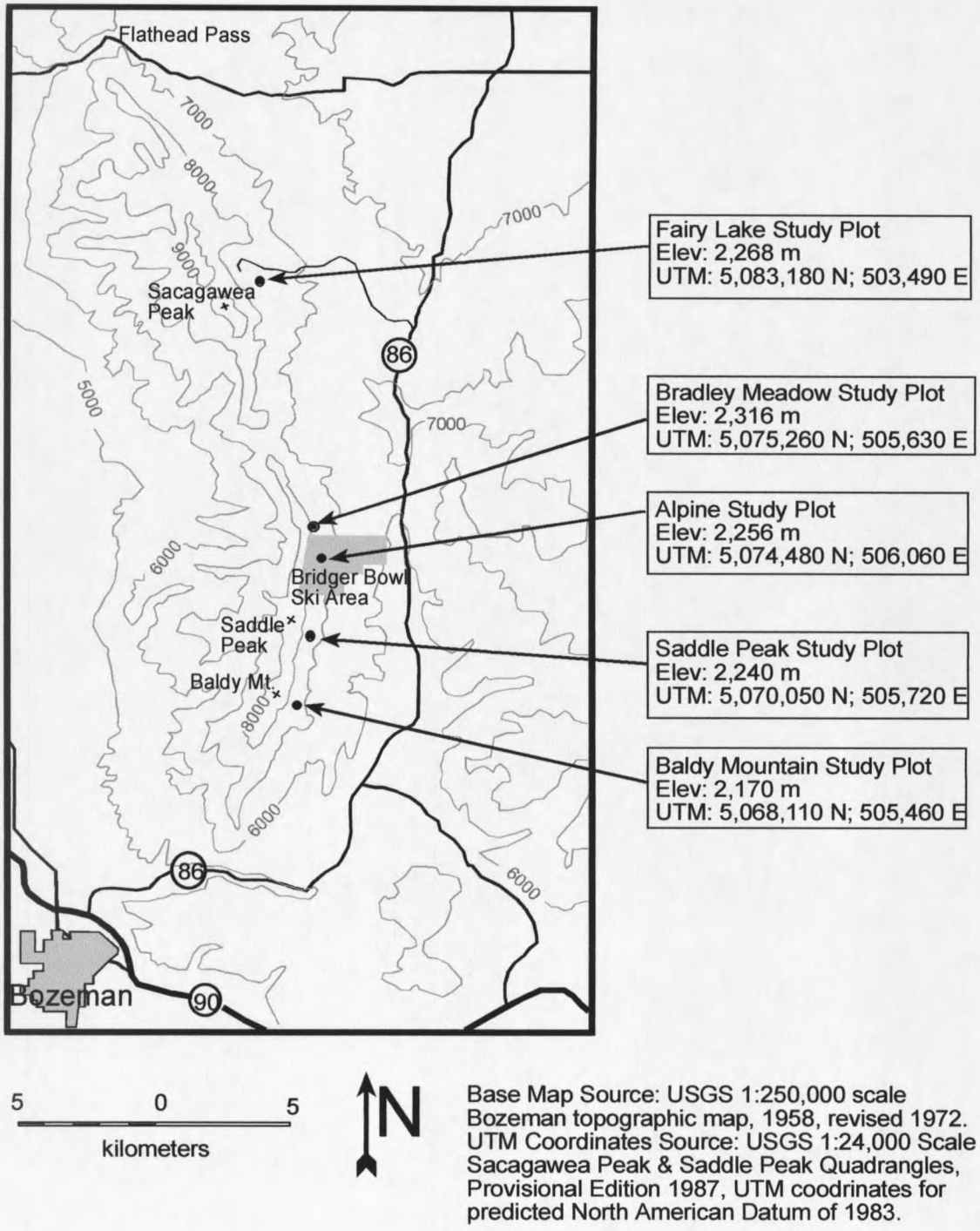
5) safety:

   - slope angle of 25-30° and no more than 35°
   - observer safety, with no significant threat from adjoining avalanche paths, a generally safe approach, and no terrain traps below the study slope.

During the winter of 1999/2000 four final Bridger Range study plot sites were chosen: Baldy Mountain, Saddle Peak, Bradley Meadow, and Fairy Lake (Figure 2). These study plot sites were selected based on: 1) the criteria listed above, 2) the availability of four complete sets of QLCT field equipment, and 3) the likely availability of no more than four skilled teams of observers and sufficient transportation support for four teams. Public USFS lands encompassed all four sites and a Special Use Permit was obtained for the study plots from the Gallatin National Forest Bozeman Ranger District.

The north-most portion of "Bradley Meadow", located immediately north of the Bridger Bowl ski area boundary, was selected as the primary study plot based on its easy access via the ski area (with their permission), for its proximity to the Bridger Bowl Ski Area Alpine study plot (Figure 2), and for its generally central location, north-to-south, among the four study plots. Bradley Meadow is also of sufficient size to accommodate a time series of snowpack monitoring snowpits in one area while leaving enough undisturbed snow for multiple 900 m^2 sampling plots for the multi-pit data collection effort described below. Bradley (1970) and Birkeland (1995) also conducted their research at the Bradley Meadow site.

Figure 2: Bridger Range Study Plots Map. The Bridger Bowl Alpine Study Plot was used exclusively to collect climate data.



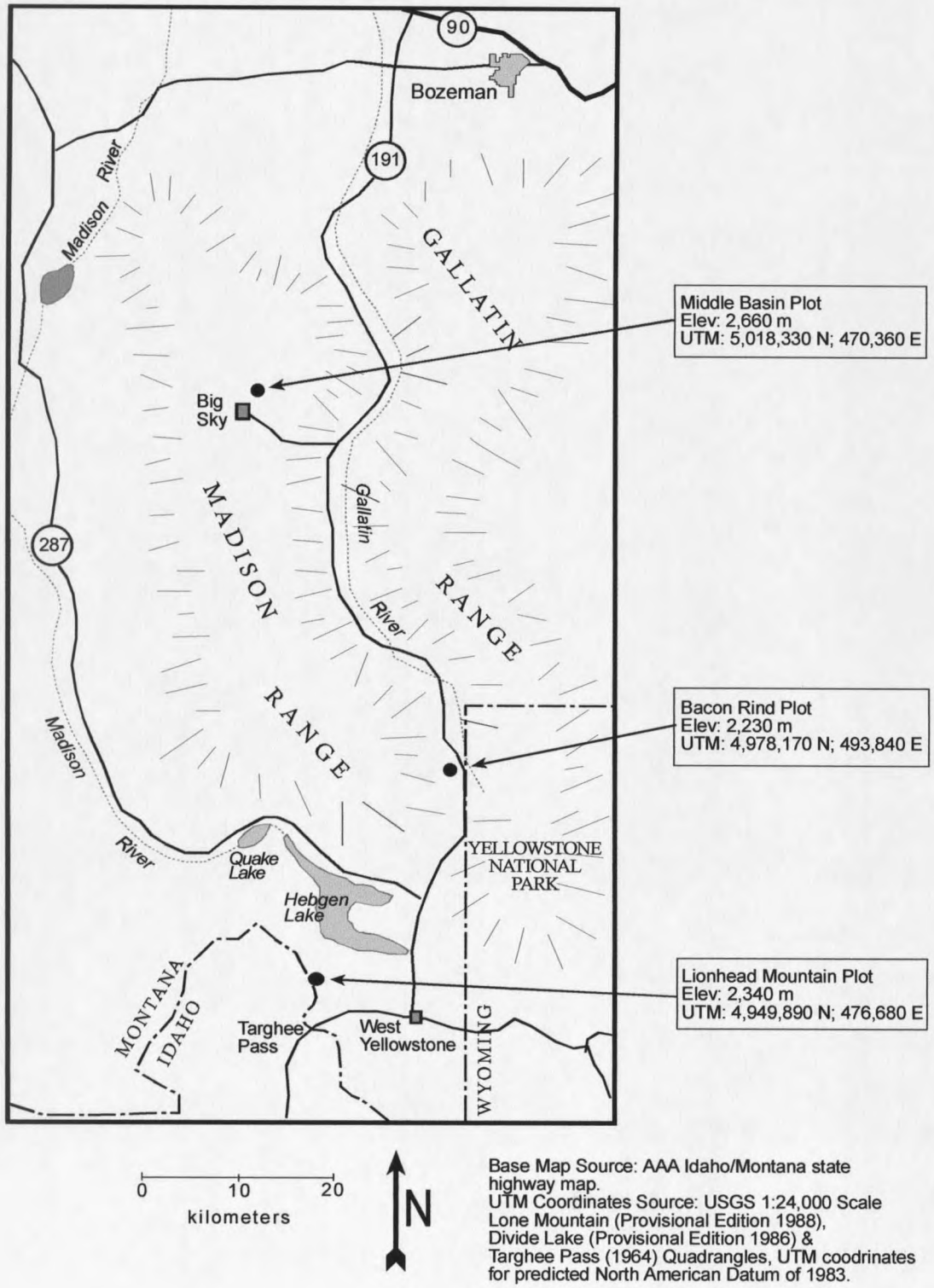
Base Map Source: USGS 1:250,000 scale Bozeman topographic map, 1958, revised 1972.
UTM Coordinates Source: USGS 1:24,000 Scale Sacagawea Peak & Saddle Peak Quadrangles, Provisional Edition 1987, UTM coodrinates for predicted North American Datum of 1983.

The Baldy Mountain and Saddle Peak study plots are located south of the Bridger Bowl ski area and both required the use of snowmobiles for access. Permission was obtained from a private landowner to gain direct access to USFS lands en-route to these study plots, and from the USFS to utilize motorized transportation in this area of the Bridger Range. The fourth study plot is located in the northern portion of the Bridger Range on a slope adjoining the Fairy Lake outlet; this site also required a snowmobile for reasonable access. Snowmobile use in this area in unrestricted. All four Bridger Range study plot sites are found on the eastern limb of the Bridger Range anticlinorium and lie at the adjoining contacts of the Morrison Formation, Ellis Group, and Kootenai Formation (Skipp et al., 1999).

Due to the very slow development of satisfactory snowpack conditions in the Bridger Range study area during the early 2000/2001 season, and the risk of losing a second season of data collection, two study plot stability-sampling trials were performed elsewhere. We conducted the first trial of that season on 1/3/01 near Bacon Rind Creek in Yellowstone National Park (Figure 3) on an open, east-southeast-facing slope some 150 meters above the valley floor with a planar surface, 32° slope angle, no apparent vegetation or rock outcroppings, and an apparent lack of skier disturbance. The site presented an ideal proxy "study plot" for a stability-sampling trial, even if subsequent collection of avalanche occurrence or storm data was unlikely.

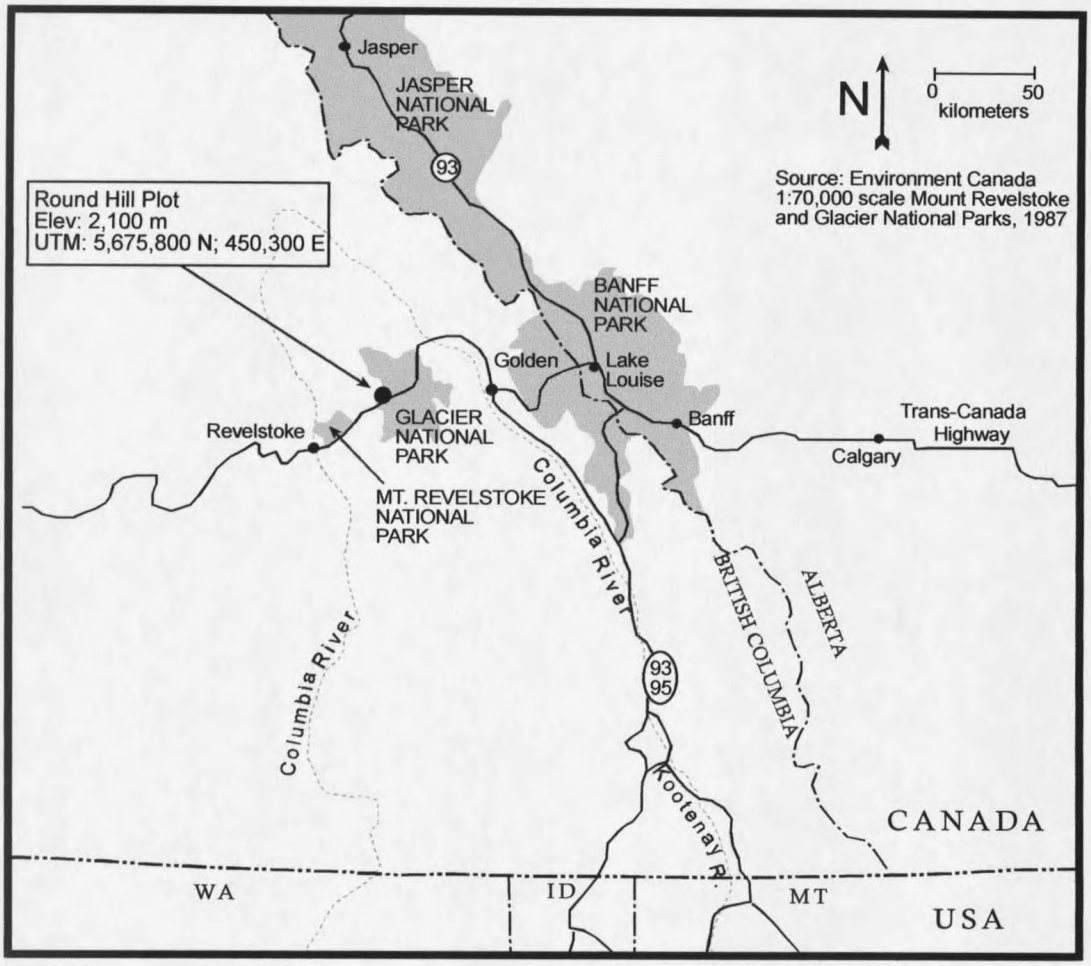
Next, on 2/4/01 we conducted the second study plot stability-sampling trial of the season near the Fidelity Mountain research facility at Rogers Pass, British Columbia, at the "Round Hill" study site (Figure 4). This site differed from the study plots used for the

Figure 3: Madison Range Study Sites Map.



Base Map Source: AAA Idaho/Montana state highway map.
UTM Coordinates Source: USGS 1:24,000 Scale Lone Mountain (Provisional Edition 1988), Divide Lake (Provisional Edition 1986) & Targhee Pass (1964) Quadrangles, UTM coodrinates for predicted North American Datum of 1983.

Figure 4: Round Hill Study Site Map



balance of the trials in its location relative to nearby starting zones. The Round Hill site is a low-angle avalanche starting zone adjoining steeper avalanche starting zones routinely monitored by the Rogers Pass avalanche safety program. Nearby starting zones with slope angles of 35° to 40° are routine target areas for explosive hazard reduction since they threaten the Trans-Canada Highway.

Parks Canada avalanche personnel proposed and first inspected the Round Hill site before Landry and Deems entered the slope. Given the recent sensitivity of a buried layer of surface hoar, deposited on 1/28/01, selecting a relatively low-angle study site was imperative to minimize risk to the data collection team. The Round Hill site presented an apparently planar surface (which proved to be a slight optical illusion produced by very "flat" light and, instead, consisted of two parallel surfaces separated by some 50 cm in relief), a slope angle of 27°-30°, an absence of vegetation or rock outcrops, and protection from wind drifting.

In early April, under the increasing sun angle, the snowpack began to approach 0° C snow temperatures throughout on the east- and south-facing aspects of the study area. Because very warm, or "wet" (0° C) snow exhibits rapid changes in stability occurring over periods of a few hours, and since the study plot stability-sampling trials require several hours to execute, further stability-sampling trials were not conducted. Snowpack monitoring at the Bradley Meadow study plot and Bridger Bowl Ski Area Alpine study plot weather data collection ceased in early April.

Avalanche Cycle Capture

My strategy for this research utilized the presence or absence of "direct action" natural avalanches, produced by a single storm, as a measurement of starting zone stability against which a model of starting zone stability could be compared. The model combined extrapolated, pre-storm measurements of study plot stability with the amount of new loading produced by the storm to estimate starting zone stability. Under the

correct circumstances, data collection teams of three persons each were prepared to simultaneously deploy to all four Bridger Range study plots to conduct extensive stability tests (described below) immediately prior to a predicted avalanche cycle. I monitored imminent avalanche cycles through frequent visits to the Bradley Meadow study plot to perform formal snowpits and stability tests, assessing the vulnerability of the snowpack to a storm load, and by monitoring National Weather Service and Gallatin National Forest Avalanche Center short-term weather forecasts. If those routine stability tests performed at Bradley Meadow found snowpack conditions susceptible to a new snow load likely to be deposited by an approaching storm, then all four data collection teams would simultaneously deploy to conduct multi-pit study plot stability sampling trials (described in the following two sections) just prior to the approaching (presumably) critical storm. At least two members of each team were skilled and experienced field observers and all teams were fully equipped and trained for self-rescue in avalanche terrain. Team leaders (and some assistants) were briefed on the layout of their particular study plots and the data collection strategy (see below).

Precipitation and wind data obtained from Bridger Bowl Ski Area's Alpine study plot for the subsequent storm provided the remaining inputs, in addition to study plot stability data, for the starting zone stability model. Finally, field observations of natural avalanche occurrences, logged as quickly as visibility allowed during and after the storm, completed the 'capture' of an avalanche cycle in the study area.

One avalanche cycle (Storm #4, December 17-22, 1999) was successfully documented using these methods, mapping 24 separate avalanches and logging storm

data obtained from Bridger Bowl Ski Area's Alpine study plot. Stability data were collected from a single pit at the Bradley Meadow study plot on December 17, as Storm #4 commenced. This set of stability data, associated with the subsequent Storm #4 avalanche cycle observations, was used during the development of the GIS stability extrapolation model (described in the Stability Modeling section following) to verify model functions.

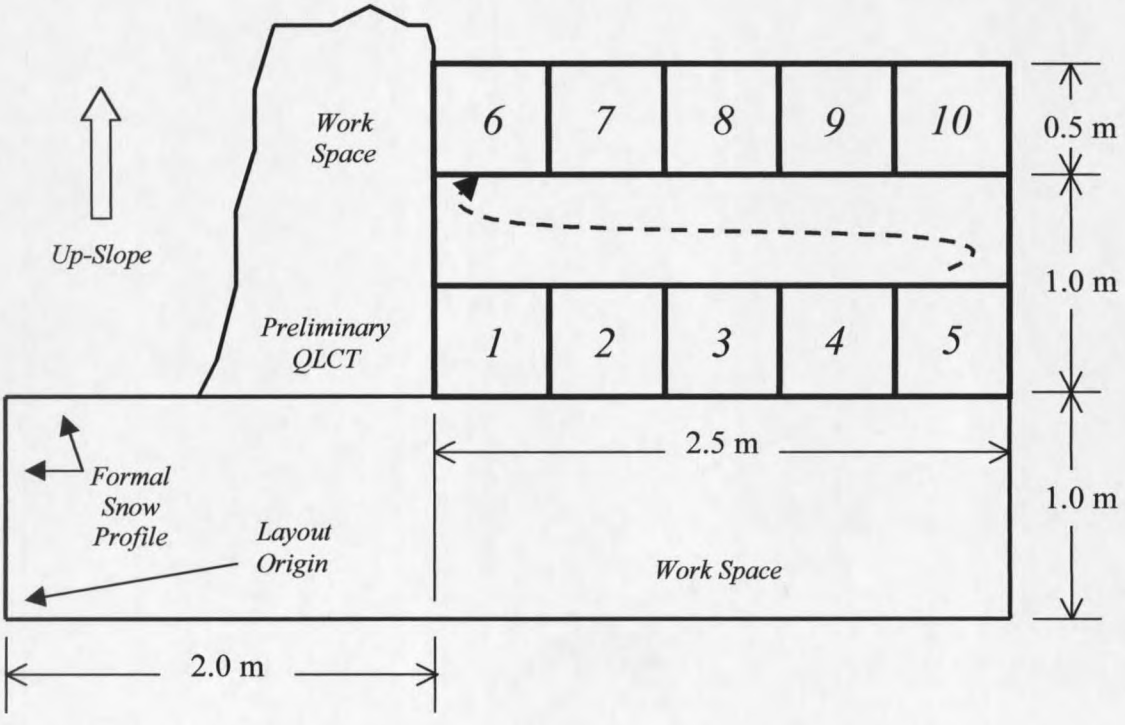
Quantified Loaded Column Stability Test

This study employed the quantified loaded column stability test (QLCT) to collect in-situ measurements of snowpack stability. The QLCT offers an objective, quantifiable method for measuring shear strength in a sloping snowpack. Final development of the stability test methodology and equipment, and comparative trials, during the winter of 1999/2000 culminated in the presentation of the method at the International Snow Science Workshop 2000 (Landry et al., 2001a) and publication of the method (Landry et al., 2001b). All data collection teams received hands-on field training in the execution of the loaded column test and related data collection techniques during the 1999/2000 season and/or early in the 2000/2001 season. The QLCT measures shear stress at the moment of shear fracture (or collapse) in an isolated column of snow. Results are calculated in units of newtons per square meter (N/m^2). Planar, "Q1"or "Q2" shear fracture results as well as column collapses (in depth hoar) were logged as valid test results (Birkeland and Johnson, 1999); very rough "Q3" shear results were rejected. Size effects associated with the two nominal QLCT sample areas (0.04 m^2 and 0.08 m^2), and

the shear stress produced by the snow in the isolated column itself, are calculated during the test procedure (Landry et al., 2001b). Those computations yield a size-corrected value for the total shear stress acting upon the weak layer at the moment of fracture using the notation τ_{∞} when applied to a single QLCT, $\bar{\tau}_{\infty}$ when the mean of all valid QLCTs in a single snowpit is computed, and $\bar{\tau}_{\infty(Plot)}$ when the mean of all tests in a 900m^2 stability sampling trial is computed. These three forms of τ_{∞} represent a measure of the 'strength' of the snowpack at those respective scales.

A standard snowpit layout was designed for this study (Figure 5). Ten QLCT were performed, per pit, in two rows of five test "cells" measuring 50 cm by 50 cm each, with the second row of cells one meter (on-slope distance) uphill of the face of the first row.

Figure 5: Standard Snowpit Layout. Sequence of Ten QLCT Cells Shown.

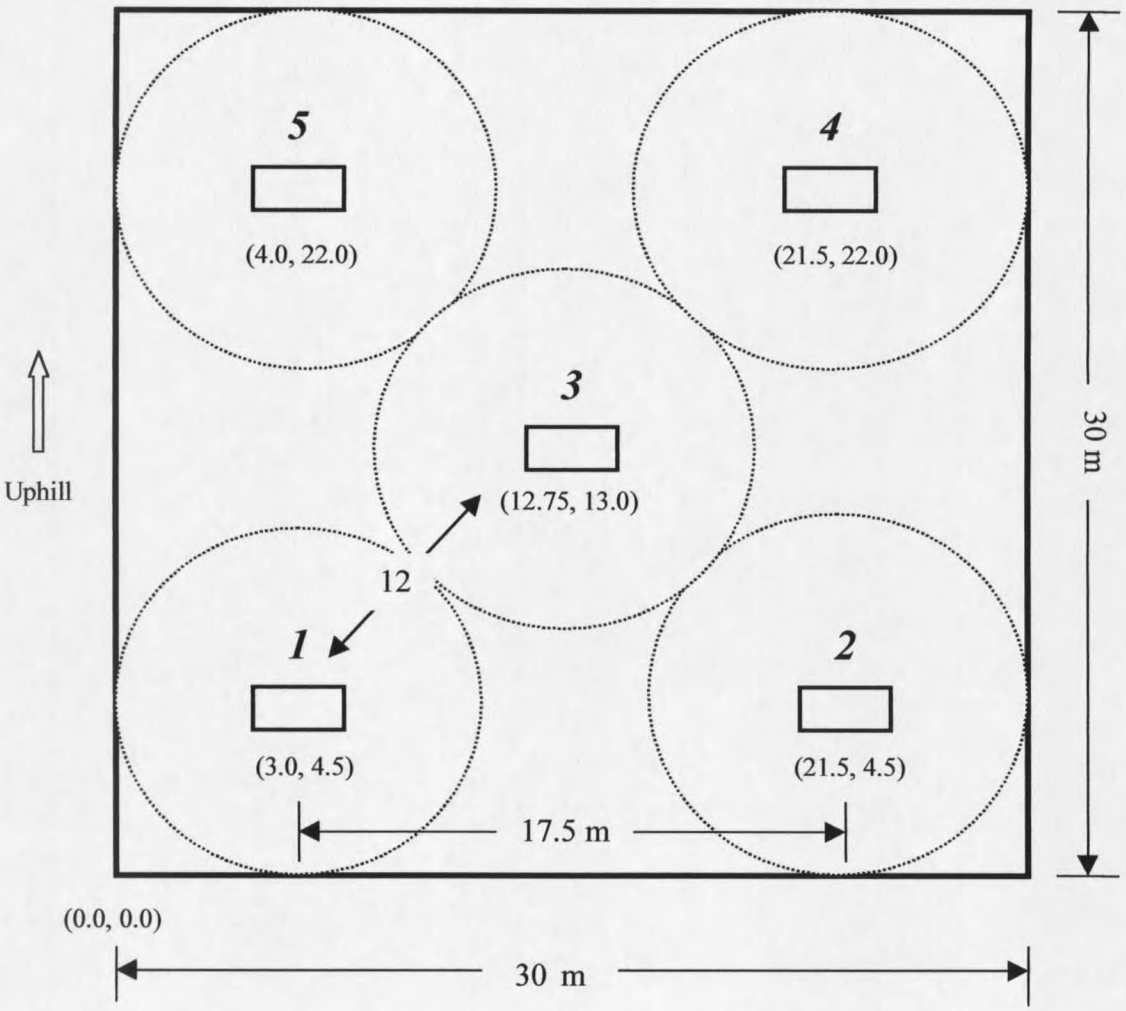


Observers performed one or more preliminary QLCT and collected formal snow profile data to the observer's left of the first row of five cells (Figure 5). Once the appropriate QLCT mode and load plate had been selected based on the preliminary QLCT and formal profile, one QLCT was performed in each of the ten test cells, moving from left to right in each row. Typically, the observer and one assistant worked in a pit.Given the sample-size of ten (nominally, sometimes fewer) QLCT per pit, the precision achieved in a given pit was occasionally evaluated based on the *t*-distribution (with n - 1 degrees of freedom, using a 95% confidence level) for the measured mean strength at shear, in N/m^2 (Landry et al., 2001b). The deduced margin of error, expressed in N/m^2, was converted to its snow-water (SWE) equivalent using the ratio of 118.9 N/m^2 per 25 mm SWE on a 38° slope.

Study Plot Stability Sampling Design

This study employed a systematic sampling scheme to measure snowpack stability at five sampling snowpits within a given study plot (Figure 6). Since a random sampling scheme could not be relied upon to obtain a spatially representative sample of the study plot, a 30m by 30m area at each of the four study area study plots was subdivided into five tangent, circular sub-areas of equal size. Then, a grid of ten QLCTs (Figure 5) was centered over the center-point of each circular sub-area. The 900 m^2 study plot layout origin (lower left) corner was located a known distance from a marked "monument" (tree or stake) in the field. Cartesian coordinate values from that origin point determined individual pit layout (lower left) corners (Figure 5).

Figure 6: Study Plot Stability Sampling Trials Layout, Pits #1 through #5. (Numbers in brackets are Cartesian coordinates for the 'layout origin' of a snowpit's layout (Figure 5), in meters from the lower-left (0, 0) 'origin' corner of the plot).



Data collection teams conducted the five snowpits by moving uphill in a sequence designed to avoid contamination of a down-slope pit prior to sampling. Observers dug the first of the five snowpits, shown as pit 1 in Figure 6, to the ground surface using the standard snowpit layout (Figure 5). First, they performed a formal snowpack profile documenting the entire snowpack's temperature profile, stratigraphy, layer hardnesses,

grain types and sizes, density profile, and other routine data. Potential weak layers were initially identified using the compression (tap) test. Then, "preliminary" QLCTs pinpointed the weakest weak layer in the stratigraphy and their results determined which QLCT mode, load plate, and force gauge to deploy for the ten subsequent logged QLCTs at pit 1.

The standard snowpit layout (Figure 5) at study plot pits 2-5 (Figure 6) was modified by shortening the width of the pit face to the left of the ten-cell QLCT grid from two meters to one meter. In each of the remaining four snowpits, compression tests and one or more preliminary QLCT were performed to the left of the ten-cell QLCT grid to confirm the subject weak layer and slab, and the appropriate QLCT setup. Slab density and thickness measurements were also collected at each pit. In the case of ambiguity about which weak layer was weakest, and most likely to respond to the QLCT, multiple weak layer/slab measurements were obtained and each weak layer was labeled on the formal snowpack profile performed at pit 1. Significant departures from the snowpack stratigraphy in pit 1 were noted as they were found in pits 2-5.

Study Plot Stability Sampling Sessions

Winter of 1999/2000

During the winter of 1999/2000 fieldwork focused on the final selection of four Bridger Range study plots, development and analysis of the quantified loaded column test (QLCT) method (Landry et al., 2001), field training of data collection team leaders and

assistants in the QLCT method, and field testing of the avalanche observation and storm data collection methods.

QLCT training for the data collection team training was completed by mid-season. However, due to below-average precipitation and an unusually stable and strong mid- and late-season snowpack, no full-blown 900 m^2 study plot stability-sampling trials were performed during the latter portion of the season.

Winters of 2000/2001 and 2001/2002

Data collection teams performed seven 900 m^2 stability-sampling study plot trials during the 2000/2001 season and four trials during the 2001/2002 season (Table 3). The first trial was conducted on 1/3/01 at a site near Bacon Rind Creek in the upper Gallatin River canyon of southwest Montana, the second, on 1/27/01, at a location uphill and left of the 900 m^2 Bradley Meadow study plot being reserved for simultaneous trials at all Bridger Range study plots, and the third trial was performed on 2/4/01 at Round Hill, near the Fidelity research station operated by Parks Canada near Rogers Pass, British Columbia. On February 28th, 2001, three data collection teams successfully completed stability sampling trials at the Bridger Range study area Baldy Mountain, Saddle Peak, and Bradley Meadow study plots. I instructed the teams to target, where present, a specific weak layer of large faceted grains 20-30 cm above the ground for the stability-sampling trials at each study plot. This layer had been monitored throughout the season at the Bradley Meadow study site since forming during December 2000. A set of ten QLCT conducted there on February 16th (Pit #14, Appendix H) showed that the layer was approaching strengths that would exceed the ability of the QLCT to measure.

Table 3: Study Plot Stability-Sampling Trials Summary. (Mean plot strength ($\bar{\tau}_{\infty(Plot)}$), mean plot stability ($S_{QCLT(Plot)}$), a unit-less ratio, and the type of weak layer tested are shown).

Study Plot	Date	Team Leader	$\bar{\tau}_{\infty(Plot)}$ (N/m^2)	Stability $S_{QLCT(Plot)}$	Weak Layer Type
Bacon Rind (BRSP)	1/3/01	Landry	533	2.08	Depth Hoar
Bradley Meadow (BMSP)	1/27/01	Deems	588	5.44	New Forms
Round Hill (RHSP)	2/4/01	Landry & Deems	851	2.62	Surface Hoar
Baldy Mountain (BLSP)	2/18/01	Landry	1,125	1.60	Depth Hoar
Saddle Peak (SPSP)	2/18/01	Birkeland	1,482	1.85	Depth Hoar
Bradley Meadow (BMSP)	2/18/01	Deems	1,657	1.30	Depth Hoar
Bradley Meadow (BMSP)	3/17/01	Landry	433	3.12	Near-Surface Facets
Middle Basin (MBP)	12/7/01	Landry	696	2.03	Facets and Depth Hoar
Lionhead Mountain (LMP)	1/9/02	Landry	375	2.53	Surface Hoar
Lionhead Mountain (LMP)	1/15/02	Landry	523	3.08	Surface Hoar
Lionhead Mountain (LMP)	1/26/02	Landry	1,084	2.43	Surface Hoar

Given the absence of other weak layers in the study area snowpack, and the ongoing drought conditions that seemed unlikely to yield any future avalanche cycle in association with this weak layer, we decided to proceed with the stability sampling trials at all four study plots even if no subsequent avalanche observations were likely. A fourth data collection team was also dispatched on 2/18/01 to the Fairy Lake study plot but, upon arrival, found the study plot heavily disturbed by snowmobile tracks and unsuitable for stability sampling. None-the-less, the team confirmed the presence of the expected

"target" weak layer of faceted grains at 30 cm above the ground. The final, seventh trial of the 2000/2001 season was conducted on 3/17/01 at Bradley Meadow, uphill and right of the 900 m^2 study plot utilized during the trials on 2/18/01.

Once again, due to an unusually stable snowpack throughout the Bridger Range during the early and middle portions of the 2001/2002 winter, data collection efforts were forced to find locations outside the Bridger Range study area (Table 3). The first 2001/2002 trial was conducted near Big Sky, Montana, on the ridge separating Beehive and Middle basins (Figure 3). All three remaining trials were conducted south of Lionhead Mountain, 15 km west of West Yellowstone, Montana (Figure 3).

These eleven trials provided measures of variation in stability at several spatial scales of resolution: from one QLCT test to the next (0.25 m^2), within a single snowpit (3.75 m^2), within a study plot (900 m^2), and between study plots (at distances ≥2 km). In addition, this set of trials spanned a wide variety of weak-layer types, a broad range in stability ($S_{QLCT(Plot)}$, Table 3), and nearly the full range of shear strength detectable by the QLCT method ($\bar{\tau}_{\infty(Plot)}$, Table 3).

Avalanche Starting Zones Atlas

Avalanche terrain is frequently documented in an avalanche "atlas" (McClung and Schaerer, 1993). I prepared an abridged avalanche reference "atlas" for the study area designating the selected starting zones and upper tracks of 159 specific avalanche "paths" on the slopes east of the N-S-trending spine of the Bridger Range, from south of Baldy Mountain north to Flathead Pass (Landry, 2000). Avalanche paths are typically

subdivided into at least three elements: 1) the starting zone, where the initial mass of the avalanche releases, 2) the runout zone, where the avalanche slows and stops, depositing debris, and 3) the track connecting the starting zone and the runout zone (Martinelli, 1974). For the purposes of this study, which focuses on the presence or absence in a starting zone of a fresh avalanche produced by storm precipitation and wind loading, only starting zones and upper tracks were mapped; maximum runout zones were not analyzed or mapped.

For this study, I defined avalanche path starting zones within the study area based on their maximum potential avalanche magnitude. A minimum starting zone size was defined using the force- and mass-based Canadian avalanche size classification scheme (CAA/NRCC, 1995). This study included only starting zones capable of Canadian Class 2 (capable of harming a person) or larger events (Table 4). Avalanche terrain within or nearby the Bridger Bowl ski area was also eliminated from the study area because of the

Table 4. Canadian Snow Avalanche Size Classification System. (CAA/NRCC, 1995)

Canadian Size Class	Avalanche Destructive Potential	Typical Mass (tons)	Typical Path Length
1	Relatively harmless to people	<10 t	10 m
2	Could bury, injure, or kill a person	10^2 t	100 m
3	Could bury and destroy a car, damage a truck, destroy a small building, or break a few trees	10^3 t	1,000 m
4	Could destroy a railway car, large truck, several buildings, or a forest area up to 4 hectares (~ 10 acres)	10^4 t	2,000 m
5	Largest snow avalanche known. Could destroy a village or a forest of 40 hectares (~100 acres)	10^5 t	3,000 m

intensive explosive avalanche hazard mitigation program conducted within the ski area and "out-of bounds" skier disturbances of the snowpack in areas immediately adjacent to the ski area.

Applying the Canadian Class 2 minimum-size threshold criterion required estimation of potential avalanche magnitude of small starting zones. For instance, a slab of 1.0 meters thickness and 200 kg/m^3 mean density would require a starting zone area of at least 500 m^2 and a slab releasing approximately 25 meters in width and 20 meters in fall-line height in order to qualify as a Canadian Class 2 event. Due to the scale of the study area, and the large number of small avalanche paths, detailed field measurements of path lengths or starting zone areas were impractical and not conducted in the Bridger Range. However, by comparing 1:24,000 USGS topographic avalanche path maps of starting zones in Colorado, which I analyzed and classified according to the Canadian method, with 1:24,000 USGS maps of the Bridger Range, I was able to determine which Bridger Range starting zones met the minimum Canadian Class 2 threshold and to estimate their maximum potential event Class.

Estimation of the maximum spatial extent of a starting zone, and of the magnitude of maximum events, presumes that a long return-period, dry-slab avalanche of at least 1 meter thickness releases in the starting zone (Mears, 1996). Such events typically involve a deep underlying snowpack spanning minor terrain or vegetation barriers and connecting what are more frequently observed as independently behaving "pockets" within the long return-period event starting zone. I mapped the selected Bridger Range

long return-period starting zones based on my estimation of the maximum possible extent of 1-meter thick dry-slab avalanche fracture lines.

The techniques used for verifying the starting zones meeting the Canadian Class 2 threshold included:

1. visual observations and photography of field evidence of avalanche paths (including slope steepness, terrain, surface roughness, and vegetation patterns) from some starting zones, runouts, and tracks themselves, and from the valley floor below
2. preliminary starting zone and track mapping on the Saddle Peak, Sacagawea Peak, and Flathead Pass U.S.G.S. 1:24,000 scale 7.5' quadrangles, sketching estimated starting zone boundaries and making map measurements of starting zone and path (estimated length) dimensions for comparison to classified Colorado paths and Canadian size criteria
3. consultation from experienced Bridger Range avalanche observer Ron Johnson of the Gallatin National Forest Avalanche Center (Johnson, 2000 pers. comm.)
4. final mapping of the avalanche starting zones and tracks on the Saddle Peak, Sacagawea Peak, and Flathead Pass U.S.G.S. 1:24,000 scale 7.5' quadrangles

To facilitate field observation, I labeled individual starting zones according to their location north and south of USGS named geographic landmarks in the Bridger Range. For example, the first paths located to the north and south of Baldy Mountain were designated "BM – 1n" (first starting zone north of Baldy Mountain) and "BM – 1s" (first

starting zone south of Baldy Mountain), avoiding replication of the prefix initials. In areas without USGS place-names, I adopted commonly used local names such as "Wolverine Basin" as reference points, or a stream drainage was used to designate a segment of the Range (e.g., "South Fork Flathead Creek" and "Mill [Creek] Peak").

Color photographs of 15 segments of the Range taken from those observation points points along Montana State Highway 86 or the Flathead Pass Road showed early-season snowcover (and some early season avalanches), Those color photographs of the starting zones, and a tabular list and map of the starting zones shown in each segment, were used to prepare the atlas reference pages for each segment of the Range. Arrows connect the tabular list of the starting zones to the photograph and the map. The detailed path measurements (starting zone, track, runout zone) and avalanche histories typically presented in a comprehensive avalanche atlas were beyond the scope of this study.

Avalanche Observations

All but 23 of the 159 selected Bridger Range study area starting zones can be viewed with binoculars or a field scope from Montana State Highway 86 or the Flathead Pass Road. Copies of each Bridger Range Path Atlas reference page were used to map the spatial magnitude of actual natural avalanche occurrences. Field observations made on the ground were recorded on log sheets listing each path and noting the estimated size of the avalanche and other observations, such as the estimated height of the crown fracture. In addition to noting the size of the event by the Canadian classification scheme, the observer estimated the size of the event using the American size scale (Perla and

Martinelli, 1976). The American size-classification system describes the *relative* size of an avalanche, compared to the maximum potential avalanche in a given path, using an ordinal scale from 1 to 5. For instance, according to the American scale, a "medium" or average event in any given path is a Class 3 event, regardless of whether the path is 200 meters in length or 1,000 meters in length. Similarly, an American Class 4 or 5 avalanche which reaches or exceeds the maximum historic runout distance of the path may be the result of an avalanche of as little as 10^2 tons mass or as much as 10^5 tons, depending on the particular path being observed. Utilizing both the Canadian and American size classification systems, and sketching the avalanche on a topographic map, assured thorough documentation of an avalanche. Whenever possible, photographs of recent avalanches were taken to supplement other field observations.

GIS "BASEDAT" Preparation

A geographic model of the study area was required to model starting zone stability. Accordingly, I developed a geographic information system (GIS) from a digital elevation model (DEM) of the Bridger Range study area (Aspinall, 2000 pers. comm.) using ArcView 3.2 software (ESRI, 1999) and its attendant modules Spatial Analyst and 3-D Analyst. DEMs provide a grid of geo-referenced points (x, y), where x represents longitude and y represents latitude, and each point's elevation value (z). GIS software can depict a DEM as a "regular" grid of cells. Terrain attributes such as contours, slope angle (Ψ), and slope aspect (xyz) can be derived from DEM data using spatial algorithms within the GIS software. A "triangulated irregular net" (TIN) can also be derived from a

DEM and draped over the grid. Both grid and TIN formats were utilized in this project, as described below.

The United States Geological Survey has prepared DEMs of mountain areas in the U.S., including the Bridger Range, with a grid cell spacing of 30 meters; elevation values are given for the center of each 30 m square cell. USGS has also prepared DEMs for some mountain areas at a grid spacing of 10 m, and even 1 m. Since these are not universally available, and are very expensive to produce, the standard USGS Level II 30m DEM has been utilized for this research in the Bridger Range. USGS states that elevation (*z*) RMS (root mean square) error for the Level II 30 m DEM is ±7 m.

DEM accuracy, in GIS-derived slope angle and slope aspect classifications, was evaluated by Ouren and Landry (2000) over an area of 400 km^2 in northern Yellowstone National Park using ArcView Ver. 3.2 and a USGS Level II 10 m DEM. ArcView 3.2 uses the Horn method (Jones, 1998) for deriving slope angle from a DEM grid. Increasing the cell size (area) of a DEM had the effect of reducing slope angles in the mountainous topography examined by the study. This effect was non-linear and produced the largest proportion of reduction in the steepest slopes. The proportion of slopes represented as ≥30° was reduced from 14.6% of all cells in the 10m DEM to 12.7% in the USGS Level II 30 m DEM of the same area, a reduction in cells ≥30° of some 13%. Ouren and Landry found that increasing or decreasing the cell size of a DEM had negligible effects on the classification of slope aspects.

A triangular irregular network (TIN) was derived from the study area DEM aggregating the "regular" (square) DEM grid cells into "irregular" (triangular) groups

linked by terrain attributes such as aspect and slope angle. The creation of a TIN from a DEM in ArcView 3.2 requires the specification of a "*z tolerance*" variable, the maximum variation in elevation allowed between cells which otherwise share similar slope angle and aspect attributes. Using small *z tolerance* values results in the creation of an increased number of smaller triangular cells derived from relatively few grid cells, while a large *z tolerance* value produces fewer, larger triangular cells aggregating more grid cells. An "optimal" TIN, given the underlying resolution of the DEM, is a compromise balancing the redundancy of too many small TIN cells, dissecting terrain into identical and unnecessarily precise elements, against the loss of detail resulting from too few large TIN cells that over-aggregate what an experienced avalanche forecaster could expect to be uniquely behaving starting zone terrain elements.

An optimal *z tolerance* value was selected by comparing resultant TINs to 1:24,000 USGS topographic maps and using direct observation and knowledge of the study area terrain. In the Bridger Range study area the TIN *z tolerance* was set at 25 m. The resulting TIN most nearly matched how I, as an experienced avalanche forecaster, would subdivide the study area avalanche starting zones into forecast-able elements, or terrain "units" likely to behave in concert during "average" conditions.

Once generated, the optimal TIN was converted to an ArcView shapefile wherein each TIN was given a unique ID number. (The slope and aspect attributes of the originating DEM grid cells were also preserved.) Then, the TIN shapefile was used to classify each of the DEM grid cells as an element of the particular TIN cell (or TINs)

which overlaid it. Cells at TIN nodes, and under the sides of the TIN's legs, were classified as members of all the adjoining TINs.

Study plot locations at the study areas were plotted in GIS "point themes" using coordinates obtained with GPS units with error of ±15 m. The presence or absence of trees in the study area's DEM grid cells was evaluated using U.S. Forest Service digital vegetation cover data for the Bridger Range obtained from the Gallatin National Forest GIS office (USFS, 2000). These data were derived by the USFS from ortho-photos at a scale of 1:15,000 and then re-plotted at 1:24,000 scale as ArcInfo polygons of tree species and maturity classifications. I aggregated those ArcInfo polygons into ArcView 3.2 shape files and compared them to USGS 1:24,000 scale 'quad' mapping of vegetation, and to field observation of the tree-cover at specific sites, modifying the selection of USFS vegetation classifications until a "best fit" was achieved. An ArcView "mask" grid theme was then prepared, identifying DEM cells with trees of sufficient density and height (as coded in the USFS data) to preclude avalanche initiation based on my experience regarding avalanche formation on tree-covered slopes.

In order to model the influence of snow drift on starting zone stability, source and deposition areas had to be identified within the GIS. First, the DEM cells constituting the ridge crest in the study area were located and used to produce a *Ridge* point theme. In the Bridger Range study area this was facilitated by the north-south orientation of the Range, and its single spine. Next, windward fetch and leeward deposition cells were identified by modifying Fohn's (1980) findings for the horizontal extent of blowing snow processes about a ridge-crest. In the Bridger Range study area, prevailing winds at ridge crest are

known to be westerly (Gauer, personal communication). Given that, and Gauer's recommendations, windward fetch cells were classified *Wind* by selecting all cells due west of a ridge-crest cell that were ≤200 m below the ridge-crest cell. Likewise, leeward deposition cells were classified *Lee* by selecting all cells due east of a ridge crest cell that were ≤ 100 m below the ridge-crest cell. A Bridger Range point theme containing those *Wind* (ward) and *Lee* (ward) cells was created.

All identified avalanche path starting zones (and upper tracks) were plotted as polygons in an ArcView shapefile theme for each study area, using DEM derived contour lines and digital raster graphic themes as aids to geo-reference their location on the DEM grids. The abridged avalanche starting zone atlas was used as the source data for the Bridger Range study area. Next, the avalanche starting zone themes were used to overlay the TIN shapefiles in order to identify the particular TINs constituting (in whole or in part) a particular starting zone. Individual TIN cells were classified as members of a given avalanche path starting zone, or of no (known) path.

Finally, a single "BASEDAT" theme was constructed for the study area by joining each of the GIS elements described above into a single theme containing all of the spatial information required to model starting zone stability (Table 5).

Table 5. GIS "BASEDAT" Theme Variables.

BASEDAT Attributes	Description	Data Class	Source
x	East/west location	IV	GIS derived from 30 m DEM
y	North/south location	IV	GIS derived from 30 m DEM
z	Elevation	IV	GIS derived from 30 m DEM
xyz	Aspect	IV	GIS derived from 30 m DEM
ψ	Slope angle	IV	GIS derived from 30 m DEM
Ridge	Bridger Range crest cell	IV	GIS derived from 30 m DEM
Wind	Blowing snow fetch cell	IV	GIS derived (assumes winds 270°)
Lee	Blowing snow deposition cell	IV	GIS derived (assumes winds 270°)
Tin	Triangulated irregular net	IV	GIS derived from 30 m DEM
Path	Avalanche path shapes	IV	Empirically mapped at 1:24,000
SP	Study plot points	IV	Physically located with GPS

Stability Modeling

Using Class IV (terrain) geographic inputs of the BASEDAT GIS, snow water equivalent (SWE) distribution and starting zone stability are modeled from extrapolated Class I and II data using spatial and physical functions (Table 6).

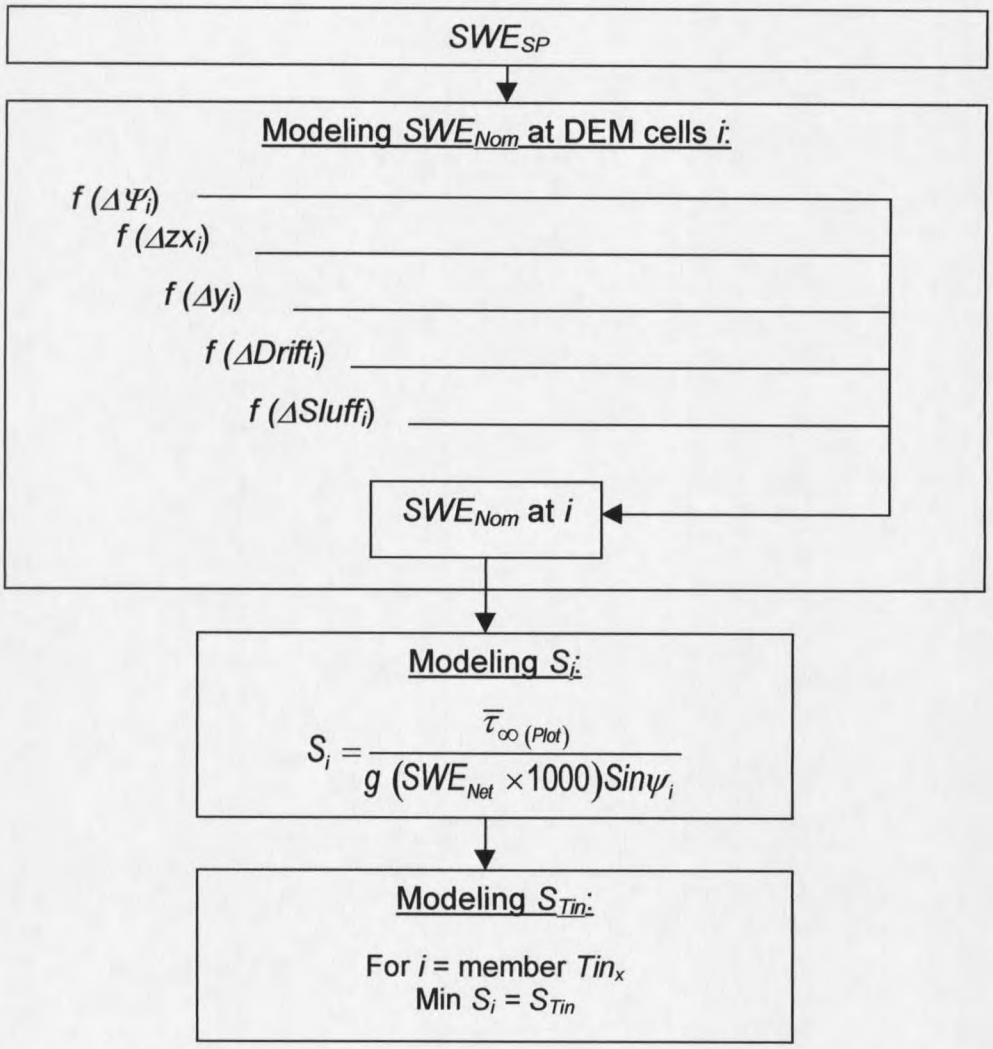
In general terms, SWE_{Plot} measured at study plots was successively modeled in the study area avalanche starting zones in five additive iterations by applying three geographic functions ($\Delta\Psi$, Δzx, and Δy) and two physical functions ($\Delta Drift$, $\Delta Sluff$) to the BASEDAT 30m DEM grid cells, as shown schematically in Figure 7. The stability ratio S_i was calculated for each 30m DEM grid cell. Then, a stability ratio S_{Tin} was determined for each starting zone TIN cell by selecting the lowest DEM grid cell value, S_i, within a given TIN. The lowest (least stable) grid cell stability value (S_i) contained within a starting zone TIN was considered a reasonable proxy for the

development of a stability "deficit zone" and that cell's value was used to characterize stability within that entire TIN cell, as S_{Tin}.

Table 6. Stability Model Data and Variables.

Model Variables	Description	Data Class	Data Source/Model Function
SWE_{Plot}	Snow water equivalent of slab at study plot	Class II	Measured at study plots
SWE_{Nom}	Nominal snow water equivalent at grid cell *i*, by location	Modeled Class II	Effect on SWE_{Plot} of $\Delta\Psi_i$, Δzx, Δy, $\Delta Drift$, *and* $\Delta Sluff$ functions at DEM cell *i*
SWE_{Test}	Water equivalent of study plot mean shear strength at shear fracture	Class I	$\overline{\tau}_{\infty(Plot)}$ measured by QLCT at study plots, converted to its water equivalent
S_{Plot}	Stability ratio S_{QLCT} at study plot	Class I	$\frac{g \sin \psi_{SP} SWE_{Test}}{g \sin \psi_{SP} SWE_{SP}}$
S_i	Stability ratio S_{QLCT} at grid cell *i*	Modeled Class I	$\frac{g \sin \psi_{SP} SWE_{Test}}{g \sin \psi_i SWE_{Nom}}$
S_{Tin}	Stability ratio S_{QLCT} at starting zone TIN using lowest S_i value among cells *i* within TIN	Modeled Class I	$\frac{g \sin \psi_{SP} SWE_{Test}}{\mathrm{Min}(g \sin \psi_i SWE_{nom})}$

Figure 7: Extrapolated Study Plot Stability Model.



When a grid cell *i* lying on the boundary of two TIN cells contained the lowest value S_i in one or both TIN cells, that value was used for S_{Tin} in the respective TIN cells. Thereafter, TIN cells formed the basis for the modeling of patterns of starting zone stability and, later, for spatial analysis of patterns of actual avalanching compared to the patterns of stability predicted by the model. A value of $S_{Tin} \leq 1.0$ was interpreted as a TIN that had avalanched. Following the extrapolation of pre-storm study plot stability

measurements to the starting zones, the model used study plot measurements of subsequent storm precipitation to re-calculate S_{Tin}. Maps of TINs that achieved the critical value $S_{Tin} \leq 1.0$ were compared to maps of actual observed avalanches plotted in the BASEDAT starting zone map.

The sequence of the model's five successive iterations begins with the "spatial" functions and the best-understood spatial effect, change in slope angle ($\Delta\Psi$). Slope angle is a significant term in the equation for calculating the shear stress (τ_{Slab}) produced by a snow slab overlying weak layer on a slope:

$$\tau_{Slab} = \rho g h Sin\psi \qquad (3)$$

where ρ is snow density (kg/m^3), g is acceleration (9.8), and h is slab thickness (m) measured normal to the slope. The second iteration of the model applies another well-documented spatial effect on *SWE* in mountain ranges, Δzx, the combined effect of change in elevation and "easting" (distance in the downwind direction from ridge crest). Then, a "place holder" was created for a third iteration in which a function Δy, representing the effects on *SWE* of change in location along the long axis of a mountain range, could be applied if such an effect could be described for the study area. These three functions completed the objective application of spatial controls on SWE_{Nom}. With each modification of SWE_{Nom} at a grid cell i, the stability ratios S_i and S_{Tin} were recalculated.

Next, the "process" functions *ΔDrift* and *ΔSluff* were applied in order to modify SWE_{Nom} for each grid cell i and then recalculate S_i and S_{Tin}. The function for *ΔDrift* is

based on Föhn (1980), as previously discussed. The function *ΔSluff* utilizes a hydrologic algorithm for flow accumulation contained in ArcView 3.2. The model requires setting the minimum slope angle of cells *i* at which snow sluffing begins (default = 60°) and the maximum slope angle for cells *i* at which sluffs will stop (default = 35°), depositing the accumulated quantity SWE_{Nom} which moved downslope from the grid cells "upstream".

Thus, during the first model iteration, only the BASEDAT slope angle ψ_i at each 30m DEM cell was used, along with the SWE_{Plot} and $\overline{\tau}_{\infty(Plot)}$ values measured at a study plot, to recalculate a stability ratio S_i at each grid cell. No other spatial functions or physical functions were applied to SWE_{Plot} during this first run and the stability ratio S_{Tin} differed from S_{Plot} only by the difference in slope angle.

Next, the spatial function Δzx was applied to the SWE_{Nom} values at each grid cell obtained from the $\Delta\Psi$ iteration. That is, the application of the next spatial function in the sequence applied to the cumulative effects on SWE_{Nom} of all preceding spatial functions to produce a new set of S_i and S_{Tin} values. In the Bridger Range study area, Pipp and Locke's (1998) function for Δz was adapted to BASEDAT inputs and model variables, as follows:

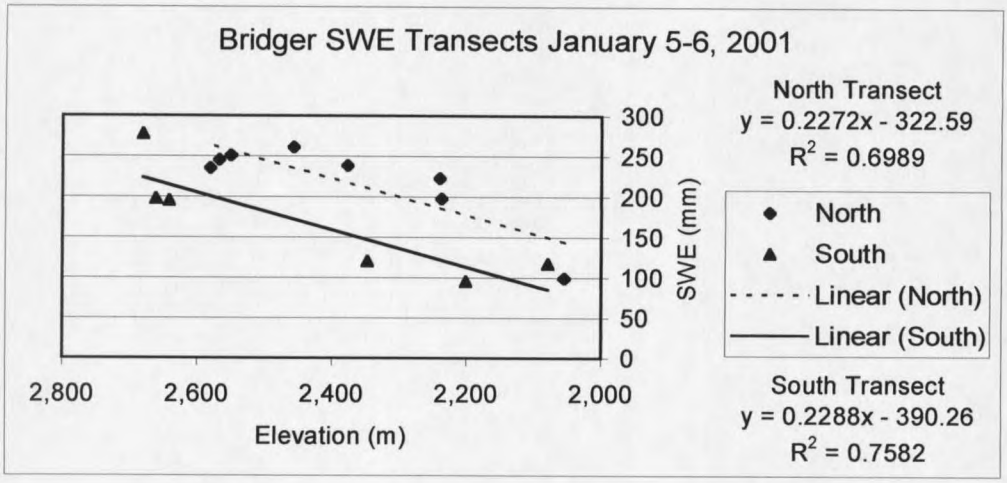
$$f_{\Delta zx(Pipp)}(SWE_{Nom(i)}) = SWE_{Plot}\left[\frac{-887+628\left(\frac{z_i}{1000}\right)}{-887+628\left(\frac{z_{SP}}{1000}\right)}\right] \qquad (4)$$

However, the Pipp and Locke (1998) study area was biased toward lower elevation areas at distances from the ridge crest that reduced the influence of the orographic precipitation enhancement produced by the ridge crest. For that reason, in order to better model the effects of Δzx within the elevational and easting bounds of the avalanche terrain on the east-facing side of the Bridger Range, measurements of total snowpack SWE were made during the 2000/2001 winter along two east/west transects located at the Bridger Bowl Ski Area north and south boundaries. The north transect was at approximately 45° 49' 45"N and the south at approximately 45° 48' 24" N. The SWE measurements were made to the ground surface, and normal to the slope, at each point on the transect using a "Snowmetrics" brand sampling tube calibrated directly to mm SWE. The data obtained from these transects are included (Appendix A). The results of the SWE analysis of these transects are presented here, rather than under Results, since they formed the basis for a second, alternative Δzx model function (Figure 7).

The three points nearest the ridge in each transect were spaced approximately 30m (measured horizontally) apart in an attempt to reveal a wind drift effect on SWE supplementing the elevation effect being investigated and, also, to match the 30m DEM grid size. The first SWE measurement was located 30m (horizontally) from the ridge crest. No measurement of SWE was made on the ridge crest proper.

The north SWE transect did, in fact, show an increase in SWE immediately downslope of the ridge extending east (to the right in Figure 8) to the fourth data point located some 106 meters (horizontally) from the ridge. This result conformed to field observations of cornice formation at the ridge-crest. The south SWE transect, however,

Figure 8: Bridger Range SWE Transects, January 2001.



showed the opposite pattern, with a rapid reduction of SWE moving east from the ridge, despite similar observations of substantial cornicing at ridge-crest and a fetch area on the windward side of the ridge-crest.

Therefore, the data were inclusive regarding a predictable, cumulative leeward enhancement by drifting snow of snowpack SWE at the sample points immediately east of the ridge-crest. However, both the complete north and south SWE transects clearly show an elevation/easting effect on SWE distribution similar to that found by Pipp and Locke (1998), and others. An alternative to the Pipp Δzx function called the Landry Δzx function was derived from the aggregation of the two transects, which had very similar slopes and differed only in their y-intercept values, as follows:

$$f_{\Delta zx(Landry)}(SWE_{Nom(i)}) = SWE_{Plot}\left[\frac{-307+209\left(\frac{z_i}{1000}\right)}{-307+209\left(\frac{z_{SP}}{1000}\right)}\right] \qquad (5)$$

Next, a place was held in the model for a final spatial effect function (Δy) to be applied to the cumulative effects of $\Delta\Psi$ and Δzx on SWE_{Nom}. However, no systematic evidence regarding Δy effects in the Bridger Range were obtained from simultaneous study plot measurements of total SWE and a value of $\Delta y = 1.0$, for no effect, was utilized.

Finally, two physical processes were modeled – snow drifting by wind, and snow sluffing during storms from over-steep terrain onto lower-angle terrain. The movement of snow by wind, during storms, from windward slopes west of the Bridger crest onto leeward slopes, was incorporated into the model as the *ΔDrift* function. Föhn's (1980) comparatively simple, two-dimensional physical wind drift model (Equation 10) was applied, at the 30m DEM cells designated *Wind* in BASEDAT, to the value SWE_{Nom} previously produced by the application of the spatial effect functions Δzx and Δy, as follows:

$$f_{\Delta Drift(Fohn)}[SWE_{Nom}(i_{Lee})] = SWE_{Nom}(i_{Lee}) + \frac{\max\left(k\bar{u}^3 \left\{ m/d \right\}, \left[\frac{\sum SWE_{Nom}(i_{Wind(y)})}{2} \right] \right)}{Count(i_{Lee(y)})} \quad (6)$$

where SWE_{Nom} for each grid cell i designated "Lee" in BASEDAT equaled the underlying value SWE_{Nom} at that cell *plus* one-half of the total SWE_{Nom} in all the *Wind* fetch cells having the same y (latitude) value and not covered by trees (as represented in BASEDAT by the value for *Veg*), multiplied by the product of a constant k and the 24-hour wind speed at ridge-crest, with $k = 8\times10^{-5} s^3 d^{-1} m^{-2}$, divided by the number of *Lee*

cells with the same y value. Wind direction was assumed to be 270° (due west). Mean 24-hour hour wind speed ($\overline{u}$) data was obtained from Bridger Bowl ridge crest study plot and converted to units of meters-per-second before model input.

The *ΔSluff* function was applied last, following the drift function, and caused all accumulated storm SWE in grid cells i with a slope angle of 60° or more to move downslope, on the steepest vector out of a cell to the adjoining cell and continue until reaching the first cell i with a slope angle of 35° or less. Hydrological flow modeling functions contained in ArcView 3.2 were adapted for this element of the stability model.

In addition, each forecaster also made an inductive estimate of the amount of new SWE_{Plot}, based upon the results of the first set of ten QLCT performed at the study plot, that would initiate avalanching in the local starting zones, by aspect. These estimates were entered as a special case by the model for eventual comparison to the model's estimation of the critical increment of SWE_{Nom} that would bring the value for S_{Tin} to 1.0. Qualitative principles regarding the spatial effects on stability caused by changes in aspect and elevation, and the avalanche forecasting experience of the researcher and his team leaders, were used to make these determinations.

Each iterative model run was stored as a unique case in a database containing values of S_{Tin} for each study area TIN. Maps of actual natural avalanches that were the result of storm loading immediately subsequent to study plot data collection were also stored as stability cases with binary S_{Tin} values (1 = Avalanche, 0 = No avalanche) for each TIN.

The influences on weak layers within the snowpack of terrain substrate and curvature, micro-scale wind action, free water presence in the snowpack, and temporal changes in snowpack stability require exceedingly complex physical models, as well as higher resolution data inputs, and are therefore beyond the scope of this research and were not incorporated in this study's model.

Storm Weather Data Collection

Storm weather data were obtained in twenty-four hour increments, from 9 AM to 9 AM, from the Bridger Bowl ski area Ski Patrol's records. Daily totals of storm SWE are measured with a Balfour tipping bucket gauge at the ski area's Alpine study plot at an elevation of 2,255 meters. Daily average wind speed and direction are measured and logged electronically at the ski area's Ridge study plot at an elevation of 2,590 m.

Data Analysis

Throughout these analyses the term 'variation' refers to absolute differences between measurements or observations (e.g., standard deviation) while the term 'variability' refers to the relative rate of variation among sets of observations or measurements, as given by their coefficients of variation.

Inter-Study-Plot Variability

Coefficients of Variation. The size-corrected QLCT "strength" (maximum shear stress at snow fracture), τ_{∞}, was calculated in units of N/m^2 (Landry et al., 2001b) for each valid QLCT at each of the five sampling snowpits within the 900 m^2 study plot.

Given a minimum of at least three valid results at a pit, a coefficient of variation of the mean, size-corrected shear strength of the pit, $CV\ \overline{\tau}_{\infty}$, was calculated to provide an index of variability in strength within individual pits. The value of $CV\overline{\tau}_{\infty}$ represents the relative magnitude of the sample standard deviation s in shear strength as a proportion (percentage) of the mean strength $\overline{\tau}_{\infty}$ of a given pit, as follows:

$$CV\overline{\tau}_{\infty} = s/\overline{\tau}_{\infty} \tag{7}$$

Consistent QLCT results in a pit resulted in a low standard deviation of strength and commensurately low variability in strength, $CV\overline{\tau}_{\infty}$, for the pit. A few QLCT results that varied substantially from the balance of the tests in a pit increased the standard deviation of strength and the variability index of strength, $CV\overline{\tau}_{\infty}$, regardless of the actual magnitude of the standard deviation. Therefore, an individual pit could exhibit low values of strength and a low-magnitude standard deviation of strength for the QLCT results (in actual N/m^2), but high variability when some QLCT results varied substantially from others. Similarly, pits exhibiting high strength but relatively consistent results (low variation among higher-magnitude strengths) could exhibit low variability.

A coefficient of variation of strength for each plot, $CV\ \overline{\tau}_{\infty(Plot)}$, was also calculated, pooling all valid QLCT values τ_{∞} at a plot and calculating their sample standard deviation s, as follows:

$$CV\overline{\tau}_{\infty Plot} = s_{Plot}/\overline{\tau}_{\infty(Plot)} \tag{8}$$

Z Score of Strength. A Z score was calculated for each valid QLCT at a plot, expressing each individual QLCT strength result τ_{∞} in terms of its departure, in sample standard deviations s, from the mean plot strength $\overline{\tau}_{\infty(Plot)}$ (all valid QLCT results aggregated), as follows:

$$Z(\tau_{\infty}) = \frac{\tau_{\infty} - \overline{\tau}_{\infty(Plot)}}{s} \tag{9}$$

These Z scores are presented in oblique-view charts of the respective study plots. In the charts, the plot mean strength $\overline{\tau}_{\infty(Plot)}$ "surface" is represented by the Z-score of 0 (zero) and bars show the scores above- and below-mean, in units of standard deviations, for individual QLCTs. The oblique-view chart layout replicates the 900 m^2 stability sampling trials pit layout (Figure 6), with (nominally) fifty test QLCT cells arrayed as clusters of ten cells (Figure 5) in each of the five stability-sampling pits in a plot.

Stability Ratio S_{QLCT}. Measurements were made at each stability sampling trial pit, approximately one meter left of the front row of QLCT, of the thickness of the slab overlying a subject weak layer and its water content, and of the slope angle. The shear stress τ_{Slab} produced by the in-situ snow lying over the subject weak layer was calculated (Landry et al., 2001b) and the stability ratio S_{QLCT}, the ratio of strength to stress, at a given pit, was computed as follows (the calculation of plot mean stability averaged all valid individual measurements of strength in the numerator and all stress measurements in the denominator):

$$S_{QLCT} = \overline{\tau}_{\infty} / \tau_{Slab} \tag{10}$$

Z Score of Stability S_{QLCT}. As with strength, a Z score of stability S_{QLCT} was calculated for each individual valid QLCT at a plot (Landry et al., 2001b) using the single measurement of stress collected for each pit in the denominator of the ratio $\tau_\infty / \tau_{Slab}$. The Z score of stability expresses each individual QLCT stability result S_{QLCT} in terms of its departure, in sample standard deviations s, from the mean plot stability $S_{QLCT(Plot)}$ (all valid S_{QLCT} results pooled), as follows:

$$Z\left(S_{QLCT}\right) = \frac{S_{QLCT} - \overline{S}_{QLCT(Plot)}}{s} \qquad (11)$$

These Z scores are also presented in oblique-view charts of the respective study plots, as described above for Z scores of strength.

Two-Sample t-Tests. For each pit in a given plot, adapted two-sample t-test analyses were used to evaluate the hypotheses of "no difference" between a single pit's mean strength $\overline{\tau}_\infty$ and its plot's mean strength $\overline{\tau}_{\infty(Plot)}$, and between a single pit's stability S_{QLCT} and its plot's mean stability $S_{QLCT(Plot)}$. This adaptation of the two-sample t-test analysis evaluates whether the mean strength $\overline{\tau}_\infty$ and stability S_{QLCT} in any single snowpit within a carefully selected study plot will reliably represent mean plot strength $\overline{\tau}_{\infty(Plot)}$ and mean plot stability $S_{QLCT(Plot)}$ throughout the study plot (including the single pit) and, therefore, whether that study plot represents a single "stability population". Thus, in this application of the two-sample t-test, the assumption that samples are drawn

from two separate populations has been relaxed. This is accomplished by pooling a single snowpit with the remaining four snowpits to obtain mean study plot stability. If a particularly strong/weak or stable/unstable pit were not pooled with the remaining four pits, study plot stability variability would be underestimated and made to appear more consistent than was actually measured.

In their measurements of snow resistance, a proxy for snow strength, Birkeland et al. (1995) evaluated and eliminated the potential for spatial autocorrelation among snow resistance measurements by re-sampling their 1-meter test-grid data at a spacing of 5 meters. In this study, the shortest distance between stability measurement sites - snowpits in the 900 m^2 study plot sampling scheme - is approximately 12 meters, more than doubling Birkeland's spacing between sample locations.

Before the *t*-test analyses I first conducted *F*-tests to evaluate any difference in variances between the pit mean strength $\bar{\tau}_\infty$ and pit stability S_{QLCT} and their study plot counterparts. Then, two-sample *t*-tests were conducted, comparing single-pit data to the pooled data from all pits at a given study plot. The *t*-test evaluates a null hypothesis of "no difference" between sample means for small samples ($n < 30$). Based on *F*-test results, the appropriate two-sample *t*-test was applied, using the "pooled variance" form of the two-sampled *t*-test when the *F*-test failed to reject the null hypothesis of no difference in variability, or the "separate variance" form of the two-sample *t*-test when the *F*-test rejected the null hypothesis.

In the context of this study of avalanche forecasting methods, probabilities p from the two-tailed, two-sample t-tests were compared to a significance level of $\alpha = 0.05$, the highest acceptable threshold for a Type I error, but all p values are reported.

Appendices D and E present complete F-test and t-test analyses of strength for all 2000/2001 and 2001/2002 trials, respectively, and Appendices F and G present complete F-test and t-test analyses of stability for all 2000/2001 and 2001/2002 trials, respectively.

Intra-Study-Plot Stability Variability

This comparison of study plots tests the hypothesis that the Bridger Range is a single "avalanche region" (Birkeland, 1997) that may, on a given day, contain multiple study plot locations exhibiting the same stability. In order to test for difference in mean strength and stability between Bridger Range 900 m^2 study plots sampled on 2/18/01 I first conducted an F-test of pooled results at each plot to evaluate whether pairs of plots exhibited a significant difference in variance for strength and stability. Then, two-sample t-tests were conducted, comparing the mean strength $\overline{\tau}_{\infty(Plot)}$ and mean stability $S_{QLCT(Plot)}$ at one study plot to $\overline{\tau}_{\infty(Plot)}$ and $S_{QLCT(Plot)}$ at another study plot. The t-test evaluates a null hypothesis of "no difference" between sample means for small samples ($n < 30$). Based on F-test results, the appropriate two-sample t-test was applied, using the "pooled variance" form of the two-sampled t-test when the F-test indicated no difference in variances or the "separate variance" form of the two-sampled t-test when the F-test rejected the hypothesis of no difference in variances. The two-sample t-test assumes that samples are drawn from separate populations and are, therefore, independent. Given a

minimum spacing between study plots of approximately two kilometers, spatial autocorrelation among study plots is considered highly unlikely. Again, in the context of this study of avalanche forecasting methods, probabilities p from the two-tailed, two-sample t-tests were compared to a significance level of $\alpha = 0.05$, the highest acceptable threshold for a Type I error, but all p values are reported.

Stability Model Evaluation

Had they been observed, maps of actual natural avalanche cycles in the study area, subsequent to 900 m^2 study plot stability sampling trials, were to be compared to the GIS-generated maps of modeled local stability, with three objectives. First, the ability of the models to predict the spatial distribution of avalanching was to be evaluated. Second, the ability of the models to predict a critical load threshold for the pre-storm snowpack would be evaluated by comparing the modeled storm net loading, the pre-storm critical load threshold model, and the actual avalanche occurrences. And third, spatial analyses would also seek spatial patterns in the 'degree of uncertainty' encountered when applying the stability models to terrain that is increasingly distant from the study plot where stability was measured. Unfortunately, as discussed under Results, since no significant natural avalanche cycles occurred, another approach to model evaluation was required.

RESULTS AND DISCUSSION

Winter of 2000/2001

Analysis of the seven separate study plot stability sampling trials performed during the winter of 2000/2001 revealed an unexpected variety in the magnitude and pattern of variations in snowpack stability. Significant variation occurred at all scales and in several spatial patterns. Complete results for all 2000/2001 season study plot stability-sampling trials, including all valid QLCT τ_∞ results, Z scores, S_{QLCT} values, and τ_{Slab} data, are provided in chronological order (Appendix B). All 2000/2001 snowpack profiles referred to are provided in chronological order (Appendix H).

Weather and Snowpack

The 2000/2001 season proved to be the second unusually dry winter in a row in the Bridger Range study area. As a consequence, at mid-season we determined that any opportunity to conduct the 900 m^2 study plot stability-sampling trials would be exploited, particularly any opportunity to conduct simultaneous trials at all four Bridger Range study plots, regardless of the likelihood of a storm-triggered avalanche cycle immediately after those trials. However, winter's onset offered no hints of the drought to come.

After a series of small weather disturbances throughout November, culminating in Storm #1 on November 30th which delivered 25 cm of snow containing 28 mm SWE, the snowpack at the Alpine study plot at Bridger Bowl Ski Area totaled 85 cm depth on

December 1st. Total December 1st snowpack depth at the nearby Bradley Meadow study plot was somewhat lower, at approximately 60 cm. Storm #1 was of sufficient intensity and duration to initiate a moderately extensive avalanche cycle of Class 3 (US) slab events running on one or more of the weak layers of faceted grains developing in the shallow snowpack. Profile #1, of November 15th, at Bradley Meadow study plot, revealed those weak layers (Appendix H).

The first nine days of December were dry, with air temperatures ranging from -11° C to 7° C. Following a weak disturbance on the 10th, cold air advected into the study area. The Alpine study plot season-low temperature (-25° C) occurred on the morning of the 11th. Another series of three small storms increased the Alpine study plot snowpack total depth to 120 cm by January 1st while the total depth at the Bradley Meadow study plot was approximately 130 cm. Profile #2 on December 12th (Appendix H) revealed the formation of a ±50 cm thick slab overlying a layer of heavily faceted, 1-3 mm grains, approaching "cup" characteristics, located 30 cm above the ground. These grains had developed under strong snow-temperature gradients driven by the cold weather in mid-December. This layer of faceted grains persisted throughout the season and provided a weak layer for the study plot stability-sampling trials conducted on February 18th. By January 1st, the slab above the layer of 1-3 mm faceted grains observed at 30cm above the ground had thickened to almost 80 cm and the snowpack showed signs of increasing stability. The season total SWE at Alpine study plot, as of January 1st, was 100 mm of H_2O, the total of 47 mm received during November storms and 53 mm during December, or just 52% of the 17-year average season total SWE through December (Table 2).

The year 2001 began with a strong, but not unprecedented, "January thaw" lasting almost two weeks. This period of dry and warm weather afforded an opportunity to conduct two SWE transects running east from the Bridger Range ridge crest (as discussed under Methods – Stability Modeling) on January 5th and 6th. Thick melt-freeze crusts developed on south-, southeast-, and east-facing aspects throughout the Bridger Range during this period. Cooler weather, more typical of January in the study area, resumed mid-month, with four days of light precipitation totaling 15 cm of new snow. Storm #5, on January 20th, with 23 cm of new snow containing 23 mm of SWE, produced only a very minor cycle of Class 1 and 2 (US) loose-snow and "extra-soft slab" activity. By January 21st the snowpack had regained its New Year's Day depth of 130 cm at Bradley Meadow. A small disturbance on January 26th delivered 8 cm of snow with light winds. Cool temperatures during and after Storm #5 and the January 26th disturbance, with lows near -10° C and highs near 0°, minimized new-snow settlement and strengthening, creating the opportunity to conduct a 900 m^2 study plot stability-sampling trial next to the Bradley Meadow study plot in a weak layer 10-15 cm below the snowpack surface. January 2001 storms contributed only another 51 mm SWE, bringing the season total SWE to 151 mm H_2O, only 50% of the 17-year average season total SWE through January (Table 2).

Storms #6 and #7 in early February produced modest increments of 5-15 cm of new snow loading to the snowpack and resulted in no extensive avalanching in the Bridger Range study area. The snowpack at the Bradley Meadow and Alpine study plots remained at depth 150 cm for most of February. By mid-month, the slab overlying the

still-recognizable weak layer of (now 2-4 mm) faceted grains 30 cm above the ground had thickened to 100 cm at Bradley Meadow, as seen in Profile #14, February 16th (Appendix H). Due to the substantial load represented by the overlying slab, the weak layer had gradually gained strength and required additional loads the equivalent of a minimum of 50 mm SWE in order to trigger weak layer failure during QLCTs. Given the weather trend, and the improbability that a single storm large enough to initiate a natural deep-slab avalanche cycle would arrive in the near future, simultaneous stability-sampling trials were conducted at three of the four Bridger Range study area study plots on February 18th. It was assumed that the weak layer of 2-4 mm faceted grains 30 cm above the ground found at Bradley Meadow on February 16th would be present at all four study plots. February ended with only 54 mm additional SWE for the month and a season total SWE of 205 mm, just 54% of the 17-year average season total SWE at the end of February (Table 2). Since November 30th, no significant natural slab avalanche cycle had occurred in the Bridger Range study area.

Early March delivered a warming trend with temperatures as high as +11° C (March 9th). On March 11th a small disturbance resulted in 5 cm of new snow at the Alpine study plot. Overnight lows reached -9° C. On March 12th a brief episode of freezing rain, up to ridge-crest elevations (2,800 m) in the southern Bridger Range, produced a 1-2 mm thick ice crust at the snow surface. Storm #8 on March 14th and 15th deposited a 35 cm layer of new snow on top of the frozen-rain ice crust. The Storm #8 new-snow slab bonded well to the frozen-rain ice crust, but a steep temperature gradient in the snow immediately below the ice crust had produced 'near-surface faceting' facets (Birkeland, 1998) of the

new-snow grains deposited on the 10th of March. Storm #8 produced a small natural avalanche cycle of five events up to Class 3 (US) running in the near-surface weak layer just below the ice crust. No deep-slab activity failing lower in the snowpack was observed. On March 17th a third stability-sampling session was performed at Bradley Meadow using a 900 m^2 area immediately uphill and north of the site of the February 18th trials. This trial measured the stability of the Storm #8 slab/frozen-rain crust/near-surface facet ensemble found in Profile #19 (Appendix H) rather than the deep-slab scenario tested during the February 18th trials.

March concluded with a period of storm from the 25th through the 31st totaling 51 cm of new snow. Altogether, March delivered 91 mm in additional SWE bringing the season total SWE to 296 mm, only 59% of the 17-year average of 500 mm for the period (Table 2).

Inter-Study-Plot Variability

Each of the seven 2000/2001 study plot stability-sampling trials is evaluated individually, in chronological order, comparing individual pits to their plot's means of strength, stress, and stability. Complete 2000/2001 stability-sampling study plot trials results for *t*-tests of snowpack strength are shown in Appendix D, and for *t*-tests of snowpack stability in Appendix F.

Bacon Rind Trials - 1/3/01. A shallow snowpack, 48 cm deep, consisting of 18 cm of 3-5 mm "depth hoar" cup grains at the ground, and an overlying slab of 30 cm of mixed forms (Profile #4, Appendix H) was tested using the surface mode of the QLCT.

QLCT-induced shear fractures were generally Q1, occurring at the interface between the slab and weak layer; only one or two collapse failures were observed at or near the ground.

Pit-by-pit and plot-wide results of the QLCT measurements of mean total shear stress at slab fracture, referred to as mean strength, the standard deviation of strength, and a coefficient of variation in strength for the five pits and the entire Bacon Rind plot are presented (Table 7). A complete, nominal set of fifty valid QLCT results, at ten per pit, was obtained. Landry conducted the QLCTs, assisted by Birkeland. No evidence of prior disturbance, by skiers or animals, was observed at any pit location within the plot, although one set of animal tracks did traverse an un-used area in the lower left corner of the plot. Notably, Pits 3 and 5 exhibited $CV\overline{\tau}_{\infty}$ values that were almost twice those of 1, 2, and 4, and pit 3 was 29-64% stronger than the other four pits.

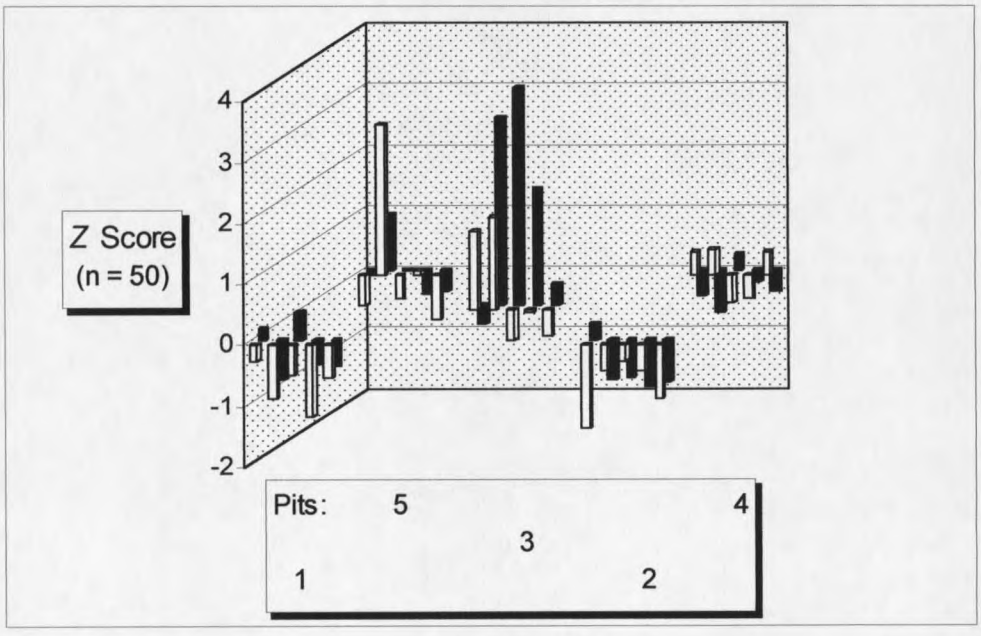
Table 7: Bacon Rind Study Plot (BRSP) 1/3/01 Trials: QLCT Results. Number of Valid Tests (n), Mean Strength ($\overline{\tau}_{\infty}$) in N/m^2, Standard Deviation (s) in N/m^2, and Coefficient of Variation of Strength ($CV\overline{\tau}_{\infty}$), by Pit and Plot.

Study Plot	Date		Pit 1	Pit 2	Pit 3	Pit 4	Pit 5	Plot
BRSP	1/3/01	n	10	10	10	10	10	50
		$\overline{\tau}_{\infty}$	460	432	710	513	549	533
		s	81	71	251	73	161	171
		$CV\overline{\tau}_{\infty}$	17.5%	16.4%	35.4%	14.2%	29.3%	32.0%

A chart of Z scores of $\overline{\tau}_{\infty}$ for the Bacon Rind trials highlights the variability in strength among the pits (Figure 9). Pit 4 Z scores show the lowest amplitude and most symmetric variation about the plot mean strength $\overline{\tau}_{\infty(Plot)}$ (i.e., $Z = 0.0$). This result is

reflected in pit 4 having the plot's lowest $CV\bar{\tau}_{\infty}$ of 14.2% and the proximity of pit 4's mean strength $\bar{\tau}_{\infty}$ of 513 N/m^2 to the plot mean value $\bar{\tau}_{\infty(Plot)}$ of 533 N/m^2 (Table 7). Pits 1 and 2, on the other hand, are dominated by Z scores falling below the plot mean $\bar{\tau}_{\infty(Plot)}$, and the range of Z score values in each pit appears larger, in the figure, than observed in pit 4, as evidenced by their slightly higher values of $CV\bar{\tau}_{\infty}$ (Table 7). Based

Figure 9: Bacon Rind Study Plot 1/3/01 Trials: Z Scores of Strength τ_{∞}. (White bars represent results in the front-row of a given pit and black bars represent back-row results. Pit locations are shown in the key below the chart).



just on their Z scores, pit 4 would appear to better represent the plot mean strength than pits 1 and 2 and, of those three pits, pit 2 would seem the least representative of plot mean strength, with the most consistently negative Z scores.

At pit 5 six of the ten Z scores are also below the plot mean $\overline{\tau}_{\infty(Plot)}$. Two of the four results above the mean are quite near the mean (at 0.11 and 0.00 standard deviations), but one result, test cell 2 (second from left, front row), is 2.45 standard deviations above the plot mean $\overline{\tau}_{\infty(Plot)}$ and, along with the cell 7 result directly uphill of cell 2, substantially increased the pit's variability. Despite the fact that Pit 5 has a much higher $CV\overline{\tau}_{\infty}$, at 29.3%, than observed in pits 1, 2, and 4, its pit mean strength $\overline{\tau}_{\infty}$, at 549 N/m^2, is closest of all the pits to the plot mean strength $\overline{\tau}_{\infty(Plot)}$ of 533 N/m^2. This would appear to be nothing more than a coincidence, since pit 3 exerted more influence on the value of $\overline{\tau}_{\infty(Plot)}$ than pit 5.

The increased range in Z scores at pit 3 is clear (Figure 9). Five Z scores are greater than 1.2 standard deviations above the plot mean, and two exceed 3.0 deviations. The pit-minimum Z score of –0.488 in cell 3 and the pit-maximum of +3.562 immediately uphill of cell 3 in cell 8 resulted in a pit range in strength of 4.05 standard deviations, a pit mean $\overline{\tau}_{\infty}$ of 710 N/m^2 (Table 7) and a pit $CV\overline{\tau}_{\infty}$ of 35.4% (Table 7). By the evidence in the Z score chart alone, it's clear that aggregating pit 3 with the remaining four pits has the effect of elevating the plot mean strength.

At the plot scale, the plot $CV\overline{\tau}_{\infty(Plot)}$ of 32.0% (Table 7) reflects variations in strength from the plot-maximum Z score in cell 8 of Pit 3 (Figure 9) of +3.562 standard deviations to the plot-minimum of –1.361 at cell 1 in pit 2, a range of 4.923 standard deviations s of 171 N/m^2, or 840 N/m^2 (Table 7).

Next, variations in shear stress at the slab/weak-layer interface were evaluated. The shear stress produced by the in-situ slab, τ_{Slab}, was calculated (Landry et al., 2001b). Among the five pits, τ_{Slab} exhibited a range of only 25 N/m^2 (Table 8). Such a small range in stress stands in contrast to the large range in strength just described and clearly does not explain the high variations in strength observed.

Table 8: Bacon Rind Study Plot (BRSP) 1/3/01 Trials: Shear Stress. In Situ Slab Shear Stress, τ_{Slab} (N/m^2), and Coefficient of Variation of Mean Plot Shear Stress, $CV\,\overline{\tau}_{Slab}$.

Study Plot	Date	τ_{Slab} Pit 1	τ_{Slab} Pit 2	τ_{Slab} Pit 3	τ_{Slab} Pit 4	τ_{Slab} Pit 5	$CV\,\overline{\tau}_{Slab}$ Plot
BRSP	1/3/01	255	244	260	269	254	3.6%

A stability ratio S_{QLCT} was calculated for each pit by dividing the pit's mean strength $\overline{\tau}_{\infty}$ by the shear stress τ_{Slab} produced by the in-situ slab at the pit (Table 9). With very little variation in the denominator of the S_{QLCT} ratio, the shear stress τ_{Slab}, the pattern of

Table 9: Bacon Rind Study Plot (BRSP) 1/3/01 Trials: Stability. Pit and Plot Stability, S_{QLCT}, and Coefficient of Variation of Mean Plot Stability, $CV\,\overline{S}_{QLCT(Plot)}$.

Study Plot	Date	S_{QLCT} Pit 1	S_{QLCT} Pit 2	S_{QLCT} Pit 3	S_{QLCT} Pit 4	S_{QLCT} Pit 5	$\overline{S}_{QLCT(Plot)}$
BRSP	1/3/01	1.81	1.77	2.73	1.90	2.16	2.08 CV = 31.3%

variation in stability among the pits is the same as the pattern of variation in strength (Table 7), with pit 2 having the lowest stability ratio S_{QLCT} and pit 3 the highest, and the $CV\ \overline{S}_{QLCT(Plot)}$ of 31.3% is quite similar to the $CV\ \overline{\tau}_{\infty}$ at 32.0%.

Next, the ability of each set of QLCT stability tests at the Bacon Rind pits to represent the plot's mean strength on 1/3/01 was analyzed (Table 10) using the relaxed adaptation of the two-sample *t*-test (two-sided, $\alpha = 0.05$) described under Methods – Data Analysis. The null hypothesis H_o of "no difference" between pit mean strength $\overline{\tau}_{\infty}$ and plot mean strength $\overline{\tau}_{\infty(Plot)}$ was evaluated and rejected in three out of five pits reflecting, again, the influence of pit 3 on $\overline{\tau}_{\infty(Plot)}$. Liberalizing the *t*-test tolerance for a Type I error to significance level $\alpha = 0.10$ did not alter that outcome.

Table 10: Bacon Rind Study Plot (BRSP) 1/3/01 Trials: *t*-Tests of Strength. Two-Sample *t*-Test (two-sided, $\alpha = 0.05$) of "No Difference" Between Mean Pit Strength ($\overline{\tau}_{\infty}$) and Mean Plot Strength ($\overline{\tau}_{\infty(Plot)}$). (All pits pooled to calculate $\overline{\tau}_{\infty(Plot)}$).

Study Plot	Date	Pit 1 $\overline{\tau}_{\infty}$ to $\overline{\tau}_{\infty(Plot)}$	Pit 2 $\overline{\tau}_{\infty}$ to $\overline{\tau}_{\infty(Plot)}$	Pit 3 $\overline{\tau}_{\infty}$ to $\overline{\tau}_{\infty(Plot)}$	Pit 4 $\overline{\tau}_{\infty}$ to $\overline{\tau}_{\infty(Plot)}$	Pit 5 $\overline{\tau}_{\infty}$ to $\overline{\tau}_{\infty(Plot)}$
BRSP	1/3/01	Reject $p = 0.048$	Reject $p = 0.004$	Reject $p = 0.008$	Fail to Reject $p = 0.556$	Fail to Reject $p = 0.788$

Finally, Hypothesis #1, that, on 1/3/01, stability at any one Bacon Rind pit would represent the plot's mean stability, was analyzed with the adapted two-sample *t*-test. The null hypothesis H_o of "no difference" between stability S_{QLCT} at a given pit and mean plot stability $\overline{S}_{QLCT(Plot)}$ was tested (Table 11). Again, since shear stress τ_{Slab} varied so little

in the Bacon Rind trials (Table 8), the results of these analyses mimic the results shown in Table 10 and the null hypothesis of "no difference" in stability is rejected in the same three of the five pits. Thus, pits 1, 2 and 3 at Bacon Rind were found unrepresentative

Table 11: Bacon Rind Study Plot (BRSP) 1/3/01 Trials: *t*-Tests of Stability. Two-Sample *t*-Test (two-sided, $\alpha = 0.05$) of "No Difference" Between Pit Stability (S_{QLCT}) and Mean Plot Stability ($\overline{S}_{QLCT(Plot)}$). (All pits pooled to calculate $\overline{S}_{QLCT(Plot)}$).

Study Plot	Date	Pit 1: S_{QLCT} to $\overline{S}_{QLCT(Plot)}$	Pit 2: S_{QLCT} to $\overline{S}_{QLCT(Plot)}$	Pit 3: S_{QLCT} to $\overline{S}_{QLCT(Plot)}$	Pit 4: S_{QLCT} to $\overline{S}_{QLCT(Plot)}$	Pit 5: S_{QLCT} to $\overline{S}_{QLCT(Plot)}$
BRSP	1/3/01	Reject $p = 0.059$	Reject $p = 0.027$	Reject $p = 0.064$	Fail to Reject $p = 0.184$	Fail to Reject $p = 0.717$

of either the mean strength or the mean stability of the plot. A graph of the *Z*-scores of the stability ratio S_{QLCT} for each valid QLCT at Bacon Rind was indistinguishable from the chart of strength in Figure 9 due to the near-constant stress shown in Table 8.

The disparity, driven by pit 3 results, in strength and stability in this trial is difficult to explain. Variations in the slab load on the weak layer were negligible, so pressure metamorphism was more-or-less constant throughout the plot. Pit 2 may have experienced periods of shading by a downslope tree, enhancing temperature gradients during the formation of the weak layer. However, this potential effect was not present at pit 1, which was only 6.5% stronger than pit 2, or at any other pits. Further, no variations in the substrate such as protruding rocks or bushes were observed, the slope was generally planar, no evidence of prior disturbance was found, and the QLCT method was

consistent throughout the trial. Absent these possible influences on its strength, some other snowpack process must have been responsible for the significantly higher strength and stability at pit 3.

Bradley Meadow Study Plot Trials - 1/27/01. On January 27th a weakness near the bottom of an 18 cm new-snow layer deposited during Storm #5, January 20th, was tested in a 900 m^2 stability-sampling trial at Bradley Meadow utilizing the surface mode of the QLCT. The subject weak layer consisted of an inter-layer band of relatively lower density, partially decomposed new-snow particles displaying incipient faceting (Profile #7, Appendix H). The observers obtained consistent Q2 shears during the QLCTs. Some QCLTs resulted in simultaneous failures in the Storm #5 weakness and a layer of faceted grains near the bottom of the snowpack (the weak layer eventually tested on February 18th). Only QLCT results in the Storm #5 weak layer are analyzed here. Jeff Deems conducted all QLCTs, with Landry assisting, obtaining a near-complete set of 46 of 50 possible valid QLCT results, with only four tests either failing in a different weak layer or rejected due to apparent prior disturbance (possible ski track in pit 4).

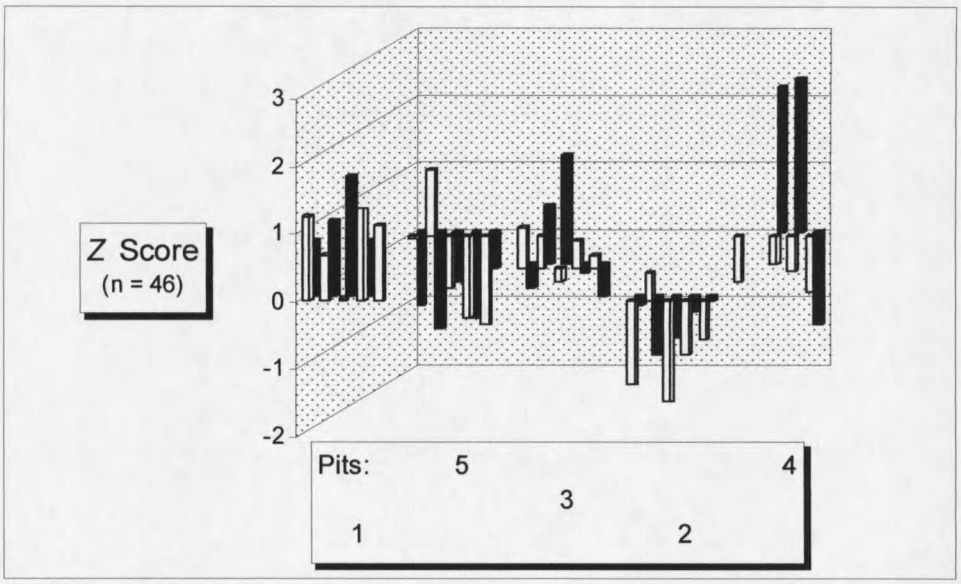
Pit-by-pit and plot-wide results of the QLCT measurements of weak-layer shear strength and its variation among the five pits and across the plot were summarized (Table 12). Individual pits exhibited a wide range in their $CV\ \bar{\tau}_{\infty}$ values, from a low of only 9.1% at pit 1, the pit with the highest value of mean strength $\bar{\tau}_{\infty}$, to a high of 33.0% in pit 4, the pit whose value of $\bar{\tau}_{\infty}$ was, coincidentally, closest to the plot mean strength $\bar{\tau}_{\infty(Plot)}$.

Table 12: Bradley Meadow Study Plot (BMSP) 1/27/01 Trials: QLCT Results. Number of Valid Tests (n), Mean Strength ($\bar{\tau}_{\infty}$) in N/m^2, Standard Deviation (s) in N/m^2, and Coefficient of Variation of strength ($CV\bar{\tau}_{\infty}$), by Pit and Plot.

Study Plot	Date		Pit 1	Pit 2	Pit 3	Pit 4	Pit 5	Plot
BMSP	1/27/01	n	9	10	10	7	10	46
		$\bar{\tau}_{\infty}$	721	514	629	601	490	588
		s	65	77	85	199	99	134
		$CV\bar{\tau}_{\infty}$	9.1%	15.0%	13.5%	33.0%	20.2%	22.8%

The overall (all valid QLCT results pooled), plot-wide $CV\ \bar{\tau}_{\infty(Plot)}$, at 22.8%, was surprising low, given the week-old age of the weak layer, the rapidity with which new snow usually gains strength under "pressure metamorphism" (settlement produced by overburden) (Perla and Martinelli, 1976) and the observed variability of the overlying slab, discussed below. Z scores of strength τ_{∞} are shown in a chart of each valid QLCT in the trial (Figure 10). The pit 4 results include a gap representing a non-result at cell 2 in the front (white) row, and two missing results at cells 6 and 7 in the back (black) row. Pit 1 has one missing result at cell 10 in the back row. Pits 2 and 5 produced results substantially below the mean plot strength $\bar{\tau}_{\infty(Plot)}$. Conversely, all of the pit 1 and most of the pit 3 Z scores were above the plot mean; pit 3 did include four below-mean results. Further, pit 4 produced results departing substantially from the mean in both directions, as reflected in its 33.0% CV in pit strength $\bar{\tau}_{\infty}$.

Figure 10: Bradley Meadow Study Plot 1/27/01 Trials: Z Scores of Strength τ_{∞}. (White bars represent results in the front-row of a given pit and black bars represent back-row results. Pit locations are shown in the key below the chart).



Despite pit 4 displaying the widest variability in strength, ranging from –1.367 standard deviations below-mean at cell 10 to 2.288 above-mean at cell 9, pit 4's mean strength $\bar{\tau}_{\infty}$ of 601 N/m^2 fell closest to the plot mean $\bar{\tau}_{\infty(Plot)}$ of 588 N/m^2 (Table 12). Interestingly, the strongest and weakest QLCT results in pit 4 were in adjoining cells (cells 9 and 10). Pit 2 produced the weakest result in the plot at –1.496 standard deviations below-mean in cell 3. The plot-wide range in measured strength was from 388 N/m^2 in pit 2, cell 3, to 894 N/m^2 in pit 4, cell 9, for a total range of 506 N/m^2.

To an avalanche forecaster digging a single pit at this site in that day, any one of pits 1, 2, 3 or 5 might have seemed likely, given their generally low values of $CV\bar{\tau}_{\infty}$, to represent plot-wide mean strength in a plot that would be expected, given additional

sampling, to exhibit similarly low overall variation in strength. In fact, however, it was pit 4, the pit with the most variability by a factor of at least 50%, that displayed the mean pit strength $\bar{\tau}_{\infty}$, at 601 N/m^2, closest of all pits to the plot mean of 588 N/m^2 (Table 12). In the chart of Z scores (Figure 10), pit 4 doesn't appear to overwhelm the remaining pits with a large number especially weak or strong QLCTs. In the chart of Z scores, the distribution of above- and below-mean scores in pit 4 appears balanced (Figure 10) compared to the other individual pits. But, if viewed collectively, the Z scores in pits 1, 2, 3 and 5 can also be seen to balance each other around the mean plot strength (Figure 10). Whether any single pit is representative of mean plot stability is examined below.

First, values for shear stress τ_{Slab} at each pit are shown (Table 13). Unlike the remarkably uniform slab and shear stress observed at Bacon Rind, the new snow slab deposited by Storm #5 and the January 26th disturbance at Bradley Meadow showed substantial variations in thickness and water content producing a corresponding 31.5% $CV\tau_{Slab}$, despite only small variations in slope angle among the pits.

Table 13: Bradley Meadow Study Plot (BMSP) 1/27/01 Trials: Shear Stress. Pit Shear Stress τ_{Slab} (N/m^2), and Coefficient of Variation of Mean Plot Shear Stress, $CV\bar{\tau}_{Slab}$.

Study Plot	Date	τ_{Slab} Pit 1	τ_{Slab} Pit 2	τ_{Slab} Pit 3	τ_{Slab} Pit 4	τ_{Slab} Pit 5	$CV\bar{\tau}_{Slab}$ Plot
BMSP	1/27/01	162	67	105	105	103	31.5%

Pit 2 had the lowest τ_{Slab} and the lowest mean pit strength $\bar{\tau}_{\infty}$ (Table 12), while pit 1 had the highest τ_{Slab} and highest mean pit strength $\bar{\tau}_{\infty}$. This might be explained as the result of variations in the effects of pressure metamorphism. Increased settlement and bond formation may have occurred where the slab was thickest and heaviest and where τ_{Slab} was greatest, at pit 1, while, conversely, the least settlement occurred where the slab was thinnest and τ_{Slab} was lowest, at pit 2. The cause of these variations in slab thickness (and water content) was most likely wind drift before, during, and after Storm #5, and the snow showers on January 26th.

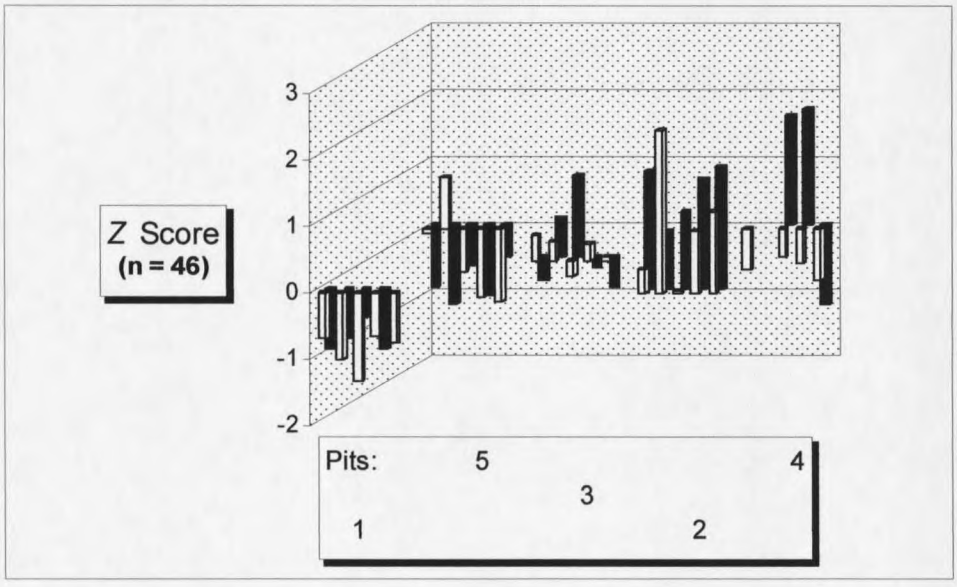
Stability ratio S_{QLCT} results for each pit and the mean plot stability $\bar{S}_{QLCT(Plot)}$ are shown in Table 14. The plot-wide CV of mean plot stability $\bar{S}_{QLCT(Plot)}$, at 22.2%, is quite similar to the CV of mean plot strength $\bar{\tau}_{\infty(Plot)}$, at 22.8%.

Table 14: Bradley Meadow Study Plot (BMSP) 1/27/01 Trials: Stability. Pit and Plot Stability, S_{QLCT}, and Coefficient of Variation of Mean Plot Stability, $CV\,\bar{S}_{QLCT(Plot)}$.

Study Plot	Date	S_{QLCT} Pit 1	S_{QLCT} Pit 2	S_{QLCT} Pit 3	S_{QLCT} Pit 4	S_{QLCT} Pit 5	$\bar{S}_{QLCT(Plot)}$
BMSP	1/27/01	4.46	7.70	6.02	5.75	4.77	5.74 $CV = 22.2\%$

A graph of the Z scores of stability calculated for each QLCT test cell (Figure 11) shows a substantially different pattern than seen in the graph of the Z scores of strength (Figure 10), a consequence of variation in shear stress τ_{Slab} over the plot (Table 13).

Figure 11: Bradley Meadow Study Plot 1/27/01 Trials: Z Scores of Stability S_{QLCT}. (White bars represent results in the front-row of a given pit and black bars represent back-row results. Pit locations are shown in the key below the chart).



While pits 3, 4 and 5 all had very similar values τ_{Slab} quite near the plot mean of 108N/m^2, and show similar scatter in Z scores about the means of strength and stability in both graphs, pits 1 and 2 show reversed distributions in the graphs. All Z scores for strength in pit 1 are above the mean in Figure 10, but all scores for stability are below-mean in Figure 11. Almost exactly the opposite pattern is seen at pit 2 in both graphs. Since a single value for stress is used for each calculation of S_{QLCT} in a pit, the net difference between the Z scores for strength and stability for each cell are constant, at a

given pit. The cause of the reversals noted at pits 1 and 2 lies in the relative magnitudes of departure from the plot mean of strength and stress.

Pit 1 had both the highest values for shear stress τ_{Slab}, at 162 N/m^2 (Table 13), and for strength $\bar{\tau}_{\infty}$, at 721 N/m^2 (Table 12). But the proportion of departure from the plot means of strength and stress at pit 1 was larger for stress τ_{Slab}, at 1.6 standard deviations above the plot mean stress of 108 N/m^2 (Table 13) than for strength $\bar{\tau}_{\infty}$, which was 1.0 standard deviations above the plot mean strength of 588 N/m^2 (Table 12). Thus, the stress value (denominator) of the S_{QLCT} ratio for pit 1 grew proportionately larger than the strength value (numerator), relative to their respective plot means, bringing stress closer to strength and driving the ratio below the plot mean stability.

At pit 2, even though the pit means of strength (514 N/m^2, Table 12) and stress (67 N/m^2, Table 13) are below the plot mean for each, the strength value remains proportionally closer, at 0.55 standard deviations below-mean $\bar{\tau}_{\infty(Plot)}$ of 588 N/m^2, than the value of stress, at 1.2 standard deviations below the plot mean stress of 108 N/m^2. Thus, at pit 2, the departure from the plot mean strength was smaller than the departure from plot mean stress, shifting the S_{QLCT} ratio toward the numerator (strength) and above the plot mean stability.

Two-sample *t*-test analyses evaluated how representative each pit's mean strength $\overline{\tau}_{\infty}$ was of the mean plot strength $\overline{\tau}_{\infty(Plot)}$ (Table 15). Interestingly, as discussed above,

Table 15: Bradley Meadow Study Plot (BMSP) 1/27/01 Trials: *t*-Tests of Strength. Two-Sample *t*-Test (two-sided, $\alpha = 0.05$) of "No Difference" Between Mean Pit Strength ($\overline{\tau}_{\infty}$) and Mean Plot Strength ($\overline{\tau}_{\infty(Plot)}$). (All pits pooled to calculate $\overline{\tau}_{\infty(Plot)}$).

Study Plot	Date	Pit 1 $\overline{\tau}_{\infty}$ to $\overline{\tau}_{\infty(Plot)}$	Pit 2 $\overline{\tau}_{\infty}$ to $\overline{\tau}_{\infty(Plot)}$	Pit 3 $\overline{\tau}_{\infty}$ to $\overline{\tau}_{\infty(Plot)}$	Pit 4 $\overline{\tau}_{\infty}$ to $\overline{\tau}_{\infty(Plot)}$	Pit 5 $\overline{\tau}_{\infty}$ to $\overline{\tau}_{\infty(Plot)}$
BMSP	1/27/01	Reject $p = 0.000$	Reject $P = 0.028$	Fail to Reject $p = 0.227$	Fail to Reject $p = 0.865$	Reject $p = 0.034$

this analysis reveals that pit 4, the pit exhibiting the largest $CV\ \overline{\tau}_{\infty}$ at 33.0% (Table 12) also produced the pit mean strength $\overline{\tau}_{\infty}$ (601 N/m^2 (Table 12)) most representative of $\overline{\tau}_{\infty(Plot)}$ (588 N/m^2 (Table 12)). Conversely, pit 1, with the lowest $CV\overline{\tau}_{\infty}$ of 9.1% ($\overline{\tau}_{\infty}$ of 721 N/m^2) was the most unrepresentative of the plot mean $\overline{\tau}_{\infty(Plot)}$ (588 N/m^2). While this result is striking, it appears to be case-specific and is not construed to indicate that pits with low variability cannot represent the mean strength of a study plot.

Finally, two-sample *t*-test analyses of stability S_{QLCT} is applied (Table 16). The same pattern of results seen in Table 15 is observed, showing that pits 1, 2 and 5 are unrepresentative of either plot mean strength or plot stability. Graphic evidence of this pattern is seen in the chart of stability *Z* scores (Figure 11), with pit-wide variance above- or below-mean stability in pits 1, 2 and 5, juxtaposed to more balanced distributions of the *Z* scores about the mean at pits 3 and 4.

Table 16: Bradley Meadow Study Plot (BMSP) 1/27/01 Trials: *t*-Tests of Stability. Two-Sample *t*-Test (two-sided, $\alpha = 0.05$) of "No Difference" Between Pit Stability (S_{QLCT}) and Mean Plot Stability ($\overline{S}_{QLCT(Plot)}$). (All pits pooled to calculate $\overline{S}_{QLCT(Plot)}$).

Study Plot	Date	Pit 1: S_{QLCT} to $\overline{S}_{QLCT(Plot)}$	Pit 2: S_{QLCT} to $\overline{S}_{QLCT(Plot)}$	Pit 3: S_{QLCT} to $\overline{S}_{QLCT(Plot)}$	Pit 4: S_{QLCT} to $\overline{S}_{QLCT(Plot)}$	Pit 5: S_{QLCT} to $\overline{S}_{QLCT(Plot)}$
BMSP	1/27/01	Reject $p = 0.000$	Reject $p = 0.001$	Fail to Reject $p = 0.473$	Fail to Reject $p = 0.981$	Reject $p = 0.060$

Round Hill Trials - 2/4/01. This trial produced stability-sampling results from a low-angle avalanche starting zone, rather than a "representative" study plot, utilizing the same methods and sampling design as previous trials. A layer of 4-6 mm buried surface hoar existed above a thin melt-freeze crust some 50 cm below the snowpack surface and it consistently produced "easy" (compression test) shear results for Parks Canada avalanche forecasters at the nearby Fidelity study plot since being deposited on January 28th.

Given time constraints, two teams of observers conducted the trials. John Kelly (Parks Canada), previously trained and assisted, on 2/4/01, by Landry, collected QLCT data from pits 1, 3 and 5. Jeff Deems, assisted by Johann Schleiss (Parks Canada), collected data in pits 2 and 4. At the conclusion of pits 1, 2, 3 and 4, a total of 37 valid QLCT results had been obtained from the 1/28/01 buried surface hoar weak layer. In many QLCTs, a second layer of buried surface hoar deposited on 1/21/01, lying some 10 cm below the 1/28/01 layer, failed simultaneously with the 1/28/01 layer. Only the 1/28/01 weak layer results are analyzed here. All 37 valid QLCT results were Q1.

Then, as Deems and Schleiss prepared to depart the site, and during preparation of pit 5 by Landry and Kelly, the final pit of the trial, the study site collapsed with an audible "whoomph". This collapse was quite likely triggered by the massive disturbance involved in performing the stability-sampling trials since no precipitation or wind loading was occurring. No visible cracking or snow movement was observed due, we assumed, to the low slope angle. Subsequently, Kelly and Landry could not ascertain precisely which weak layer had collapsed and conducted the final set of ten QLCTs in pit 5. However, no valid QLCT results were obtained from the 1/28/01 weak layer in pit 5, as all ten tests failed in the deeper layer of surface hoar.

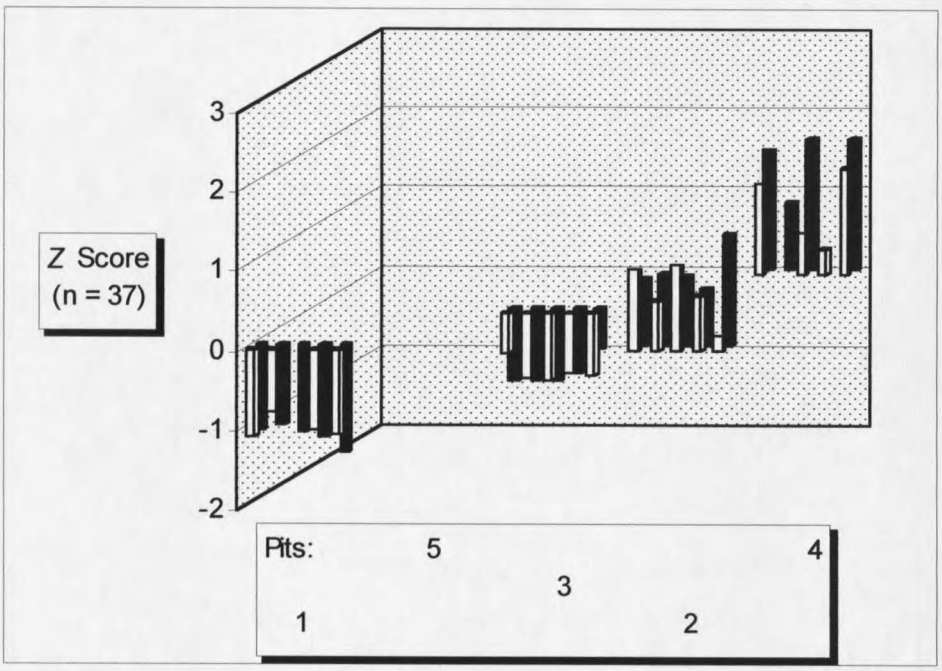
Dramatically differing results exhibiting a strong spatial pattern of strength variation were obtained from the four successfully sampled pits (Table 17). While coefficients of variation in strength within individual pits were generally low and similar, mean strengths $\bar{\tau}_\infty$ for pits 1 and 3 were only 30-40% of the values for $\bar{\tau}_\infty$ at pits 2 and 4, creating a dramatic distinction between the two sides of the plot.

Table 17: Round Hill (RH) 2/4/01 Trials: QLCT Results. Number of Valid Tests (n), Mean Strength ($\bar{\tau}_\infty$) in N/m^2, Standard Deviation (s) in N/m^2, and Coefficient of Variation of strength ($CV\bar{\tau}_\infty$), by Pit and Plot.

Study Plot	Date		Pit 1	Pit 2	Pit 3	Pit 4	Pit 5	Plot
RH	2/4/01	n	9	10	10	8	*No Result*	37
		$\bar{\tau}_\infty$	391	1,174	508	1,299		831
		s	60	133	64	214		417
		$CV\bar{\tau}_\infty$	15.4%	11.3%	12.5%	16.5%		50.2%

This strong pattern of variation is easily seen in a chart of Z scores of strength (Figure 12). Z scores at pit 1 and pit 3 all fall well below the plot mean while all pit 2 and 4 scores are well above the mean, with one exception (cell 5 of pit 2). This spatial

Figure 12: Round Hill 2/4/01 Trials: Z Scores of Strength τ_∞. (White bars represent results in the front-row of a given pit and black bars represent back-row results. Pit locations are shown in the key below the chart. No results in pit 5.)



variation in strength differs from the previous trials in the large-scale pattern of difference, bisecting the plot into two distinctly different populations of strength. Clearly, utilizing two data collection teams could explain those differences. However, given the prior QLCT training of the two teams by Landry, the magnitude of variation in these results exceeds any plausible amount of variability introduced by using two different QLCT operators during the trial.

Shear stress τ_{Slab} produced by the in-situ slab lying above the 1/28/01 surface hoar weak layer showed a similar pattern of variation (Table 18). Again, pit 1 had the lowest value of τ_{Slab} while pit 4 had the highest (of the four pits with valid QLCT results), but the differences in stress are less than the differences in strength.

Table 18: Round Hill (RH) 2/4/01 Trials: Shear Stress. Pit Shear Stress, τ_{Slab} (N/m^2), and Coefficient of Variation of Mean Plot Shear Stress, $CV\ \overline{\tau}_{Slab}$.

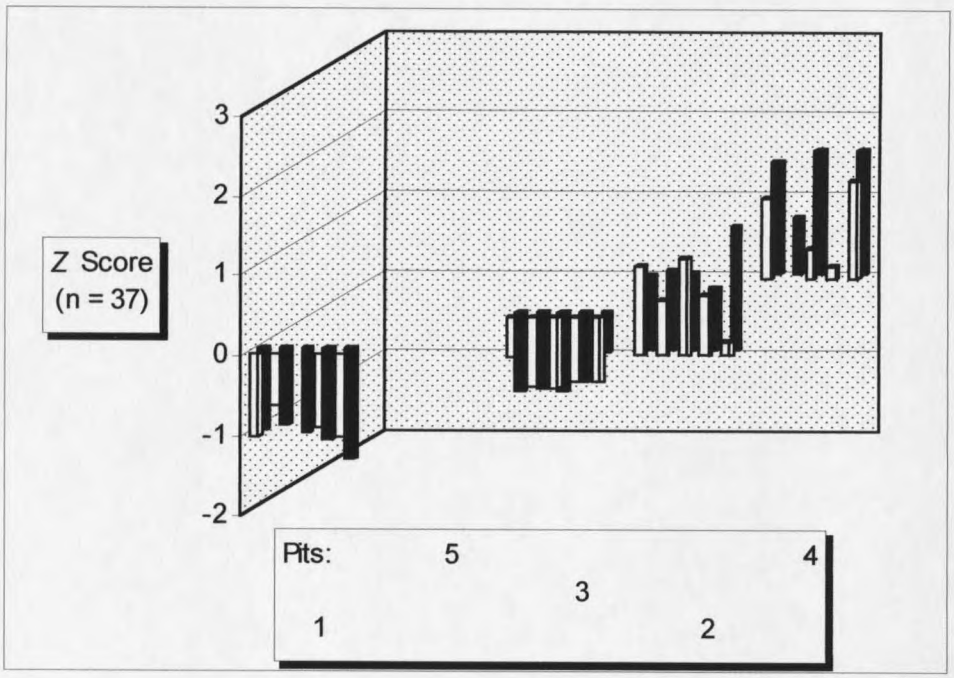
Study Plot	Date	τ_{Slab} Pit 1	τ_{Slab} Pit 2	τ_{Slab} Pit 3	τ_{Slab} Pit 4	τ_{Slab} Pit 5	$CV\,\overline{\tau}_{Slab}$ Plot
RH	2/4/01	269	323	304	348	*nr*	10.2%

Since stress varied in the same pattern, if not the same magnitude, as strength, variations in the stability ratio S_{QLCT} followed the established pattern too (Table 19), but with a plot-wide $CV\ S_{QLCT}$ of 43.7%, somewhat less than the $CV\ \overline{\tau}_{\infty}$, at 50.2%. A chart of the pattern of variation in stability using Z scores of S_{QLCT} (Figure 13) also appears to be nearly identical to the chart of Z scores of strength $\overline{\tau}_{\infty}$ (Figure 12).

Table 19: Round Hill (RH) 2/4/01 Trials: Stability. Pit and Plot Stability, S_{QLCT}, and Coefficient of Variation of Mean Plot Stability, $CV\,\overline{S}_{QLCT(Plot)}$.

Study Plot	Date	S_{QLCT} Pit 1	S_{QLCT} Pit 2	S_{QLCT} Pit 3	S_{QLCT} Pit 4	S_{QLCT} Pit 5	$\overline{S}_{QLCT(Plot)}$
RH	2/4/01	1.45	3.63	1.67	3.73	nr	2.60 $CV = 43.7\%$

Figure 13: Round Hill 2/4/01 Trials: Z Scores of Stability S_{QLCT}. (White bars represent results in the front-row of a given pit and black bars represent back-row results. Pit locations are shown in the key below the chart. No valid results were obtained in pit 5.)



Given this consistent pattern and magnitude of variation between the left side of the plot and the right side, any one of the four pits at Round Hill would seem unlikely to predict the mean strength or stability of two of the other three pits, or of the plot. The apparent inability of any single pit to represent plot strength or stability was verified by the two-sampled t-test analyses which show that no single pit was representative of plot mean strength or stability (Tables 20 and 21).

Table 20: Round Hill (RH) 2/4/01 Trials: *t*-Tests of Strength. Two-Sample *t*-Test (two-sided, $\alpha = 0.05$) of "No Difference" in Pit Mean Strength ($\overline{\tau}_{\infty}$) and Plot Mean Strength ($\overline{\tau}_{\infty(Plot)}$). (All pits pooled to calculate $\overline{\tau}_{\infty(Plot)}$).

Study Plot	Date	Pit 1 $\overline{\tau}_{\infty}$ to $\overline{\tau}_{\infty(Plot)}$	Pit 2 $\overline{\tau}_{\infty}$ to $\overline{\tau}_{\infty(Plot)}$	Pit 3 $\overline{\tau}_{\infty}$ to $\overline{\tau}_{\infty(Plot)}$	Pit 4 $\overline{\tau}_{\infty}$ to $\overline{\tau}_{\infty(Plot)}$	Pit 5 $\overline{\tau}_{\infty}$ to $\overline{\tau}_{\infty(Plot)}$
RH	2/4/01	Reject $p = 0.000$	Reject $p = 0.000$	Reject $p = 0.000$	Reject $p = 0.000$	nr

Table 21: Round Hill (RH) 2/4/01 Trials: *t*-Tests of Stability. Pit-to-Plot Two-Sample *t*-Test (two-sided, $\alpha = 0.05$) of "No Difference" Between Pit Stability (S_{QLCT}) and Mean Plot Stability ($\overline{S}_{QLCT(Plot)}$). (All pits pooled to calculate $\overline{S}_{QLCT(Plot)}$).

Study Plot	Date	Pit 1: S_{QLCT} to $\overline{S}_{QLCT(Plot)}$	Pit 2: S_{QLCT} to $\overline{S}_{QLCT(Plot)}$	Pit 3: S_{QLCT} to $\overline{S}_{QLCT(Plot)}$	Pit 4: S_{QLCT} to $\overline{S}_{QLCT(Plot)}$	Pit 5: S_{QLCT} to $\overline{S}_{QLCT(Plot)}$
RH	2/4/01	Reject $p = 0.000$	Reject $p = 0.000$	Reject $p = 0.000$	Reject $p = 0.001$	nr

The Round Hill trial offered an object lesson to the data collection team in the potential for critical spatial variations of stability, by a factor of two or more, within a distance of only 12 meters, the approximate distance from pit 3 to pits 2 or 4, even when individual pits presented comparatively minor internal variability in strength. Or, as noted by Deems while on-site, stability on this apparently uniform slope decreased by more than 50% within the equivalent of one or two turns by a skier.

A very subtle change in slope aspect offered one possible explanation of these results. Cross-slope curvature placed pits 2 and 4 in a slightly more south-facing portion of the

southeast-facing 900 m^2 plot than pits 1, 3 and 5. Increased exposure to the sun can cause standing, unburied surface hoar to "wilt" and eventually lay flat, resulting in increased strength once buried, compared to intact surface hoar on "cooler" slope aspects. The in-plot differences in slope aspect at Round Hill were too small to reliably measure with the tools at hand but, nonetheless, may have been sufficient to contribute to the observed differences in strength. Perhaps the subtle differences in slope aspect also resulted in differing rates of creep within the plot whereby the more south-facing pits 2 and 4 experienced higher creep rates, compressing and strengthening the weak layer, while the surface hoar in the remaining pits remained more upright and vulnerable to rapid loading (Jamieson and Schweizer, 1998).

Baldy Mountain Study Plot Trials - 2/18/01. Data collection teams were deployed to all four Bridger Range study area study plots, including the Baldy Mountain study plot, on February 18th with the intention of conducting simultaneous stability-sampling trials in a 10-15 cm thick weak layer of large, faceted grains located approximately 20-30 cm above the ground. If present at a given study plot, the trials would attempt to measure the strength and stability of this particular weak layer, hereafter referred to as the 2/18/01 trials "target weak layer".

The standard formal snowpit performed on 2/18/01 at the pit 1 location of the Baldy Mountain study plot did reveal the presence of the target weak layer of large faceted grains, lying some 10 cm thick between 20-30 cm above the ground. However, in pit 1 an even weaker layer of basal facets immediately above the ground consistently failed (during the ten QLCT) before the so-called target weak layer above it and no valid results

were obtained from the target weak layer. In pit 2 three additional responding weak layers produced QLCT results in eight of the ten QLCTs, before the target weak layer could respond, bringing the total number of weak layers identified to five. Only two valid (primary failure) QLCT results were obtained for the target weak layer in pit 2.

This complex array of responding weak layers ultimately yielded only 19 valid results for the target weak layer, still more than any other weak layer, with six results from pit 3, seven from pit 4, four from pit 5, just two from pit 2, and none from pit 1. Shear quality in the valid tests ranged from Q1 to Q2. The final tally of valid tests of target weak layer strength and variation, by pit and plot, is presented (Table 22).

Table 22: Baldy Mountain Study Plot (BLSP) 2/18/01 Trials: QLCT Results. Number of Valid Tests (n), Mean Strength ($\overline{\tau}_{\infty}$) in N/m^2, Standard Deviation (s) in N/m^2, and Coefficient of Variation of strength ($CV\overline{\tau}_{\infty}$), by Pit and Plot. (A minimum of three valid results was required to compute a CV of $\overline{\tau}_{\infty}$ in a given pit).

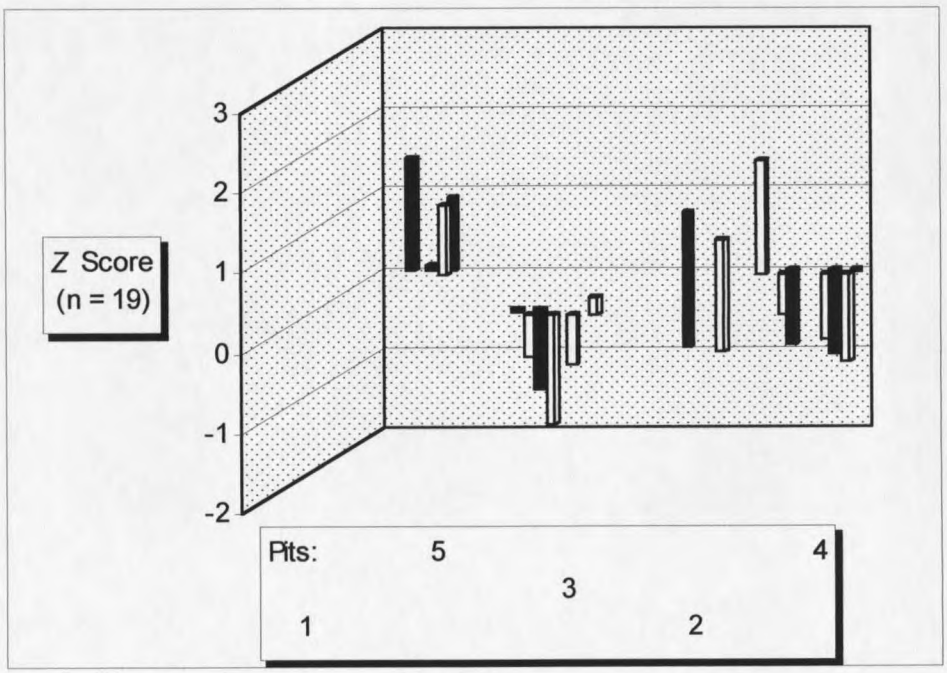
Study Plot	Date		Pit 1	Pit 2	Pit 3	Pit 4	Pit 5	Plot
BLSP	2/18/01	n	*No Results*	2	6	7	4	19
		$\overline{\tau}_{\infty}$		1,569	961	1,005	1,361	1,125
		s		61	170	259	159	289
		$CV\overline{\tau}_{\infty}$		nr	17.7%	25.7%	11.7%	25.7%

However, the results presented in Table 22 fail to fully represent the complexity of the snowpack and its stability, as just described. The fact that less than one-half of the study plot's QLCT stability-sampling cells produced a result in the target weak layer suggests that no single pit could reliably represent all of the plot's stability

configurations, with five different slab/weak layer combinations eventually observed. None-the-less, with that caveat noted, and for the purpose of making comparisons with the other Bridger Range study plots sampling the target weak layer that day, a full array of analyses of the target weak layer was performed.

A chart displays the Z scores of strength for those 19 valid results (Figure 14). The calculations of these Z scores included only valid results for the target weak layer and, consequently, the figure does not fully depict the complexity of the snowpack at the Baldy Mountain study plot. The figure includes gaps, or empty areas, where QLCT results were obtained from weak layers besides the target weak layer.

Figure 14: Baldy Mountain Study Plot 2/18/01 Trials: Z Scores of Strength τ_{∞}. (White bars represent results in the front-row of a given pit and black bars represent back-row results. Pit locations are shown in the key below the chart. No valid results were obtained in pit 1, two in pit 2, six in pit 3, seven in pit 4, and four in pit 5.)



Measurements of the in-situ slab overlying the target weak layer and calculations of the shear stress also show a considerable amount of variation among the four pits producing valid QLCT results (Table 23). Interestingly, pit 2 produced the strongest value for strength $\overline{\tau}_{\infty}$, albeit with only two out of ten possible valid results in the target weak layer, and was also the pit with the largest value for in-situ slab shear stress τ_{Slab}. Further, pit 3, with the lowest value of mean pit strength $\overline{\tau}_{\infty}$ was the location of the second-lowest value of stress τ_{Slab}.

Table 23: Baldy Mountain Study Plot (BLSP) 2/18/01 Trials: Shear Stress. Pit Shear Stress, τ_{Slab} (N/m^2), and Coefficients of Variation of Mean Plot Shear Stress, $CV\overline{\tau}_{Slab}$.

Study Plot	Date	τ_{Slab} Pit 1	τ_{Slab} Pit 2	τ_{Slab} Pit 3	τ_{Slab} Pit 4	τ_{Slab} Pit 5	$CV\overline{\tau}_{Slab}$ Plot
BLSP	2/18/01	nr	920	556	519	813	27.8%

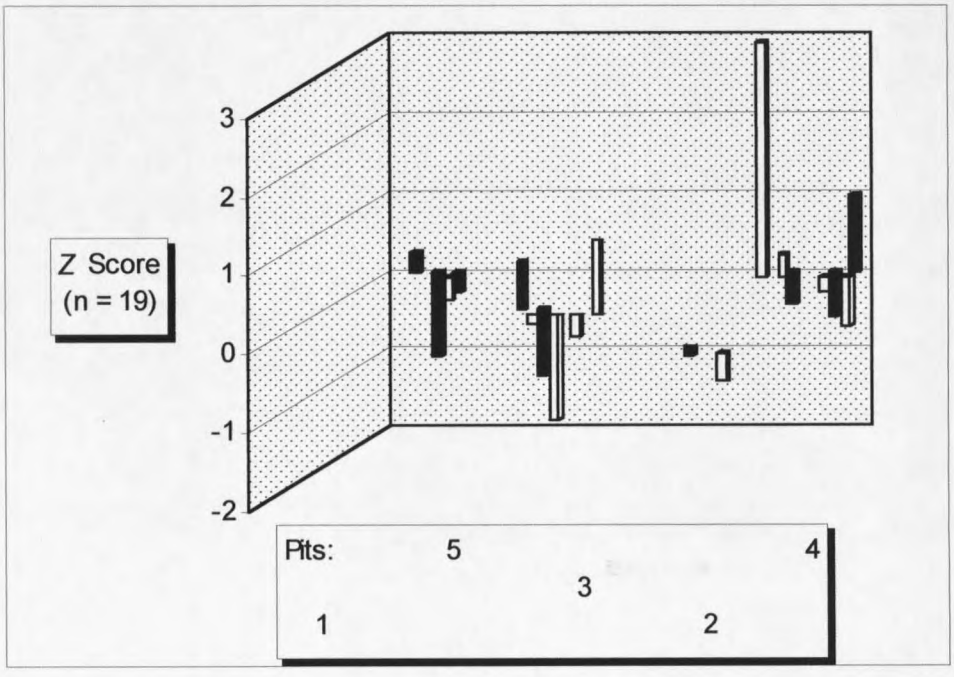
With substantial variations in both stress and strength, the pattern of stability differs from the pattern of variations in strength. Values of S_{QLCT} were calculated for the four pits with valid results, and for the plot (Table 24). Overall, pooling all individual S_{QLCT} results, the plot shows less variability in stability, at $CV\ \overline{S}_{QLCT(Plot)}$ of 20.0%, than in strength, at $CV\ \overline{\tau}_{\infty(Plot)}$ of 25.7%, or stress, at $CV\tau_{Slab}$ of 27.8%. No particular significance is attributed to this result given the small sample sizes, especially in pit 2.

Table 24: Baldy Mountain Study Plot (BLSP) 2/18/01 Trials: Stability. Pit and Plot Stability, S_{QLCT}, and Coefficient of Variation of Mean Plot Stability, $CV\ \overline{S}_{QLCT(Plot)}$.

Study Plot	Date	S_{QLCT} Pit 1	S_{QLCT} Pit 2	S_{QLCT} Pit 3	S_{QLCT} Pit 4	S_{QLCT} Pit 5	$\overline{S}_{QLCT(Plot)}$
BLSP	2/18/01	nr	2.82	1.73	1.94	1.67	1.79 $CV = 20.1\%$

Comparing the chart of Z scores of strength (Figure 14) to the chart of Z scores of stability (Figure 15) shows the influence of the variations in stress on the pattern of mean plot stability. Both Z scores in pit 2 (Figure 15) show slightly below-mean stability

Figure 15: Baldy Mountain Study Plot 2/18/01 Trials: Z Scores of Stability S_{QLCT}. (White bars represent results in the front-row of a given pit and black bars represent back-row results. No valid results were obtained in pit 1, two in pit 2, six in pit 3, seven in pit 4, and four in pit 5.)



as opposed to substantially above-mean strength, the effect of above-average shear stress. Three out of four results at pit 5 show Z scores of stability below the plot mean versus four of four with above-average strength. Pit 5 had the most-nearly-average shear stress. Pit 3 happens to display near-mean stability, balancing above-average strength with below-average stress and pit 4 shows the effect of having the lowest value of stress in the plot, with the maximum Z score for stability in the plot.

Continuing the analyses, two-sample t-tests compared the mean strength and stability of individual pits to the plot mean strength and stability. The results of t-tests of strength (Table 25) and of stability (Table 26) are shown. Pit 2 has been disqualified from these t-test analyses due to the small sample size of less than three valid results.

Table 25: Baldy Mountain Study Plot (BLSP) 2/18/01 Trials: t-Tests of Strength. Two-Sample t-Test (two-sided, $\alpha = 0.05$) of "No Difference" in Pit Mean Strength ($\overline{\tau}_{\infty}$) and Plot Mean Strength ($\overline{\tau}_{\infty(Plot)}$). (All pits pooled to calculate $\overline{\tau}_{\infty(Plot)}$).

Study Plot	Date	Pit 1 $\overline{\tau}_{\infty}$ to $\overline{\tau}_{\infty(Plot)}$	Pit 2 $\overline{\tau}_{\infty}$ to $\overline{\tau}_{\infty(Plot)}$	Pit 3 $\overline{\tau}_{\infty}$ to $\overline{\tau}_{\infty(Plot)}$	Pit 4 $\overline{\tau}_{\infty}$ to $\overline{\tau}_{\infty(Plot)}$	Pit 5 $\overline{\tau}_{\infty}$ to $\overline{\tau}_{\infty(Plot)}$
BLSP	2/18/01	No valid results	Less than 3 valid results	Fail to Reject $p = 0.204$	Fail to Reject $p = 0.343$	Fail to Reject $p = 0.134$

Table 26: Baldy Mountain Study Plot (BLSP) 2/18/01 Trials: *t*-Tests of Stability. Two-Sample *t*-Test (two-sided, $\alpha = 0.05$) of "No Difference" Between Pit Stability (S_{QLCT}) and Mean Plot Stability ($\overline{S}_{QLCT(Plot)}$),. (All pits pooled to calculate $\overline{S}_{QLCT(Plot)}$).

Study Plot	Date	Pit 1: S_{QLCT} to $\overline{S}_{QLCT(Plot)}$	Pit 2: S_{QLCT} to $\overline{S}_{QLCT(Plot)}$	Pit 3: S_{QLCT} to $\overline{S}_{QLCT(Plot)}$	Pit 4: S_{QLCT} to $\overline{S}_{QLCT(Plot)}$	Pit 5: S_{QLCT} to $\overline{S}_{QLCT(Plot)}$
BLSP	2/18/01	No valid results	Less than 3 valid results	Fail to Reject $p = 0.710$	Fail to Reject $p = 0.420$	Fail to Reject $p = 0.536$

By default, pits 1 and 2 are deemed unrepresentative of either mean plot (target weak layer) strength or stability, given only zero and two valid QLCT results, respectively. The evidence (*p* value) in support of the null hypothesis of "no difference" between pit and plot mean strength in pits 3, 4 and 5 is not particularly strong. And, although the evidence in support of the null hypothesis of "no difference" in pit and plot stability is somewhat stronger for those three pits, it must be acknowledged that only seventeen of thirty, or 57% of the stability-sampling cells in those pits produced a valid QLCT result in the target weak layer. The remaining thirteen results were distributed among four other weak layers, thus begging the question of how to define strength and stability in those pits, and that plot.

Regardless of how they were defined, I concluded that plot strength and stability were not as well represented by pits 3, 4 and 5 as these *t*-test analyses of the target weak layer suggested and, based on the empirical evidence, those pits did not represent the totality of either at the plot. Certainly, as an experienced avalanche forecaster, and the leader of this data collection team, I was perplexed by the extreme heterogeneity at this study plot, and

only diligent data recording by assistants Chuck Lindsay and Stuart Dominick enabled us to capture this complex "portrait" of spatial variation.

While the expected weak layer of basal facets was found, per Profile #14 dug at Bradley Meadow two days earlier, so were several other unexpected and even weaker weak layers located higher up in the snowpack. The snowpack at the Baldy Profile #15, at 111 cm, was 27 cm shallower than Profile #14 at Bradley Meadow. The Baldy Mountain Study Plot is also 86 meters lower than the Bradley Meadow Study Plot, and both plots are exposed to wind effects, including scouring. Perhaps the combined effects of its lower elevation, exposure to wind scouring, and a location at the southern end of the Bridger Range produce a typically shallower snowpack at the Baldy Mountain Study Plot than at Bradley Meadow. A wind-effected plot would be prone to developing a more complex stratigraphy than a nearby sheltered plot, such as the Saddle Peak Plot (see below).

Saddle Peak Study Plot Trials - 2/18/01. Karl Birkeland, assisted by Doug Chabot and Zach Matthews, conducted the Saddle Peak study plot trials on 2/18/01, finding the target weak layer of large faceted grains in place, some 20 cm above the ground, as anticipated by the 2/16/01 results from Bradley Meadow described above. Unlike the Baldy Mountain study plot just 2 km to the south, the Saddle Peak site yielded 47 out of 50 possible valid QLCT results from the target weak layer. Shear quality was variable, ranging from Q1 shears to acceptable Q3 collapses. The customary summary of the values of pit mean strength and its variability throughout the plot is given (Table 27).

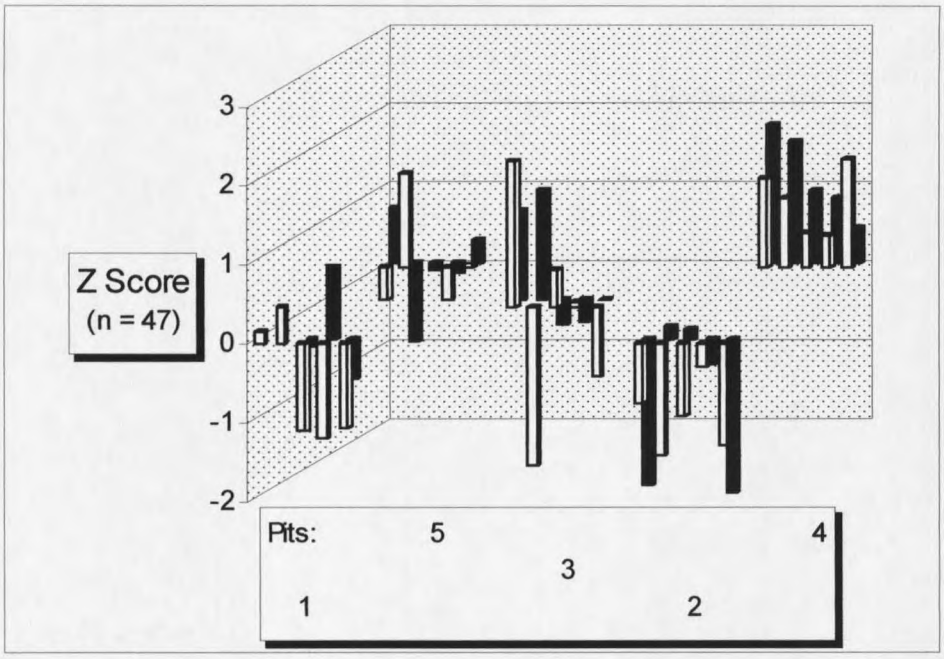
Table 27: Saddle Peak Study Plot (SPSP) 2/18/01 Trials: QLCT Results. Number of Valid Tests (n), Mean Strength ($\overline{\tau}_{\infty}$) in N/m^2, Standard Deviation (s) in N/m^2, and Coefficient of Variation of strength ($CV\,\overline{\tau}_{\infty}$), by Pit and Plot.

Study Plot	Date		Pit 1	Pit 2	Pit 3	Pit 4	Pit 5	Plot
SPSP	2/18/01	n	8	10	10	10	9	47
		$\overline{\tau}_{\infty}$	1,367	1,162	1,552	1,846	1,490	1,482
		s	298	289	458	177	243	375
		$CV\,\overline{\tau}_{\infty}$	21.8%	24.8%	30.1%	9.6%	16.3%	25.3%

At values of τ_{∞} reaching a maximum of 2,174 N/m^2, the target weak layer was nearly too strong to measure at Saddle Peak, using the QLCT equipment available. However, post-trials laboratory testing of the equipment confirmed its ability to accurately measure within this range of strength and confirmed these results. Given the completeness of this data set, subsequent analyses of variations in strength and stability must be considered good indicators of plot-wide characteristics.

A chart of Z Scores of individual QLCT measurements of strength τ_{∞} presents at least three different patterns (Figure 16). In pits 1, 5 and, most strikingly, in pit 3, the weakest and strongest QLCT results in the pits were in adjoining test cells, either next to one another in the same row (as in pit 3) or immediately above (uphill of) or below (downhill of) each other in their respective rows. And, the weakest and strongest QLCT results in the entire plot were from cell 1 (at 2,174 N/m^2) and cell 2 (951 N/m^2) of pit 3, spanning a range of 4.23 standard deviations of plot mean strength $\overline{\tau}_{\infty(Plot)}$. Although pit 3 presented the most in-pit variability, at $CV\ \overline{\tau}_{\infty}$ of 30.1%, substantial in-pit variability was the norm at Saddle Peak, with the exception of pit 4.

Figure 16: Saddle Peak Study Plot 2/18/01 Trials: Z Scores of Strength τ_{∞}. (White bars represent results in the front-row of a given pit and black bars represent back-row results.)



Besides strong inter-pit variability, strong intra-pit variation was also found at Saddle Peak. Pit 4 presented a complete set of ten Z scores, all above the plot mean. Pit 4 had the lowest value $CV\bar{\tau}_{\infty}$ in the plot, at 9.6% (Table 27). Conversely, eight of pit 2's Z scores were below the mean and the remaining two results were only slightly above the plot mean. The difference in pit mean strengths $\bar{\tau}_{\infty}$ from pit 4 to pit 2 was 684 N/m^2, or 1.8 standard deviations s of plot mean strength (Table 27). Based on the chart, neither pit seemed likely to represent the plot mean strength well.

In addition to pits showing uniform departure from the plot mean strength, three pits exhibited an array of Z scores lying both above and below the mean plot strength.

Although not self evident in Figure 16, pit 5 had the pit mean strength $\bar{\tau}_{\infty}$, at 1,490 N/m^2, nearest to the plot mean strength $\bar{\tau}_{\infty(Plot)}$ of 1,482 N/m^2 (Table 27). Pit 5 was followed closely by pit 3, the pit with the most variability in the plot, at CV $\bar{\tau}_{\infty}$ of 30.1%, with a pit mean strength of 1,522 N/m^2 (Table 27). However, that coincidence of high variability of strength within a particular pit with a pit mean strength close to the plot mean strength seemed to be dependent on the results of other pits.

Shear stress produced by the in-situ slab overlying the target weak layer also varied among the pits, but not in the same pattern as strength (Table 28). The rate of variation in the shear stress was modest, with a $CV\bar{\tau}_{Slab}$ of 15.9%, but rather large in actual value (N/m^2), given a plot mean shear stress of 833 N/m^2, and a range of 331 N/m^2. The range

Table 28: Saddle Peak Study Plot (SPSP) 2/18/01 Trials: Shear Stress. Pit Shear Stress, τ_{Slab} (N/m^2), and Coefficient of Variation of Mean Plot Shear Stress, $CV\bar{\tau}_{Slab}$.

Study Plot	Date	τ_{Slab} Pit 1	τ_{Slab} Pit 2	τ_{Slab} Pit 3	τ_{Slab} Pit 4	τ_{Slab} Pit 5	$CV\bar{\tau}_{Slab}$ Plot
SPSP	2/18/01	679	739	730	853	1010	15.9%

of snow water equivalence (SWE) contained in the in-situ slab was 69 mm, from a low of 158 mm at pit 1 to a high of 227 mm at pit 5 (Appendix B). Since this slab represented the accumulation of snow since mid-December, these variations could be attributed to the effects of wind drifting during and between storms rather than variations in actual precipitation, a highly implausible explanation over an area of only 900 m^2. The Saddle

Peak study plot was, among the three plots tested on February 18th, the most sheltered site but, as the SWE data suggest, still not immune from wind drifting effects.

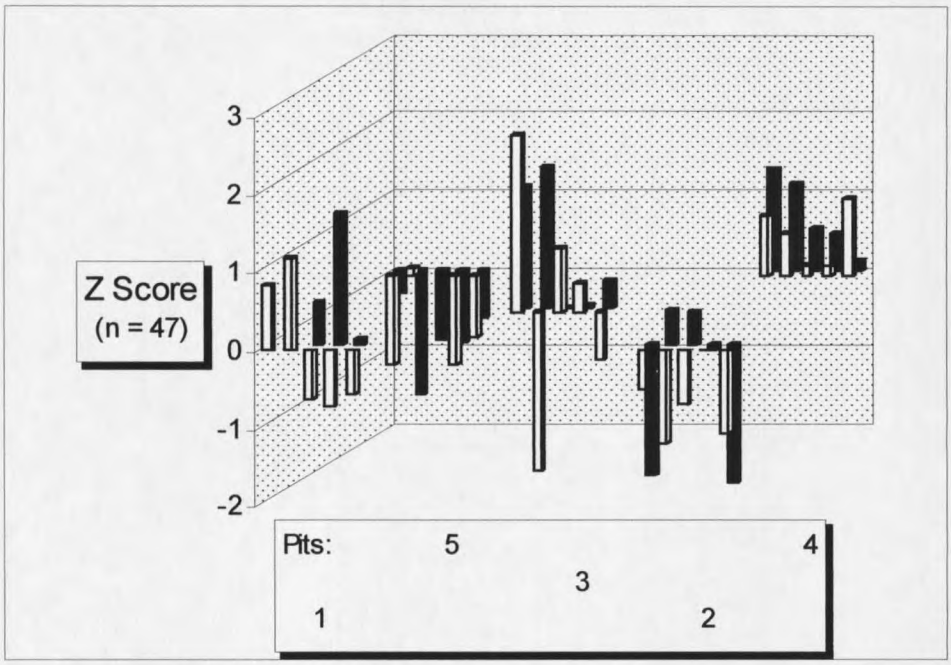
Interestingly, the previously observed pattern (Bradley Meadow 1/27/01 trials) of the pit with the least shear stress exhibiting the weakest strength, and the pit with the most stress having the most strength, did not occur at Saddle Peak, even at these high values. Pit 5 at Saddle Peak had the median strength but the highest stress. Pit 2 had the lowest strength but the median value of shear stress. Perhaps the distribution of stress (primarily a function of slab SWE, given near-equal slope angles) on 2/18/01 was different from the distribution of snow during the early formation of the target weak layer of large faceted grains. Once formed, large faceted grains and their more advanced forms, cup crystals and depth hoar, are known to be more resistant changes in strength due to pressure metamorphism (slab overburden) than other crystal forms.

This complicated pattern of relationships between strength and stress resulted in a different ordering of pit stability (Table 29). The two strongest pits, pits 4 and 3 (Table 27), remain the most stable, in the same order, but the remainder of pits are shuffled. A chart of Z scores of stability (Figure 17) resembles the Z scores of strength Figure 16, but with substantial shifts about the plot mean driven by variations in stress.

Table 29: Saddle Peak Study Plot (SPSP) 2/18/01 Trials: Stability. Pit and Plot Stability, S_{QLCT}, and Coefficient of Variation of Mean Plot Stability, $CV\,\overline{S}_{QLCT(Plot)}$.

Study Plot	Date	S_{QLCT} Pit 1	S_{QLCT} Pit 2	S_{QLCT} Pit 3	S_{QLCT} Pit 4	S_{QLCT} Pit 5	$\overline{S}_{QLCT(Plot)}$
SPSP	2/18/01	2.01	1.57	2.09	2.16	1.48	1.86 $CV = 26.1\%$

Figure 17: Saddle Peak Study Plot 2/18/01 Trials: *Z* Scores of Stability S_{QLCT}. (White bars represent results in the front-row of a given pit and black bars represent back-row results).



For example, at pit 1, relatively higher strength (Table 27) than stress (Table 28), compared to their respective plot means, resulted in a shift upwards in *Z* scores to above-average stability (Figure 17), versus below-average strength (Figure 16). Conversely, at pit 5 comparatively higher stress (the plot maximum) than strength (the plot median) produced the lowest stability in the plot. A similar relationship in pit 2 also resulted in below-average stability, slightly higher than at pit 5 due to a larger absolute difference between strength and stress at pit 2. Pit 3, with the 2nd highest strength and 2nd lowest value of stress made a small shift upward in its distribution of *Z* scores for stability (Figure 17). Further, pit 4, with the second-highest value of stress, shows a shift downward in its *Z* scores of stability (Figure 17) from its *Z* scores for strength (Figure

16), toward the mean. Nonetheless, pit 4 preserves its rank as the most stable pit in the plot with a larger difference between strength (Table 27) and stress (Table 28), of 993 N/m^2, than at pit 3, where the difference was 792 N/m^2.

A review of the chart of Z scores of strength (Figure 16) suggests that pits 2 and 4 depart too much from the plot mean to perform as representatives of plot mean strength. Two-sampled t-tests comparing pit mean strength $\overline{\tau}_{\infty}$ to aggregated plot mean strength $\overline{\tau}_{\infty(Plot)}$ verify this (Table 30). Pit 5 is found most representative of plot mean strength, followed by pit 3. In the Saddle Peak trials, as opposed to the Bradley Meadow 1/27/01 trials, the pit with the most variation in strength (Figure 16, Table 27) was not the most representative of plot mean strength, but was still second-best.

Table 30: Saddle Peak Study Plot (SPSP) 2/18/01 Trials: t-Tests of Strength. Two-Sample t-Test (two-sided, $\alpha = 0.05$) of "No Difference" in Pit Mean Strength ($\overline{\tau}_{\infty}$) and Plot Mean Strength ($\overline{\tau}_{\infty(Plot)}$). (All pits pooled to calculate $\overline{\tau}_{\infty(Plot)}$).

Study Plot	Date	Pit 1 $\overline{\tau}_{\infty}$ to $\overline{\tau}_{\infty(Plot)}$	Pit 2 $\overline{\tau}_{\infty}$ to $\overline{\tau}_{\infty(Plot)}$	Pit 3 $\overline{\tau}_{\infty}$ to $\overline{\tau}_{\infty(Plot)}$	Pit 4 $\overline{\tau}_{\infty}$ to $\overline{\tau}_{\infty(Plot)}$	Pit 5 $\overline{\tau}_{\infty}$ to $\overline{\tau}_{\infty(Plot)}$
SPSP	2/18/01	Fail to Reject $p = 0.417$	Reject $p = 0.014$	Fail to Reject $p = 0.771$	Reject $p = 0.004$	Fail to Reject $p = 0.952$

The t-test analyses of stability (Table 31) differ from the t-test results for strength above (Table 30). In addition to finding pits 2 and 4 unrepresentative of mean plot stability, pit 5 is also rejected. This result is easily recognized in the chart of Z scores of

Table 31: Saddle Peak Study Plot (SPSP) 2/18/01 Trials: *t*-Tests of Stability. Two-Sample *t*-Test (two-sided, $\alpha = 0.05$) of "No Difference" Between Pit Stability S_{QLCT} and Mean Plot Stability $\overline{S}_{QLCT(Plot)}$. (All pits pooled to calculate $\overline{S}_{QLCT(Plot)}$).

Study Plot	Date	Pit 1: S_{QLCT} to $\overline{S}_{QLCT(Plot)}$	Pit 2: S_{QLCT} to $\overline{S}_{QLCT(Plot)}$	Pit 3: S_{QLCT} to $\overline{S}_{QLCT(Plot)}$	Pit 4: S_{QLCT} to $\overline{S}_{QLCT(Plot)}$	Pit 5: S_{QLCT} to $\overline{S}_{QLCT(Plot)}$
SPSP	2/18/01	Fail to Reject $p = 0.418$	Reject $p = 0.083$	Fail to Reject $p = 0.221$	Reject $p = 0.004$	Reject $p = 0.001$

stability, where the entire pit shows scores well below the plot mean (Figure 17). In addition, the evidence in support of the null hypothesis of "no difference" between pit and plot mean stability for pits 1 ($p = 0.418$) and pit 3 ($p = 0.221$) is not particularly strong. Overall, three of five Saddle Peak study plot pits were clearly unrepresentative of mean plot stability, and the remaining two had *t*-statistics suggesting that their means are between 0.8 and 1.2 standard deviations above the plot mean (Appendix F).

Substantial variations in slab thickness, water content, and shear stress were found throughout the plot on 2/18/01. Since wind drift is the likely explanation for these variations, it is reasonable to assume that variations in snowpack height were prevalent throughout the winter. It is not known whether a "typical" spatial pattern of drifting prevails at the Saddle Peak Study Plot, or whether drifting produces ever-changing patterns of thicker/thinner areas within the snowpack. Since the winter of 2000/2001 was notably dry, storms were infrequent, limiting the amount of snow available for wind drifting. Prolonged periods between wind drift events occurred where thinner- and

thicker-than-average areas of the plot snowpack persisted and experienced higher or lower temperature gradients. Once the tested weak layer was buried, those variations in the temperature gradient affecting the weak layer could have produced, over time, wide variations in the strength of the weak layer. As the winter progressed, a generally thicker but still variable increase in the slab thickness would have also contributed varying amounts of shear stress, and pressure-induced metamorphism, to the snowpack processes affecting the weak layer. In short, the cumulative effects of wind drift at the Saddle Peak Study Plot may decrease the likelihood, over time, of finding a single snowpit that represents the weak layer or slab conditions extant over the plot once a weak layer is buried.

This explanation could explain the kind of pit-to-pit differences between pits 2 and 4 but it does not explain how the strongest and weakest QLCT results found in the entire 900 m^2 plot could occur within 50 cm of each other, in the same pit. In the context of pit 3, the result in cell 2 appears to be an "outlier", perhaps the result of disturbance during the preparation of the QLCT (Figure 16). However, the pit 3 cell 2 result was more "typical" of several pit 2 results, 12 meters away, if still the weakest. Similarly, pit 3 cell 1 was more "typical" of the strength observed in pit 4, also 12 meters away, if still the strongest. Thus, what appeared to be weak/strong outlier results in a given pit simply reflected a larger-scale range in strengths present throughout the plot. Variations in slab thickness of sufficient magnitude to account for these differences in strength are not plausible over these cell-to-cell distances of 50 cm. Further, other terrain-based variables, such as slope aspect, or substrate, were constant throughout the plot. Some

other, undetermined snowpack process appears to have controlled the scale of variation in snowpack strength at pit 3 in the Saddle Peak Study Plot on 2/18/01.

Bradley Meadow Study Plot Trials - 2/18/01. These trials proved to be as problematic as the Baldy Mountain trials eight kilometers to the south. Team leader Jeff Deems, assisted by Jim Rasmussen and Mark Schaffer, did locate the 2/18/01 target weak layer of large (1-2 mm) facets in Profile #17 (Appendix H) at pit 1, but at a height of 41 cm above the ground rather than at 20-30 cm, as observed at Bradley Meadow in the pre-trials Profile #14 conducted on 2/16/01 (Appendix H). Pit 1 was unexpectedly deep, with a total snow depth of 215 cm, over one meter deeper than observed at pit 1 at either Baldy Mountain (111 cm, Profile #15) or Saddle Peak (102 cm, Profile #16) (Appendix H). Pit 1's (Profile #17) total depth on 2/18/01 was also 77 cm deeper than Profile #14 of 2/16/01 (Appendix H), dug only 20-30 meters distant from pit 1. Even with nothing more than this evidence, Bradley Meadow revealed major variations in snowpack characteristics.

A summary of the pit mean strengths and their variation reveals the magnitude of variation in strengths eventually observed at Bradley Meadow (Table 32). However, these data underestimate the actual variation since all ten stability sampling cells at pit 1 proved to be too strong to measure with the QLCT equipment at hand, and no column failures could be observed. At the maximum range of the test equipment used, the strength at all ten of the cells in pit 1 exceeded 2,660 N/m^2, but their actual strength and variation was undetermined. And, at pit 3, eight tests exceeded the QLCT measurement range. At pit 5, five tests were not logged due to ambiguity in their point of fracture in a

Table 32: Bradley Meadow Study Plot (BMSP) 2/18/01 Trials: QLCT Results. Number of Valid Tests (n), Mean Strength ($\overline{\tau}_{\infty}$) in N/m^2, Standard Deviation (s) in N/m^2, and Coefficient of Variation of strength ($CV\overline{\tau}_{\infty}$), by Pit and Plot.

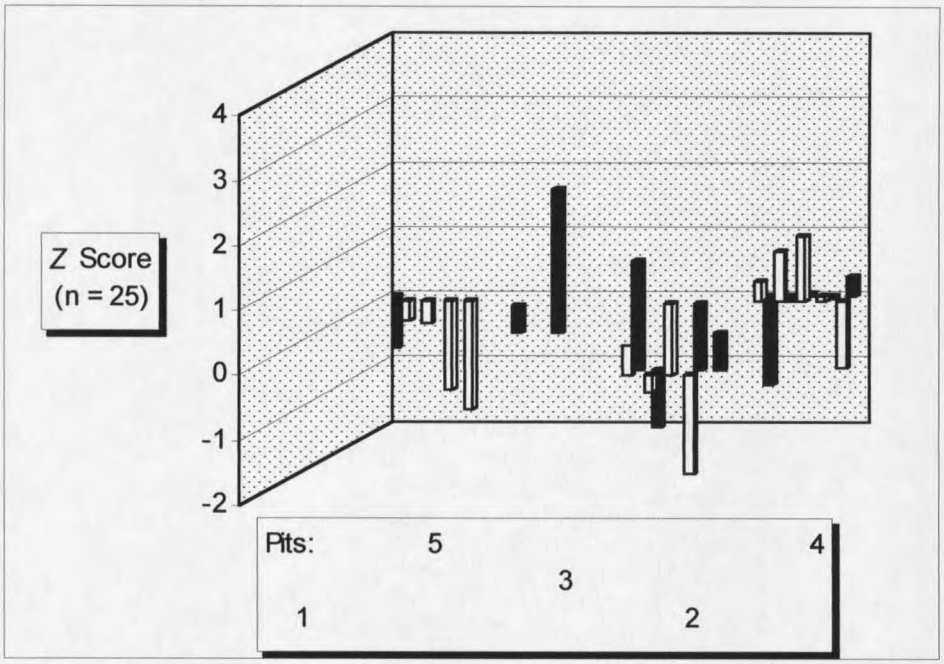
Study Plot	Date		Pit 1	Pit 2	Pit 3	Pit 4	Pit 5	Plot
BMSP	2/18/01	n	*None*	8	2	10	5	25
		$\overline{\tau}_{\infty}$	*> 2,660*	1,746	2,131	1,650	1,338	1,657
		s	*NA*	376	443	253	212	351
		$CV\overline{\tau}_{\infty}$	*NA*	21.6%	20.8%	15.3%	15.9%	21.2%

layer of basal facets much thicker than observed at pit 1, and only tests that had clearly failed near the top of the layer of faceted grains were logged. Given the number of exceedingly strong tests, and rejected tests, actual variability in strength was undetermined but can reasonably be presumed to be underestimated by a $CV\overline{\tau}_{\infty(Plot)}$ of only 21.2%. Since no measure of variance was available for the missing data, and could not reasonably be estimated, the minimum strength value of 2,660 N/m^2 was not applied to the ten pit 1 cells or the missing data in pit 5.

A chart of the twenty-five valid Z scores of strength highlighted the amount of missing data (Figure 18). The data collection team was unable to obtain any strength data for the subject weak layer at pit 1, only five valid results at pit 5, two at pit 3, and eight results were logged at pit 2. Only pit 4 produced a complete array of ten valid QLCT results. Therefore, only twenty-five valid Z scores were calculated, out of a possible fifty. Since 40% of the valid results were at pit 4, that single pit had a large influence on determining the mean strength of the twenty-five valid tests and, as a consequence, eight

of the ten results at pit 4 exhibited Z scores within one standard deviation of the plot mean strength (Appendix B).

Figure 18: Bradley Meadow Study Plot 2/18/01 Trials: Z Scores of Strength τ_{∞}. (White bars represent results in the front-row of a given pit and black bars represent back-row results.)



Pit 2 exhibited more variability in strength than pit 4, at $CV\overline{\tau}_{\infty}$ values of 21.6% and 15.3%, respectively (Table 32), and this was also seen in the larger range of Z scores of between cell 4 and cell 6 at pit 2 (Figure 18). Cell 5 in pit 5 produced the weakest valid result in the plot, with a Z score of –1.688 (Appendix B) and an actual strength of 1,066 N/m^2 (Appendix B), and cell 8 in pit 3 produced the measured maximum, at 2,419 N/m^2 (Appendix B). This established a measured range in strength of approximately 1,353 N/m^2. Assuming that strength in pit 1 was at least 2,660 N/m^2, the range in strength was

estimated to be at least 1,594 N/m^2. By either standard, the range of variation in strength observed at Bradley Meadow that day seemed to render 'plot mean strength' meaningless information for an avalanche forecaster concerned with estimating how much new-snow SWE would constitute a critical load for the snowpack.

Shear stress produced by the in-situ slab at Bradley meadow exhibited similar variation (Table 33). Incomplete slab data at pit 5 prevented the calculation of τ_{Slab} there. Nonetheless, the four pits for which τ_{Slab} was obtained presented a range in shear stress of 1,386 N/m^2, comparable to the low estimate of the range in strength.

Table 33: Bradley Meadow Study Plot (BMSP) 2/18/01 Trials: Shear Stress. Pit Shear Stress, τ_{Slab} (N/m^2), and Coefficient of Variation of Mean Plot Shear Stress, $CV\overline{\tau}_{Slab}$.

Study Plot	Date	τ_{Slab} Pit 1	τ_{Slab} Pit 2	τ_{Slab} Pit 3	τ_{Slab} Pit 4	τ_{Slab} Pit 5	$CV\overline{\tau}_{Slab}$ Plot
BMSP	2/18/01	2,335	1,199	1,676	949	Missing	47.9%

With no valid strength data for pit 1, and missing stress data at pit 2, and only two valid strength results at pit 3 (which preclude a reasonable estimate of variance at pit 3), stability ratios S_{QLCT} could be computed for only pits 2 and 4 (Table 34). Clearly, the amount of missing data compromised the calculation of a plot mean stability, and its variability. The value of $CV\overline{S}_{QLCT(Plot)}$ shown was considered an underestimate of plot mean stability. No chart of Z scores of stability was prepared due to the preponderance of missing data and the consequent skewing of plot mean stability.

Table 34: Bradley Meadow Study Plot (BMSP) 2/18/01 Trials: Stability. Pit and Plot Stability, S_{QLCT}, and Coefficient of Variation of Mean Plot Stability, $CV\,\overline{S}_{QLCT(Plot)}$.

Study Plot	Date	S_{QLCT} Pit 1	S_{QLCT} Pit 2	S_{QLCT} Pit 3	S_{QLCT} Pit 4	S_{QLCT} Pit 5	$\overline{S}_{QLCT(Plot)}$
BMSP	2/18/01	*nr*	1.46	*nr*	1.74	*nr*	1.59 $CV = 20.4\%$

Setting aside the influence of non-results at pit 1 and 5, strength data from pits 2, 3, 4 and 5 were evaluated for differences between their measured pit mean strength and the measured plot mean strength using the usual two-sample *t*-test method (Table 35). Predictably, pits 4 and 2, which contain 72% of the valid results at the plot, were found to be representative of the *measured* plot mean strength. However, in the absence of fifteen additional test cells exceeding 2,660 N/m^2 in strength, and with unknown variance, these *t*-test results were inconclusive.

Table 35: Bradley Meadow Study Plot (BMSP) 2/18/01 Trials: *t*-Tests of Strength. Two-Sample *t*-Test (two-sided, $\alpha = 0.05$) of "No Difference" in Pit Mean Strength ($\overline{\tau}_{\infty}$) and Plot Mean Strength ($\overline{\tau}_{\infty(Plot)}$). (All pits pooled to calculate $\overline{\tau}_{\infty(Plot)}$).

Study Plot	Date	Pit 1 $\overline{\tau}_{\infty}$ to $\overline{\tau}_{\infty(Plot)}$	Pit 2 $\overline{\tau}_{\infty}$ to $\overline{\tau}_{\infty(Plot)}$	Pit 3 $\overline{\tau}_{\infty}$ to $\overline{\tau}_{\infty(Plot)}$	Pit 4 $\overline{\tau}_{\infty}$ to $\overline{\tau}_{\infty(Plot)}$	Pit 5 $\overline{\tau}_{\infty}$ to $\overline{\tau}_{\infty(Plot)}$
BMSP	2/18/01	*No valid results*	Fail to Reject $p = 0.535$	Reject $p = 0.091$	Fail to Reject $p = 0.968$	Reject $p = 0.0062$

No *t*-test analyses of pit-to-plot stability were prepared for the reasons described above regarding presentation of Z scores of stability. This set of compromised analyses

for the 2/18/01 trials suggested, and on-site common sense indicated to the observers, that what appeared to experienced avalanche forecasters to be a potentially nominal site for a study plot had proven to be exactly the opposite.

On 2/18/01, Bradley Meadow study plot was clearly *not* a site where a single snowpit would reliably represent the strength or stability of the entire study plot. Of all the factors that might have been responsible for the variation observed on 2/18/01, the effects of wind drifting was considered the most likely explanation, particularly since the snow overlying the weak layer was two months old and subject to many significant wind drifting events. Previous research at Bradley Meadow has shown wind drifting to be a significant factor in the spatial variation of snowpack properties (Birkeland et al., 1995). The age of the weak layer itself is another likely cause of the observed variability. No skier or other disturbance was observed at the study plot prior to the trials.

Bradley Meadow Study Plot Trials - 3/17/01. The final 900 m^2 study plot stability-sampling trials of the 2000/2001 winter was conducted in a 9 cm layer of small (0.5-1.0 mm), near-surface faceted crystals, lying immediately beneath a thin (1 mm), frozen-rain ice crust lying 10 cm below the snow surface. These trials were performed in an undisturbed area uphill and north of the plot used for the 2/18/01 trials. I prepared and conducted all QLCTs, assisted by Karl Birkeland and Dan Miller.

Numerous preliminary QLCT were required to refine a technique for cutting through the thin ice crust with a minimum of disturbance to the delicate crust/weak layer interface. The surface mode of the QLCT was employed using the large load plate (area 0.08 m^2). While some disturbance to the weak layer/ice crust interface at the edges of the

isolated column was unavoidable, I attempted to maintain consistent technique while cutting the column to create a constant level of disturbance throughout the trials. None-the-less, four test cells were ruined during preparation. The forty-six valid QLCT results logged exhibited shear fractures of consistent Q1 quality, approximately 1 cm below the ice crust. Interestingly, five tests, two in pit 4, and three in pit 5, produced "double" fractures in the isolated column, one in the target weak layer below the ice crust, and a second, simultaneous result in the layer of large facets tested during the 2/18/01 trials.

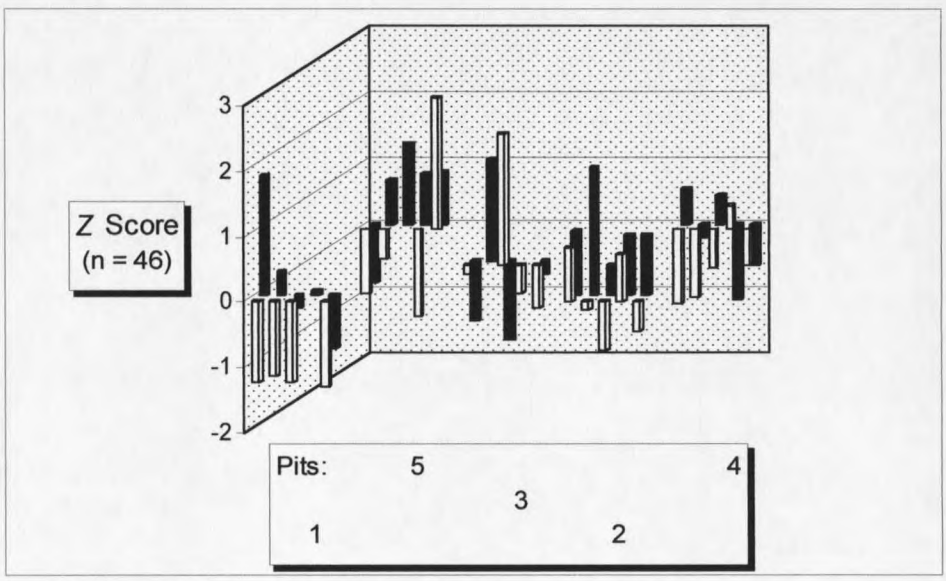
An examination of variations in pit and plot mean strengths revealed substantial coefficients of variation of 19-32% within individual pits, and equaling 27% plot-wide (Table 36). Given the young age of the weak layer of near-surface facets (formed within the previous ten days), and the uniformity of the ice crust and overlying slab (see below), some unknown portion of this variation was attributed to disturbance during QLCT column preparation, as discussed. The effects of prolonged burial or widely varying shear stress that could be expected with a deeply buried weak layer did not seem to be a plausible explanation for this variability.

Table 36: Bradley Meadow Study Plot (BMSP) 3/17/01 Trials: QLCT Results. Number of Valid Tests (n), Mean Strength ($\bar{\tau}_\infty$) in N/m^2, Standard Deviation (s) in N/m^2, and Coefficient of Variation of strength ($CV\bar{\tau}_\infty$), by Pit and Plot.

Study Plot	Date		Pit 1	Pit 2	Pit 3	Pit 4	Pit 5	Plot
BMSP	3/17/01	n	9	10	8	10	9	46
		$\bar{\tau}_\infty$	386	496	434	389	459	433
		s	123	93	136	77	135	117
		$CV\bar{\tau}_\infty$	31.9%	18.8%	31.4%	19.8%	29.5%	27.0%

A chart of Z scores of strength (Figure 19) revealed a generally random scatter of scores about the plot mean, with no pit exhibiting uniformly above- or below-average results. Most pits displayed a substantial range in Z scores, from a plot low of 1.699 standard deviations at pit 4 to a plot high of 3.365 standard deviations at pit 5 (Appendix B). Pit 3, the pit with the second-highest range in Z scores by 0.116 standard deviations (Appendix B), and the second-highest $CV\,\bar{\tau}_{\infty}$ (by 0.5%), had the pit mean strength $\bar{\tau}_{\infty}$, at 434 N/m^2, closest to the plot mean strength $\bar{\tau}_{\infty(Plot)}$ of 433 N/m^2 (Table 36). The chart of Z scores may show evidence of changing QLCT column preparation technique during the trials. Pit 1, performed first, yielded below-average strength, particularly in the first set of five tests (front row) where one test cell (4) was ruined during preparation. The

Figure 19: Bradley Meadow Study Plot 3/17/01 Trials: Z Scores of Strength τ_{∞}. (White bars represent results in the front-row of a given pit and black bars represent back-row results.)



second row began, in cell 6, with a substantially above-average result. Those pit 1 results may show "improving" technique whereby less disturbance was created to the weak layer while cutting through the ice crust. This "skill" in column preparation was then perhaps sustained at a relatively consistent level as the trials progressed, with pits 2, 3, and 5, in that order, until fatigue or time pressures may have resulted in lower skill and more disturbance, producing one ruined test cell (3) and below-average mean pit strength, in pit 4, the final pit.

Variations in shear stress among the pits was extremely small, as previously noted (Table 37). In fact, the in-situ snow above the weak layer exhibited the least variability in shear stress observed during the 2000/2001 winter trials at $CV\overline{\tau}_{Slab}$ of 1.9%. This was attributed to the absence of wind during and after Storm #8, on March 15th and 16th, depositing the layer of 10 cm (settled) of new snow above the frozen-rain crust with remarkable uniformity. Slope angles were similar at all five pits.

Table 37: Bradley Meadow Study Plot (BMSP) 3/17/01 Trials: Shear Stress. Pit Shear Stress, τ_{Slab} (N/m^2), and Coefficient of Variation of Mean Plot Shear Stress, $CV\overline{\tau}_{Slab}$.

Study Plot	Date	τ_{Slab} Pit 1	τ_{Slab} Pit 2	τ_{Slab} Pit 3	τ_{Slab} Pit 4	τ_{Slab} Pit 5	$CV\overline{\tau}_{Slab}$ Plot
BMSP	3/17/01	137	141	137	138	142	1.9%

With nearly constant shear stress across the study plot, variations in stability were driven by variations in strength among the pits, and the plot-wide coefficient of variation

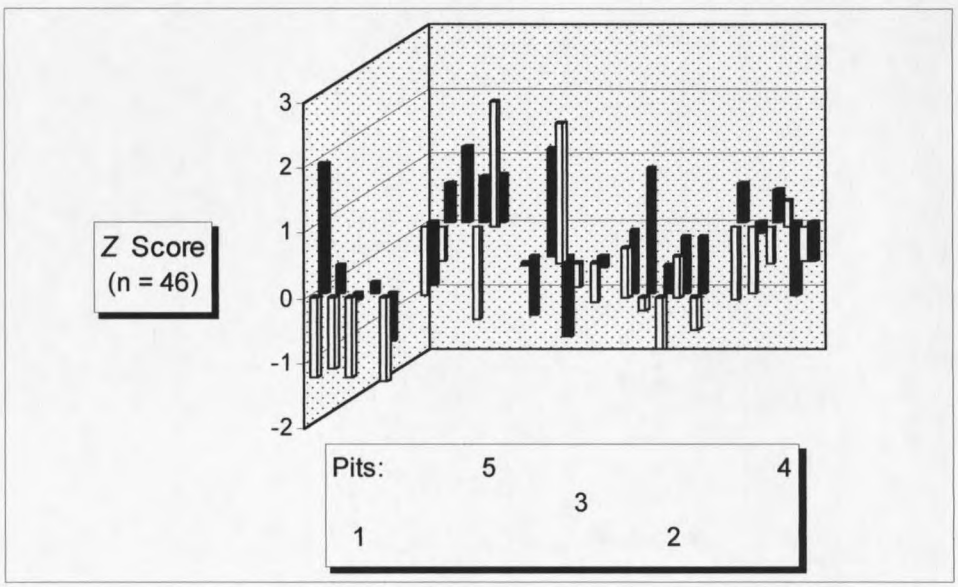
in stability, $CV\ \overline{S}_{QLCT(Plot)}$, of 26.6% (Table 38) was almost identical to the plot-wide variability of strength, $CV\overline{\tau}_{\infty(Plot)}$, of 27.0% (Table 36).

Table 38: Bradley Meadow Study Plot (BMSP) 3/17/01 Trials: Stability. Pit and Plot Stability, S_{QLCT}, and Coefficient of Variation of Mean Plot Stability, $CV\,\overline{S}_{QLCT(Plot)}$.

Study Plot	Date	S_{QLCT} Pit 1	S_{QLCT} Pit 2	S_{QLCT} Pit 3	S_{QLCT} Pit 4	S_{QLCT} Pit 5	$\overline{S}_{QLCT(Plot)}$
BMSP	3/17/01	2.82	3.52	3.18	2.82	3.22	3.11 $CV = 26.6\%$

With near-constant shear stress plot-wide, a chart of Z scores of stability (Figure 20) was virtually identical to the chart of Z scores of strength (Figure 19). These charts reveal no apparent difference between their patterns of strength and stability.

Figure 20: Bradley Meadow Study Plot 3/17/01 Trials: Z Scores of Stability S_{QLCT}. (White bars represent results in the front-row of a given pit and black bars represent back-row results).



Given a pit mean strength $\overline{\tau}_{\infty}$ within 1 N/m^2 of the plot mean strength $\overline{\tau}_{\infty(Plot)}$ (Table 36), pit 3 seemed assured of being a strong representative of plot-wide strength and *t*-test analyses of the strength results confirmed this (Table 39). The *t*-statistic for pit 5 suggests that it, too, represented plot mean strength well, if not as well as pit 3. In fact, the *t*-test analyses failed to find any pit unrepresentative of plot mean strength, although the evidence for the null hypothesis of "no difference" between $\overline{\tau}_{\infty}$ and $\overline{\tau}_{\infty(Plot)}$ was not particularly strong for pits 1, 2 or 4.

Table 39: Bradley Meadow Study Plot (BMSP) 3/17/01 Trials: *t*-Tests of Strength. Two-Sample *t*-Test (two-sided, $\alpha = 0.05$) of "No Difference" in Pit Mean Strength ($\overline{\tau}_{\infty}$) and Plot Mean Strength ($\overline{\tau}_{\infty(Plot)}$). (All pits pooled to calculate $\overline{\tau}_{\infty(Plot)}$).

Study Plot	Date	Pit 1 $\overline{\tau}_{\infty}$ to $\overline{\tau}_{\infty(Plot)}$	Pit 2 $\overline{\tau}_{\infty}$ to $\overline{\tau}_{\infty(Plot)}$	Pit 3 $\overline{\tau}_{\infty}$ to $\overline{\tau}_{\infty(Plot)}$	Pit 4 $\overline{\tau}_{\infty}$ to $\overline{\tau}_{\infty(Plot)}$	Pit 5 $\overline{\tau}_{\infty}$ to $\overline{\tau}_{\infty(Plot)}$
BMSP	3/17/01	Fail to Reject $p = 0.273$	Fail to Reject $p = 0.118$	Fail to Reject $p = 0.983$	Fail to Reject $p = 0.260$	Fail to Reject $p = 0.555$

As the preceding analyses of variations in strength, stress and stability showed, *t*-tests of pit-to-plot differences also found every pit representative of mean plot stability (Table 40). In all cases except pit 3, the evidence for the representative-ness of each pit was slightly stronger for stability than for strength. Pit 3 was the most representative of plot-wide stability, but pit 5 produced a *p*-value nearly as large as pit 3. Pit 2 remained the weakest representative of plot strength or stability with *t*-statistics indicating pit means 1.590 and 1.456 standard deviations above plot means, respectively (Appendix D).

Table 40: Bradley Meadow Study Plot (BMSP) 3/17/01 Trials: *t*-Tests of Stability. Two-Sample *t*-Test (two-sided, $\alpha = 0.05$) of "No Difference" Between Pit Stability S_{QLCT} and Mean Plot Stability $\overline{S}_{QLCT(Plot)}$. (All pits pooled to calculate $\overline{S}_{QLCT(Plot)}$).

Study Plot	Date	Pit 1: S_{QLCT} to $\overline{S}_{QLCT(Plot)}$	Pit 2: S_{QLCT} to $\overline{S}_{QLCT(Plot)}$	Pit 3: S_{QLCT} to $\overline{S}_{QLCT(Plot)}$	Pit 4: S_{QLCT} to $\overline{S}_{QLCT(Plot)}$	Pit 5: S_{QLCT} to $\overline{S}_{QLCT(Plot)}$
BMSP	3/17/01	Fail to Reject $p = 0.342$	Fail to Reject $p = 0.151$	Fail to Reject $p = 0.850$	Fail to Reject $p = 0.292$	Fail to Reject $p = 0.722$

The Bradley Meadow 3/17/01 stability sampling trials revealed the inherent difficulty of sampling snowpack stability without altering that stability in the course of conducting the measurements. While all of the stability sampling trials were subject to variations in QLCT technique, the delicate bond between the ice crust and the weak layer in this particular trial posed, by far, the most difficult conditions encountered during the winter of 2000/2001. (Any stability test involving the isolation of a column of snow would have encountered the same difficulties). The results of the 3/17/01 Bradley Meadow trial undoubtedly contained measurements of both variations in measurement technique and variations in strength that could not be quantified separately. Given that qualification, these trials produced the only set of five pits found representative of their study plot, despite variations introduced by the sampling method. This was, in fact, the outcome expected by the sampling team, given the conditions leading to the formation of the weak layer, ice crust, and new-snow slab, and the "young" age of the entire configuration.

Intra-Study-Plot Variability

Comparisons of plot-wide strength, in-situ slab-generated shear stress, and stability were prepared for all simultaneously conducted study plot trials in order to evaluate whether one study plot represented stability characteristics at other study plots in its avalanche region.

Bridger Range Study Plot Trials - 2/18/01. Three stability-sampling study plots trials were conducted simultaneously in the Bridger Range on 2/18/01, at the Baldy Mountain, Saddle Peak, and Bradley Meadow study plots, as described in the preceding discussion of inter-plot variation in stability. Those analyses found that significant variability existed at each plot. That variability was of sufficient magnitude to conclude that the heterogeneity of stability within those plots was unlikely to be represented by a single pit. The following analyses investigated whether the variability of stability factors displayed at one of those plots was representative of the variability at another plot.

A summary of mean plot strength and coefficient of variation was prepared for the three plots (Table 41). The similarity of $CV\bar{\tau}_{\infty(Plot)}$ values is misleading since these only represented variability in the weak layer targeted for the trials. At Baldy Mountain four additional weak layers were found, adding additional variation. At Bradley Meadow fifteen QLCT test cells were too strong to measure and no results were logged, thereby lowering the overall strength and variability recorded at the plot.

Table 41: Bridger Range Study Plots 2/18/01 Trials: Plot Mean Strength. Number of Valid QLCT Tests (n), Plot Mean Strength ($\overline{\tau}_{\infty(Plot)}$) in N/m^2, Standard Deviation (s) in N/m^2, and Plot Coefficient of Variation of Strength ($CV\overline{\tau}_{\infty(Plot)}$).

Trials Date	*Strength*	Baldy Mountain	Saddle Peak	Bradley Meadow
2/18/01	n	19	47	25
	$\overline{\tau}_{\infty(Plot)}$	1,125 N/m^2	1,482 N/m^2	1,655 N/m^2
	s	289 N/m^2	375 N/m^2	349 N/m^2
	$CV\overline{\tau}_{\infty(Plot)}$	25.7%	25.3%	21.0%

Variation in the mean shear stress produced by the in-situ slab above the target weak layer at each plot showed similar variability (Table 42). The Bradley Meadow study plot presented not only the highest value of mean shear stress but also the largest coefficient of variation, triple that of the Saddle Peak study plot. The measurements of shear stress were considered more reliable than the measures of plot-wide strength since no measurements of stress were missing at Baldy Mountain or Saddle Peak and only one measurement (out of five) was missing at Bradley Meadow.

Table 42: Bridger Range Study Plots 2/18/01 Trials: Plot Mean Shear Stress. Mean Stress $\overline{\tau}_{Slab(Plot)}$ (N/m^2), and Coefficient of Variation of Mean Plot Shear Stress, $CV\overline{\tau}_{Slab(Plot)}$.

Trials Date	*Shear Stress*	Baldy Mountain	Saddle Peak	Bradley Meadow
2/18/01	$\overline{\tau}_{Slab(Plot)}$	702 N/m^2	833 N/m^2	1,274 N/m^2
	$CV\overline{\tau}_{Slab(Plot)}$	27.8%	15.9%	47.9%

A summary of mean plot stability and its variability is presented (Table 43), but with the same caveats applied to the summary of strength above (Table 41). At the Baldy

Table 43: Bridger Range Study Plots 2/18/01 Trials: Plot Mean Stability. Mean Stability $\overline{S}_{QLCT(Plot)}$ (unit-less ratio), and Coefficient of Variation of Mean Plot Stability, $CV\ \overline{S}_{QLCT(Plot)}$.

Trials Date	*Stability*	Baldy Mountain	Saddle Peak	Bradley Meadow
2/18/01	$\overline{S}_{QLCT(Plot)}$	1.79	1.86	1.58
	$CV\ \overline{S}_{QLCT(Plot)}$	20.1%	26.1%	20.4%

Mountain study plot the stability ratio represents only the nineteen results from the targeted weak layer and does not account for the stability of the four additional weak layers found there. At Bradley Meadow, since plot-wide strength was substantially underestimated by the valid (actually measured) results, due to the fifteen missing results showing strengths of at least 2,660 N/m2, the numerator of the stability ratio is also underestimated. Therefore, the value of the ratio is smaller (less stable) than would have been the case had a complete set of strength measurements been obtained.

Two-sample *t*-test analyses (Table 44) evaluated the hypothesis of "no difference" in mean strength between each of these three study plot's mean strength $\overline{\tau}_{\infty(Plot)}$, despite the many flaws in the data and the tempting, common-sense, conclusion that the three plots had clearly different mean strengths and variations of strength. The results indicated that none of the plots could represent the strength of another plot in spite of known differences in strength that the evaluated data did not capture. Had all the differences in

strength at Baldy Mountain and Bradley Meadow been accounted for by the data evaluated by the *t*-test the "reject" result would certainly have been even more conclusive.

Table 44: Bridger Range Study Plots 2/18/01 Trials: *t*-Tests of Strength. Plot-to-Plot, Two-Sample *t*-Test (two-sided, $\alpha = 0.05$) of "No Difference" between Plot Mean Strengths $\overline{\tau}_{\infty(Plot)}$.

Trials Date	*t-Test*	Baldy Mountain to Saddle Peak	Saddle Peak to Bradley Meadow	Baldy Mountain to Bradley Meadow
2/18/01	*t*-Test Result	Reject	Reject	Reject
	p Value	0.000	0.000	0.060

Finally, leaving no stone unturned, *t*-test analyses of differences in mean plot stability were performed (Table 45). Given the aforementioned flaws in the data being evaluated

Table 45: Bridger Range Study Plots, 2/18/01 Trials: *t*-Tests of Stability. Plot-to-Plot, Two-Sample *t*-Test (two-sided, $\alpha = 0.05$) of "No Difference" between Plot Mean Stability $\overline{S}_{QLCT(Plot)}$.

Trials Date	*t-Test*	Baldy Mountain to Saddle Peak	Saddle Peak to Bradley Meadow	Baldy Mountain to Bradley Meadow
2/18/01	*t*-Test Result	Fail to Reject	Reject	Reject
	p Value	0.553	0.019	0.059

for Baldy Mountain study plot, it was not surprising that no significant difference was found between the mean stability at Baldy Mountain and the mean stability at Saddle Peak. Only results from the targeted weak layer at Baldy Mountain were included in the *t*-test analysis, ignoring the other thirty-one results at Baldy Mountain from four

additional weak layer/slab combinations. That result was of interest, since it found significant similarity in stability in the targeted weak layer/slab ensemble at both study plots. However, I concluded that, in its totality, mean stability at Baldy Mountain was not representative of mean stability at Saddle Peak, and vice-versa, since the majority of stability-sampling results at Baldy Mountain found weak layer/slab ensembles different from the forty-seven valid tests produced in the target weak layer and slab at Saddle Peak.

Significant differences in stability were found between Saddle Peak and Bradley Meadow, and between Baldy Mountain and Bradley Meadow, despite the absence from the data evaluated by the *t*-tests of fifteen strength measurements exceeding 2,660 N/m^2 at Bradley. Had the additional fifteen tests been measurable, the magnitude of difference in means between the two plots would have increased.

Summary: In summary, none of the three Bridger Range study plots sampled on 2/18/01 were found representative of either plot-wide strength or stability at any other study plot on that day. A clue to the possible cause of this variability was found in the steadily increasing amount of mean plot shear stress produced by the in-situ slab, varying from 702 N/m^2 at Baldy Mountain, to 833 N/m^2 at Saddle Peak, to 1,274 N/m^2 at Bradley Meadow. Since all three study plots shared similar slope angles (25-31°), those differences in shear stress were primarily a function of differences in mean slab SWE between those three study plots, at 147 mm, 191 mm and 270 mm, respectively, for a maximum difference of 127 mm. A maximum difference in elevation (Baldy Mountain to Bradley Meadow) of 166 meters would account for approximately 35 mm difference in

SWE between the two plots, according to the SWE analysis conducted on 1/5 and 1/6/01 (Equation 5, page 50).

Therefore, 88 mm of the difference in SWE was unaccounted for by differences in elevation (Δz effect) and, instead, may have represented evidence of a spatial variation in SWE caused by differences in location along the north/south axis of the Bridger Range study area. The possibility of such a Δy effect on precipitation was anticipated during development of the GIS stability model, based on the observations of experienced Bridger Range observers.

Alternatively, the differences may have been the result of underestimated differences in the plots' exposure to wind drift, just as the substantial variations in SWE at individual plots were attributed to local wind drifting. No study plot wind data was collected to refute or support this hypothesis. No matter what caused the progressive increases in SWE and shear stress (Table 42) among the plots, however, those greater shear stresses were considered a plausible explanation for the progressively greater strength (Table 41) also found by moving from south (Baldy Mountain) to north (Bradley Meadow) through the three plots.

Finally, despite all the differences in strength, stress, and stability among the three plots, the target weak layer of large, faceted grains was found at all three sampled study plots that day, and at effectively the same stratigraphic location within the snowpack. The target weak layer was also found at the fourth, un-sampled study plot at Fairy Lake. This was a comparatively thick weak layer formed over the course of many weeks. As such, it was more likely that this particular weak layer would be found at multiple

locations than would have been other thinner, more easily disturbed types of weak layers such as surface hoar, or a shallow layer of small faceted grains. Even so, while none of the plots were found representative of the strength or stability of another plot on 2/18/01, it could be argued (empirically) that each plot provided evidence that the target weak layer was present throughout the study area that day, at the study plots' elevations and slope aspects. On the other hand, neither the Saddle Peak nor Bradley Meadow study plot provided any indication that four additional weak layers, besides the targeted weak layer, would be found at the Baldy Mountain plot and frequently prove more sensitive than the target weak layer. Thus, even the ability of study plots to reveal the simple absence or presence of weak layers, on 2/18/01, was confounded by spatial variations.

Winter of 2001/2002

Four 900 m^2 plot stability-sampling trials were conducted during the 2001/2002 season. Due to unusually stable conditions throughout early- and mid-winter, no trials were performed at Bridger Range study plots. Instead, one stability-sampling trial was performed at a slope in Middle Basin (Figure 3) near Big Sky, Montana, and three trials were conducted near and within an avalanche path south of Lionhead Peak (Figure 3), on the Idaho/Montana border west of West Yellowstone, Montana.

Weather and Snowpack

The extremely dry summer and fall drought of 2001 in Southwest Montana was finally broken by a multi-day rain and snowstorm beginning October 11th. A visit to the Bridger Range Bradley Meadow Study Plot on October 16th, to install study plot

perimeter signs, found 40-60 cm of dense, moist snow covering the plot. Subsequent dry and warm weather produced repeated melt-freeze cycles in this new snow layer, slowly ablating and consolidating the snowpack in the Bridger Range study area and eventually melting south-facing slopes and lower elevation east-facing slopes back to bare ground by month-end. By November 19th, under continued drought and unusually warm temperatures, the northeast-facing Baldy Mountain Study Plot had partially melted to bare ground, the Saddle Peak Study Plot remained snow-covered, and the Bradley Meadow Study Plot had begun to show vegetation through no more than 10-15 cm of snow-cover. The snow-cover at the Fairy Lake Study Plot was not observed but was presumed to resemble the coverage at Bradley Meadow.

The second notable precipitation event of the season, Storm #2, began November 21st and continued through the 25th, and totaled 64 cm of new snow containing 61 mm SWE at the Bridger Bowl Ski Area's Alpine Study Plot. A series of small storms followed, and December produced 80 mm of SWE at the Bridger Bowl Ski Area's Alpine Study Plot, or 85% of the 1984-2001 monthly average (Table 2). By January 7th the total depth at the Bradley Meadow Study Plot was 116 cm and no notable weak layers were present in the snowpack (Profile 7, Appendix I). Despite experiencing a record monthly snowfall in January, at 98.5", no persistent weak layers formed in the Bridger Range during the month of January. Avalanching was limited to direct-action activity within new-snow layers only. Given the absence of conditions favorable to data collection in the Bridger Range study area, other locations south of the Bozeman area were utilized for the four

trials performed during the 2001/2002 season. A summary of each trial is presented with the discussion of those trials' results.

Inter-Study-Plot Variability

Analysis of the four separate stability sampling trials performed during the winter of 2001/2002 revealed additional variety in the magnitude and patterns of variations in snowpack stability previously observed during the 2000/2001 season. Detailed results for all 2001/2002 season stability-sampling trials, including all valid QLCT τ_{∞} results, Z scores, S_{QLCT} values, and τ_{Slab} data, are provided in chronological order in Appendix C. All 2001/2002 snowpack profiles referred to are provided in chronological order in Appendix I. Complete 2001/2002 results for *t*-tests of snowpack strength are shown in Appendix E, and for *t*-tests of snowpack stability in Appendix G.

Middle Basin Trials – 12/7/01. The first 900 m^2 stability-sampling trial of the 2001/2002 season was conducted on a large, generally planar, east-facing, 30° open slope on the shoulder separating the Beehive Basin and Middle and Bear Basin drainages of the Spanish Peaks portion of the Madison Range (Figure 3). The slope is locally referred to as "Spanky's" run. I performed all QLCT tests, assisted by Karl Birkeland. Snow Profile #2 (Appendix I) revealed two potential weak layers on either side of a porous crust eroded by temperature-gradient faceting. Preliminary shear tests suggested that either the upper weakness "A" just above that crust (at the interface between 0.5-1 mm faceted grains at the base of the 50-55 cm overlying slab and the crust) or the lower weakness "B" just below the crust (a layer of 2-3 mm, very friable large facets and cups)

could produce the initial fracture during QLCT tests. In fact, subsequent QLCTs in the Profile #2 pit (pit 1 in the 30m x 30m study plot layout) produced seven results at the A interface and three results in weak layer B (Table 46). Later, pit 5 also produced six valid results in weak

Table 46: Middle Basin Plot (MBP) 12/7/01 Trials: QLCT Results for Pooled A and B Weak Layers. Number of Valid Tests (n) by Weak Layer, Number of "No Result" (NR) Tests, Mean Strength ($\bar{\tau}_\infty$) in N/m^2, Standard Deviation (s) in N/m^2, and Coefficient of Variation of strength ($CV\bar{\tau}_\infty$), by Pit and Plot.

Study Plot	Date		Pit 1	Pit 2	Pit 3	Pit 4	Pit 5	Plot
MBP	12/7/01	n A	7	7	10	8	0	32
		n B	3	0	0	0	6	9
		n NR	0	3	0	2	4	9
		$\bar{\tau}_\infty$	648	693	764	710	650	696
		s	114	39	176	262	111	160
		$CV\bar{\tau}_\infty$	17.6%	5.6%	23.1%	36.9%	17.0%	23.0%

layer B, none in A, and four "no results". Given their proximity to each other, separated only by the 2-cm crust, and the likelihood that both weak layers developed simultaneously, under the same temperature gradient regime, QLCT results from both the A and B weak layers were pooled to calculate pit and plot stability. This departure from previous stability sampling plot analyses, which have focused exclusively on single weak layers, liberalizes the interpretation of the 41 valid stability test results on the premise that weak layers A and B were, effectively, a single metamorphic feature within the snowpack exhibiting local variations in development. All QLCT shear fractures were rated quality "1" on both weak layers.

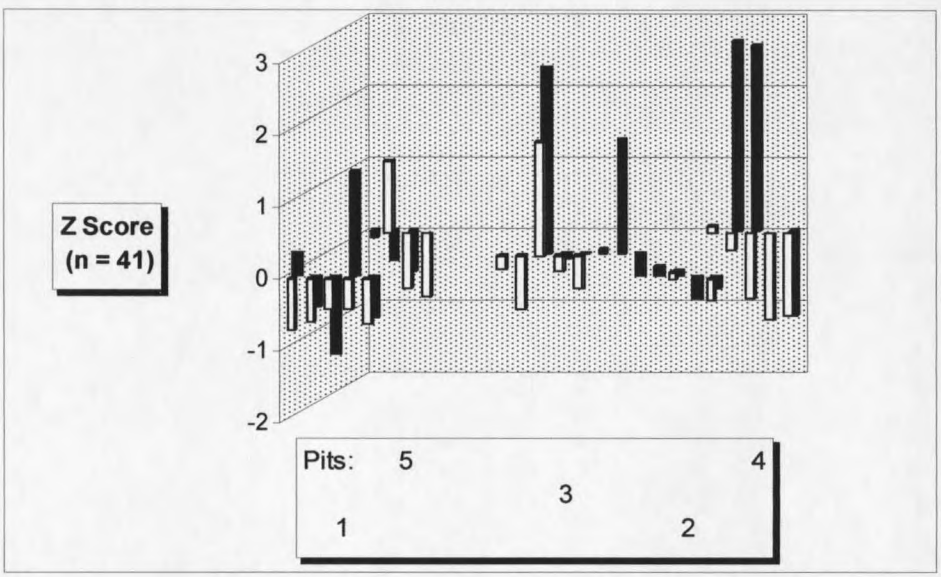
Pooling all 41 valid A and B weak layer results to calculate mean pit strength $\overline{\tau}_{\infty}$ resulted in a mean plot strength $\overline{\tau}_{\infty\,(Plot)}$ of 696 N/m^2, with a standard deviation of 160 N/m^2, and a coefficient of variation of strength for the plot $CV\overline{\tau}_{\infty\,(\mathrm{Plot})}$ of 23.0% (Table 46). However, another nine QLCT procedures yielded no valid result (logged as "NR") prior to destruction of the snow column and/or over-stressing the force gauge at forces of 19-26 kg (Appendix C). Although those nine results were excluded from the statistical analyses of the plot, since no actual fracture was observed in either weak layer A or B, those tests did provide evidence of strength in the two weak layers. Further, in pits 2 and 4 the "NR" tests occurred under forces substantially larger than the forces producing valid results, often more than twice as large (Appendix C). Thus, in the absence of valid measurements of strength for the nine "NR" results, it is clear that the calculated coefficients of variation in strength $CV\overline{\tau}_{\infty}$ for pits 2, 4 and 5 misstate the empirically observed variability in those pits.

For the purpose of estimating the effects of the nine "NR" results on the analysis of the 41 valid results, I've used the maximum forces recorded by the force gauge before ceasing the individual "NR" tests (Appendix C) to estimate strength, even though no fracture occurred. I inferred the location of a potential fracture at weak layer A or B, at some larger force, from the valid results in that pit. Using those nine estimated values for strength to recalculate pit mean strength $\overline{\tau}_{\infty}$, the values of $CV\overline{\tau}_{\infty}$ for pits 2 and 5 would increase from 5.6% to 26.1%, and from 17.0% to 35.2%, respectively. (The value of $CV\overline{\tau}_{\infty}$ for pit 5 actually drops slightly from 36.9% to 35.2%, since two valid tests exceeded the recorded maximum forces of the two "NR" tests (Appendix C)). Further,

the overall, plot-wide $CV\bar{\tau}_{\infty\,(\mathrm{Plot})}$ increases from 23.0% to 29.8%. While these estimated values of pit mean strength and coefficients of variation using "NR" results are considered legitimate empirical evidence of increased variability, only valid tests results were employed in statistical analyses of strength and stability.

A chart of Z scores of strength τ_{∞} for all valid (weak layer A or B) QLCT results reveals a wide range of variation among the five pits (Figure 21). (Note that the five results in the back row of pit 3, shown as black bars, are offset two "cells" to the right, beginning behind the center cell of the front row, and appear to merge with results from pit 2. This offset was due to damage to test cells 5 and 6 (Figure 5) during preparation).

Figure 21: Middle Basin Plot (MBP) 12/7/01 Trials: Z Scores of Pooled A and B Weak Layer Strength τ_{∞}. (White bars represent results in the front-row of a given pit and black bars represent back-row results).



Pit 1 produced ten valid results, three in weak layer B (cells 1, 2, and 10) and the balance in weak layer A. The strongest and weakest tests in the pit are in adjoining back-row cells 8 and 9 and were both from weak layer A. Pit 2 includes three missing results at test cells 1, 2 and 4, leaving only two valid results in the front row (shown as white bars), one slightly above the plot-mean strength, and the other slightly below. Five valid results are shown in the back row, three just above plot-mean strength, and two just below. When considering valid results only, pit 2 displays the lowest coefficient of variation of strength $CV\bar{\tau}_{\infty}$, at 5.6%, and the pit mean strength $\bar{\tau}_{\infty}$, at 693 N/m^2, closest to plot mean strength $\bar{\tau}_{\infty\,(Plot)}$ of 696 N/m^2. However, as discussed above, cells 1, 2 and 4 produced empirical "NR" (no result) evidence of much larger variation in strength within pit 2.

Pit 3 yielded the least confusing results, despite the "offset" in the back row: ten valid results were obtained in weak layer A. Nonetheless, substantial variability is observed, driven by two results 1.6 standard deviations above the mean (center test in front row and right-most cell in the back row) and one result 2.6 standard deviations above-mean (left-most cell in back row). The remaining seven cells tested are closely clustered between the plot mean and less than 1 standard deviation below plot-mean. When "NR" results are estimated for pits 2, 4 and 5, as discussed above, pit 3 remains near the plot-mean strength with somewhat lower variability than the plot-at-large.

Pit 4 produced eight valid results in weak layer A; cells 6 and 9, in the back row were "NR". When only valid results are considered, pit 4 displays the most variability in the plot, with two cells (7 and 8) over 2.5 standard deviations above pit-mean strength and

three cells (4, 5 and 10) at least one standard deviation below-mean. If "NR" results are estimated for pits 2, 4 and 5, then pits 4 and 5 display equally high values for $CV\,\overline{\tau}_{\infty}$, at 35.2%.

Finally, the six valid results obtained from weak layer B at pit 5, at $\overline{\tau}_{\infty} = 650$ N/m^2, are generally below the plot-mean strength. However, the four "NR" cells (1, 5, 9 and 10) in pit 5 belie the impression that pit 5 was about as weak and variable as pit 1. When the estimated strengths of the nine "NR" cells in the plot are empirically considered, as discussed earlier, pit 5 becomes the strongest pit in the plot and ties, with pit 4, for largest variability within the plot, while pit 1 remains the weakest and least-variable pit in the plot.

Variations in shear stress, produced by the slabs overlying weak layers A and B, were neither as dramatic or confusing (Table 47). An increase in slab SWE in pit 3, rather than increased slab thickness, accounted for the higher value of τ_{Slab} there (Appendix C). As observed in other trials (Bradley Meadow 1/27/01 and Round Hill 2/4/01), the same pit, pit 3 in this trial, displayed the plot's highest values for pit-mean strength $\overline{\tau}_{\infty}$ (Table 46) and shear stress τ_{Slab} (Table 47).

Table 47: Middle Basin Plot (MBP) 12/7/01 Trials: Shear Stress for Pooled A and B Weak Layers. Pit Shear Stress, τ_{Slab} (N/m^2), and Coefficient of Variation of Mean Plot Shear Stress, $CV\,\overline{\tau}_{Slab}$. (*na* indicates "not applicable" in the pit).

Study Plot	Date	τ_{Slab} Pit 1	τ_{Slab} Pit 2	τ_{Slab} Pit 3	τ_{Slab} Pit 4	τ_{Slab} Pit 5	$CV\,\overline{\tau}_{Slab}$ Plot
MBP	12/7/01	322 (A) 377 (B)	305 (A) *na* (B)	399 (A) *na* (B)	325 (A) *na* (B)	*na* (A) 374 (B)	12.4% (A) 0.6% (B)

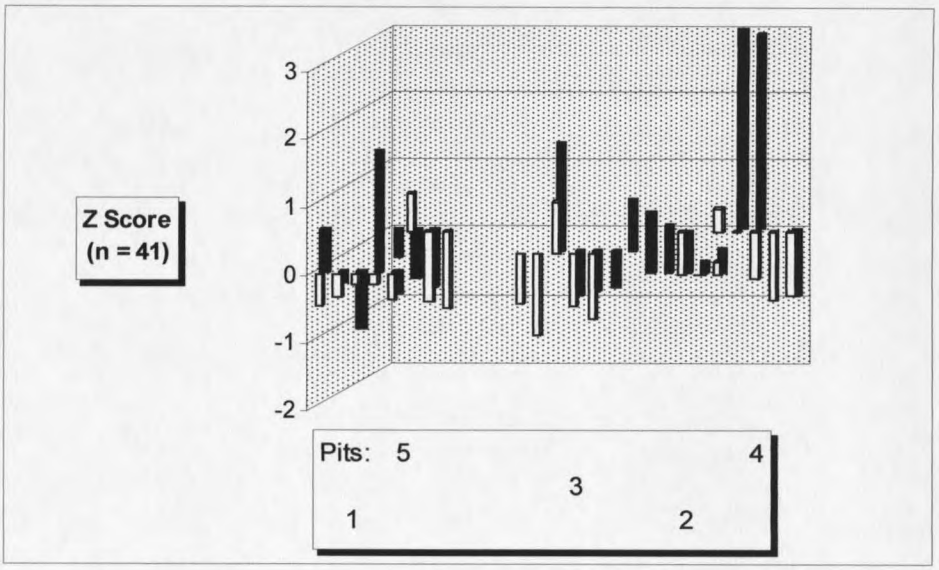
Combining valid strength $\overline{\tau}_{\infty}$ data (Table 46) with shear stress τ_{Slab} data (Table 47) for each pit yields a stability ratio S_{QLCT} for each pit and a mean stability ratio for the plot $\overline{S}_{QLCT(Plot)}$ (Table 48). Pit 5 presents the lowest stability ratio because the second-lowest

Table 48: Middle Basin Plot (MBP) 12/7/01 Trials: Stability for Pooled A and B Weak Layers. Pit and Plot Stability, S_{QLCT}, and Coefficient of Variation of Mean Plot Stability, $CV\,\overline{S}_{QLCT(Plot)}$.

Study Plot	Date	S_{QLCT} Pit 1	S_{QLCT} Pit 2	S_{QLCT} Pit 3	S_{QLCT} Pit 4	S_{QLCT} Pit 5	$\overline{S}_{QLCT(Plot)}$
MBP	12/7/01	2.01	2.27	1.91	2.19	1.74	2.03 CV = 23.7% (n = 41)

pit-mean strength in the plot, at 650 N/m^2 (Table 46) is associated with a relatively high value for pit shear stress, at 374 N/m^2 (Table 47). Conversely, seven of the ten QLCT results in pit 1, from weak layer A, are somewhat stronger ($\overline{\tau}_{\infty(A)}$ = 670 N/m^2), and are associated with a comparatively lower value for pit shear stress ($\tau_{Slab(A)}$ = 322 N/m^2), offsetting the three comparatively weaker B weak layer QLCT results. The variability among stability ratios S_{QLCT} based on the 41 valid QLCT results, at $CV\,\overline{S}_{QLCT(Plot)}$ = 23.7%, is comparable to that observed in most of the 2000/2001 trials. A chart of Z scores of stability S_{QLCT} (Figure 22) appears quite similar, in general pattern, to the chart of Z scores of strength τ_{∞} (Figure 21). Above-plot-mean S_{QLCT} values in cells 6 and 9 in

Figure 22: Middle Basin Plot (MBP) 12/7/01 Trials: *Z* Scores of Pooled A and B Weak Layer Stability S_{QLCT}. (White bars represent results in the front-row of a given pit and black bars represent back-row results).



pit 1 are offset by below-mean cells to bring pit 1 closest to the plot-mean stability S_{QLCT}. Pit 2 has the stability ratio farthest from the plot mean since all seven cells with valid results produced S_{QLCT} values above the plot-mean (Appendix C).

However, the stability pattern produced by valid results (Figure 22) is altered when estimated strength values for the nine "NR" cells in the plot are considered. When estimated "NR" results are included in calculations of pit and plot stability S_{QLCT}, pit 5 (four "NR" tests), rather than exhibiting the lowest stability ratio, rises in rank to fall closest to the plot-mean S_{QLCT}. Further, pits 3 and 1, both with no "NR" tests, both drop in rank to present the lowest and second lowest stability ratios, respectively. Pit 4 (2 "NR" tests) and pit 2 (3 "NR" tests) retain the same positions with above-average stability ratios. And, when the nine "NR" results are used to estimate plot-wide stability,

the pit (5) exhibiting the largest increase in strength variability $CV\bar{\tau}_{\infty}$, from 17.0% (without four "NR" tests) to 35.2% (with four estimated "NR" test results), captures the (increased, from 2.02 to 2.27) plot-mean stability better than the pit (1) with the least strength variability and with no "NR" tests.

When only the 41 valid QLCT results QLCT results from weak layers A and B are pooled in the calculation of pit- and plot-mean strength, *t*-tests for "no difference" in those means yield no pits whose mean strength is statistically different from the (pooled pit) plot-mean (Table 49). Pit 2 produces the strongest evidence of "no difference" between pit- and plot-mean strength despite having a significantly different (lower) variance (in strength) than the plot (Figure 21, Appendix E). Pits 1 and 4 also exhibited significantly different variance (lower and higher, respectively) in strength than the plot (Appendix E). The *t*-test results for pits 1 and 3 show the least compelling *p* values (Table 49) supporting the "no difference" hypothesis.

Table 49: Middle Basin Plot (MBP) 12/7/01 Trials: *t*-Tests of Strength for Pooled A and B Weak Layers. Two-Sample *t*-Test (two-sided, $\alpha = 0.05$) of "No Difference" in Pit Mean Strength ($\bar{\tau}_{\infty}$) and Plot Mean Strength ($\bar{\tau}_{\infty(Plot)}$). (All pits pooled to calculate $\bar{\tau}_{\infty(Plot)}$).

Study Plot	Date	Pit 1 $\bar{\tau}_{\infty}$ to $\bar{\tau}_{\infty(Plot)}$	Pit 2 $\bar{\tau}_{\infty}$ to $\bar{\tau}_{\infty(Plot)}$	Pit 3 $\bar{\tau}_{\infty}$ to $\bar{\tau}_{\infty(Plot)}$	Pit 4 $\bar{\tau}_{\infty}$ to $\bar{\tau}_{\infty(Plot)}$	Pit 5 $\bar{\tau}_{\infty}$ to $\bar{\tau}_{\infty(Plot)}$
MBP	12/7/01	Fail to Reject $p = 0.286$	Fail to Reject $p = 0.904$	Fail to Reject $p = 0.248$	Fail to Reject $p = 0.892$	Fail to Reject $p = 0.503$

If the nine estimated "NR" results are included in the calculations of pit- and plot-mean strength, pit 4 still presents very strong evidence of "no difference" between pit-and plot-mean strength (p = 0.993) and pits 2, 3 and 5 continue to yield "no difference" results. Pit-mean strength in pit 1, however, is found unrepresentative of plot-mean strength (p = 0.013). And, when "NR" results are included, only pit 1 shows a variance (in strength) significantly different than plot-wide variance.

Similar results are obtained with t-tests of "no difference" between pit- and plot-mean stability. When only the 41 valid QLCT results from weak layers A and B are pooled to calculate pit- and plot-mean stability, all five pits are found representative of plot-mean stability (Table 50). In contrast to the t-test results for strength, however, the roles of pits 1 and 2 are now reversed. Now pit 1 presents the strongest evidence of "no difference" while pit 2 presents the second-weakest p value. Only pit 4 displays a significantly different variance in stability (larger) than the plot overall, due to the results in cells 7 and 8 (Figure 22, Appendix E).

Table 50: Middle Basin Plot (MBP) 12/7/01 Trials: t-Tests of Stability for Pooled A and B Weak Layers. Two-Sample t-Test (two-sided, $\alpha = 0.05$) of "No Difference" Between Pit Stability S_{QLCT} and Mean Plot Stability $\overline{S}_{QLCT(Plot)}$. (All pits pooled to calculate $\overline{S}_{QLCT(Plot)}$).

Study Plot	Date	Pit 1: S_{QLCT} to $\overline{S}_{QLCT(Plot)}$	Pit 2: S_{QLCT} to $\overline{S}_{QLCT(Plot)}$	Pit 3: S_{QLCT} to $\overline{S}_{QLCT(Plot)}$	Pit 4: S_{QLCT} to $\overline{S}_{QLCT(Plot)}$	Pit 5: S_{QLCT} to $\overline{S}_{QLCT(Plot)}$
MBP	12/7/01	Fail to Reject p = 0.932	Fail to Reject p = 0.190	Fail to Reject p = 0.502	Fail to Reject p = 0.605	Fail to Reject p = 0.164

However, again, if the nine estimated "NR" results are included in the calculations of pit- and plot-mean stability, *t*-tests of "no difference" between pit- and (pooled pit) plot-mean stability yield different results. When estimated "NR" results are included, both pit 1 and pit 2 are found unrepresentative of plot-mean stability (at $p = 0.094$ and $p = 0.086$, respectively) and the evidence for "no difference" at pit 3 is also rather weak ($p = 0.124$).

This trial, like the Baldy Mountain Study Plot trial of 2/18/01, has revealed the difficulties in describing plot stability when multiple, highly variable weak layers exist within a plot. In contrast to the Baldy Mountain 2/18/01 case, where five distinctly different and non-proximate weak layers were revealed, I have elected to pool the results of the metamorphically related and proximate weak layers found in this trial, as explained above. This decision has the initial effect of including pit 5, where only B weak layer results were obtained, in the analysis of pit-to-plot relationships. If only weak layer A results were evaluated, pit 5 would have to be found empirically unrepresentative of study plot strength or stability.

Further, as in the Bradley Meadows Study Plot trials of 2/18/01, this trial also produced a number of no-result ("NR") QLCT tests in which the strength of the weak layer(s) exceeded either/both the strength of the overlying snow column or the capacity of the force gauge. These "NR" results produced un-quantified empirical evidence of substantial strength in those test cells (often confirmed with subsequent "hard" or "hard-plus" compression test results on the remaining column). As shown above, incorporating estimated (minimum) strengths of the nine "NR" tests in my analysis yields substantially different results than are obtained when "NR" results are excluded. Although I tallied

both sets of pooled A and B weak layer *t*-test results, showing the "NR-inclusive" results parenthetically as alternative results (Table 67), it was my judgement that the more empirical "NR-inclusive" analysis of pit-to-plot stability relationships best reflected the conditions present at the Middle Basin Plot on 12/7/01.

This analysis proceeded on the premise that weak layers A and B were formed under the same temperature-gradient regime. However, weak layer B, consisting of cup-shaped faceted crystals below a heavily eroded melt-freeze crust, was not always present. Perhaps local pockets of lower density snow, produced by blowing snow collecting in depressions in the layer of snow remaining from October storms, were subjected to strong temperature gradients forming faceted grains prior to the formation of the upper crust during a period of thaw. Then, a renewed temperature gradient could have enhanced the now-buried facets (weak layer B) while eroding, partially or completely, the overlying melt-freeze crust. When additional snow fell a persisting temperature gradient would have begun faceting at the base of the new slab (weak layer A). Where the melt-freeze crust above weak layer B was completely eroded, weak layers A and B could have merged into a single layer. Such a sequence of events could explain the highly variable distribution of weak layer B, and relative variations in strength between A and B.

No clear pattern in the relationship of shear stress to strength emerges either since, after including "NR" results, the next-weakest pit (3) contained the highest shear stress, while the next-strongest pit (2) is associated with the lowest shear stress. At pit 3 both weak layers A and B were present but A was weaker in eight of the ten cells, while the remaining two cells failed simultaneously in A and B. Conversely, at pit 5, where the

highest strength was associated with the second-highest shear stress, although weak layer A was present in all cells, layer B was weaker in all six cells actually producing fracture. Perhaps variation in the "bridging" capacity of the melt-freeze crust overlying weak layer B resulted in varying relative (compared to A) strength produced by pressure metamorphism from the overlying slab.

While the age of weak layer B may have been somewhat more variable, perhaps related to episodes of blowing snow re-distribution, weak layer A was of a younger and comparatively uniform age throughout the plot, arriving in a single storm. Thereafter, any persistent temperature gradient regime would have been generally consistent throughout the plot, as suggested by the quite low variability of snow depth on 12/7/01, at *CV* 4.7%. Additionally, although younger, weak layer A proved weaker than B in pit 3, perhaps due to the strength of the crust between them. Weak layer age also does not seem to be related to the observed patterns of strength.

In summary, when "NR" results are accounted for, this trial yielded no clear clues about snowpack processes that could explain why two pits (1 and 2) were not representative of plot stability on 12/7/01, or why the other three pits were (Appendix G).

Lionhead Mountain Plot Trials – 1/9/02. Given the continued absence of testable weak layers in the Bridger Range study plots in early January (Profile #7, Appendix I), a stability-sampling trial was conducted on 1/9/02 at a site near Lionhead Mountain, 15 km west of West Yellowstone, Montana (Figure 3). We tested a layer of 15-20 mm surface hoar buried under a 25 cm slab having an average density of 140 kg/m^3 (Profile #9, Appendix I). This surface hoar formed from December 21st-26th and was subsequently

buried by a pair of small storms December 27th-28th and January 2nd-3rd (Johnson, personal communication). A northeast-facing and generally planar site, well-sheltered from ridgecrest wind, and showing no evidence of skier or snowmobile disturbance, was selected for the trial. Several "rollers", chunks of snow falling from upslope trees, had trundled down this slope and their "traces" were noted whenever they intersected a stability sampling point. No systematic "roller" effect was observed. Slope angles varied from 25 to 28 degrees. Due to the known sensitivity of the weak layer, steeper slopes had some potential to collapse during the trial and were, therefore, unsafe to work on.

In addition to the standard stability-sampling grid used during this research, consisting of 50 QLCT tests spread among five pits (performed by Landry, assisted by Zach Matthews), several other forms of data were collected within the 900 m^2 plot. Karl Birkeland (assisted by Dan Miller) collected 84 snow resistance profiles utilizing the Swiss Snow Micro-Pen (SMP), a motorized, digital penetrometer, Ron Johnson performed 50 stuffblock (SB) stability tests, and Birkeland and Miller conducted four Rutschblock stability tests. The results of these other tests will be summarized below.

Fifty valid QLCT results were obtained, all displaying clean, Q1 shears (Table 51). The uniqueness of this trial is immediately apparent when noting that three of the five pits produced coefficients of variation in strength $CV\bar{\tau}_{\infty}$ of 6.0% or less. Further, the plot-wide value $CV\bar{\tau}_{\infty(Plot)}$ was 10.4%. In all eight previous trials, the lowest plot-wide value $CV\bar{\tau}_{\infty(Plot)}$ obtained for a (complete or near-complete) set of 46-50 valid QLCT

results was 22.8%, on 1/27/01 at the Bradley Meadow study plot, testing a new-snow weakness (Table 12).

Table 51: Lionhead Mountain Plot (LMP) 1/9/02 Trials: QLCT Results. Number of Valid Tests (n), Mean Strength ($\bar{\tau}_{\infty}$) in N/m^2, Standard Deviation (s) in N/m^2, and Coefficient of Variation of strength ($CV\bar{\tau}_{\infty}$), by Pit and Plot.

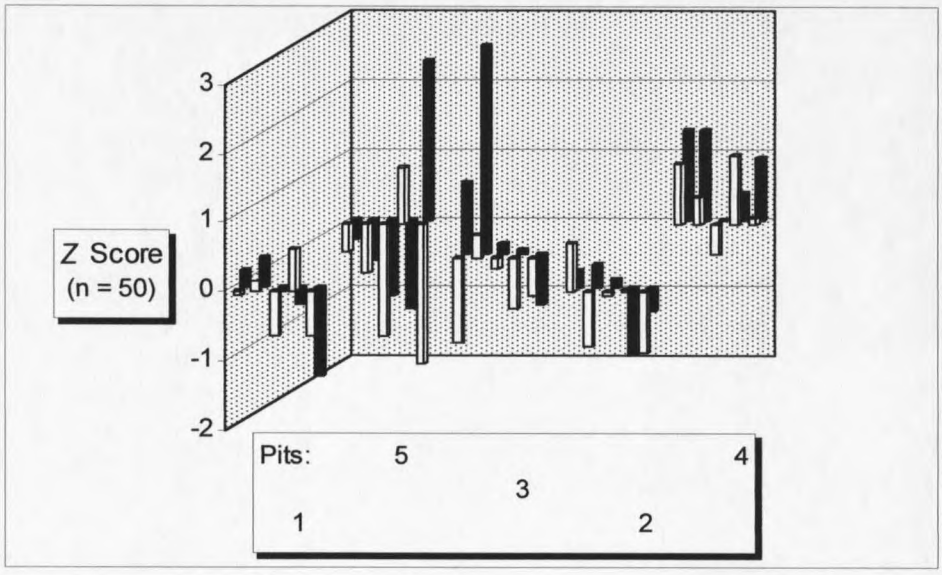
Study Plot	Date		Pit 1	Pit 2	Pit 3	Pit 4	Pit 5	Plot
LMP	1/9/02	n	10	10	10	10	10	50
		$\bar{\tau}_{\infty}$	369	368	383	398	357	375
		s	22	22	57	23	49	39
		$CV\bar{\tau}_{\infty}$	6.0%	6.0%	14.9%	5.7%	13.7%	10.4%

It is noteworthy that the actual standard deviation s (39 N/m^2) of plot-wide strength $\bar{\tau}_{\infty(Plot)}$ (375 N/m^2) in this trial (Appendix C) was 67% less than the previous lowest plot-wide value of 117 N/m^2, at the Bradley Meadow study plot on 3/17/01. On a hypothetical 38° slope nearby at Lionhead on 1/9/02, one standard deviation s of plot-mean strength $\bar{\tau}_{\infty(Plot)}$ was the equivalent of only an 8 mm SWE load (with no change in mean strength). Further, based on the t-distribution method for estimating precision (Landry et al., 2001b), with sample-size of ten valid QLCT in each pit, the (95% confidence level) margin of error of pit-mean strength on 1/9/02 was from < 30 N/m^2 (pits 1 and 2) to approximately 40 N/m^2 (pit 3), or from < 6 mm SWE to 8.4 mm SWE. The strength data from these five pits produced a substantially more meaningful level of resolution (to an avalanche forecaster) than observed in the next-best previous trial, at

Bradley Meadow on 3/17/01, where the strength margin-of-error range was equivalent to a 15-25 mm SWE load (95% confidence level).

A chart of the fifty Z scores of strength (Figure 23) highlights the effects test cells 7 in pit 3 ($Z = 3.957$) and 10 in pit 5 ($Z = 3.164$) had on the plot-wide variation of strength, balanced somewhat by cell 5 in pit 5 ($Z = -1.986$) (Appendix C). Only pit 4 presented a clear bias toward above-plot-average strength.

Figure 23: Lionhead Mountain Plot 1/9/02 Trials: Z Scores of Strength τ_{∞}. (White bars represent results in the front-row of a given pit and black bars represent back-row results. Pit locations are shown in the key below the chart).



Just as the strength of the 1/9/02 trials weak layer was substantially more consistent than observed in previous trials, the shear stress produced by the overlying slab was also very uniform among the pits (Table 52), varying by only 15 N/m^2 (equivalent to 2 mm variations in SWE load on a 38° slope). Interestingly, as observed during previous trials,

Table 52: Lionhead Mountain Plot (LMP) 1/9/02 Trials: Shear Stress. Pit Shear Stress, τ_{Slab} (N/m^2), and Coefficient of Variation of Mean Plot Shear Stress, $CV\overline{\tau}_{Slab}$.

Study Plot	Date	τ_{Slab} Pit 1	τ_{Slab} Pit 2	τ_{Slab} Pit 3	τ_{Slab} Pit 4	τ_{Slab} Pit 5	$CV\overline{\tau}_{Slab}$ Plot
LMP	1/9/02	150	141	147	156	147	3.8%

the pit with the highest shear stress τ_{Slab}, pit 4, was also the pit with the highest mean strength $\overline{\tau}_{\infty}$ (Table 51), but the actual differences in shear stress among the five pits were quite small.

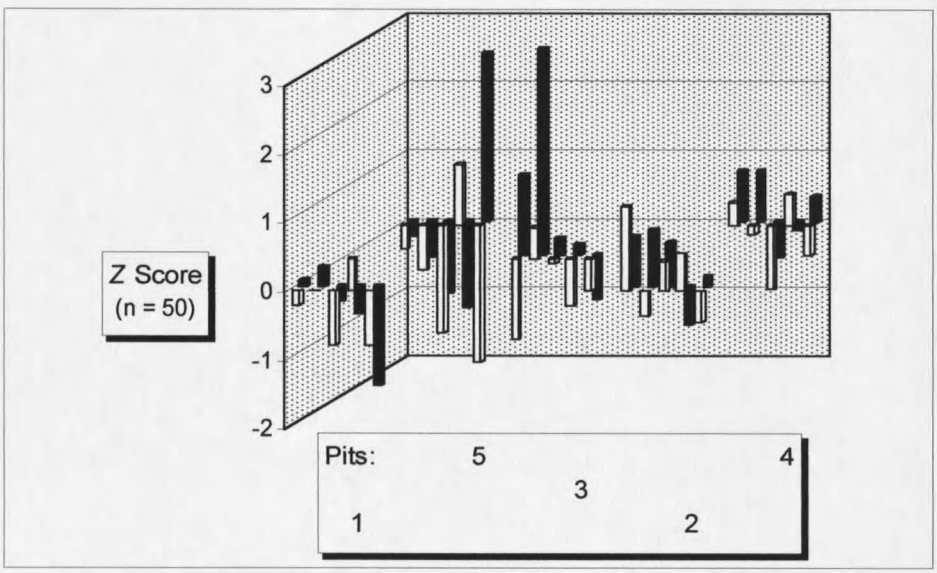
Given generally consistent values for strength and stress, it follows that the calculated stability ratios would be similar among the five pits as well. This was the case, as the coefficient of variation $CV\,\overline{S}_{QLCT(Plot)}$ of 10.2% indicates (Table 53). Again, among the eight previous 900 m^2 trials, the lowest value of the coefficient of variation in plot-mean stability $CV\,\overline{S}_{QLCT(Plot)}$ obtained for a (complete or near-complete) set of 46-50 valid QLCT results was 22.2%, on 1/27/01 at the Bradley Meadow study plot, testing a new-snow weakness (Table 14).

Table 53: Lionhead Mountain Plot (LMP) 1/9/02 Trials: Stability. Pit and Plot Stability, S_{QLCT}, and Coefficient of Variation of Mean Plot Stability, $CV\,\overline{S}_{QLCT(Plot)}$.

Study Plot	Date	S_{QLCT} Pit 1	S_{QLCT} Pit 2	S_{QLCT} Pit 3	S_{QLCT} Pit 4	S_{QLCT} Pit 5	$\overline{S}_{QLCT(Plot)}$
LMP	1/9/02	2.45	2.62	2.61	2.55	2.42	2.53 $CV = 10.2\%$

A chart of Z scores of stability (Figure 24) presented a slightly different pattern than the chart of Z scores of strength (Figure 23). Pit 4 now presents a generally random scatter of Z scores of stability about the plot mean, since above-average strength (Table 51) was offset by above average slab shear stress (Table 52).

Figure 24: Lionhead Mountain Plot 1/9/02 Trials: Z Scores of Stability S_{QLCT}. (White bars represent results in the front-row of a given pit and black bars represent back-row results. Pit locations are shown in the key below the chart).



Two-sampled t-test analyses of pit-to-plot differences in strength (Table 54) highlighted the above-plot-mean QLCT results at pit 4, shown in the chart of Z scores of strength (Figure 23). Only pit 4 departed significantly from plot-mean strength; the remaining four pits proved to be statistically representative of plot-wide mean strength.

Table 54: Lionhead Mountain Plot (LMP) 1/9/02 Trials: Stability: *t*-Tests of Strength. Two-Sample *t*-Test (two-sided, $\alpha = 0.05$) of "No Difference" in Pit Mean Strength ($\overline{\tau}_{\infty}$) and Plot Mean Strength ($\overline{\tau}_{\infty(Plot)}$). (All pits pooled to calculate $\overline{\tau}_{\infty(Plot)}$).

Study Plot	Date	Pit 1 $\overline{\tau}_{\infty}$ to $\overline{\tau}_{\infty(Plot)}$	Pit 2 $\overline{\tau}_{\infty}$ to $\overline{\tau}_{\infty(Plot)}$	Pit 3 $\overline{\tau}_{\infty}$ to $\overline{\tau}_{\infty(Plot)}$	Pit 4 $\overline{\tau}_{\infty}$ to $\overline{\tau}_{\infty(Plot)}$	Pit 5 $\overline{\tau}_{\infty}$ to $\overline{\tau}_{\infty(Plot)}$
LMP	1/9/02	Fail to Reject $p = 0.501$	Fail to Reject $p = 0.464$	Fail to Reject $p = 0.672$	Reject $p = 0.019$	Fail to Reject $p = 0.197$

However, two-sampled *t*-test analysis of differences in stability (Table 55) also revealed the counterbalancing effect on the stability ratio S_{QLCT} of the higher value of shear stress τ_{Slab} at pit 4. Accordingly, all five pits were found statistically representative of the plot-wide stability ratio $\overline{S}_{QLCT(Plot)}$ of 2.53. Among the nine stability-sampling

Table 55: Lionhead Mountain Plot (LMP) 1/9/02 Trials: *t*-Tests of Stability. Two-Sample *t*-Test (two-sided, $\alpha = 0.05$) of "No Difference" Between Pit Stability S_{QLCT} and Mean Plot Stability $\overline{S}_{QLCT(Plot)}$. (All pits pooled to calculate $\overline{S}_{QLCT(Plot)}$).

Study Plot	Date	Pit 1: S_{QLCT} to $\overline{S}_{QLCT(Plot)}$	Pit 2: S_{QLCT} to $\overline{S}_{QLCT(Plot)}$	Pit 3: S_{QLCT} to $\overline{S}_{QLCT(Plot)}$	Pit 4: S_{QLCT} to $\overline{S}_{QLCT(Plot)}$	Pit 5: S_{QLCT} to $\overline{S}_{QLCT(Plot)}$
LMP	1/9/02	Fail to Reject $p = 0.216$	Fail to Reject $p = 0.317$	Fail to Reject $p = 0.542$	Fail to Reject $p = 0.788$	Fail to Reject $p = 0.259$

trials performed to-date, only one previous trial had produced five pits representative of plot-wide stability, the Bradley Meadows study plot trial of 3/17/01 performed in a layer

of near-surface facets; the plot-wide stability ratio $\overline{S}_{QLCT(Plot)}$ at BMSP on 3/17/01 was 3.11 (Table 38).

Not surprisingly, the additional stability tests performed within the 900 m^2 Lionhead Mountain plot on 1/9/02 – Stuffblock (SB), Rutschblock (RB) and compression (CT) tests – also produced very consistent results. (I routinely conducted two compression tests at each of the five pits within the 900m^2 plots throughout this research in order to verify the location of weak layers). Among these, the SB, RB, and CT all produce ordinal scores based upon successive increments of dynamic loading, while the SMP generates continuous measurements of resistance to penetration.

Six of the ten CT's were ranked "Easy", fracturing after only 2 taps (mode) from the wrist, and the range was from 1 to 4 taps from the wrist. Forty (80%) of the fifty SB's fractured at drop-height 10 cm (mode), with a range from 0 cm (static load of 4.5-5 kg) to a drop-height of 20 cm. All four RB's were rated an "easy" 2, fracturing with a partial "half-step" onto the isolated block. All of these test methods produced Q1 shears.

Snow Micro-Pen results were unavailable at the time of this writing.

Altogether, the 1/9/02 trials results depicted, by a wide margin, the lowest magnitude variations of strength and stability, with the least variability, observed to-date during this research. Based on the relatively young age of the buried surface hoar, and its substantial thickness, a comparatively uniform stability-sampling trial outcome was anticipated by the team. Nevertheless, the very small variations in strength measured by the QLCT, and the consistently low variability in strength in pits 1, 2 and 4, provided reassuring evidence that the QLCT could detect "uniform" conditions with a minimal level of

observer-introduced "noise" in the data. In fact, all stability test methods produced relatively uniform results that day, albeit at different increments of precision.

Given the observed consistency in the weak layer's thickness, and in the overlying soft slab (Table 52), it is plausible that, once the overlying slab was deposited, pressure metamorphism and/or penetration of the surface hoar into the snow below it (Davis et al., 1998; Jamieson and Schweizer, 2000) occurred at relatively uniform rates throughout the plot. The overlying slab contained an average of 34 mm SWE. This load accumulated at a modest rate between 12/26/01 and 1/3/02 and no additional slab load was added during the seven days prior to the trials. Thus, on 1/9/02 the weak layer was tested for strength following a period of snowpack creep under constant, and comparatively low (SWE), load. That combination of a uniformly deposited weak layer of surface hoar, covered by a uniform and minor load, and followed by a period of creep under a constant load, prior to strength measurements, could explain why all five pits represented plot-wide stability. Despite very small variations in strength at the pit scale, each pit contained enough range in strength to capture the (also small) range of variation at the plot scale. Thus, the 1/9/02 trials revealed a "characteristic scale" (Phillips, 1999a) of stability, the scale at which (for the moment) stability could be reliably sampled, that was at least as large as the 900 m^2 plot.

Lionhead Mountain Plot Trials – 1/15/02. A follow-up trial at Lionhead was conducted on 1/15/02 in order to investigate changes in strength and stability, and the variability of strength and stability, in the surface hoar weak layer tested on 1/9/02. Looking up-slope, the lower-left (origin) corner of the 1/15/02 900 m^2 stability-sampling

plot was located 45 m to the right of the upper-right corner of the 1/9/02 900 m^2 plot, in the lower track/runout zone of an avalanche path locally referred to as "Ski Hill". Fresh snowmobile tracks were observed some 75 m to the right (looking up-slope) of the selected site, along with one obscured ski track. No other evidence of disturbance was evident on the slope. Slope aspect varied only slightly, from 38° on 1/9/02 to 46° on 1/15/02; both plots were considered northeast-facing slopes. Slope angles were slightly more consistent at the 1/15/02 plot, ranging from 26°-27° (Appendix C). Forty-eight valid QLCT results were performed by Landry, assisted by Jeff Deems, all producing Q1 shears (Table 56).

Table 56: Lionhead Mountain Plot (LMP) 1/15/02 Trials: QLCT Results. Number of Valid Tests (n), Mean Strength ($\overline{\tau}_{\infty}$) in N/m^2, Standard Deviation (s) in N/m^2, and Coefficient of Variation of strength ($CV\overline{\tau}_{\infty}$), by Pit and Plot.

Study Plot	Date		Pit 1	Pit 2	Pit 3	Pit 4	Pit 5	Plot
LMP	1/15/02	n	10	10	9	10	9	48
		$\overline{\tau}_{\infty}$	486	557	545	528	497	523
		s	43	56	74	32	31	55
		$CV\overline{\tau}_{\infty}$	8.9%	10.0%	13.5%	6.1%	6.2%	10.5%

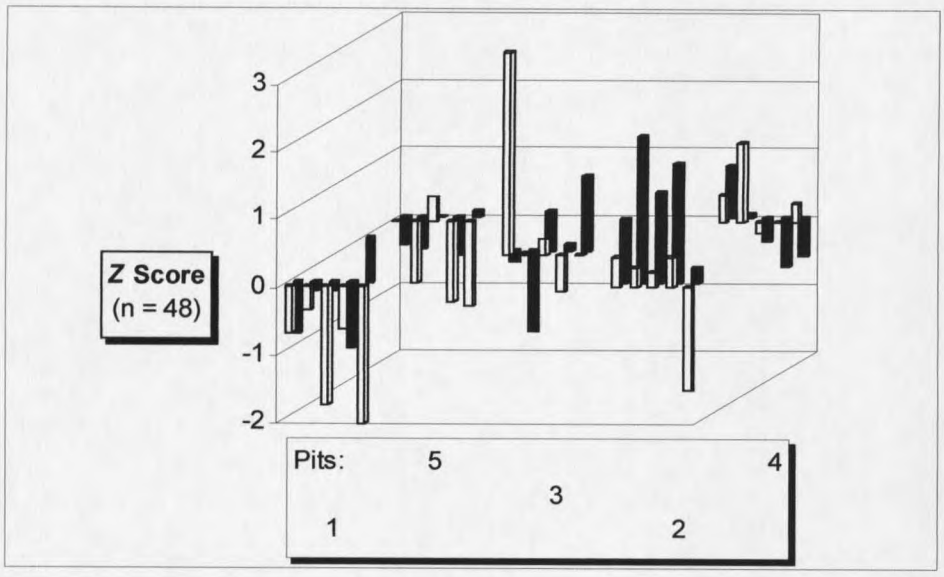
On 1/15/02 the surface hoar weak layer was approximately 50% thinner in the snowpit face than on 1/9/02, apparently due to settlement, and the 6-10 mm surface hoar grains were noticeably less well-defined, degrading by rounding and necking with adjoining mixed forms (Profile 10, Appendix I).

As was done during the 1/9/02 trials, Karl Birkeland collected 121 Snow Micro-Pen (SMP) profiles throughout the plot, assisted by Michael Cooperstein. Birkeland and Cooperstein also conducted 10 stuffblock tests. Bob Brown performed two Rutschblock tests and also collected an intact sample of the buried surface hoar weak layer, sandwiched between its adjoining layers, for 3-d analysis.

QLCT results (Table 56) revealed that the 1/15/02 plot was stronger than the 1/9/02 plot, increasing by 148 N/m^2 (39%) from a plot-mean strength $\overline{\tau}_{\infty(Plot)}$ values of 375 N/m^2 on 1/9/02 to 523 N/m^2 on 1/15/02. But, somewhat surprisingly, variability was virtually the same at $CV\overline{\tau}_{\infty(Plot)}$ values of 10.5% and 10.4% respectively, since the standard deviations s of strength, at 39 and 59 N/m^2 respectively, varied in approximately equivalent proportion to strength. Whether or not these results hid subtle statistically significant differences between pit- and plot-mean strength, however, remained to be determined by the t-test procedure.

First, a chart of Z scores of individual QLCT strength τ_{∞} results revealed apparent pit-to-plot differences (Figure 25). Pits 1, 2 and 5 all displayed a clear bias to above-plot-mean (pit 2) or below-plot-mean strength (pits 1 and 5), while pits 3 and 4 show more balanced scatter about the plot-mean strength.

Figure 25: Lionhead Mountain Plot 1/15/02 Trials: Z Scores of Strength τ_{∞}. (White bars represent results in the front-row of a given pit and black bars represent back-row results. Pit locations are shown in the key below the chart).



Only a few cm of new snow accumulated at the Lionhead Mountain plot between 1/9/02 and 1/15/02, resulting in only slightly higher values for the overlying slab thickness and SWE (Appendix C). Consequently, shear stress values were also only 15% higher on 1/15/02, ranging from 163-178 N/m^2 (Table 57) versus 141-156 N/m^2 on 1/9/02. Variability in shear stress was low and essentially the same on both days, at 3.6% and 3.8% respectively. Therefore, any increased variability in strength or stability seen

Table 57: Lionhead Mountain Plot (LMP) 1/15/02 Trials: Shear Stress. Pit Shear Stress, τ_{Slab} (N/m^2), and Coefficient of Variation of Mean Plot Shear Stress, $CV\overline{\tau}_{Slab}$.

Study Plot	Date	τ_{Slab} Pit 1	τ_{Slab} Pit 2	τ_{Slab} Pit 3	τ_{Slab} Pit 4	τ_{Slab} Pit 5	$CV\overline{\tau}_{Slab}$ Plot
LMP	1/15/02	165	174	163	178	169	3.6%

on 1/15/02 was probably not attributable to an increase in the variation, or actual amount, of shear stress over the plot. Nor could a change in slope angles, exposure to wind, small variations in slope aspect around minor undulations in the snowpack's surface (reflecting the ground surface), exposure to tree "drops", or other terrain-based factors plausibly explain the increased strength. Those factors were effectively constant between the plots as well. Instead, snowpack processes such as creep and surface hoar penetration of the underlying layer (Davis et al., 1998; Jamieson and Schweizer, 2000) under a near-constant load, rather than under an increasing load, and/or temperature-induced metamorphism (rounding and necking), provided plausible explanations for the observed increase in strength.

As during the 1/9/02 trials, the consistency of shear stress observed throughout the plot on 1/15/02, combined with low variations in strength (Table 56), yielded five similar pit values for the stability ratio S_{QLCT} (Table 58). The plot-wide stability ratio $S_{QLCT(Plot)}$

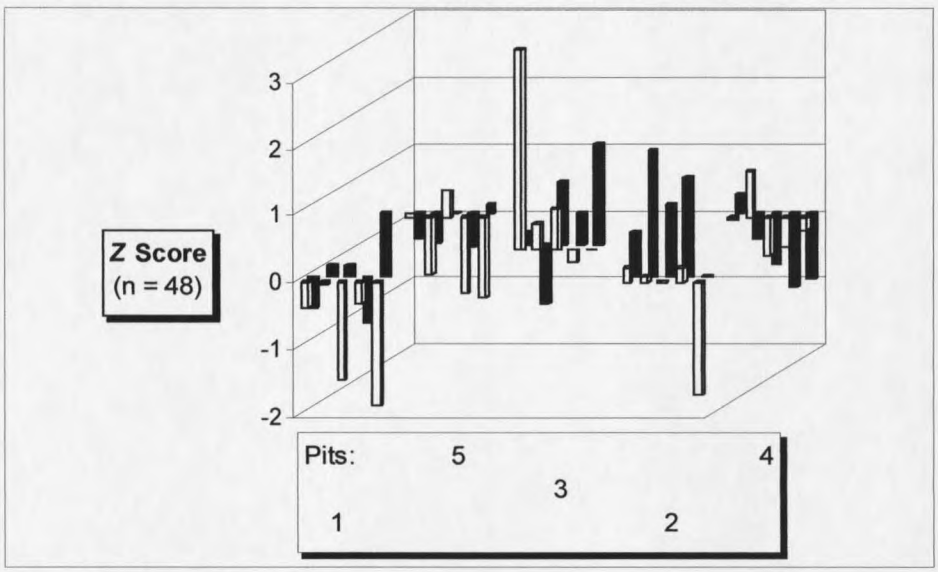
Table 58: Lionhead Mountain Plot (LMP) 1/15/02 Trials: Stability. Pit and Plot Stability, S_{QLCT}, and Coefficient of Variation of Mean Plot Stability, $CV\,\overline{S}_{QLCT(Plot)}$.

Study Plot	Date	S_{QLCT} Pit 1	S_{QLCT} Pit 2	S_{QLCT} Pit 3	S_{QLCT} Pit 4	S_{QLCT} Pit 5	$\overline{S}_{QLCT(Plot)}$
LMP	1/15/02	2.95	3.21	3.34	2.97	2.94	3.08 $CV = 10.6\%$

was higher (more stable) on 1/15/02 than on 1/9/02, because plot-wide strength increased almost 40% from 1/9/02 to 1/15/02, while shear stress increased only 15% during the same period.

A chart of Z scores of stability (Figure 26) presented several pits apparently skewed toward above- or below-plot-mean stability (Table 58). The low standard deviation s of $S_{QLCT(Plot)}$, at 0.325 (Appendix C) amplified individual cell results.

Figure 26: Lionhead Mountain Plot 1/15/02 Trials: Z Scores of Stability S_{QLCT}. (White bars represent results in the front-row of a given pit and black bars represent back-row results. Pit locations are shown in the key below the chart).



As in all previous trials, two-sample t-tests were performed to reveal any statistically significant pit-to-plot differences in strength or stability on 1/15/02. As suggested by the chart of Z scores of strength (Figure 25), pits 1, 2, and 5 were all found unrepresentative of plot-mean strength (Table 59). On 1/9/02, only one pit (pit 4) was unrepresentative.

Table 59: Lionhead Mountain Plot (LMP) 1/15/02 Trials: Stability: *t*-Tests of Strength. Two-Sample *t*-Test (two-sided, $\alpha = 0.05$) of "No Difference" in Pit Mean Strength ($\overline{\tau}_{\infty}$) and Plot Mean Strength ($\overline{\tau}_{\infty(Plot)}$). (All pits pooled to calculate $\overline{\tau}_{\infty(Plot)}$).

Study Plot	Date	Pit 1 $\overline{\tau}_{\infty}$ to $\overline{\tau}_{\infty(Plot)}$	Pit 2 $\overline{\tau}_{\infty}$ to $\overline{\tau}_{\infty(Plot)}$	Pit 3 $\overline{\tau}_{\infty}$ to $\overline{\tau}_{\infty(Plot)}$	Pit 4 $\overline{\tau}_{\infty}$ to $\overline{\tau}_{\infty(Plot)}$	Pit 5 $\overline{\tau}_{\infty}$ to $\overline{\tau}_{\infty(Plot)}$
LMP	1/15/02	Reject $p = 0.054$	Reject $p = 0.080$	Fail to Reject $p = 0.295$	Fail to Reject $p = 0.675$	Reject $p = 0.061$

Further, *t*-tests of pit-to-plot stability found pit 3, the most variable pit in the plot (Table 56), and pit 5, the pit with the lowest stability ratio (Table 58), both unrepresentative of plot-mean stability on 1/15/02 (Table 60). This result is not readily apparent in the chart of Z scores of stability (Figure 26), where pits 2 and 4 also seem to depart substantially from the plot mean. In pit 4, however, pit-mean strength, at 528 N/m^2, was very near the plot-mean strength of 523 N/m^2, overcoming the effect of the

Table 60: Lionhead Mountain Plot (LMP) 1/15/02 Trials: *t*-Tests of Stability. Two-Sample *t*-Test (two-sided, $\alpha = 0.05$) of "No Difference" Between Pit Stability S_{QLCT} and Mean Plot Stability $\overline{S}_{QLCT(Plot)}$. (All pits pooled to calculate $\overline{S}_{QLCT(Plot)}$).

Study Plot	Date	Pit 1: S_{QLCT} to $\overline{S}_{QLCT(Plot)}$	Pit 2: S_{QLCT} to $\overline{S}_{QLCT(Plot)}$	Pit 3: S_{QLCT} to $\overline{S}_{QLCT(Plot)}$	Pit 4: S_{QLCT} to $\overline{S}_{QLCT(Plot)}$	Pit 5: S_{QLCT} to $\overline{S}_{QLCT(Plot)}$
LMP	1/15/02	Fail to Reject $p = 0.258$	Fail to Reject $p = 0.255$	Reject $p = 0.045$	Fail to Reject $p = 0.146$	Reject $p = 0.083$

differences in standard deviation (Table 56). Conversely, in pit 2, the standard deviation of strength of 56 N/m^2, nearly identical to the plot-wide standard deviation of 55 N/m^2, counterbalanced the 34 N/m^2 difference in strength (Table 56). In contrast, on 1/9/02, no pits were found statistically unrepresentative of plot-mean stability.

The curious outcome of the 1/15/02 trials data was that, despite having low plot-wide coefficients of variation in strength and stability nearly identical to those on 1/9/02, three pits had mean strengths statistically different from the plot-mean strength (versus only one pit on 1/9/02). Further, two pits had stability ratios different from the plot-mean stability (versus no pits on 1/9/02). This apparent contradiction – nearly constant variability between the two trials, with decreased representative-ness in the latter – can be explained by examining the Z scores of individual pits in the 1/15/02 trials. As in all previous analyses of the 900m^2 stability sampling trials data, all valid QLCT results were pooled to calculate the plot-wide means of strength and stability. Then, a Z score was computed for each valid QLCT test cell comparing that cell's computed strength and stability to the pooled, plot-wide mean results, respectively. Thus, it was possible for an individual pit, such as pit 5, to simultaneously exhibit low inter-pit variability in strength ($CV\bar{\tau}_{\infty}$ = 6.2%) and a mean Z score of -0.471 (mean of all valid Z scores in the pit), or a departure of –0.471 (plot-wide) standard deviations of 55 N/m^2 from the (plot-mean) strength of 523 N/m^2 (Appendix C). A similar calculation for the mean Z score of pit 5 stability found a departure of –0.431 standard deviations from the pooled, plot-wide mean stability ratio of 3.08, despite low inter-pit variability in stability at

$CV\,\bar{S}_{QLCT} = 6.2\%$. Both differences, at pit 5, were found significantly different from the plot-means of strength and stability by the *t*-test.

From a practical perspective, the *t*-test analyses of the 1/15/02 trials were arguably inconsequential, despite the finding of statistically unrepresentative pits. As during the 1/9/02 trials, the margin of error (95% confidence level) for pit-mean strength remained low, ranging from < 30 N/m^2 (pit 5) to 60 N/m^2 (pit 3), or from < 6 mm SWE to 12 mm SWE. Further, the plot-wide standard deviation in strength amounted to a critical load (on a 38° slope, assuming the same strength) of 11 mm SWE, or a range in critical load (± 1 standard deviation) from 64 to 87 mm SWE (Appendix C).

In an avalanche forecasting context, those high levels of resolution in pit-mean strength, and the narrow range in critical load SWE, might have overridden the fine distinctions in pit-mean strengths and stability drawn by the *t*-tests. Despite the *t*-test results showing two pits unrepresentative of plot-wide stability, all five pits in the 1/15/02 plot provided stability information as useful to an avalanche forecaster as the five pits of 1/9/02, all of which were representative of plot-wide stability. That is, the low-magnitude margins of error in strength measurements (95% confidence level) described above are small enough that a forecaster would still find the results from all five pits useful, given how near the strength of pits 3 and 5 were to the others.

Nevertheless, the *t*-test analyses of the weak layer's strength and stability during the 1/15/02 trials did detect an incipient and statistically significant trend towards spatial divergence (Schumm, 1991). That is, over time, the stability characteristics of pits 3 and 5 had begun to significantly depart from those of pits 1, 2 and 4, even under the same

general snowpack (creep) conditions and process. Importantly, that divergence trend was *between, but not within* the five pits in the plot suggesting that the spatial scale of this divergence was larger than a pit but smaller than the plot. This trend may have been related to the slow rate of change in the load and shear stress acting on the weak layer. A third trial was conducted at Lionhead on 1/26/02 to pursue additional evidence of changing spatial and temporal patterns of strength and stability.

Lionhead Mountain Plot Trials – 1/26/02. The third trial at Lionhead was performed 20 meters downslope from the 1/15/02 trials, testing the same December 21st-26th surface hoar weak layer tested on 1/9/02 and 1/15/02, now one month old. The undisturbed, planar site offered slope angles only slightly lower than those of the 1/15 trials and identical exposure to wind-drift and snow roller disturbances. A small conifer, less than 3 meters tall, stood some 4 meters downslope of pit 2. This "dark body" may have been close enough to pit 2 for long-wave radiation emitted by the tree to effect the development of the surface hoar layer being tested. However, no apparent visual differences in the weak layer were observed.

During the period since the 1/15 Lionhead trials a nearby SNOTEL location (Madison Plateau) had logged 2.6" (aprox. 66 mm) of new SWE, much of which arrived on 1/21 and 1/22/02. A pit nearby (Profile #11, Appendix I) on 1/21, dug during an aborted attempt to conduct a 900 m^2 stability-sampling trial, showed a trend toward strengthening. A fresh storm had begun at dawn on the 26th and snowfall was steady throughout the day of this trial, at rates of 2-4 cm per hour, accompanied by gusty winds. Careful ski testing of small slopes during the approach to the site, the absence of any

natural activity, and the results of pit 1 at the site provided sufficient evidence that the team (Landry and Reid Sanders) could conduct the trials safely. No obvious changes in the thickness of the surface hoar weak layer since 1/21 were apparent when viewing the snowpit wall, but closer examination with a 20x hand lens revealed continuing rounding, degradation of the (dis-aggregated) individual surface hoar grains, now co-mingled among other snow forms.

A full set of 50 valid QLCT results was obtained using the bench mode of the test (Table 61). Given the increased SWE load, plot-wide strength verified the expected trend

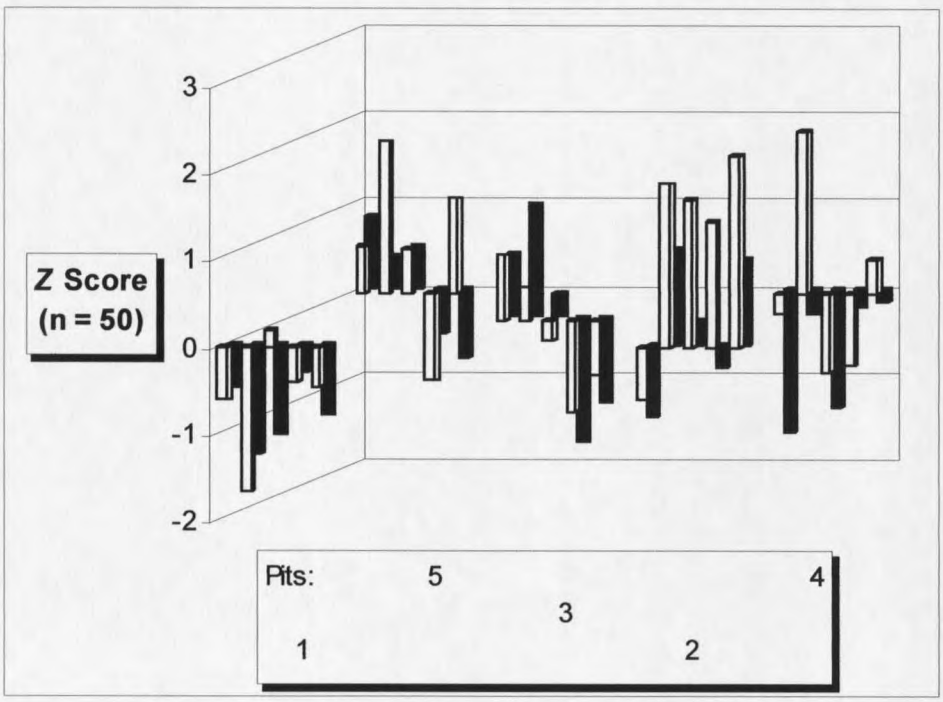
Table 61: Lionhead Mountain Plot 1/26/02 Trials: QLCT Results. Number of Valid Tests (n), Mean Strength ($\bar{\tau}_{\infty}$) in N/m^2, Standard Deviation (s) in N/m^2, and Coefficient of Variation of strength ($CV\bar{\tau}_{\infty}$), by Pit and Plot.

Study Plot	Date		Pit 1	Pit 2	Pit 3	Pit 4	Pit 5	Plot
LMP	1/26/02	n	10	10	10	10	10	50
		$\bar{\tau}_{\infty}$	955	1,234	1,066	1,019	1,145	1,084
		s	99	205	173	186	162	189
		$CV\bar{\tau}_{\infty}$	10.4%	16.6%	16.2%	18.3%	14.2%	17.5%

toward increased strength, rising from 523 N/m^2 on 1/15/02 (Table 56) to 571 N/m^2 on 1/21/02 (Profile #11, Appendix I), to 1,084 N/m^2 on 1/26/02 (Table 61). Of primary interest, however, was the increased variability in strength on 1/26, at a coefficient of variation in plot-wide strength $CV\bar{\tau}_{\infty(Plot)}$ of 17.5%, up 67% from 10.5% during the trials of 1/15/02.

Pit 1 showed the least variability in strength. A chart of Z scores of strength τ_{∞} in individual test cells showed that pit 1 was also skewed toward below-average strength, while pit 2 appeared skewed toward above-average strength (Figure 27).

Figure 27: Lionhead Mountain Plot 1/26/02 Trials: Z Scores of Strength τ_{∞}. (White bars represent results in the front-row of a given pit and black bars represent back-row results. Pit locations are shown in the key below the chart).



Despite the substantial amount of precipitation received during the period from 1/15 to 1/26/02, variation in the shear stress τ_{Slab} produced by the slab overlying the weak layer increased only 19%, from 3.6% on 1/15/02 to 4.3% on 1/26/02 (Table 62). The consistency of the snow deposition at these sites was attributed to the general absence of wind-drift. Thus, the increased variability in weak layer strength could not be explained by a correspondingly large increase in the variability of the slab-generated shear stress.

Table 62: Lionhead Mountain Plot 1/26/02 Trials: Shear Stress. Pit Shear Stress, τ_{Slab} (N/m^2), and Coefficient of Variation of Mean Plot Shear Stress, $CV\overline{\tau}_{Slab}$.

Study Plot	Date	τ_{Slab} Pit 1	τ_{Slab} Pit 2	τ_{Slab} Pit 3	τ_{Slab} Pit 4	τ_{Slab} Pit 5	$CV\overline{\tau}_{Slab}$ Plot
LMP	1/26/02	417	454	439	447	469	4.3%

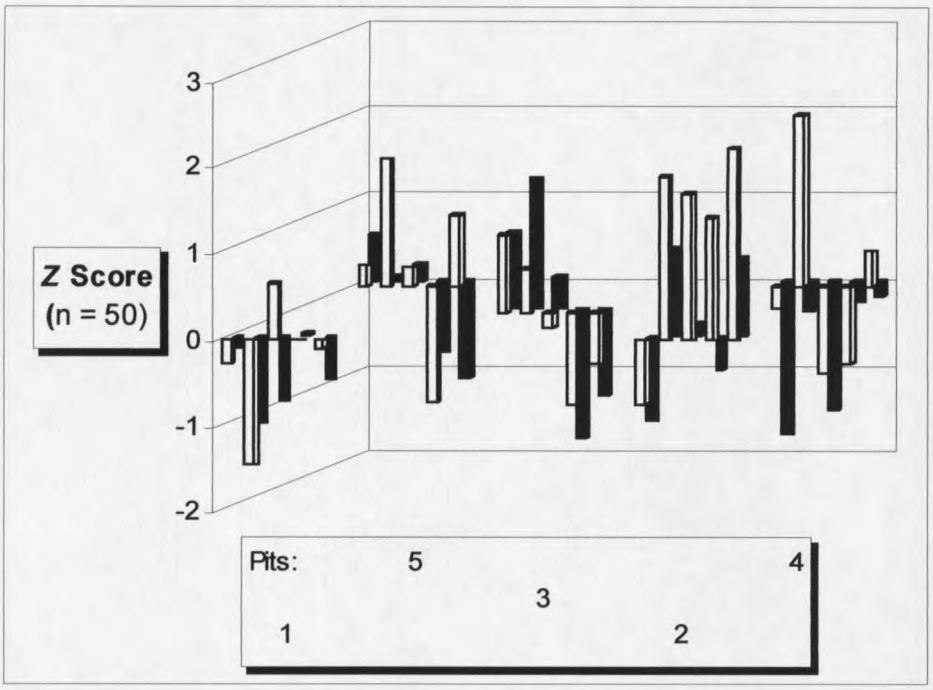
Interestingly, the pattern of variations in the shear stress τ_{Slab} during the 1/26 trials served to partially offset the variability in strength and produced a coefficient of variation in plot-wide stability $CV\,\overline{S}_{QLCT(Plot)}$ of 16.2% (Table 63), slightly lower than the coefficient of variation in plot-wide strength, at 17.5% (Table 61). As suspected, based on strength, pit 1 presented almost the lowest stability ratio S_{QLCT}, and pit 2 the highest.

Table 63: Lionhead Mountain Plot 1/26/02 Trials: Stability. Pit and Plot Stability, S_{QLCT}, and Coefficient of Variation of Mean Plot Stability, $CV\,\overline{S}_{QLCT(Plot)}$.

Study Plot	Date	S_{QLCT} Pit 1	S_{QLCT} Pit 2	S_{QLCT} Pit 3	S_{QLCT} Pit 4	S_{QLCT} Pit 5	$\overline{S}_{QLCT(Plot)}$
LMP	1/26/02	2.29	2.72	2.43	2.28	2.44	2.43 $CV = 16.2\%$

A chart of Z Scores of stability showed little difference in the pattern of variations in stability (Figure 28), compared to variations in strength (Figure 27). Pits 3 and 5 showed the most even scatter of individual test-cell Z scores about the plot-wide mean stability ratio of 2.43.

Figure 28: Lionhead Mountain Plot 1/26/02 Trials: Z Scores of Stability S_{QLCT}. (White bars represent results in the front-row of a given pit and black bars represent back-row results. Pit locations are shown in the key below the chart).



Two-sample t-test analyses of the pit-to-plot differences in strength for the five pits confirmed that pits 1 and 2 were not statistically representative of plot-wide strength (Table 64). (If the small tree near pit 2, noted earlier, had any effect on the weak layer at

Table 64: Lionhead Mountain Plot 1/26/02 Trials: Stability: t-Tests of Strength. Two-Sample t-Test (two-sided, $\alpha = 0.05$) of "No Difference" in Pit Mean Strength ($\overline{\tau}_{\infty}$) and Plot Mean Strength ($\overline{\tau}_{\infty(Plot)}$). (All pits pooled to calculate $\overline{\tau}_{\infty(Plot)}$).

Study Plot	Date	Pit 1 $\overline{\tau}_{\infty}$ to $\overline{\tau}_{\infty(Plot)}$	Pit 2 $\overline{\tau}_{\infty}$ to $\overline{\tau}_{\infty(Plot)}$	Pit 3 $\overline{\tau}_{\infty}$ to $\overline{\tau}_{\infty(Plot)}$	Pit 4 $\overline{\tau}_{\infty}$ to $\overline{\tau}_{\infty(Plot)}$	Pit 5 $\overline{\tau}_{\infty}$ to $\overline{\tau}_{\infty(Plot)}$
LMP	1/26/02	Reject $p = 0.005$	Reject $p = 0.028$	Fail to Reject $p = 0.779$	Fail to Reject $p = 0.329$	Fail to Reject $p = 0.344$

all it would have been to strengthen it, by wilting and/or inhibiting surface hoar formation, but any effect could only be speculated and no visible evidence of difference was observed). Notably, despite a plot-wide coefficient of variation in strength of 17.5%, only two pits departed significantly from plot-wide strength on 1/26/02, compared to three pits during the 1/15/02 trials (despite a plot-wide coefficient of variation in strength of only 10.5%).

Even better "representation" of stability was found on 1/26/02 with *t*-tests of pit-to-plot differences in stability (Table 65). Only one of the five pits, pit 2, was determined unrepresentative of plot-wide stability, despite a plot-wide coefficient of variation in

Table 65: Lionhead Mountain Plot 1/26/02 Trials: *t*-Tests of Stability. Two-Sample *t*-Test (two-sided, $\alpha = 0.05$) of "No Difference" Between Pit Stability S_{QLCT} and Mean Plot Stability $\overline{S}_{QLCT(Plot)}$. (All pits pooled to calculate $\overline{S}_{QLCT(Plot)}$).

Study Plot	Date	Pit 1: S_{QLCT} to $\overline{S}_{QLCT(Plot)}$	Pit 2: S_{QLCT} to $\overline{S}_{QLCT(Plot)}$	Pit 3: S_{QLCT} to $\overline{S}_{QLCT(Plot)}$	Pit 4: S_{QLCT} to $\overline{S}_{QLCT(Plot)}$	Pit 5: S_{QLCT} to $\overline{S}_{QLCT(Plot)}$
LMP	1/26/02	Fail to Reject $p = 0.287$	Reject $p = 0.045$	Fail to Reject $p = 0.971$	Fail to Reject $p = 0.280$	Fail to Reject $p = 0.952$

stability of 16.2%. Again, results were more uniform than on 1/15/02, when two pits were found unrepresentative of plot-wide stability (Table 60), with a plot-wide coefficient of variation in stability of only 10.6% (Table 58).

These results revealed different patterns of variation and "representation" than were observed during the 1/15/02 trials. Analysis of the 1/15 trials suggested that the

characteristic scale of variation in strength (and stability) was larger than a pit but smaller than the plot. Divergence in strength had become greater between pits than within pits, so individual pits were less likely to contain a range of strength or stability representative of plot-wide strength or stability. (Slab shear stress was nearly constant throughout the plots on 1/15 and 1/26). Subsequently, by 1/26, the characteristic scale of stability had approached (or perhaps reached, if the above-average strength in pit 2 is attributed to the nearby tree) the scale of the plot, despite increased variability at both scales. Between 1/15 and 1/26 variability of strength increased most rapidly at the pit scale. Pit representation of plot-wide strength and stability was better on 1/26 than on 1/15 because more of the 1/26 pits contained a range of strength representative of the increased plot-wide range in strength.

What factors governing snowpack processes changed between 1/15 and 1/26, producing rapid divergent (increased) variability in strength at the pit scale simultaneously with converging variability at the plot scale? Substantial and sometimes rapid loading (55 mm SWE) between 1/15 and 1/26 produced a 107% increase in strength in eleven days. That gain in strength occurred at roughly twice the rate of the 40% increase in strength between 1/9 and 1/15, when only 4 mm SWE of load was added to the snowpack over six days. While a temperature gradient through the weak layer did diminish slightly between 1/9 and 1/15 (Profiles 9 & 10, Appendix I), the bulk of this strengthening in the surface hoar was attributed to pressure metamorphism and substrate penetration induced by loading.

Under a near-constant load, variability in strength at the pit scale actually decreased slightly from 1/9 to 1/15, averaging 8.9% on 1/15 (mean of individual pits' $CV\bar{\tau}_{\infty}$, Table 56), down from 9.3% on 1/9. But, under substantial and sometimes rapid new loading between 1/15 and 1/26, variability in strength at the pit scale increased to 15.1% on 1/26 (mean of individual pits' $CV\bar{\tau}_{\infty}$, Table 61) indicating that the standard deviation of strength had grown faster than the mean of strength. At the larger plot scale, variability in strength changed very little between 1/9 and 1/15, from 10.4% to 10.5%, since mean strength and the standard deviation of strength changed proportionately, but then jumped to 17.5% on 1/26, a 67% increase. It is reasonable to assume that the substantial gross increase in the load on the weak layer, and sometimes-rapid rates of loading from 1/15 to 1/26, produced increased and, at times, *accelerating* creep rates in the snowpack.

These 1/26 results suggest that accelerating snowpack creep had the "global" effect of mobilizing the overlying slab on this slope, overwhelming local (pit-to-pit) variations in the stress/strength relationship at the weak layer and producing somewhat more variable in-pit *and* more uniform plot-wide distribution of shear strength. If this relationship between changing creep rates and scales of variation holds, a subsequent cessation in new loading, and decelerating creep rates, could have produce renewed divergence and poorer representation of strength (and stability), where differences between pits became larger than differences within pits again. However, an increasing depth of burial (and corresponding increase in age) of the weak layer could also eventually insulate the weak layer from near-surface changes in creep rates, enabling divergence to dominate future

changes in strength. Unfortunately, time and safety constraints made it impossible to perform another stability-sampling trial at this site prior to this writing.

Bridger Range Stability Model.

As previously discussed, the Bridger Range experienced two consecutive drought winters, in 1999/2000 and 2000/2001, followed by a notably stable winter in 2001/2002. The Bridger Range stability model was designed to extrapolate study plot stability measurements collected just prior to a storm whose load triggered an avalanche cycle in the study area. Actual avalanches would then have been compared to the model's predicted pattern of avalanching.

Weather and snowpack conditions, however, did not provide the opportunity to implement the model in that way. Instead, stability data from five Bridger Range stability-sampling trials during the 2000/2001 season were extrapolated even though no avalanching related to a subsequent storm was observed. Since all five trials were conducted in the southern portion of the Bridger Range study area, study plot stability was extrapolated only to the southern half of the Range, south of Ross Pass. All valid QLCT result from the five 2000/2001 trials were used to model stability in the starting zones mapped in the southern study area avalanche starting zones atlas (pg. 41).

No actual natural avalanches were observed in the Bridger Range coincident with or immediately after the five 2000/2001 trials. Several model runs, however, produced "critical" stability ratios $S_{Tin} < 1.0$ in numerous starting zones, indicating that those starting zones had exceeded a critical stability threshold and, according to the model, should have avalanched. For example, the pit with the highest (most stable) stability ratio

S_{QLCT} in the Saddle Peak Study Plot trials of 2/18/01, pit 4 (at S_{QLCT} = 2.16, Table 29), produced critical values of S_{Tin} < 1.0 in thirty-nine (68%) of the 57 mapped southern Bridger Range starting zones. Further, the pit with the lowest stability ratio S_{QLCT} in the Saddle Peak Study Plot trials of 2/18/01, pit 4 (at S_{QLCT} = 1.48, Table 29), produced critical values of S_{Tin} < 1.0 in fifty-seven (100%) of the 57 mapped southern Bridger Range starting zones. However, again, no natural avalanches were observed anywhere in the southern Bridger Range on 2/18/01 or during the weeks thereafter. Similar gross over-predictions of avalanching were produced by model runs associated with the 2/18/02 trials.

These "false-positive" results were attributed, in part, to the inability of the model to realistically estimate either change in snowpack depth (and water content) produced by changes in elevation (the Δzx function) or the effects of wind-drift redistribution of snow at and below ridgeline (the $\Delta Drift$ function). Actual snowpack SWE transect measurements were made to estimate a linear elevation effect Δzx. A simple model of ridge-crest wind drift was adopted and winds were (realistically) assumed to be uni-directional, from the west, at the ridge crest. Further, in the absence (by design) of snowpack data from elevations above the study plots, the model made no attempt to quantify changes over time in weak layer strength resulting from increased (or decreased) load or change of slope-aspect. The combined effects of these shortcomings resulted in inexorably increasing shear stresses, with increased altitude, but no offsetting increases in weak layer strength.

QLCT Trials

On three occasions QLCT results were compared to shear frame results (Table 66). The objective of the trials was to compare, in large grids of side-by-side tests, measured values and the variance in strength between the shear frame, an established test method, and the QLCT. Two of those trials were conducted in a layer of buried surface hoar at Rogers Pass, British Columbia, in March 2000 using the bench mode of the QLCT and a 0.025 m^2 shear frame (Landry et al., 2001b). Statistically different mean strengths were obtained in both of those trials, perhaps due to force-vector differences between the two methods (Landry et al., 2001b). However, the rates of variation in the results proved more similar.

Table 66: QLCT vs. Shear Frame Trials. Comparing Number of Tests (n), Mean Strength ($\overline{\tau}_{\infty}$), Standard Deviation of Strength (s), and Coefficient of Variation of Strength ($CV\overline{\tau}_{\infty}$).

	Rogers Pass – Cheops Plot 3/15/00		Rogers Pass – Fidelity Plot 3/16/00		Bacon Rind Plot 1/9/01	
	QLCT	SF	QLCT	SF	QLCT	SF
n	13	12	22	22	13	24
$\overline{\tau}_{\infty}$	2,085	1,469	1,804	2,303	819	945
s	318	190	201	270	248	229
$CV\overline{\tau}_{\infty}$	15.2%	12.9%	11.2%	11.7%	30.3%	24.3%

Larger differences in the coefficients of variation were found testing a layer of depth hoar at the Bacon Rind Plot on 1/9/01 using the surface mode of the QLCT and a 0.009 m^2 shear frame. Again, force-vector differences between the two methods could explain

those differences, since the shear frame introduces shear stress only, at the weak layer/slab interface, while the QLCT introduces shear and normal stresses. Several QLCT tests on 1/9/01 produced fracture at a different location than was measured by the shear frame and were not included in the analysis, resulting in a smaller sample of QLCT results.

Comparisons between the QLCT and the Stuffblock (SB), compression (CT), or Rutschblock (RB) tests could not be quantified since the latter tests produce ordinal ratings of strength and involve dynamic loads with cumulative effects. Of those, the CT may produce the most resolution in results, but all three tests yield results in force increments that preclude sensitivity to the small differences in strength detectable with the QLCT.

However, as noted earlier, sets of 50 SB, 10 CT, and four RB collected on 1/9/02 within the 900 m^2 plot all produced highly consistent results that were qualitatively analogous to the 10.4% coefficient of variation in strength measured by the QLCT (surface mode). Of the 50 SB, 40 (80%) had a "drop height" of 10 cm. Of the ten CT, six fractured with 2 taps from the wrist and the range was from 1 to 4 taps. And, all four RB fractured at score 2. Another set of tests performed by Birkeland and Johnson at the Middle Basin Plot on 12/28/01 produced 24 SB test scores ranging from 20cm to 80cm drop-heights, with 12 tests producing the mode drop-height of 40 cm, while 24 QLCT produced a mean strength of 1,134 N/m^2 and a standard deviation of 245 N/m^2, for a *CV* of strength of 21.6%. Again, although no direct comparison of strengths is possible, SB and QLCT results seemed to present similar variability in the Middle Basin trial.

CONCLUSIONS

Sampling Method

Collecting any type of field measurements of snowpack stability on inclined study plot slopes poses difficulties associated with slope disturbances created by the presence of the observer(s) and by variation introduced by the test procedure and/or the tester's technique. Paradoxically, measuring those effects requires producing the effects – a familiar dilemma in observing physical processes. The stability sampling trials at Round Hill on 2/4/01 provided the most striking example of observer disturbance, with the collapse of the entire slope during preparation of the final pit (pit 5). The Bradley Meadow trials on 3/17/01 required extra care during stability test preparation in order not to inadvertently damage the delicate relationship between the weak layer and overlying ice crust. Despite these potential sources of observer-introduced 'noise' in the QLCT results, this research proceeded on the premise that such disturbances were generally constant on a given day.

Still, the highly variable QLCT results obtained during the 2000/2001 season trials gave me, and others, pause. How much of that surprising variability was an artifact of the QLCT method itself? Was one QLCT mode more prone to background, operator-induced variation than another? Were different operators producing different effects on that background variation? Obviously, some residual variation would be found in any

snow stability testing method, and in any observer's technique, but was the QLCT producing more than other methods? Preliminary side-by-side comparative trials of the QLCT (bench mode) and 0.025 m^2 shear frame at Rogers Pass, British Columbia, in March 2000 (Landry et al, 2001), had produced approximate parity in the results. This suggested that, on those days, any residual noise in QLCT data was not substantially different than that obtained with the 0.025 m^2 shear frame (when operated by trained experts). Still, the variability observed during the 2000/2001 trials had routinely exceeded other reported quantified shear frame test results (Föhn, 1988; Jamieson ,1995).

Those doubts were largely assuaged by the three Lionhead Mountain Plot trials of January 2002. On 1/9/02, using the QLCT in surface mode, three pits in the plot (30 valid tests) produced coefficients of variation of strength of 6% or less, a hitherto unseen low index of variability (Appendix C). Pits 1 and 2 both produced standard deviations of strength of 22 N/m^2 against pit-mean strengths of 368 N/m^2 and 369 N/m^2, respectively. Then, during the subsequent 1/15 trials, using surface mode again, another two pits (19 tests) produced coefficients of variation of strength of only 6% (Appendix C). Further, the actual variations in plot-wide strength on both days were also quite low, with standard deviations in strength of 39 N/m^2 and 55 N/m^2, on plot-wide mean strengths of 375 N/m^2 and 523 N/m^2, respectively. Although the variability of strength was generally higher during the 1/26/02 trials, using the QLCT bench mode, that result was consistent with the increased strength of the weak layer. No observer-induced effects, such as localized collapsing, were observed during any of the Lionhead Mountain Plot trials.

It is reasonable to attribute some portion of the 6% coefficients of variation of strength observed in the five Lionhead Mountain Plot pits to actual variation in the strength of the surface hoar weak layer, given slight undulations in the snow surface producing small variations in aspect and 'sky view'. If real variations in strength accounted for one-half of the 6% variability then perhaps the residual, background variation introduced by the surface mode QLCT method, and variations in the observer's (my) technique, was as low as 3% in those pits on those days. Repeated measurements detecting very small standard deviations of strength provided reassuring evidence that at least the surface mode of the QLCT (using the 2-20 kg force gauge) could be executed with low levels of induced variation when testing a relatively weak surface hoar weak layer. Similarly, the Lionhead Mountain Plot trials of 1/26 provided evidence that bench mode could measure lower levels of variability than were observed during the bench mode trials of 2000/2001. Since bench mode was employed when testing stronger weak layers than can be tested with surface mode, and increased variability in strength was frequently associated with stronger snow in these trials, a substantial portion of the 17.5% coefficient of variation in strength on 1/26/02 was also attributed to real variations in the strengthening surface hoar weak layer. By using a lever-like apparatus to apply force to the load plate through the 2-20 kg force gauge, the load rate is controlled. Therefore, operator-induced variation caused by uncontrolled loading is thought to be no worse, and perhaps even lower, in bench mode than in surface mode, even at the higher strengths being tested. Bench mode does, however, entail substantially more preparation of the snow sample prior to testing and those procedures inevitably introduce additional

increment of background variation, compared to surface mode. Nonetheless, results from both QLCT test modes are reported here with some confidence that they include no more introduced variation, and perhaps less, than the shear frame method, when both methods are performed by experts. However, additional comparative QLCT vs. shear frame trials, and a method for reconciling effects on weak layer strength produced by differences between shear frame and QLCT force vectors, are needed.

Study Plot Stability and Hypothesis #1

Of the fifty-four snowpits sampled for stability (collecting 468 valid QLCT results), sixteen pits (29.6%) were found statistically unrepresentative of their respective study plots. Another eight (14.8%), or ten (18.5%, if the "NR" results are included in the analysis of the Middle basin Plot trials of 12/7/01), were deemed unrepresentative based on conclusive empirical evidence such as unquantified QLCT results, where strength exceeded our measurement capacities, or the presence of multiple weak layers (Table 67). The remaining thirty pits (55.6%), or twenty-eight (51.9%, when the "NR" results at the Middle Basin Plot are included in the analysis), were found statistically representative of their study plots (Table 67). In short, Hypothesis #1, that a single snowpit would represent mean stability throughout a carefully selected plot, was refuted as often as not. These results fail to reduce uncertainty regarding the representative-ness of stability test results from a single snowpit and, therefore, recommend rejecting Hypothesis #1.

However, while those roughly equal proportions of unrepresentative and representative pits from all eleven trials produced substantial evidence against Hypothesis

#1, those proportions were not always indicative of results at particular plots. At one extreme, the Round Hill trial on 2/4/01 produced no pits representative of plot-wide stability (Table 67). On the other hand, three trials - Bradley Meadow on 3/17/01, Middle Basin on 12/7/01, and Lionhead Mountain on 1/9/02 - produced no *un*representative pits (Table 67). Other trials, such as Bacon Rind and Lionhead on 1/15/02 and 1/26/02, produced a mixture of representative and unrepresentative pits (Table 67).

No periodicity in stability or its components was observed at the spatial scales of this study, such as the 2.5-3.0 m cross-slope 'wavelength' in shear strength variations observed by Conway and Abrahamson (1988). Also, none of the 468 valid stability tests conducted during the trials revealed the presence of 'imperfections' or 'deficit zones' now considered responsible for natural slab release (Schweizer, 1999), at least not at the scale of the individual tests (nominally 0.04 to 0.08 m^2). (The Round Hill trial did initiate a slope-wide weak layer fracture but the massive disturbance of the slope during the trial likely triggered this collapse). Rather, each of the eleven 900 m^2 stability-sampling plot trials revealed unique configurations of in-pit and in-plot variations in stability and its components – strength and stress.

The large proportion of either statistically or empirically unrepresentative pits in these trials cannot be attributed to the types of geographic controls – changes in elevation, slope aspect, distance from ridgecrest – that Birkeland (1997; 2001) and Dexter (1986)

Table 67: Stability-Sampling Trials Summary. (Bracketed values represent inclusion of "NR" QLCT results).

Plot	Date	Plot Mean Stability	*CV* Stability	Plot Mean Strength (N/m^2)	*CV* Strength	Pits Statistically Representative of Plot Stability	Pits Statistically Unrepresentative of Plot Stability	Pits Empirically Unrepresentative of Plot Stability
Bacon Rind	1/4/01	2.08	31.3%	533	32.0%	2	3	0
Bradley Meadow	1/27/01	5.74	22.2%	588	22.8%	2	3	0
Round Hill	2/4/01	2.60	43.7%	831	50.2%	0	4	0
Baldy Mountain[a]	2/18/01	1.79	20.1%	1,125	25.7%	0	0	5
Saddle Peak	2/18/01	1.86	26.1%	1,482	25.3%	2	3	0
Bradley Meadow[b]	2/18/01	1.59	20.4%	1,657	21.2%	2 (0)	0	3 (5)
Bradley Meadow	3/17/01	3.11	26.6%	433	27.0%	5	0	0
Middle Basin	12/7/01	2.03	23.7%	696	23.0%	5 (3)	0	0 (2)
Lionhead Mtn.	1/9/02	2.53	10.2%	375	10.4%	5	0	0
Lionhead Mtn.	1/15/02	3.08	10.6%	523	10.5%	3	2	0
Lionhead Mtn.	1/26/02	2.43	16.2%	1,084	17.5%	4	1	0
					Totals	30 (26)	16	8 (12)
					%	55.6% (48.2%)	29.6%	14.8% (22.2%)

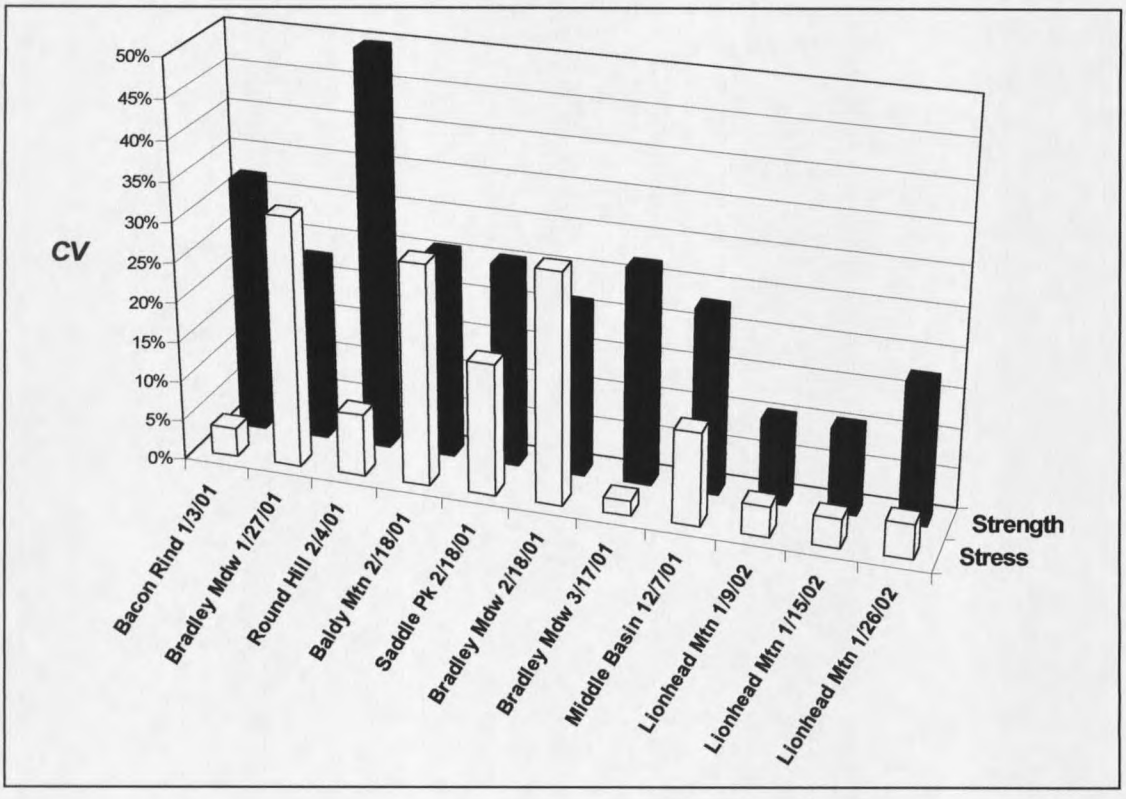
[a] Stability and strength data computed for QLCT results from subject weak layer only; five weak layers identified
[b] Stability and strength data computed for valid QLCT results only; numerous tests exceeded strength measuring capacity of equipment

correlated to variations in snowpack characteristics at large spatial scales. Nor were the kind of substrate irregularities, such as rock outcrops or logs, known to produce localized variations in snowpack strength observed in the plots (Birkeland et al., 1995; Arons et al., 1998). Within the comparatively small-scale, carefully selected 900 m^2 plots employed in this study, variations in those geographic controls were minimized, by experimental design. Rather, other physical controls, such as variations in load and loading rates on weak layers, and the age of weak layers, may help explain the variability observed. Chalmers and Jamieson (2000) found a relationship between gradual increases in the slab load over a surface hoar weak layer and increases in the shear strength of the surface hoar, with increasing loads (over time) producing increased stability. Johnson and Jamieson (2000) found a similar result in a study of faceted weak layers. In both of those studies, increases in load and changes in weak layer strength correlated over extended time periods of up to 90 days. Such physical controls affecting stability could be expected to occur at many spatial scales, including the study plot scale used in this study.

Thus, substantial plot-scale variations in shear stress produced by the in-situ slab load might have offered a plausible explanation for similar variations in weak layer strength in the eleven stability-sampling trials. Instead, these eleven trials produced a wide variety of relationships between the variability of shear stress and strength (Figure 29). For example, at Bradley Meadow during the 1/27/01 trial the coefficient of variation in shear stress was high, at 31.5%, and the coefficient of variation in strength was 22.8% (Figure 29). However, at Bacon Rind on 1/3/01 the coefficient of variation in shear stress was very low, at only 3.6%, but the coefficient of variation in strength was 32.0% (Figure 29).

At Round Hill on 2/4/01 the coefficient of variation in shear stress was also low, at 10.2%, but the coefficient of variation in strength was very large, at 50.2% (Figure 29).

Figure 29: Comparisons of Coefficients of Variation (*CV*) in Stress and Strength. (White bars represent plot-wide stress and black bars represent plot-wide strength.)



Those observed differences suggest that variability in stress and strength can vary by as much as a factor approaching ten, a range substantially larger than Föhn's finding (1988, p. 272) that, "...during stable or meta-stable conditions ... stability varies with the same order of magnitude (15-30%) as other snowpack parameters". (The plot-mean stability ratio S_{QLCT} was 2.08 at Bacon Rind on 1/3/01 and 2.60 at Round Hill on 2/4/01). Subdividing the trials according to whether a majority or a minority of pits were

representative of plot stability, a comparison of layer characteristics of the eleven trials performed in this study revealed yet another ambiguous perspective on these results (Table 68).

Table 68: Stability-Sampling Trials' Weak Layer and Slab Characteristics. Grouped according to representation of plot-wide stability.

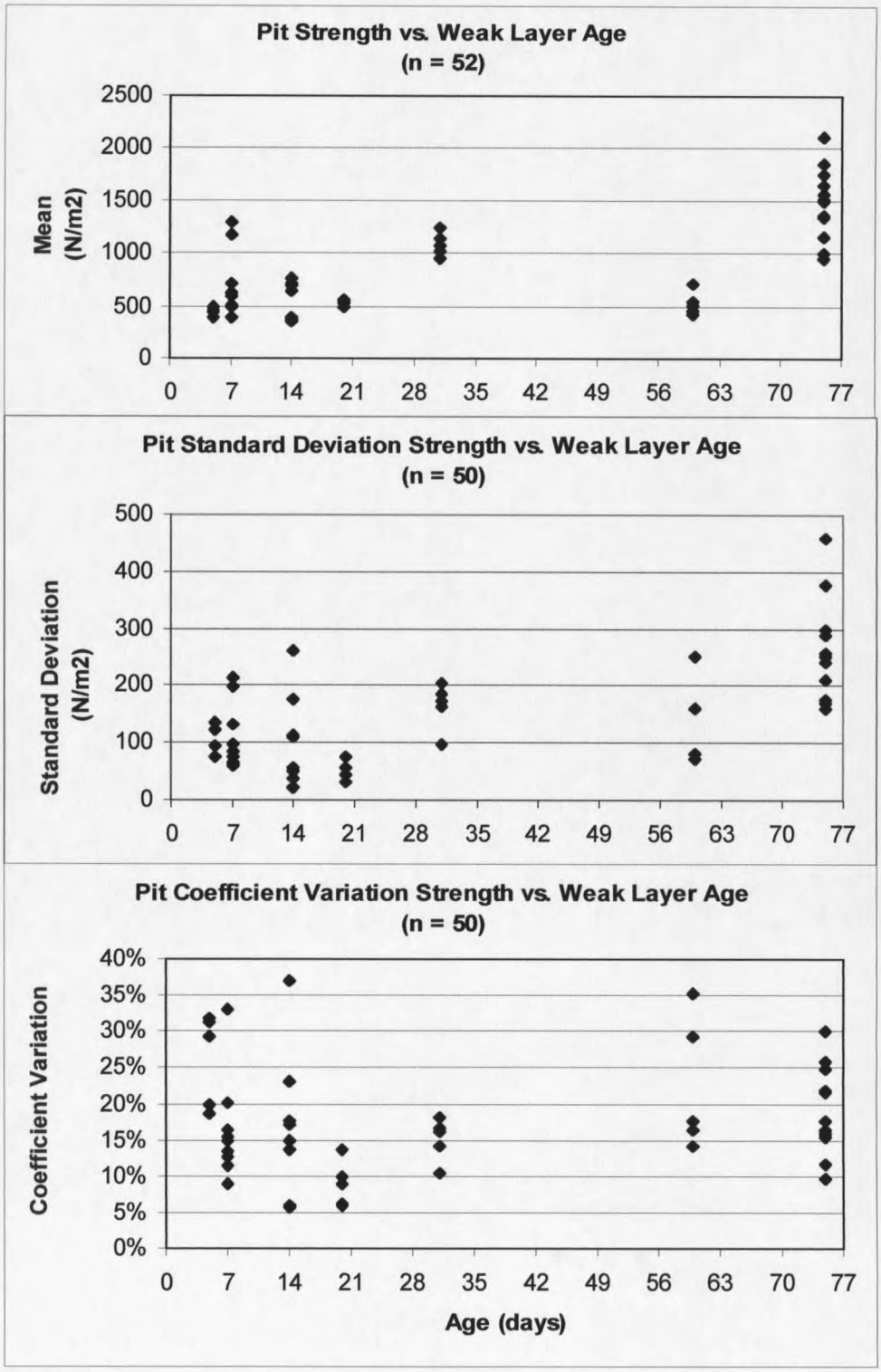
Trials	Pits Statistically Representative of Plot Stability	Weak Layer Type	Mean Slab Shear Stress (N/m^2)	*CV* Slab Shear Stress	Weak Layer Age
Bradley Meadow 3/17/01	5 of 5	Near-Surface Facets	139	1.9%	≅5 days
Lionhead 1/9/02	5 of 5	Surface Hoar	148	3.8%	14 days
Middle Basin 12/7/01	5 (3) of 5	Facets & Depth Hoar	345	11.7%	≅14 days
Lionhead 1/26/02	4 of 5	Surface Hoar	452	4.3%	31 days
Lionhead 1/15/02	3 of 5	Surface Hoar	170	3.6%	20 days
Bradley Meadow 1/27/01	2 of 5	New Forms	108	31.5%	7 days
Bacon Rind 1/4/01	2 of 5	Depth Hoar	257	3.6%	≅60 days
Saddle Peak 2/18/01	2 of 5	Depth Hoar	833	15.9%	≅75 days
Bradley Meadow 2/18/01	2 (0) of 5	Depth Hoar	1,274	47.9%	≅75 days
Round Hill 2/4/01	0 of 4	Surface Hoar	325	10.2%	7 days
Baldy Mountain 2/18/01	0 of 5	Depth Hoar	702	27.8%	≅75 days

The possibility of distinguishing between the two groups of results based on the mean shear stress and age of the weak layer is confounded by large variations within those groups and overlap between the two groups. For instance, the Middle Basin 12/7/01 and Round Hill 2/4/01 trials had very similar shear stress and weak layer age attributes, but exactly opposite "representative-ness" results (Table 68).

In his study of spatial variations in snow resistance, Birkeland et al. (1995) concluded that 'compounding factors', in addition to depth (load, in effect), contribute to snow strength. Evidently, snowpack processes operating at spatial (and perhaps temporal) scales different than the scale of variation in slab load were responsible for the inability of pits to represent plot-wide stability in trials such as Bacon Rind and Round Hill.

As noted earlier, the age of weak layers emerged as a potential predictor of consistency throughout a plot. However, when all eleven stability sampling trials are evaluated together, that hypothesis is not supported by a plot of weak layer age compared to pit mean strength, the standard deviation of pit-mean strength, and the coefficient of variation of pit mean strength (Figure 30). Although a discernible trend toward increasing strength with age is seen, a cluster of results at age 60 days contradicts the trend, and a considerable range in strength occurred in pits with young weak layers. The standard deviation of pit-mean strength mirrors the pattern of strength, with overlap in the magnitude of variations between young and old weak layers. Further, no age-driven pattern emerges in the coefficients of variation. Clearly, combining the different weak-

Figure 30: Weak Layer Age vs. Measures of Pit Strength. All valid pits, all trials.

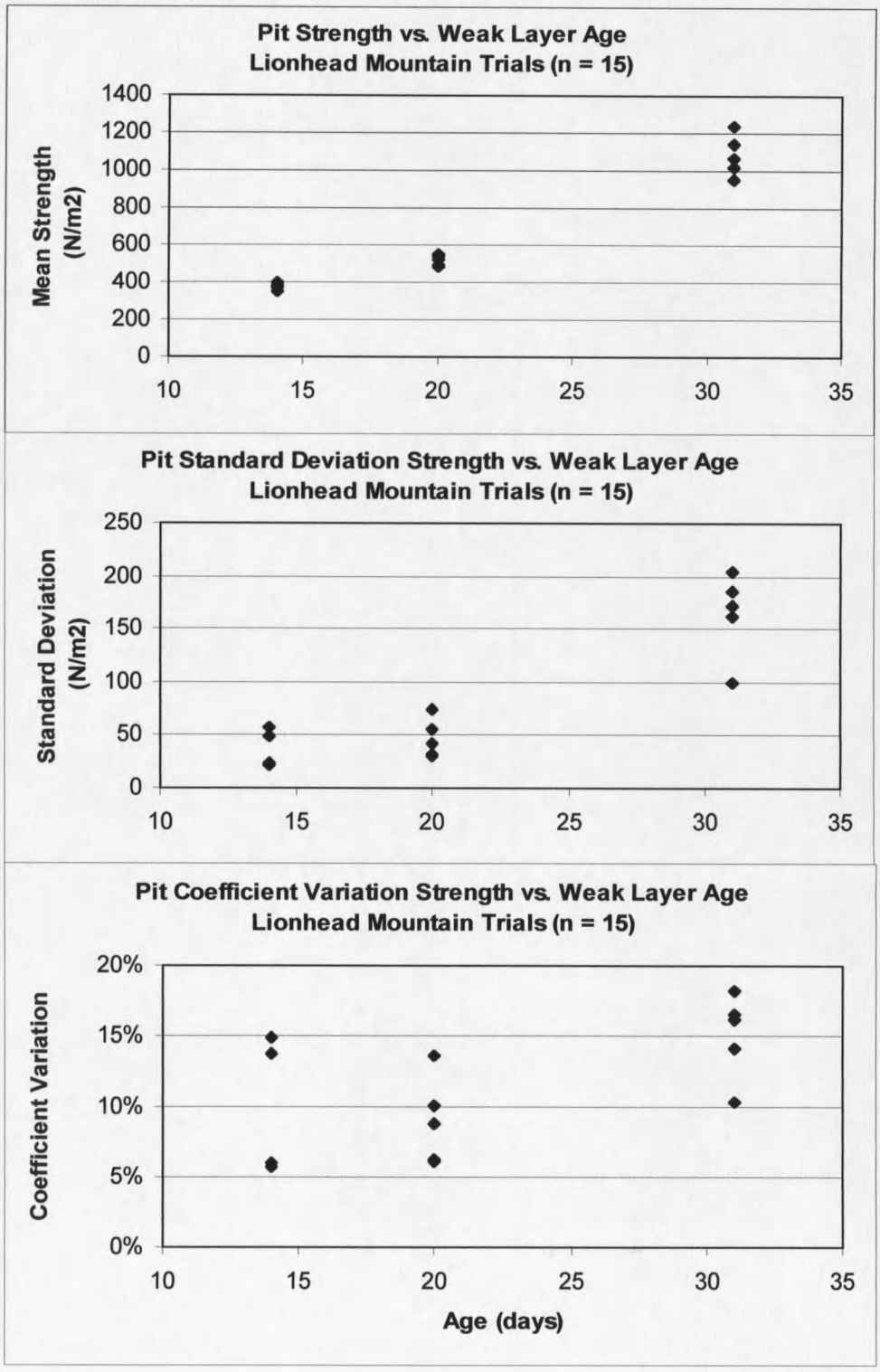


layer types observed in these trials (Table 68) contributes scatter to this analysis, and this chart (Figure 30) does not enable identification of which of pits were representative of plots.

However, a similar examination of the three trials performed at Lionhead Mountain Plot on 1/9/02, 1/15/02, and 1/26/02 does suggest a relationship between the age of a weak layer and variations in strength (Figure 31). The surface hoar weak layer deposited between 12/21 and 12/26/01 was tested in all three trials for a total of fifteen valid pits. A majority of pits in each trial was representative of plot-wide stability (Table 68), but *t*-tests found one pit unrepresentative of plot-wide strength on 1/9/02 (Table 54), three unrepresentative pits on 1/15/02, and two pits were unrepresentative of plot-wide strength on 1/26/02.

When the weak layer was 14 days old (1/9/02), all five pits produced similar mean strengths (too closely clustered to distinguish in Figure 31) but two pits showed higher variation in strength than the other three. Consequently, the same two pits also produced larger coefficients of variation. Subsequently, a trend toward increasing variation in strength with increasing age was observed at Lionhead culminating in one pit (pit 1) exhibiting substantially less variation than the remaining four pits on 1/26/02. This trend seems consistent with investigations of changes in surface hoar weak layer strength under increasing loads (Chalmers and Jamieson, 2000), although the weak layer gained additional strength between 1/9 and 1/15/02 without a substantial increase in slab load

Figure 31: Lionhead Plot Trials Weak Layer Age vs. Measures of Pit Strength. Fifteen valid pits, 1/9/02, 1/15/02 and 1/26/02 trials.



and shear stress suggesting that creep under a constant load also produces increasing strength over time. Interestingly, the mean plot-wide coefficients of variation in strength and stability were nearly identical from 1/9 to 1/15/02.

The relationships between weak layer age, strength, and variability of strength at the Lionhead Mountain Plot trials were complicated by differences in load rates. Further, although shear stress exhibited very low rates of variation in all three trials, even small variations in shear stress did produce pit-wise differences between *t*-tests of strength and *t*-tests of stability at each plot. These factors interacted dynamically to produce unexpected results such as reduced representative-ness from 1/9 to 1/15, at equivalent rates of variability in strength and stability, followed by improved representative-ness on 1/26/02, despite larger variability in strength and stability (Table 67). Weak layer age alone, and associated changes in strength over time due to creep, metamorphism, and increasing load, cannot explain the results of this study.

Therefore, with eleven different plot-wide patterns of stability presented by eleven different stability-sampling trials, uncertainty about the scale of spatial variation in snowpack stability remains. Rather than finding occasional "anomalous" variations in stability within these plots, the uniform stability predicted by Hypothesis #1 was observed in only three of eleven trials during this study, and no clear basis for predicting that result in those three plots was found. Further, with no more than 55.6% (30 of 54) of stability-sampling pits proving statistically representative of their seven plots, and in the absence of any consistent patterns of spatial variations in the components of stability that could explain that variability, Hypothesis #1 must be rejected. "Class I" stability test data

(LaChapelle, 1980) were, as often as not, unrepresentative of stability at one or more spatial scales – within a single pit, between pits only 12 m apart, within a single 900 m^2 study plot, and between geographically similar study plots as close as 2 km apart.

Extrapolation of Study Plot Stability and Stability Modeling

This study attempted to construct a simple GIS-based snowpack stability model of the Bridger Range of Montana, with very poor results. Hypotheses #2 and #3 addressed the extrapolation of presumably reliable study plot stability measurements at a single pit (Hypothesis #1) and the research design anticipated modeling and then observing actual patterns of study area stability in order to test Hypotheses #2 and #3. Just as would be the case in many avalanche forecasting programs, in this study stability measurements would not be conducted in avalanche starting zones for safety reasons. Rather, stability measurements were to be collected at "representative plots" in the Bridger Range and then extrapolated, in a GIS, to adjoining avalanche terrain. Unfortunately, two consecutive drought winters and an unusually stable third winter foiled the effort to conduct simultaneous Bridger Range study area stability-sampling trials just prior to a cycle of natural avalanches triggered by a storm. (Simultaneous stability-sampling trials at three study plots on 2/18/01 enabled plot-to-plot comparisons of stability and found that none of the study plots was representative of any other. No subsequent storm or avalanche activity occurred.) None-the-less, stability data collected during the Bridger Range study area trials were used as inputs to the GIS stability extrapolation model

developed for this study yielding the highly unsatisfactory "false-positive" results described earlier (Results – Bridger Range Stability Model).

A "simpler is better" approach was adopted throughout the GIS-based stability model development in this study on the hypothesis that gross patterns in stability in a comparatively small and simple mountain range could be approximated. The model's results belied that premise. The model clearly failed to estimate the combined effects of changes in elevation and of wind-drift on snowpack processes in the study area avalanche starting zones. Further, the model made no attempt to estimate the extremely complex processes changing the strength of weak layers, or other spatially controlled variations in the snowpack (i.e., changes by slope aspect), or the effects of time on avalanche formation processes. In short, the complexity of snowpack and avalanche formation processes could not be distilled into a few basic elements.

More fundamentally, however, this research found "uniform" stability at only three of eleven plots. The GIS model's underlying hypothesis that a single study plot snowpit would produce a reliable, representative measurement of plot-scale stability was rejected in the majority of the eleven stability-sampling trials performed in the Bridger Range study area and elsewhere. Given the poor representation by pits of plot stability in this study, even if a vastly more sophisticated deterministic model of snowpack and avalanche formation processes had been developed, the extrapolation of study-plot stability in a GIS-based model of avalanche terrain would still have entailed a high degree of uncertainty. Therefore, at a minimum, incorporating Class I stability-test data within deterministic avalanche forecasting models would seem to require a substantially

improved understanding of spatial and temporal variations in avalanche formation processes. In my opinion, these complex processes could elude generalization by even the most sophisticated deterministic GIS modeling approach since even defining an appropriate stability input to the model would be problematic. Other applications of GIS, focused on presenting and performing spatial analyses of historic avalanche data (i.e., Stoffel et al., 1998; McCollister et al., 2000), seem more likely to improve our understanding of these dynamic systems.

Implications for Conventional Avalanche Forecasting

Sufficient uncertainty in stability test results at a single study plot pit remains for avalanche forecasters to discount that information in lieu of other, lower-entropy Class I stability data. But, do these results suggest that conducting stability tests at carefully selected study plots is unhelpful or, worse, misleading?

As an experienced avalanche forecaster, I do not believe that rejecting Hypothesis #1 necessitates, or even recommends, that experienced avalanche professionals abandon the use of study plot stability tests, particularly when such tests are used to monitor change over time. It is my opinion that *experienced* forecasters learn to give appropriate weight to such tests, within their iterative information collecting and evaluation processes, and presume spatial variation to be the norm. Experienced forecasters acquire a sophisticated capacity (unmatched by any model or expert system) to weight, integrate, and extrapolate stability test information with other Class I, II and III information based on their

underlying understanding of avalanche formation processes and their cumulative experience in observing avalanche behavior.

Stability test results from study plots *and other "targeted" sampling locations* (McClung, in press) are typically perceived as clues to spatial patterns of snowpack characteristics. McClung (in press) argues that "avalanche forecasting is the prediction of current and future snow *instability* in space and time" and, as such, must confront biases in human perception. If snow stability sampling methods are unlikely to reveal instability then human perception will be poor. He adds that random sampling does not optimize chances of locating instabilities and further notes that regular sampling across study slopes is "likely to be very inconclusive", as this study has confirmed in many (but not all) trials. Rather, McClung and others (Fredston and Fesler, 1994) advocates "targeted sampling" of sites suspected to represent the worst-case stability scenario on a given day. It has been my experience that it sometimes is impossible to conduct such targeted sampling safely and a forecaster must interpret a spatially limited sampling, estimating the kind of variations that more extensive targeted sampling might reveal. This recommends that forecasters learn to recognize snowpack and weather regimes that are likely to increase or decrease spatial variations in the components of snowpack (*in*)stability and calibrate all forms of Class I information they obtain, including stability test results, accordingly.

Scales of Spatial Variation in Stability and Suggestions for Future Research

This research investigated whether, on a given day, a single pit could represent the spectrum of local (plot-scale) variations in stability. Within the 3.75 m^2 area of each of the fifty-four pits, standard deviations of strength varied widely, from 22-23 N/m^2 at Lionhead Mountain on 1/9/02 (Appendix C), to 458 N/m^2 at Saddle Peak (pit 3) on 2/18/01 (Appendix B). Some pits were notably uniform and, at the same time, significantly different from other pits in the plot. Pits containing larger variations often did represent the variability of the plot. At Saddle Peak pit 3, on 2/18/01, the single strongest and single weakest QLCT results within the entire study plot were found in *adjoining* test cells, only 0.5 m apart (Figure 16). Ultimately, a range of "characteristic scale(s)" (Phillips, 1999a) of stability were observed and only three of the eleven plots produced a full complement of five pits exhibiting variation in stability representative of their plots on that day. Those fifteen pits and three plots captured snapshots of stability at moments in time. However, stability is clearly not a static phenomenon. Deficit zones may begin, grow, and either propagate catastrophic fracturing when a critical stress/strength threshold is reached, or to heal over time (Schweizer, 1999). Predicting avalanche formation processes will require a better understanding of the factors driving spatial and temporal changes in the characteristic scales of snowpack stability, or perhaps instability, and its components.

The three Lionhead Mountain trials during January of 2002 provided some tantalizing evidence of changes in the characteristic scale of stability over time, possibly driven by

the waxing and waning of snowpack creep rates. Our three intermittent trials at Lionhead, over a span of seventeen days, provided glimpses of the compounding effects of changes in load, creep rates, and pressure metamorphism over time. In a sense, our measurements briefly captured the 'system state' of the snowpack on that slope, and my analysis attempted to describe changes in stability in terms of 'convergence' and 'divergence', borrowing the language of so-called 'earth surface systems' presented by Phillips (1999b) and Schumm (1991). Additional stability-sampling trials (at a safe site), making frequent measurements of changes in stability over time and continuous measurements of snowpack system elements, and applying earth surface system concepts such as divergence and convergence, could improve our understanding of spatial and temporal variations in avalanche formation processes at their characteristic scales.

REFERENCES CITED

Armstrong, B. R. and K. Williams. 1986. *The Avalanche Book.* Fulcrum, Golden, Colorado, USA, 222 pp.

Armstrong, R. L. 1991. Snow properties research and data management. In *Snow Science: Reflections on the past, Perspectives on the Future.* Proceedings of the Alta symposium, The Center for Snow Science, Alta, Utah, USA, p. 1-9.

Armstrong, R. L. and E. LaChapelle, 1976. Avalanche forecast methods. In *Avalanche Release and Snowpack Characteristics: San Juan Mountains, Colorado.* University of Colorado Institute of Arctic and Alpine Research, Occasional Paper No. 19, p. 41-65.

Armstrong, R. L. and B. R. Armstrong. 1988. Snow and avalanche climates of the western United States. In *Avalanche Formation, Movement and Effects,* Proceedings of the Davos Symposium. IAHS Publ. No. 162, p. 281-294.

Arons, E. M., S.C. Colbeck and J.M.N.T Gray. 1998. Depth-hoar growth rates near a rocky outcrop. *Journal of Glaciology* 44(148), p. 477-484.

Aspinall, R. J. 2000. Personal communication. Geographic Information and Analysis Center, Montana State University, Bozeman, Montana.

Bader, H. P. and B. Salm. 1990. On the mechanics of snow slab release. *Cold Regions Science and Technology,* Vol. 17, No. 3, p. 287-300.

Balk, B., K. Elder and J. Baron. 1998. Using geostatistical methods to estimate snow water equivalence distribution in a mountain watershed. In *Proceedings of 66th Annual Western Snow Conference,* Snowbird, Utah, USA, p. 100-111.

Barry, R. G. 1992. *Mountain Weather and Climate.* Routledge: New York, 402 pp.

Birkeland, K. W. 1997. Spatial and temporal variations in snow stability and snowpack conditions throughout the Bridger Mountains, Montana. Ph.D. Dissertation, Department of Geography, Arizona State University, Tempe, Arizona, USA, 205 pp.

Birkeland, K. W. 1998. Terminology and predominant processes associated with the formation of weak layers of near-surface faceted crystals in the mountain snowpack. *Arctic and Alpine Research* 30(2), p. 193-199.

Birkeland, K. W. 2000. Personal communication. National Avalanche Center, United States Forest Service, Bozeman, Montana.

Birkeland, K.W. 2001. Spatial patterns of snow stability throughout a small mountain range. *Journal of Glaciology,* Vol. 47, No.157, p. 176-186.

Birkeland, K.W., K.J. Hansen, and R.L. Brown. 1995. The spatial variability of snow resistance on potential avalanche slopes. *Journal of Glaciology* 41(137), p. 183-190.

Birkeland, K.W. and C. Mock. 1996. Atmospheric circulation patterns associated with heavy snowfall events, Bridger Bowl, Montana, USA. *Mountain Research and Development,* Vol.16, No. 3, p. 281-286.

Birkeland, K. W. and R. Johnson. 1999. The stuffblock snow stability test: comparability with the rutschblock, usefulness in different snow climates, and repeatability between observers. *Cold Regions Science & Technology* 30, p. 115-123.

Bolognesi, R. M. 1998. Nivolog: an avalanche forecasting support system. In *Proceedings of the 1998 International Snow Science Workshop*, Sunriver, Oregon, USA, p. 412-418.

Bolognesi, R., M. Denuelle, L. Dexter. 1996. Avalanche forecasting with GIS. In *Proceedings of the 1996 International Snow Science Workshop in Banff,* p. 11-13. Canadian Avalanche Association, Revelstoke, BC, Canada.

Bradley, C. 1970. The location and timing of deep slab avalanches. *Journal of Glaciology*, Vol. 9, No. 56, p. 253-261.

Bridger Bowl Ski Patrol. 2001. Personal communication from Peter Carse.

Buisson, L. and C. Chartier. 1989. Avalanche starting zone analysis by use of a knowledge-based system. *Annals of Glaciology,* Vol. 13, p. 27-30.

CAA/NRCC and Schleiss, V. 1995. Weather observation sites and procedures. In *Appendix A, Observation Guidelines and Recording Standards for Weather, Snowpack and Avalanches.* Canadian Avalanche Association, NRCC Technical memorandum No. 132, p. 61-62.

Caine, N. 1975. An elevational control of peak snowpack variability. *Water Resources Bulletin*, Vol. 11, No. 3, p. 613-621.

Chalmers, T.S. and J.B. Jamieson. 2000. Contrasting stability trends of two surface hoar layers in the Columbia Mountains, British Columbia, Canada. In *Proceedings of the 2000 International Snow Science Workshop*, Big Sky, Montana, USA, p. 94-100.

Chernouss, P. A. and Yu. V. Federenko. 1998. Probabilistic evaluation of snow-slab stability on mountain slopes. *Annals of Glaciology*, Vol. 26, p. 303-306.

Conway, H. and J. Abrahamson. 1984. Snow stability index. *Journal of Glaciology*, Vol. 30, No. 106, p.321-327.

Conway, H. and J. Abrahamson. 1988. Snow-slope stability – a probabilistic approach. *Journal of Glaciology*, Vol. 34, No.117, p. 170-177.

Davis, R. E., B.J. Jamieson and C. Johnston. 1998. Observations on buried surface hoar in British Columbia, Canada; section analyses of layer evolution. In *Proceedings of the 1998 International Snow Science Workshop*, Sunriver, Oregon, USA, p. 86-92.

Dexter, L. R. 1986. Aspect and elevation effects on the structure of the seasonal snow cover in Colorado. Ph.D. Dissertation, Department of Geography, University of Colorado, Boulder, Colorado, USA, 229 pp.

Durand, Y., G. Giraud, E. Brun, L Merindol and E. Martin. 1999. A computer-based system simulating snowpack structures as a tool for regional avalanche forecasting. *Journal of Glaciology*, Vol. 45, No. 151, p. 469-484.

ESRI. 1999. ArcView v. 3.2. Environmental Research Systems, Inc. Redlands, California, USA.

Farnes, P. E. 1995. Estimating monthly distribution of average annual precipitation in mountainous areas of Montana. In *Proceedings of 63rd Annual Western Snow Conference*, Sparks, Nevada, USA, p. 78-86.

Föhn, P. M. B. 1980. Snow transport over mountain crests. *Journal of Glaciology*, Vol. 26, No. 94, p. 469-480.

Föhn, P. M. B. 1987a. The "Rutschblock" as a practical tool for slope stability evaluation. In *Avalanche Formation, Movement, and Effects*, Proceedings of the Davos Symposium. IAHS publ. No. 162, p. 223-228.

Föhn, P. M. B. 1987b. The stability index and various triggering mechanisms. In *Avalanche Formation, Movement and Effects,* Proceedings of the Davos Symposium. IAHS Publ. No.162, p. 195-207.

Föhn, P. M. B. 1988. Snowcover Stability Tests and the Aereal Variability of Snow Strength. In *Proceedings of the 1988 International Snow Science Workshop*, Whistler, British Columbia, Canada, p. 262-273.

Fredston, J. and D. Fessler. 1994. Snow sense - a guide to evaluating snow avalanche hazard. *Alaska Mountain Safety Center*, Anchorage, Alaska, USA, 116 pp.

Gauer, P. 1999. Blowing and drifting snow in alpine terrain: a physically-based numerical model and related field measurements. Mitt. Eidgenöss. Inst. Schnee-Lawinenforsch. 58: 128 S.

Gauer, P. 2000. Personal communication. Montana State University Department of Civil Engineering, Bozeman, Montana.

Giraud, G, E. Brun, Y. Durand and E. Martin. 1994. Validations of objective models to simulate snow cover stratigraphy and avalanche risk for avalanche forecasting. In *Proceedings of the 1994 International Snow Science Workshop*, Snowbird, Utah, USA, p. 509-517.

Good, W. and W. Ammann. 1994. Modeling local avalanche forecast: a review. In *Proceedings of the 1994 International Symposium on Snow and Related Manifestations, Manali*, p. 19-25.

Greene, E.M., G. E. Liston, and R.A Pielke, Sr. 1999. Simulation of above-treeline snowdrift using a numerical snow-transport model. *Cold Regions Science and Technology*, Vol. 30, 1999, p. 135-144.

Ingersoll, G. P., D. H. Campbell, and N.E. Spahr. 1996. Snow depth variability in a small alpine watershed. In *Proceedings of the 64th Annual Western Snow Conference*, Bend, Oregon, USA, p. 159-162.

Jamieson, J. B. 1995. Avalanche prediction for persistent snow slabs. Ph.D. Dissertation, Department of Civil Engineering, University of Calgary, Calgary, Alberta, 255 pp.

Jamieson, J.B. and C.D. Johnston. 1992. Experience with Rutschblocks. In *Proceedings of the 1992 International Snow Science Workshop*, Breckenridge, Colorado, USA, p. 150-159.

Jamieson, B. and C.D. Johnston. 1994. Monitoring a shear frame stability index and skier-triggered slab avalanches involving persistent weak layers. In *Proceedings of the 1994 International Snow Science Workshop*, Snowbird, Utah, USA, p. 14-21.

Jamieson, J.B. and T. Geldsetzer. 1996. *Avalanche accidents in Canada – Volume 4*. Canadian Avalanche Association, Revelstoke, BC, Canada, 193 pp.

Jamieson, J.B. and C. Johnston. 1997. The compression test for snow stability. In *Proceedings of the 1996 International Snow Science Workshop in Banff*, p. 118-125. Canadian Avalanche Association, Revelstoke, BC, Canada.

Jamieson, J.B. and J. Schweizer. 2000. Texture and strength changes of buried surface hoar layers with implications for dry snow-slab avalanche release. *Journal of Glaciology*, Vol. 46, No. 152, p. 151-160

Johnson, G. and B.J. Jamieson. 2000. Strength changes of layers of faceted snow crystals in the Columbia and Rocky Mountain snowpack climates in southwestern Canada. In *Proceedings of the 2000 International Snow Science Workshop*, Big Sky, Montana, USA, p. 86-93.

Johnson, R. 2000. Personal communication. Gallatin National Forest Avalanche Center, United States Forest Service, Bozeman, Montana.

Johnson, R. 2002. Personal communication. Gallatin National Forest Avalanche Center, United States Forest Service, Bozeman, Montana.

Johnson, R. and K. W. Birkeland. 1998. Effectively using and interpreting stability tests. In *Proceedings of the 1998 International Snow Science Workshop*, Sun River, Oregon, USA, p. 562-565.

Jones, K.H. 1998. A comparison of algorithms used to compute hill slope as a property of the DEM. *Computers & Geosciences*, Vol. 24, No. 4, p. 315-323.

Judson, A., C. Leaf, and G. Brink. 1980. A process-oriented model for simulating avalanche danger. *Journal of Glaciology*, Vol. 26, No. 94, p.53-63.

LaChapelle, E.R. 1966. Avalanche forecasting - a modern synthesis. In *International Symposium on the Scientific Aspects of Snow and Ice Avalanches*, IAHS publ. No. 69, 350-356.

LaChapelle, E. R. 1980. The fundamental processes in conventional avalanche forecasting. *Journal of Glaciology*, Vol. 26, No. 94, p. 75-84.

Landry, C. C. 1994. Avalanche hazard risk management for the Yule marble quarry. In *Proceedings of the 1994 International Snow Science Workshop*, Snowbird, Utah, USA, p. 548-563.

Landry, C. C. 1998. 1997/98 Yule Creek Avalanche Services avalanche season review: Yule Creek quarry operation. Unpublished memorandum to Colorado Yule Marble Company from Yule Creek Avalanche Services, 23 pp.

Landry, C. C. 1998. A "loaded column" test – ready for prime time? Unpublished Yule Creek Avalanche Services Irregular Communiqué No. 4, 11 pp.

Landry, C. C. 1999. Experimental loaded column test procedure. Unpublished Yule Creek Avalanche Services memorandum, 14 pp.

Landry, C. C. 2000. Unpublished Bridger Range avalanche starting zone atlas. On file with Department of Earth Sciences, Montana State University, Bozeman, Montana.

Landry, C.C., J. Borkowski, and R.L. Brown. 2001a. Quantified loaded column stability test: mechanics, methodology, and preliminary trials. In *Proceedings of the 2000 International Snow Science Workshop*, Big Sky, Montana, USA, p. 230-237.

Landry, C.C., J. Borkowski, and R.L. Brown. 2001b. Quantified loaded column stability test: mechanics, procedure, sample-size selection, and trials. *Cold Regions Science and Technology*, Vol. 33, p. 103-121.

Liston, G. E. and M. Sturm. 1998. A snow-transport model for complex terrain. *Journal of Glaciology*, Vol. 44, No. 148, p. 498-516.

Logan, N. and D. Atkins. 1996. *The snowy torrents – avalanche accidents in the United States, 1980-86.* Colorado Geological Survey Special Publication No. 39, 265 pp.

Martinelli, M., Jr. 1974. *Snow avalanche sites, their identification and evaluation.* U.S. Department of Agriculture, Forest Service, Agriculture Information Bulletin 360, 26 pp.

McClung, D.M. 1977. Direct simple shear tests on snow and their relation to slab avalanche formation. *Journal of Glaciology* Vol. 19 (81), p. 101-109.

McClung, D.M. 1994. Use of expert knowledge in avalanche forecasting. In *Proceedings of the 1994 International Symposium on Snow and Related Manifestations, Manali*, p. 417-424.

McClung, D.M. 1998. The seven elements of avalanche forecasting. In *Proceedings of the 1998 International Snow Science Workshop*, Sunriver, Oregon, USA, p. 426.

McClung, D.M. 2000. Predictions in avalanche forecasting. *Annals of Glaciology,* Vol. 31, p. 377-381.

McClung, D.M. In press. The elements of applied avalanche forecasting Part I: the human issues. *Natural Hazards.*

McClung, D. and P. Schaerer, 1993. *The Avalanche Handbook.* The Mountaineers, Seattle, Washington, USA, 272 pp.

McClung, D. and J. Schweizer. 1999. Skier triggering, snow temperatures and the stability index for dry-slab avalanche initiation. *Journal of Glaciology* Vol. 45 (150), p. 190-200.

McCollister, C., K. Birkeland, K. Hansen and R. Aspinall. 2000. Using GIS to visualize historical avalanche data. In *Proceedings of the 2000 International Snow Science Workshop*, Big Sky, Montana, USA, p. 439.

McPartland, J. T. 1971. Snowpack accumulation in relation to terrain and meteorological factors in Southwest Montana. M.S. Thesis, Department of Earth Sciences, Montana State University, Bozeman, Montana, USA, 106 pp.

Mears, A. 1996. Dry-slab density and thickness during major storms. In *Proceedings of the 1996 International Snow Science Workshop in Banff*, p. 91. Canadian Avalanche Association, Revelstoke, BC, Canada.

Mock, C.J. and K.W. Birkeland. 2000. Snow avalanche climatology of the western United States mountain ranges. *Bulletin of the American Meteorological Society* 81(10), p. 2367-2392.

Narita, H. 1980. Mechanical behavior and structure of snow under uniaxial tensile stress. *Journal of Glaciology*, Vol. 26, No. 94, p. 275-282.

Owenby, J. R. and D. S. Ezell. 1992. Monthly station normals of temperature, precipitation, and heating and cooling degree days, 1961-1990, Montana. National Climatic Data Center, Asheville, N.C., USA.

Ouren, D. and C. C. Landry. 2000. Unpublished student report, Department of Earth Sciences, Montana State University, Bozeman, Montana.

Perla, R. and M. Martinelli Jr. 1976 (revised 1978). *Avalanche Handbook.* U.S. Department of Agriculture Handbook 489. Washington, D.C.: U.S. Government Printing Office, 238 pp.

Perla, R. and T. M. H. Beck. 1983. Experience with shear frames. *Journal of Glaciology*, Vol. 29, No. 103, p. 485-491.

Phillips, J. D. 1999a. Earth surface systems – complexity, order and scale. Malden and Oxford: Blackwell.

Phillips, J. D. 1999b. Divergence, convergence, and self-organization in landscapes. *Annals of the Association of American Geographers*, 89(3), p. 466-488.

Pipp, M. J. and W.W. Locke. 1998. Local scale variability in storm snowfall and seasonal snowpack distribution in the Bridger Range, Montana. In *Proceedings of the 66th Annual Western Snow Conference*, Snowbird, Utah, USA, p. 26-37.

Rink, C. 1987. Doctrine of geosystems and statistical methods as a means of avalanche forecast. In *Avalanche Formation, Movement and Effects,* Proceedings of the Davos Symposium. IAHS Publ. No. 162, p. 581-582.

Schaerer, P. 1991. Suggestions for snow research. In *Snow Science: Reflections on the past, Perspectives on the Future.* Proceedings of the Alta symposium, The Center for Snow Science, Alta, Utah, USA, p. 32-41.

Schumm, S. A. 1991. To interpret the earth: ten ways to be wrong. Cambridge University Press, Cambridge and New York.

Schweizer, J. 1999. Review of dry snow slab avalanche release. *Cold Regions Science and Technology*, Vol. 30, p. 43-57.

Schweizer, J. and P.M.B. Föhn. 1996. Avalanche forecasting – an expert system approach. *Journal of Glaciology*, Vol. 42, No. 141, p.318-332.

Schleiss, V.G. 1989. Rogers pass avalanche atlas – Glacier National park, British Columbia, Canada. Canadian Parks Service, Revelstoke, British Columbia, Canada. 313 pp.

Skipp, B., D. R. Lageson and W.J. McKinnis. 1999. Geologic Map of the Sedan Quadrangle, Gallatin and Park Counties, Montana. USGS Geologic Investigations Series I-2634, 1999.

Sommerfeld, R. A. 1980. Statistical models of snow strength. *Journal of Glaciology*, V. 26 (94), 1980, p. 217-223.

Sommerfeld, R. A. and J. Smith. 1998. Modeling snowdrift distribution in a small mountain watershed: spatial and temporal limitations. In *Proceedings of 66th Annual Western Snow Conference*, Snowbird, Utah, USA, p. 116-122.

Stoffel, A., R. Meister and J. Schweizer. 1998. Spatial characteristics of avalanche activity in an alpine valley – a GIS approach. *Annals of Glaciology*, Vol. 26, p.329-336.

USFS. 2000. ArcInfo vegetation coverages, Gallatin National Forest, Bozeman, Montana, USA.

WAN. 1995. WestWide Avalanche Network, Post Office Box 8067, Alta, Utah 84092-8067, USA.

Winstral, A., K. Elder and R. Davis. 1998. Characterization of wind induced snow redistribution with GIS derived parameters. In *Proceedings of the 66th Annual Meeting Western Snow Conference*, Snowbird, Utah, USA, p. 9-18.

APPENDICES

APPENDIX A

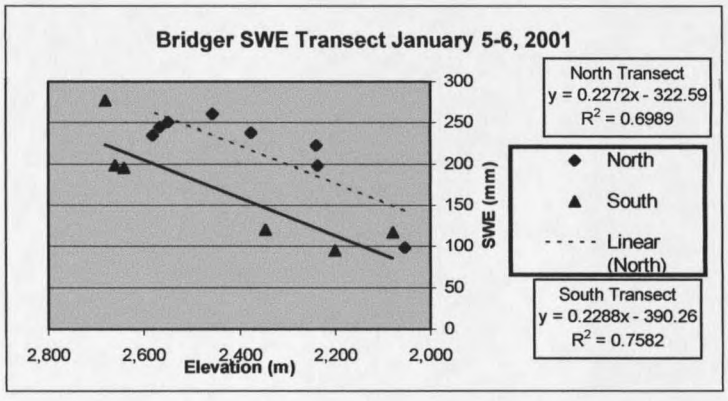
SOUTHERN BRIDGER RANGE *SWE* TRANSECT

Southern Bridger Range SWE Transects - January 5-6, 2001*
(* ALSP as of 1/12/01 - no intervening precip)

Transect	Sample Point	UTM Coord N/S	N/S Var Ridge	UTM Coord E/W	E/W Var Ridge	Est. Elev (ft)	Est. Elev (m)	Var Elev (m)	Snowpack Thickness	Total SWE	Density *p*
North	Ridge	5,074,915		505,215	0	8,526	2,599	0			
	1	5,074,927	12	505,247	32	8,469	2,581	-17	1.03	235	228
	2	5,074,939	24	505,277	62	8,422	2,567	-32	1.19	245	206
	3	5,074,950	35	505,308	93	8,365	2,550	-49	1.09	251	230
	4	5,075,055	140	505,321	106	8,060	2,457	-142	1.10	261	237
	5	5,075,075	160	505,559	344	7,800	2,377	-221	1.10	238	216
	6	5,074,969	54	506,057	842	7,350	2,240	-358	0.90	223	248
	7	5,074,928	13	507,100	1,885	6,740	2,054	-544	0.50	99	197
	ALSP	5,074,746	-181	506,043	828	7,340	2,237	-361	0.68	198	290
South	Ridge	5,072,190	0	505,134	0	8,795	2,681	0			
	1	5,072,195	5	505,168	34	8,731	2,661	-20	1.10	277	252
	2	5,072,201	11	505,197	63	8,667	2,642	-39	0.91	198	218
	3	5,072,201	11	505,232	98	8,603	2,622	-59	0.94	195	208
	4	5,071,998	-192	505,631	497	7,700	2,347	-334	0.65	120	185
	5	5,072,362	172	506,158	1,024	7,220	2,201	-480	0.38	95	250
	6	5,072,814	624	506,914	1,780	6,820	2,079	-602	0.56	117	211

Graph Data

	Elev	SWE
N1	2,581	235
N2	2,567	245
N3	2,550	251
N4	2,457	261
N5	2,377	238
N6	2,240	223
N7	2,054	99
ALSP	2,237	198
S1	2,681	277
S2	2,661	198
S3	2,642	195
S4	2,347	120
S5	2,201	95
S6	2,079	117



APPENDIX B

2000/2001 Study Plot Trials QLCT Results

Bacon Rind 30m x 30m Study Plot Stability-Sampling Trials: 1/3/01

Location		QLCT Data Surface Mode					Pit Results *(TauInf correction term C = 0.771)				Z Score	Z Score	Location	
Pit #	Cell #	Slope	H2O Nor	H Nor	TauSlab	Test kg	TauInfin (N/m2)*	S QLCT	Pit-Wise		TauInfin	S QLCT	Pit #	Cell #
1	1	30	52	0.29	255	6.65	489	1.919	Mean =	460	-0.258	-0.240	1	1
1	2	30	52	0.29	255	4.05	383	1.501	Std Dev'n =	81	-0.882	-0.882	2	1
1	3	30	52	0.29	255	5.60	446	1.750	Coef. Var'n =	17.5%	-0.510	-0.500	3	1
1	4	30	52	0.29	255	2.75	329	1.293	Median =	451	-1.193	-1.204	4	1
1	5	30	52	0.29	255	5.50	442	1.734			-0.534	-0.524	5	1
1	6	30	52	0.29	255	8.45	562	2.208			0.173	0.204	6	1
1	7	30	52	0.29	255	5.05	423	1.662			-0.642	-0.635	7	1
1	8	30	52	0.29	255	9.60	610	2.392	SQLCT =	1.81	0.448	0.488	8	1
1	9	30	52	0.29	255	6.05	464	1.822	Crit(38) -1s =	26	-0.402	-0.388	9	1
1	10	30	52	0.29	255	5.85	456	1.790	Crit(38) +1s =	60	-0.450	-0.438	10	1
2	1	32	47	0.28	244	2.15	301	1.232	Mean =	432	-1.361	-1.297	1	2
2	2	32	47	0.28	244	5.90	460	1.884	Std Dev'n =	71	-0.429	-0.294	2	2
2	3	32	47	0.28	244	6.50	485	1.988	Coef. Var'n =	16.4%	-0.279	-0.133	3	2
2	4	32	47	0.28	244	5.85	458	1.875	Median =	424	-0.441	-0.307	4	2
2	5	32	47	0.28	244	4.15	386	1.580			-0.864	-0.762	5	2
2	6	32	47	0.28	244	8.60	574	2.353			0.243	0.429	6	2
2	7	32	47	0.28	244	5.00	422	1.727			-0.652	-0.534	7	2
2	8	32	47	0.28	244	5.10	426	1.745	SQLCT =	1.77	-0.628	-0.508	8	2
2	9	32	47	0.28	244	4.45	398	1.632	Crit(38) -1s =	25	-0.789	-0.682	9	2
2	10	32	47	0.28	244	4.85	415	1.701	Crit(38) +1s =	55	-0.690	-0.575	10	2
3	1	30	53	0.29	260	13.00	752	2.897	Mean =	710	1.285	1.265	1	3
3	2	30	53	0.29	260	14.00	793	3.054	Std Dev'n =	251	1.525	1.508	2	3
3	3	30	53	0.29	260	5.60	450	1.732	Coef. Var'n =	35.4%	-0.488	-0.528	3	3
3	4	30	53	0.29	260	7.40	523	2.015	Median =	671	-0.057	-0.092	4	3
3	5	30	53	0.29	260	5.80	458	1.763			-0.440	-0.480	5	3
3	6	30	53	0.29	260	6.35	480	1.850			-0.308	-0.346	6	3
3	7	30	53	0.29	260	20.40	1,055	4.062			3.059	3.059	7	3
3	8	30	53	0.29	260	22.50	1,141	4.393	SQLCT =	2.73	3.562	3.568	8	3
3	9	30	53	0.29	260	15.60	859	3.306	Crit(38) -1s =	42	1.909	1.895	9	3
3	10	30	53	0.29	260	9.00	589	2.267	Crit(38) +1s =	148	0.327	0.296	10	3
4	1	30	55	0.30	269	9.05	598	2.220	Mean =	513	0.383	0.224	1	4
4	2	30	55	0.30	269	9.20	604	2.243	Std Dev'n =	73	0.419	0.259	2	4
4	3	30	55	0.30	269	5.50	453	1.682	Coef. Var'n =	14.2%	-0.468	-0.605	3	4
4	4	30	55	0.30	269	5.75	463	1.719	Median =	483	-0.408	-0.547	4	4
4	5	30	55	0.30	269	9.05	598	2.220			0.383	0.224	5	4
4	6	30	55	0.30	269	5.65	459	1.704			-0.432	-0.570	6	4
4	7	30	55	0.30	269	4.55	414	1.537			-0.695	-0.827	7	4
4	8	30	55	0.30	269	8.50	576	2.137	SQLCT =	1.90	0.251	0.095	8	4
4	9	30	55	0.30	269	6.55	496	1.841	Crit(38) -1s =	36	-0.216	-0.360	9	4
4	10	30	55	0.30	269	5.90	470	1.742	Crit(38) +1s =	67	-0.372	-0.512	10	4
5	1	32	49	0.28	254	5.40	447	1.755	Mean =	549	-0.506	-0.492	1	5
5	2	32	49	0.28	254	17.30	952	3.740	Std Dev'n =	161	2.454	2.563	2	5
5	3	32	49	0.28	254	5.80	464	1.822	Coef. Var'n =	29.3%	-0.407	-0.389	3	5
5	4	32	49	0.28	254	7.75	546	2.147	Median =	493	0.078	0.111	4	5
5	5	32	49	0.28	254	4.45	406	1.597			-0.742	-0.736	5	5
5	6	32	49	0.28	254	7.00	515	2.022			-0.108	-0.081	6	5
5	7	32	49	0.28	254	11.00	684	2.689			0.887	0.946	7	5
5	8	32	49	0.28	254	7.45	534	2.097	SQLCT =	2.16	0.004	0.034	8	5
5	9	32	49	0.28	254	5.90	468	1.839	Crit(38) -1s =	28	-0.382	-0.364	9	5
5	10	32	49	0.28	254	6.00	472	1.855	Crit(38) +1s =	96	-0.357	-0.338	10	5
						Max	1,141			n =	50	50		
						Min	301			Sum =	0.000	0.000		

Plate Wgt.	0.50	kg
C Factor :	0.771	

TauSlab Data					(N/m2)
Loc	Slope	Slab	H Nor	H2O Nor	TauSlab
1	30	A	0.29	52	255
2	32	A	0.28	47	244
3	30	A	0.29	53	260
4	30	A	0.30	55	269
5	32	A	0.28	49	254
Mean	30.8		0.29	51	257
Std D	1.1		0.01	3	9
CV	3.6%		2.9%	6.2%	3.6%

Plot Summary		
n =	50	
Mean TauInfin =	533	N/m2
Std Dev'n =	171	N/m2
CV TauInfin =	32.02%	
SQLCT =	2.075	Mean of pooled pit SQLCT
Std Dev'n =	0.650	
CV SQLCT =	31.32%	
Crit(38) Mean =	58	mm (TauInfin mean)
Crit(38) -1s =	23	mm (TauInfin - 1 SD)
Crit(38) +1s =	94	mm (TauInfin + 1 SD)

Bradley Meadow 30m x 30m Study Plot Stability-Sampling Trials: 1/27/01

Location		QLCT Data Surface Mode					Pit Results *(TauInf correction term C = 0.771)				Z Score	Z Score	Location	
Pit #	Cell #	Slope	H2O Nor	H Nor	TauSlab	Test kg	TauInfin (N/m2)*	S QLCT	Pit-Wise		TauInfin	S QLCT	Pit #	Cell #
1	1	29	34	0.21	162	15.2	753	4.663	Mean =	721	1.239	-0.698	1	1
1	2	29	34	0.21	162	13.3	677	4.192	Std Dev'n =	65	0.670	-0.996	2	1
1	3	29	34	0.21	162	11.2	593	3.672	Coef. Var'n =	9.1%	0.041	-1.325	3	1
1	4	29	34	0.21	162	15.6	769	4.762	Median =	737	1.359	-0.635	4	1
1	5	29	34	0.21	162	14.8	737	4.564			1.119	-0.761	5	1
1	6	29	34	0.21	162	13.8	697	4.316			0.820	-0.917	6	1
1	7	29	34	0.21	162	14.8	737	4.564			1.119	-0.761	7	1
1	8	29	34	0.21	162	17.0	825	5.110	SQLCT =	4.46	1.778	-0.416	8	1
1	9	29	34	0.21	162	13.8	697	4.316	Crit(38) -1s =	104	0.820	-0.917	9	1
1	10	29	34	0.21	162				Crit(38) +1s =	131			10	1
2	1	27	15	0.115	67	9.2	422	6.324	Mean =	514	-1.239	0.352	1	2
2	2	27	15	0.115	67	15.0	644	9.644	Std Dev'n =	77	0.419	2.450	2	2
2	3	27	15	0.115	67	8.3	388	5.809	Coef. Var'n =	15.0%	-1.496	0.026	3	2
2	4	27	15	0.115	67	10.8	483	7.240	Median =	510	-0.782	0.930	4	2
2	5	27	15	0.115	67	11.6	514	7.698			-0.553	1.220	5	2
2	6	27	15	0.115	67	13.1	571	8.557			-0.124	1.762	6	2
2	7	27	15	0.115	67	10.6	476	7.125			-0.839	0.858	7	2
2	8	27	15	0.115	67	11.4	506	7.583	SQLCT =	7.70	-0.610	1.147	8	2
2	9	27	15	0.115	67	12.8	560	8.385	Crit(38) -1s =	78	-0.210	1.654	9	2
2	10	27	15	0.115	67	13.3	579	8.671	Crit(38) +1s =	110	-0.067	1.835	10	2
3	1	29	22	0.13	105	14.2	669	6.403	Mean =	629	0.611	0.402	1	3
3	2	29	22	0.13	105	13.8	653	6.250	Std Dev'n =	85	0.491	0.305	2	3
3	3	29	22	0.13	105	11.6	565	5.407	Coef. Var'n =	13.5%	-0.168	-0.228	3	3
3	4	29	22	0.13	105	13.6	645	6.173	Median =	629	0.431	0.256	4	3
3	5	29	22	0.13	105	12.8	613	5.867			0.191	0.063	5	3
3	6	29	22	0.13	105	11.0	541	5.177			-0.348	-0.373	6	3
3	7	29	22	0.13	105	15.0	701	6.710			0.850	0.595	7	3
3	8	29	22	0.13	105	17.6	805	7.706	SQLCT =	6.02	1.629	1.225	8	3
3	9	29	22	0.13	105	11.8	573	5.484	Crit(38) -1s =	92	-0.108	-0.179	9	3
3	10	29	22	0.13	105	10.6	525	5.024	Crit(38) +1s =	128	-0.468	-0.470	10	3
4	1	29	22	0.135	105	10.0	501	4.794	Mean =	601	-0.648	-0.615	1	4
4	2	29	22	0.135	105				Std Dev'n =	199			2	4
4	3	29	22	0.135	105	10.8	533	5.101	Coef. Var'n =	33.0%	-0.408	-0.422	3	4
4	4	29	22	0.135	105	10.5	521	4.986	Median =	521	-0.498	-0.494	4	4
4	5	29	22	0.135	105	9.4	477	4.564			-0.827	-0.761	5	4
4	6	29	22	0.135	105								6	4
4	7	29	22	0.135	105								7	4
4	8	29	22	0.135	105	19.4	878	8.396	SQLCT =	5.75	2.168	1.661	8	4
4	9	29	22	0.135	105	19.8	894	8.549	Crit(38) -1s =	63	2.288	1.757	9	4
4	10	29	22	0.135	105	7.6	405	3.874	Crit(38) +1s =	146	-1.367	-1.196	10	4
5	1	30	21	0.145	103	11.8	582	5.660	Mean =	490	-0.040	-0.068	1	5
5	2	30	21	0.145	103	15.2	721	7.011	Std Dev'n =	99	1.001	0.786	2	5
5	3	30	21	0.145	103	9.5	488	4.745	Coef. Var'n =	20.2%	-0.743	-0.646	3	5
5	4	30	21	0.145	103	8.0	427	4.149	Median =	466	-1.202	-1.023	4	5
5	5	30	21	0.145	103	7.7	415	4.030			-1.294	-1.098	5	5
5	6	30	21	0.145	103	8.4	443	4.308			-1.080	-0.922	6	5
5	7	30	21	0.145	103	7.3	398	3.871			-1.416	-1.198	7	5
5	8	30	21	0.145	103	9.6	492	4.785	SQLCT =	4.77	-0.713	-0.621	8	5
5	9	30	21	0.145	103	7.8	419	4.070	Crit(38) -1s =	61	-1.263	-1.073	9	5
5	10	30	21	0.145	103	10.2	517	5.024	Crit(38) +1s =	102	-0.529	-0.470	10	5
						Max	894			n =	46	46		
						Min	388			Sum =	0.000	0.000		

Plate Wgt:	0.50	m2
C Factor :	0.771	

TauSlab Data					(N/m2)
Loc	Slope	Slab	H Nor	H2O Nor	TauSlab
1	29	A	0.210	34	162
2	27	A	0.115	15	67
3	29	A	0.130	22	105
4	29	A	0.135	22	105
5	30	A	0.145	21	103
Mean	28.8		0.15	23	108
Std D	1.1		0.04	7	34
CV	3.8%		25.1%	30.3%	31.5%

Plot Summary		
n =	46	
Mean TauInfin =	588	N/m2
Std Dev'n =	134	N/m2
CV TauInfin =	22.75%	
SQLCT =	5.768	Mean of pooled pit SQLCT
Std Dev'n =	1.583	
CV SQLCT =	27.44%	
Crit(38) Mean =	90	mm (TauInfin mean)
Crit(38) -1s =	61	mm (TauInfin - 1 SD)
Crit(38) +1s =	118	mm (TauInfin + 1 SD)

Round Hill 30m x 30m Study Plot Stability-Sampling Trials: 2/4/01 Profile #: 12 Weak Layer: A

Location		QLCT Data Bench Mode				Pit Results *(TauInf correction term C = var)				Z Score	Z Score	Location	
Pit #	*Cell #*	*Slope*	*H2OCol*	*Test kg*	*H2Otest*	*TauInfin (N/m2)**	*S QLCT*	*Pit-Wise*		*TauInfin*	*S QLCT*	*Cell #*	*Loc #*
1	1	28	33.25	4.50	0.14	383	1.421	Mean =	391	-1.075	-1.035	1	1
1	2	28	33.25	6.50	0.18	505	1.876	Std Dev'n =	60	-0.781	-0.634	2	1
1	3	28	33.25	nr				Coef. Var'n =	15.4%			3	1
1	4	28	33.25	5.20	0.15	425	1.580	Median =	389	-0.972	-0.894	4	1
1	5	28	33.25	4.60	0.14	389	1.444			-1.060	-1.015	5	1
1	6	28	33.25	4.70	0.14	395	1.467			-1.046	-0.995	6	1
1	7	28	33.25	5.00	0.15	413	1.535			-1.002	-0.934	7	1
1	8	28	33.25	4.50	0.14	383	1.421	SQLCT =	1.454	-1.075	-1.035	8	1
1	9	28	33.25	4.00	0.13	352	1.308	Crit(38) -1*s* =	13	-1.148	-1.135	9	1
1	10	28	33.25	2.80	0.10	279	1.035	Crit(38) +1*s* =	38	-1.324	-1.375	10	1
2	1	29	37	18.20	0.44	1252	3.875	Mean =	1,174	1.011	1.129	1	2
2	2	29	37	15.60	0.38	1090	3.375	Std Dev'n =	133	0.624	0.688	2	2
2	3	29	37	18.60	0.45	1277	3.952	Coef. Var'n =	11.3%	1.071	1.197	3	2
2	4	29	37	16.00	0.39	1115	3.452	Median =	1,184	0.683	0.756	4	2
2	5	29	37	12.60	0.32	904	2.798			0.176	0.179	5	2
2	6	29	37	17.00	0.41	1177	3.644			0.832	0.925	6	2
2	7	29	37	17.40	0.42	1202	3.721			0.892	0.993	7	2
2	8	29	37	17.20	0.42	1190	3.683	SQLCT =	3.633	0.862	0.959	8	2
2	9	29	37	16.10	0.39	1122	3.471	Crit(38) -1*s* =	151	0.698	0.773	9	2
2	10	29	37	20.70	0.50	1407	4.356	Crit(38) +1*s* =	218	1.384	1.553	10	2
3	1	28	32.25	8.20	0.22	621	2.046	Mean =	508	-0.502	-0.484	1	3
3	2	28	32.25	6.40	0.18	496	1.633	Std Dev'n =	64	-0.803	-0.848	2	3
3	3	28	32.25	6.20	0.17	484	1.593	Coef. Var'n =	12.5%	-0.832	-0.883	3	3
3	4	28	32.25	6.70	0.19	514	1.694	Median =	493	-0.759	-0.794	4	3
3	5	28	32.25	6.60	0.18	508	1.674			-0.773	-0.812	5	3
3	6	28	32.25	5.60	0.16	447	1.472			-0.920	-0.990	6	3
3	7	28	32.25	5.70	0.16	453	1.492			-0.905	-0.972	7	3
3	8	28	32.25	5.60	0.16	447	1.472	SQLCT =	1.673	-0.920	-0.990	8	3
3	9	28	32.25	6.30	0.18	490	1.613	Crit(38) -1*s* =	30	-0.817	-0.865	9	3
3	10	28	32.25	8.40	0.22	618	2.036	Crit(38) +1*s* =	56	-0.509	-0.493	10	3
4	1	30	19.5	19.60	0.45	1306	3.754	Mean =	1,299	1.141	1.022	1	4
4	2	30	19.5	nr				Std Dev'n =	214			2	4
4	3	30	19.5	15.50	0.36	1048	3.012	Coef. Var'n =	16.5%	0.522	0.368	3	4
4	4	30	19.5	14.20	0.33	966	2.777	Median =	1,350	0.325	0.160	4	4
4	5	30	19.5	21.00	0.48	1394	4.007			1.352	1.245	5	4
4	6	30	19.5	22.00	0.50	1457	4.188			1.503	1.404	6	4
4	7	30	19.5	17.60	0.41	1180	3.392			0.839	0.703	7	4
4	8	30	19.5	23.00	0.52	1520	4.369	SQLCT =	3.733	1.654	1.564	8	4
4	9	30	19.5	nr				Crit(38) -1*s* =	155			9	4
4	10	30	19.5	23.00	0.52	1520	4.369	Crit(38) +1*s* =	245	1.654	1.564	10	4
5	1			nr				Mean =				1	5
5	2			nr				Std Dev'n =				2	5
5	3			nr				Coef. Var'n =				3	5
5	4			nr				Median =				4	5
5	5			nr								5	5
5	6			nr								6	5
5	7			nr								7	5
5	8			nr				SQLCT =				8	5
5	9			nr				Crit(38) -1*s* =				9	5
5	10			nr				Crit(38) +1*s* =				10	5
					Max	1,520			n =	37	37		
					Min	279			Sum =	0.000	0.000		

Plate Wgt: 0.25 kg

TauSlab Data					(N/m2)
Loc	*Slope*	*Slab*	*H Nor*	*H2O Nor*	*TauSlab*
1	28	A	0.50	58.5	269
2	29	A	0.58	68	323
3	28	A	0.54	66	304
4	30	A	0.59	71	348
5			no results		
Mean	28.75		0.57	68	325
Std D	1.0		0.04	5	33
CV	3.3%		7.2%	7.8%	10.2%

Plot Summary		
n =	37	
Mean TauInfin =	831	N/m2
Std Dev'n =	417	N/m2
CV TauInfin =	50.18%	
SQLCT =	2.595	Mean of pooled cell SQLCT
Std Dev'n =	1.134	
CV SQLCT =	43.71%	
Crit(38) Mean =	106	mm (TauInfin mean)
Crit(38) -1*s* =	19	mm (TauInfin - 1 SD)
Crit(38) +1*s* =	194	mm (TauInfin + 1 SD)

Baldy Mountain 30m x 30m Study Plot Stability-Sampling Trials: 2/18/01 Profile #: 15 Weak Layer: C

Location		QLCT Data Bench Mode				Pit Results *(TauInf correction term C = var)				Z Score	Z Score	Location	
Pit #	Cell #	Slope	H2OCol	Test kg	H2Otest	TauInfin (N/m2)*	S QLCT	Pit-Wise		TauInfin	S QLCT	Cell #	Loc #
1	1	25		nr				Mean =				1	1
1	2	25		nr				Std Dev'n =				2	1
1	3	25		nr				Coef. Var'n =				3	1
1	4	25		nr				Median =				4	1
1	5	25		nr								5	1
1	6	25		nr								6	1
1	7	25		nr								7	1
1	8	25		nr				SQLCT =				8	1
1	9	25		nr				Crit(38) -1s =				9	1
1	10	25		nr				Crit(38) +1s =				10	1
2	1	28		nr				Mean =	1,569			1	2
2	2	28		nr				Std Dev'n =	61			2	2
2	3	28		nr				Coef. Var'n =				3	2
2	4	28		nr				Median =	1,569			4	2
2	5	28	179	16.6	0.55	1,526	1.659			1.386	-0.369	5	2
2	6	28		nr								6	2
2	7	28		nr								7	2
2	8	28	179	18.0	0.58	1,612	1.752	SQLCT =	2.823	1.683	-0.109	8	2
2	9	28		nr				Crit(38) -1s =	124			9	2
2	10	28		nr				Crit(38) +1s =	149			10	2
3	1	29		nr				Mean =	961			1	3
3	2	29	133	9.3	0.34	972	1.748	Std Dev'n =	170	-0.532	-0.119	2	3
3	3	29	133	5.4	0.26	729	1.312	Coef. Var'n =	17.7%	-1.371	-1.336	3	3
3	4	29	133	8.8	0.33	941	1.692	Median =	956	-0.640	-0.275	4	3
3	5	29	133	12.7	0.42	1,183	2.128			0.199	0.942	5	3
3	6	29	133	11.6	0.39	1,115	2.005			-0.038	0.598	6	3
3	7	29	133	7.0	0.29	829	1.491			-1.027	-0.837	7	3
3	8	29		nr				SQLCT =	1.729			8	3
3	9	29		nr				Crit(38) -1s =	49			9	3
3	10	29		nr				Crit(38) +1s =	121			10	3
4	1	30	83	20.4	0.53	1,541	2.967	Mean =	1,005	1.437	3.281	1	4
4	2	30	83	11.6	0.34	987	1.900	Std Dev'n =	259	-0.479	0.306	2	4
4	3	30		nr				Coef. Var'n =	25.7%			3	4
4	4	30	83	10.2	0.31	899	1.731	Median =	899	-0.784	-0.167	4	4
4	5	30	83	8.9	0.28	817	1.573			-1.067	-0.607	5	4
4	6	30		nr								6	4
4	7	30	83	9.5	0.29	855	1.646			-0.936	-0.404	7	4
4	8	30		nr				SQLCT =	1.935			8	4
4	9	30	83	9.0	0.28	823	1.585	Crit(38) -1s =	48	-1.045	-0.573	9	4
4	10	30	83	13.6	0.38	1,113	2.143	Crit(38) +1s =	156	-0.044	0.982	10	4
5	1	30		nr				Mean =	1,361			1	5
5	2	30		nr				Std Dev'n =	159			2	5
5	3	30		nr				Coef. Var'n =	11.7%			3	5
5	4	30	157.5	14.4	0.47	1,380	1.696	Median =	1,383	0.880	-0.263	4	5
5	5	30		nr								5	5
5	6	30		nr								6	5
5	7	30	157.5	16.8	0.53	1,531	1.882			1.402	0.255	7	5
5	8	30	157.5	10.7	0.39	1,147	1.410	SQLCT =	1.673	0.074	-1.062	8	5
5	9	30	157.5	14.5	0.48	1,386	1.704	Crit(38) -1s =	82	0.902	-0.242	9	5
5	10	30		nr				Crit(38) +1s =	149			10	5
					Max	1,612			n =	19	19		
					Min	729			Sum =	0.000	0.000		

Plate Wgt: 0.25 kg

TauSlab Data					(N/m2)
Loc	Slope	Slab	H Nor	H2O Nor	TauSlab
1	25	C	nr	nr	nr
2	28	C	0.80	200	920
3	29	C	0.70	117	556
4	30	C	0.56	106	519
5	30	C	0.69	166	813
Mean	28.4		0.69	147	702
Std D	2.1		0.10	44	196
CV	7.3%		14.3%	29.7%	27.8%

Plot Summary		
n =	19	
Mean TauInfin =	1,125	N/m2
Std Dev'n =	289	N/m2
CV TauInfin =	25.68%	
SQLCT =	1.791	Mean of pooled cell SQLCT
Std Dev'n =	0.358	
CV SQLCT =	20.01%	
Crit(38) Mean =	89	mm (TauInfin mean)
Crit(38) -1s =	28	mm (TauInfin - 1 SD)
Crit(38) +1s =	150	mm (TauInfin + 1 SD)

Saddle Peak 30m x 30m Study Plot Stability-Sampling Trials: 2/18/01 Profile #: 16 Weak Layer: A

Location		QLCT Data Bench Mode				Pit Results *(TauInf correction term C = var)				Z Score	Z Score	Location	
Pit #	Cell #	Slope	H2OCol	Test kg	H2Otest	TauInfin (N/m2)*	S QLCT	Pit-Wise		TauInfin	S QLCT	Cell #	Loc #
1	1	26	154.5	19.00	0.59	1,541	2.271	Mean =	1,367	0.159	0.835	1	1
1	2	26	154.5	21.00	0.63	1,659	2.445	Std Dev'n =	298	0.473	1.193	2	1
1	3	26	154.5	10.90	0.41	1,063	1.567	Coef. Var'n =	21.8%	-1.115	-0.611	3	1
1	4	26	154.5	10.40	0.39	1,034	1.523	Median =	1,367	-1.193	-0.701	4	1
1	5	26	154.5	11.20	0.41	1,081	1.593			-1.067	-0.558	5	1
1	6	26	154.5	nr								6	1
1	7	26	154.5	nr								7	1
1	8	26	154.5	17.40	0.55	1,447	2.132	SQLCT =	2.014	-0.093	0.550	8	1
1	9	26	154.5	23.80	0.69	1,825	2.688	Crit(38) -1s =	82	0.913	1.693	9	1
1	10	26	154.5	14.70	0.49	1,288	1.897	Crit(38) +1s =	207	-0.517	0.067	10	1
2	1	27	70.5	16.60	0.45	1,204	1.630	Mean =	1,162	-0.741	-0.482	1	2
2	2	27	70.5	12.40	0.35	951	1.288	Std Dev'n =	289	-1.414	-1.184	2	2
2	3	27	70.5	15.50	0.42	1,138	1.540	Coef. Var'n =	24.8%	-0.917	-0.666	3	2
2	4	27	70.5	19.40	0.51	1,372	1.858	Median =	1,171	-0.292	-0.013	4	2
2	5	27	70.5	13.20	0.37	999	1.353			-1.286	-1.051	5	2
2	6	27	70.5	9.60	0.29	783	1.060			-1.862	-1.653	6	2
2	7	27	70.5	22.20	0.57	1,541	2.086			0.157	0.456	7	2
2	8	27	70.5	22.00	0.57	1,529	2.070	SQLCT =	1.574	0.124	0.422	8	2
2	9	27	70.5	19.20	0.50	1,360	1.842	Crit(38) -1s =	28	-0.324	-0.046	9	2
2	10	27	70.5	9.00	0.28	747	1.011	Crit(38) +1s =	150	-1.958	-1.753	10	2
3	1	27	100	31.40	0.81	2,174	2.979	Mean =	1,522	1.843	2.291	1	3
3	2	27	100	5.00	0.22	586	0.803	Std Dev'n =	458	-2.387	-2.181	2	3
3	3	27	100	22.80	0.61	1,656	2.270	Coef. Var'n =	30.1%	0.465	0.834	3	3
3	4	27	100	20.20	0.56	1,500	2.056	Median =	1,494	0.048	0.393	4	3
3	5	27	100	14.40	0.43	1,151	1.578			-0.881	-0.589	5	3
3	6	27	100	27.00	0.71	1,909	2.616			1.138	1.545	6	3
3	7	27	100	28.60	0.74	2,005	2.748			1.394	1.816	7	3
3	8	27	100	18.00	0.51	1,368	1.874	SQLCT =	2.085	-0.304	0.021	8	3
3	9	27	100	18.20	0.51	1,380	1.891	Crit(38) -1s =	70	-0.272	0.055	9	3
3	10	27	100	20.00	0.55	1,488	2.039	Crit(38) +1s =	263	0.016	0.360	10	3
4	1	25	98.5	28.40	0.75	1,906	2.234	Mean =	1,846	1.129	0.759	1	4
4	2	25	98.5	26.80	0.71	1,813	2.125	Std Dev'n =	177	0.883	0.536	2	4
4	3	25	98.5	23.90	0.65	1,646	1.929	Coef. Var'n =	9.6%	0.437	0.133	3	4
4	4	25	98.5	23.80	0.64	1,640	1.922	Median =	1,816	0.421	0.119	4	4
4	5	25	98.5	30.10	0.79	2,004	2.349			1.391	0.995	5	4
4	6	25	98.5	32.40	0.84	2,137	2.504			1.744	1.315	6	4
4	7	25	98.5	31.00	0.81	2,056	2.410			1.529	1.121	7	4
4	8	25	98.5	26.90	0.71	1,819	2.132	SQLCT =	2.164	0.898	0.550	8	4
4	9	25	98.5	26.40	0.70	1,790	2.098	Crit(38) -1s =	172	0.821	0.481	9	4
4	10	25	98.5	24.00	0.65	1,652	1.936	Crit(38) +1s =	246	0.452	0.147	10	4
5	1	27	143.5	15.40	0.49	1,329	1.316	Mean =	1,490	-0.408	-1.128	1	5
5	2	27	143.5	25.50	0.72	1,936	1.917	Std Dev'n =	243	1.210	0.109	2	5
5	3	27	143.5	nr				Coef. Var'n =	16.3%			3	5
5	4	27	143.5	15.40	0.49	1,329	1.316	Median =	1,443	-0.408	-1.128	4	5
5	5	27	143.5	18.30	0.56	1,503	1.488			0.057	-0.773	5	5
5	6	27	143.5	22.20	0.64	1,738	1.721			0.682	-0.295	6	5
5	7	27	143.5	11.80	0.41	1,112	1.101			-0.985	-1.568	7	5
5	8	27	143.5	17.30	0.53	1,443	1.429	SQLCT =	1.475	-0.104	-0.895	8	5
5	9	27	143.5	17.10	0.53	1,431	1.417	Crit(38) -1s =	50	-0.136	-0.919	9	5
5	10	27	143.5	19.70	0.59	1,587	1.572	Crit(38) +1s =	152	0.281	-0.601	10	5
					Max	2,174			n =	47	47		
Plate Wgt:		0.25	kg		Min	586			Sum =	0.000	0.000		

TauSlab Data					(N/m2)
Loc	Slope	Slab	H Nor	H2O Nor	TauSlab
1	26	A	0.77	158	679
2	27	A	0.75	166	739
3	27	A	0.76	164	730
4	25	A	0.88	206	853
5	27	A	0.92	227	1010
Mean	26.4		0.83	191	833
Std D	0.9		0.08	31	133
CV	3.4%		9.5%	16.0%	15.9%

Plot Summary		
n =	47	
Mean TauInfin =	1,482	N/m2
Std Dev'n =	375	N/m2
CV TauInfin =	25.33%	
SQLCT =	1.864	Mean of pooled cell SQLCT
Std Dev'n =	0.487	
CV SQLCT =	26.10%	
Crit(38) Mean =	136	mm (TauInfin mean)
Crit(38) -1s =	58	mm (TauInfin - 1 SD)
Crit(38) +1s =	215	mm (TauInfin + 1 SD)

Bradley Meadow 30m x 30m Study Plot Stability-Sampling Trials: 2/18/01 Profile #: 17 Weak Layer: A

Location		QLCT Data Bench Mode				Pit Results *(TauInf correction term C = var)				Z Score	Z Score	Location	
Pit #	Cell #	Slope	H2OCol	Test kg	H2Otest	TauInfin (N/m2)*	S QLCT	Pit-Wise		TauInfin	S QLCT	Cell #	Loc #
1	1	30	198	nr				Mean =				1	1
1	2	30	198	nr				Std Dev'n =				2	1
1	3	30	198	nr				Coef. Var'n =				3	1
1	4	30	198	nr				Median =				4	1
1	5	30	198	nr								5	1
1	6	30	198	nr								6	1
1	7	30	198	nr								7	1
1	8	30	198	nr				SQLCT =				8	1
1	9	30	198	nr				Crit(38) -1s =				9	1
1	10	30	198	nr				Crit(38) +1s =				10	1
2	1	26	183.5	22.20	0.69	1,806	1.507	Mean =	1,746	0.433	-0.220	1	2
2	2	26	183.5	18.00	0.59	1,559	1.300	Std Dev'n =	376	-0.277	-0.861	2	2
2	3	26	183.5	26.20	0.78	2,042	1.704	Coef. Var'n =	21.6%	1.110	0.390	3	2
2	4	26	183.5	10.60	0.43	1,122	0.936	Median =	1,830	-1.529	-1.991	4	2
2	5	26	183.5	nr								5	2
2	6	26	183.5	29.40	0.85	2,231	1.861			1.651	0.878	6	2
2	7	26	183.5	14.40	0.51	1,346	1.123			-0.886	-1.411	7	2
2	8	26	183.5	nr				SQLCT =	1.457			8	2
2	9	26	183.5	25.60	0.76	2,007	1.674	Crit(38) -1s =	36	1.008	0.298	9	2
2	10	26	183.5	23.00	0.71	1,854	1.546	Crit(38) +1s =	194	0.568	-0.098	10	2
3	1	30	199	nr				Mean =	2,111			1	3
3	2	30	199	nr				Std Dev'n =	436			2	3
3	3	30	199	nr				Coef. Var'n =	20.7%			3	3
3	4	30	199	nr				Median =	2,111			4	3
3	5	30	199	nr								5	3
3	6	30	199	19.20	0.62	1,802	1.076			0.422	-1.558	6	3
3	7	30	199	nr								7	3
3	8	30	199	29.00	0.83	2,419	1.444	SQLCT =	(< 3 valid)	2.190	-0.417	8	3
3	9	30	199	nr				Crit(38) -1s =	0			9	3
3	10	30	199	nr				Crit(38) +1s =	183			10	3
4	1	31	176.5	19.20	0.59	1,761	1.856	Mean =	1,650	0.303	0.861	1	4
4	2	31	176.5	21.60	0.64	1,914	2.017	Std Dev'n =	253	0.740	1.359	2	4
4	3	31	176.5	23.00	0.67	2,003	2.110	Coef. Var'n =	15.3%	0.996	1.650	3	4
4	4	31	176.5	18.00	0.57	1,685	1.775	Median =	1,672	0.084	0.611	4	4
4	5	31	176.5	11.80	0.43	1,290	1.360			-1.047	-0.677	5	4
4	6	31	176.5	10.00	0.40	1,176	1.239			-1.375	-1.051	6	4
4	7	31	176.5	17.00	0.55	1,621	1.708			-0.098	0.403	7	4
4	8	31	176.5	17.60	0.56	1,659	1.748	SQLCT =	1.739	0.011	0.528	8	4
4	9	31	176.5	17.20	0.55	1,634	1.722	Crit(38) -1s =	94	-0.062	0.445	9	4
4	10	31	176.5	19.20	0.59	1,761	1.856	Crit(38) +1s =	201	0.303	0.861	10	4
5	1	30	119	nr				Mean =	1,338			1	5
5	2	30	119	18.80	0.53	1,545		Std Dev'n =	212	-0.317		2	5
5	3	30	119	18.60	0.53	1,532		Coef. Var'n =	15.9%	-0.353		3	5
5	4	30	119	13.00	0.41	1,180		Median =	1,369	-1.363		4	5
5	5	30	119	11.20	0.37	1,066				-1.688		5	5
5	6	30	119	16.00	0.47	1,369				-0.822		6	5
5	7	30	119	nr								7	5
5	8	30	119	nr				SQLCT =				8	5
5	9	30	119	nr				Crit(38) -1s =				9	5
5	10	30	119	nr				Crit(38) +1s =				10	5
					Max	2,419			n =	25	20		
					Min	1,066			Sum =	0.000	0.000		

Plate Wgt: 0.25 kg

TauSlab Data					(N/m2)
Loc	Slope	Slab	H Nor	H2O Nor	TauSlab
1	30	A	1.39	477	2335
2	26	A	1.05	279	1199
3	30	A	1.20	342	1676
4	31	A	0.74	188	949
5	30	A	missing	missing	
Mean	29.4		1.00	270	1274
Std D	1.9		0.27	121	610
CV	6.6%		27.5%	44.9%	47.9%

Plot Summary		
n =	25	
Mean TauInfin =	1,655	N/m2
Std Dev'n =	349	N/m2
CV TauInfin =	21.07%	
SQLCT =	1.578	Mean of pooled cell SQLCT
Std Dev'n =	0.323	
CV SQLCT =	20.44%	
Crit(38) Mean =	80	mm (TauInfin mean)
Crit(38) -1s =	7	mm (TauInfin - 1 SD)
Crit(38) +1s =	153	mm (TauInfin + 1 SD)

Bradley Meadow 30m x 30m Study Plot Stability-Sampling Trials: 3/17/01

Location		QLCT Data Surface Mode					Pit Results *(TauInf correction term C = 0.771)				Z Score	Z Score	Location	
Pit #	Cell #	Slope	H2O Nor	H Nor	TauSlab	Test kg	TauInfin (N/m2)*	SQLCT	Pit-Wise		TauInfin	SQLCT	Pit #	Cell #
1	1	25	33	0.2	137	4.5	286	2.094	Mean =	386	-1.257	-1.231	1	1
1	2	25	33	0.2	137	4.9	301	2.200	Std Dev'n =	123	-1.133	-1.103	2	1
1	3	25	33	0.2	137	4.5	286	2.094	Coef. Var'n =	31.9%	-1.257	-1.231	3	1
1	4	25	33	0.2	137	nr			Median =	341			4	1
1	5	25	33	0.2	137	4.3	279	2.041			-1.318	-1.295	5	1
1	6	25	33	0.2	137	14.5	648	4.741			1.838	1.964	6	1
1	7	25	33	0.2	137	9.7	474	3.471			0.352	0.430	7	1
1	8	25	33	0.2	137	8.0	413	3.021	SQLCT =	2.82	-0.174	-0.113	8	1
1	9	25	33	0.2	137	8.8	442	3.233	Crit(38) -1s =	26	0.074	0.143	9	1
1	10	25	33	0.2	137	6.0	341	2.491	Crit(38) +1s =	78	-0.792	-0.752	10	1
2	1	25	34	0.205	141	11.1	528	3.751	Mean =	496	0.813	0.769	1	2
2	2	25	34	0.205	141	8.0	416	2.955	Std Dev'n =	93	-0.146	-0.193	2	2
2	3	25	34	0.205	141	6.0	344	2.441	Coef. Var'n =	18.8%	-0.765	-0.813	3	2
2	4	25	34	0.205	141	10.7	514	3.648	Median =	521	0.689	0.645	4	2
2	5	25	34	0.205	141	7.0	380	2.698			-0.456	-0.503	5	2
2	6	25	34	0.205	141	11.7	550	3.905			0.999	0.955	6	2
2	7	25	34	0.205	141	14.8	662	4.702			1.958	1.916	7	2
2	8	25	34	0.205	141	10.0	488	3.468	SQLCT =	3.52	0.473	0.428	8	2
2	9	25	34	0.205	141	11.4	539	3.828	Crit(38) -1s =	55	0.906	0.862	9	2
2	10	25	34	0.205	141	11.4	539	3.828	Crit(38) +1s =	94	0.906	0.862	10	2
3	1	25	33	0.205	137	8.2	420	3.074	Mean =	434	-0.112	-0.049	1	3
3	2	25	33	0.205	137	nr			Std Dev'n =	136			2	3
3	3	25	33	0.205	137	15.1	670	4.900	Coef. Var'n =	31.4%	2.023	2.156	3	3
3	4	25	33	0.205	137	7.2	384	2.809	Median =	397	-0.421	-0.368	4	3
3	5	25	33	0.205	137	6.5	359	2.624			-0.638	-0.592	5	3
3	6	25	33	0.205	137	5.6	326	2.386			-0.916	-0.880	6	3
3	7	25	33	0.205	137	13.6	615	4.503			1.559	1.676	7	3
3	8	25	33	0.205	137	4.6	290	2.121	SQLCT =	3.18	-1.226	-1.199	8	3
3	9	25	33	0.205	137	nr			Crit(38) -1s =	34			9	3
3	10	25	33	0.205	137	7.9	409	2.994	Crit(38) +1s =	91	-0.205	-0.145	10	3
4	1	27	31	0.21	138	4.6	301	2.184	Mean =	389	-1.129	-1.123	1	4
4	2	27	31	0.21	138	4.9	313	2.267	Std Dev'n =	77	-1.031	-1.023	2	4
4	3	27	31	0.21	138	6.3	366	2.655	Coef. Var'n =	19.8%	-0.573	-0.555	3	4
4	4	27	31	0.21	138	9.2	477	3.458	Median =	368	0.374	0.415	4	4
4	5	27	31	0.21	138	6.4	370	2.682			-0.541	-0.521	5	4
4	6	27	31	0.21	138	9.8	500	3.624			0.570	0.615	6	4
4	7	27	31	0.21	138	7.5	412	2.987			-0.181	-0.154	7	4
4	8	27	31	0.21	138	9.5	488	3.541	SQLCT =	2.82	0.472	0.515	8	4
4	9	27	31	0.21	138	4.6	301	2.184	Crit(38) -1s =	37	-1.129	-1.123	9	4
4	10	27	31	0.21	138	6.2	362	2.627	Crit(38) +1s =	69	-0.606	-0.588	10	4
5	1	27	32	0.2	142	5.0	320	2.247	Mean =	459	-0.969	-1.047	1	5
5	2	27	32	0.2	142	6.6	381	2.676	Std Dev'n =	135	-0.446	-0.529	2	5
5	3	27	32	0.2	142	nr			Coef. Var'n =	29.5%			3	5
5	4	27	32	0.2	142	3.9	278	1.952	Median =	515	-1.328	-1.403	4	5
5	5	27	32	0.2	142	14.2	671	4.716			2.037	1.933	5	5
5	6	27	32	0.2	142	5.3	331	2.327			-0.871	-0.950	6	5
5	7	27	32	0.2	142	10.1	515	3.615			0.698	0.605	7	5
5	8	27	32	0.2	142	11.8	580	4.072	SQLCT =	3.22	1.253	1.156	8	5
5	9	27	32	0.2	142	10.4	526	3.696	Crit(38) -1s =	38	0.796	0.702	9	5
5	10	27	32	0.2	142	10.5	530	3.723	Crit(38) +1s =	95	0.828	0.735	10	5
						Max	671			n =	46	46		
						Min	278			Sum =	0.000	0.000		

Plate Wgt:	0.50 kg
C Factor :	0.771

TauSlab Data					(N/m2)
Loc	Slope	Slab	H Nor	H2O Nor	TauSlab
1	25	A	0.20	33	137
2	25	A	0.21	34	141
3	25	A	0.21	33	137
4	27	A	0.21	31	138
5	27	A	0.20	32	142
Mean	25.8		0.20	33	139
Std D	1.1		0.00	1	3
CV	4.2%		2.1%	3.5%	1.9%

Plot Summary		
n =	46	
Mean TauInfin =	433	N/m2
Std Dev'n =	117	N/m2
CV TauInfin =	26.99%	
SQLCT =	3.114	
Std Dev'n =	0.828	
CV SQLCT =	26.60%	
Crit(38) Mean =	62	mm (TauInfin mean)
Crit(38) -1s =	38	mm (TauInfin - 1 SD)
Crit(38) +1s =	87	mm (TauInfin + 1 SD)

APPENDIX C

2001/2002 Study Plot Trials QLCT Results

Middle Basin 30m x 30m Stability-Sampling Trials, 12/7/01 — Profile: 2 — Weak Layers: A, *B* (italics)

Location		QLCT Data Surface Mode					Pit Results *(TauInf correction term *C* = 0.771)				Z Score	Z Score	Location	
Pit #	*Cell #*	*Slope*	*H2O Nor*	*H Nor*	*TauSlab*	*Test kg*	*TauInfin (N/m2)**	*S QLCT*	*Pit-Wise*		*TauInfin*	*S QLCT*	*Pit #*	*Cell #*
1	1	*28*	*82*	*0.535*	*377*	*7.0*	*584*	*1.815*	Mean =	648	*-0.698*	*-0.442*	1	1
1	2	*28*	*82*	*0.535*	*377*	*7.5*	*604*	*1.876*	Std Dev'n =	114	*-0.576*	*-0.315*	2	1
1	3	28	70	0.505	322	9.3	632	1.962	Coef. Var'n =	17.6%	-0.402	-0.134	3	1
1	4	28	70	0.505	322	9.3	632	1.962	Median =	616	-0.402	-0.134	4	1
1	5	28	70	0.505	322	8.4	597	1.853			-0.621	-0.362	5	1
1	6	28	70	0.505	322	12.3	749	2.327			0.331	0.626	6	1
1	7	28	70	0.505	322	9.2	628	1.950			-0.426	-0.160	7	1
1	8	28	70	0.505	322	6.5	522	1.622	SQLCT =	2.01	-1.085	-0.844	8	1
1	9	28	70	0.505	322	16.9	930	2.886	Crit(38) -1*s* =	45	1.453	1.791	9	1
1	10	*28*	*82*	*0.535*	*377*	*7.5*	604	1.876	Crit(38) +1*s* =	93	-0.576	-0.315	10	1
2	1	26	71	0.49	305	NR (>21)			Mean =	693			1	2
2	2	26	71	0.49	305	NR (>26)			Std Dev'n =	39			2	2
2	3	26	71	0.49	305	12.3	711	2.333	Coef. Var'n =	5.6%	0.094	0.638	3	2
2	4	26	71	0.49	305	NR (>23)			Median =	708			4	2
2	5	26	71	0.49	305	10.6	648	2.125			-0.300	0.205	5	2
2	6	26	71	0.49	305	13.3	749	2.455			0.326	0.892	6	2
2	7	26	71	0.49	305	12.5	719	2.357			0.140	0.688	7	2
2	8	26	71	0.49	305	12.2	708	2.320	SQLCT =	2.27	0.071	0.612	8	2
2	9	26	71	0.49	305	10.5	645	2.113	Crit(38) -1*s* =	73	-0.324	0.180	9	2
2	10	26	71	0.49	305	11.2	671	2.198	Crit(38) +1*s* =	90	-0.161	0.358	10	2
3	1	29	84	0.52	399	8.5	668	1.674	Mean =	764	-0.176	-0.735	1	3
3	2	29	84	0.52	399	6.3	580	1.453	Std Dev'n =	176	-0.725	-1.195	2	3
3	3	29	84	0.52	399	15.6	952	2.387	Coef. Var'n =	23.1%	1.596	0.750	3	3
3	4	29	84	0.52	399	8.4	664	1.664	Median =	690	-0.201	-0.756	4	3
3	5	29	84	0.52	399	7.4	624	1.564			-0.451	-0.965	5	3
3	6	29	84	0.52	399	19.6	1,113	2.788			2.595	1.587	6	3
3	7	29	84	0.52	399	8.9	684	1.714			-0.076	-0.651	7	3
3	8	29	84	0.52	399	9.2	696	1.744	SQLCT =	1.91	-0.001	-0.589	8	3
3	9	29	84	0.52	399	9.4	704	1.764	Crit(38) -1*s* =	40	0.048	-0.547	9	3
3	10	29	84	0.52	399	15.6	952	2.387	Crit(38) +1*s* =	114	1.596	0.750	10	3
4	1	27	73	0.48	325	11.6	713	2.194	Mean =	710	0.101	0.349	1	4
4	2	27	73	0.48	325	10.2	659	2.030	Std Dev'n =	262	-0.232	0.006	2	4
4	3	27	73	0.48	325	7.4	552	1.700	Coef. Var'n =	36.9%	-0.899	-0.680	3	4
4	4	27	73	0.48	325	6.1	503	1.547	Median =	606	-1.208	-0.999	4	4
4	5	27	73	0.48	325	6.4	514	1.583			-1.137	-0.926	5	4
4	6	27	73	0.48	325	NR (>19)							6	4
4	7	27	73	0.48	325	22.3	1,121	3.453			2.650	2.973	7	4
4	8	27	73	0.48	325	22.0	1,110	3.418	SQLCT =	2.19	2.578	2.899	8	4
4	9	27	73	0.48	325	NR (>22)			Crit(38) -1*s* =	26			9	4
4	10	27	73	0.48	325	6.2	506	1.559	Crit(38) +1*s* =	136	-1.185	-0.975	10	4
5	1	*27*	*84*	*0.54*	*374*	*NR (>26)*			Mean =	*650*			1	5
5	2	*27*	*84*	*0.54*	*374*	*14.4*	*857*	*2.294*	Std Dev'n =	*111*	*1.004*	*0.557*	2	5
5	3	*27*	*84*	*0.54*	*374*	*7.0*	*575*	*1.538*	Coef. Var'n =	*17.0%*	*-0.759*	*-1.019*	3	5
5	4	*27*	*84*	*0.54*	*374*	*6.5*	*556*	*1.487*	Median =	*617*	*-0.878*	*-1.126*	4	5
5	5	*27*	*84*	*0.54*	*374*	*NR (>21)*							5	5
5	6	*27*	*84*	*0.54*	*374*	*9.8*	*682*	*1.824*			*-0.092*	*-0.423*	6	5
5	7	*27*	*84*	*0.54*	*374*	*8.4*	*628*	*1.681*			*-0.425*	*-0.721*	7	5
5	8	*27*	*84*	*0.54*	*374*	*7.8*	*605*	*1.619*	SQLCT =	*1.74*	*-0.568*	*-0.849*	8	5
5	9	*27*	*84*	*0.54*	*374*	*NR (>26)*			Crit(38) -1*s* =	*45*			9	5
5	10	*27*	*84*	*0.54*	*374*	*NR (>22)*			Crit(38) +1*s* =	*92*			10	5
						Max	1,121			n =	41	41		
						Min	503			Sum =	0.000	0.000		

Plate Wgt: 0.50 kg
C Factor : 0.771

TauSlab Data					(N/m2)
Loc	*Slope*	*Slab*	*H Nor*	*H2O Nor*	*TauSlab*
1	28	A	0.51	70	322
2	26	A	0.49	71	305
3	29	A	0.52	84	399
4	27	A	0.48	73	325
5	27	*B*	*0.54*	*84*	*374*
Mean	27.4		0.51	76	345
Std D	1.1		0.02	7	40
CV	4.2%		4.7%	9.2%	11.5%

Plot Summary		
n =	41	
Mean TauInfin =	696	N/m2
Std Dev'n =	160	N/m2
CV TauInfin =	23.03%	
SQLCT =	2.027	Mean of pooled pit SQLCT
Std Dev'n =	0.480	
CV SQLCT =	23.67%	
Crit(38) Mean =	79	mm (TauInfin mean)
Crit(38) -1*s* =	45	mm (TauInfin - 1 SD)
Crit(38) +1*s* =	112	mm (TauInfin + 1 SD)

Lionhead 30m x 30m Study Plot Stability-Sampling Trials: 1/9/02 Profile: 9 Weak Layer: A

Location		QLCT Data Surface Mode					Pit Results *(TauInf correction term C = 0.771)				Z Score	Z Score	Location	
Pit #	Cell #	Slope	H_2O_{Nor}	H_{Nor}	TauSlab	Test kg	TauInfin (N/m2)*	S_{QLCT}	Pit-Wise		TauInfin	S_{QLCT}	Cell #	Pit #
1	1	26	35	0.25	150	6.4	373	2.479	Mean =	369	-0.061	-0.197	1	1
1	2	26	35	0.25	150	6.6	380	2.528	Std Dev'n =	22	0.130	-0.006	2	1
1	3	26	35	0.25	150	5.8	350	2.330	Coef. Var'n =	6.0%	-0.633	-0.770	3	1
1	4	26	35	0.25	150	7.1	399	2.652	Median =	373	0.606	0.473	4	1
1	5	26	35	0.25	150	5.8	350	2.330			-0.633	-0.770	5	1
1	6	26	35	0.25	150	6.7	384	2.553			0.225	0.090	6	1
1	7	26	35	0.25	150	6.9	391	2.602			0.415	0.281	7	1
1	8	26	35	0.25	150	6.4	373	2.479	S_{QLCT} =	2.45	-0.061	-0.197	8	1
1	9	26	35	0.25	150	6.2	365	2.429	Crit(38) -1s =	41	-0.252	-0.388	9	1
1	10	26	35	0.25	150	5.1	324	2.157	Crit(38) +1s =	51	-1.300	-1.440	10	1
2	1	25	34	0.25	141	7.6	402	2.852	Mean =	368	0.679	1.245	1	2
2	2	25	34	0.25	141	6.0	344	2.441	Std Dev'n =	22	-0.803	-0.343	2	2
2	3	25	34	0.25	141	6.8	373	2.646	Coef. Var'n =	6.0%	-0.062	0.451	3	2
2	4	25	34	0.25	141	6.9	376	2.672	Median =	374	0.030	0.550	4	2
2	5	25	34	0.25	141	5.9	340	2.415			-0.896	-0.442	5	2
2	6	25	34	0.25	141	7.1	384	2.723			0.216	0.749	6	2
2	7	25	34	0.25	141	7.2	387	2.749			0.308	0.848	7	2
2	8	25	34	0.25	141	7.0	380	2.698	S_{QLCT} =	2.62	0.123	0.650	8	2
2	9	25	34	0.25	141	5.8	336	2.389	Crit(38) -1s =	43	-0.989	-0.541	9	2
2	10	25	34	0.25	141	6.5	362	2.569	Crit(38) +1s =	52	-0.340	0.153	10	2
3	1	27	33	0.25	147	5.1	327	2.228	Mean =	383	-1.227	-1.164	1	3
3	2	27	33	0.25	147	6.7	388	2.645	Std Dev'n =	57	0.338	0.444	2	3
3	3	27	33	0.25	147	6.2	369	2.514	Coef. Var'n =	14.9%	-0.151	-0.059	3	3
3	4	27	33	0.25	147	5.6	346	2.358	Median =	373	-0.738	-0.662	4	3
3	5	27	33	0.25	147	5.8	354	2.410			-0.543	-0.461	5	3
3	6	27	33	0.25	147	7.4	415	2.827			1.023	1.148	6	3
3	7	27	33	0.25	147	10.4	530	3.607			3.957	4.164	7	3
3	8	27	33	0.25	147	6.5	381	2.593	S_{QLCT} =	2.61	0.142	0.243	8	3
3	9	27	33	0.25	147	6.4	377	2.566	Crit(38) -1s =	38	0.044	0.142	9	3
3	10	27	33	0.25	147	5.6	346	2.358	Crit(38) +1s =	62	-0.738	-0.662	10	3
4	1	28	34	0.255	156	6.9	410	2.623	Mean =	398	0.902	0.361	1	4
4	2	28	34	0.255	156	6.4	391	2.498	Std Dev'n =	23	0.401	-0.122	2	4
4	3	28	34	0.255	156	5.6	359	2.298	Coef. Var'n =	5.7%	-0.401	-0.896	3	4
4	4	28	34	0.255	156	7.0	414	2.648	Median =	401	1.002	0.458	4	4
4	5	28	34	0.255	156	6.1	379	2.423			0.100	-0.412	5	4
4	6	28	34	0.255	156	7.3	426	2.723			1.303	0.748	6	4
4	7	28	34	0.255	156	7.3	426	2.723			1.303	0.748	7	4
4	8	28	34	0.255	156	6.0	375	2.398	S_{QLCT} =	2.55	0.000	-0.509	8	4
4	9	28	34	0.255	156	6.4	391	2.498	Crit(38) -1s =	46	0.401	-0.122	9	4
4	10	28	34	0.255	156	6.9	410	2.623	Crit(38) +1s =	56	0.902	0.361	10	4
5	1	28	32	0.245	147	5.8	360	2.446	Mean =	357	-0.382	-0.322	1	5
5	2	28	32	0.245	147	5.5	348	2.367	Std Dev'n =	49	-0.683	-0.630	2	5
5	3	28	32	0.245	147	4.6	313	2.127	Coef. Var'n =	13.7%	-1.585	-1.555	3	5
5	4	28	32	0.245	147	7.0	407	2.765	Median =	350	0.821	0.911	4	5
5	5	28	32	0.245	147	4.2	298	2.021			-1.986	-1.966	5	5
5	6	28	32	0.245	147	5.9	364	2.473			-0.282	-0.219	6	5
5	7	28	32	0.245	147	5.6	352	2.393			-0.583	-0.527	7	5
5	8	28	32	0.245	147	5.1	333	2.260	S_{QLCT} =	2.42	-1.084	-1.041	8	5
5	9	28	32	0.245	147	4.9	325	2.207	Crit(38) -1s =	34	-1.284	-1.246	9	5
5	10	28	32	0.245	147	8.5	466	3.164	Crit(38) +1s =	54	2.325	2.452	10	5
						Max	530			n =	50	50		
						Min	298			Sum =	0.000	0.000		

Plate Wgt:	0.50	kg
C Factor :	0.771	

TauSlab Data (N/m2)

Loc	Slope	Slab	H_{Nor}	H_2O_{Nor}	TauSlab
1	26	A	0.25	35	150
2	25	A	0.25	34	141
3	27	A	0.25	33	147
4	28	A	0.255	34	156
5	28	A	0.245	32	147
Mean	26.8		0.25	34	148
Std D	1.3		0.00	1.14	5.69
CV	4.9%		1.4%	3.4%	3.8%

Plot Summary

n =	50	
Mean TauInfin =	375	N/m2
Std Dev'n =	39	N/m2
CV TauInfin =	10.41%	
S_{QLCT} =	2.530	Mean of pooled pit S_{QLCT}
Std Dev'n =	0.259	
CV S_{QLCT} =	10.23%	
Crit(38) Mean =	47	mm (TauInfin mean)
Crit(38) -1s =	39	mm (TauInfin - 1 SD)
Crit(38) +1s =	55	mm (TauInfin + 1 SD)

Lionhead 30m x 30m Study Plot Stability-Sampling Trials: 1/15/02 Profile: 10 Weak Layer: A

Location		QLCT Data Surface Mode					Pit Results *(TauInf correction term C = 0.771)				Z Score	Z Score	Location	
Pit #	Cell #	Slope	H_2O_{Nor}	H_{Nor}	TauSlab	Test kg	TauInfin (N/m2)*	S_{QLCT}	Pit-Wise		TauInfin	S_{QLCT}	Cell #	Pit #
1	1	27	37	0.268	165	8.9	486	2.953	Mean =	486	-0.673	-0.393	1	1
1	2	27	37	0.268	165	9.4	505	3.069	Std Dev'n =	43	-0.324	-0.037	2	1
1	3	27	37	0.268	165	7.4	429	2.604	Coef. Var'n =	8.9%	-1.718	-1.463	3	1
1	4	27	37	0.268	165	9.0	490	2.976	Median =	488	-0.603	-0.322	4	1
1	5	27	37	0.268	165	6.9	410	2.488			-2.067	-1.819	5	1
1	6	27	37	0.268	165	8.8	482	2.929			-0.742	-0.464	6	1
1	7	27	37	0.268	165	9.7	517	3.138			-0.115	0.177	7	1
1	8	27	37	0.268	165	9.7	517	3.138	S_{QLCT} =	2.95	-0.115	0.177	8	1
1	9	27	37	0.268	165	8.5	471	2.860	$Crit_{(38)}$ -1s =	59	-0.952	-0.678	9	1
1	10	27	37	0.268	165	10.8	559	3.394	$Crit_{(38)}$ +1s =	77	0.652	0.962	10	1
2	1	27	39	0.285	174	10.3	546	3.149	Mean =	557	0.429	0.210	1	2
2	2	27	39	0.285	174	10.1	539	3.105	Std Dev'n =	56	0.289	0.075	2	2
2	3	27	39	0.285	174	10.0	535	3.083	Coef. Var'n =	10.0%	0.219	0.007	3	2
2	4	27	39	0.285	174	10.3	546	3.149	Median =	546	0.429	0.210	4	2
2	5	27	39	0.285	174	7.5	439	2.532			-1.524	-1.684	5	2
2	6	27	39	0.285	174	11.0	573	3.303			0.917	0.684	6	2
2	7	27	39	0.285	174	12.8	642	3.699			2.171	1.902	7	2
2	8	27	39	0.285	174	11.6	596	3.435	S_{QLCT} =	3.21	1.335	1.090	8	2
2	9	27	39	0.285	174	12.2	619	3.567	$Crit_{(38)}$ -1s =	69	1.753	1.496	9	2
2	10	27	39	0.285	174	10.0	535	3.083	$Crit_{(38)}$ +1s =	92	0.219	0.007	10	2
3	1	26	38	0.275	163	15.4	718	4.395	Mean =	545	3.552	4.040	1	3
3	2	26	38	0.275	163	10.2	524	3.210	Std Dev'n =	74	0.021	0.398	2	3
3	3	26	38	0.275	163	10.5	535	3.278	Coef. Var'n =	13.5%	0.224	0.608	3	3
3	4	26	38	0.275	163	9.4	494	3.028	Median =	528	-0.523	-0.162	4	3
3	5	26	38	0.275	163	nr							5	3
3	6	26	38	0.275	163	9.9	513	3.142			-0.183	0.188	6	3
3	7	26	38	0.275	163	8.4	457	2.800			-1.202	-0.863	7	3
3	8	26	38	0.275	163	11.0	554	3.392	S_{QLCT} =	3.34	0.564	0.958	8	3
3	9	26	38	0.275	163	10.3	528	3.233	$Crit_{(38)}$ -1s =	65	0.089	0.468	9	3
3	10	26	38	0.275	163	11.8	584	3.575	$Crit_{(38)}$ +1s =	96	1.107	1.519	10	3
4	1	27	40	0.275	178	10.2	546	3.068	Mean =	528	0.421	-0.038	1	4
4	2	27	40	0.275	178	11.3	588	3.304	Std Dev'n =	32	1.188	0.687	2	4
4	3	27	40	0.275	178	9.4	515	2.896	Coef. Var'n =	6.1%	-0.136	-0.566	3	4
4	4	27	40	0.275	178	9.6	523	2.939	Median =	525	0.003	-0.434	4	4
4	5	27	40	0.275	178	10.0	538	3.025			0.282	-0.170	5	4
4	6	27	40	0.275	178	10.7	565	3.175			0.770	0.291	6	4
4	7	27	40	0.275	178	9.7	527	2.961			0.073	-0.368	7	4
4	8	27	40	0.275	178	9.1	504	2.832	S_{QLCT} =	2.97	-0.345	-0.764	8	4
4	9	27	40	0.275	178	8.6	485	2.725	$Crit_{(38)}$ -1s =	67	-0.694	-1.094	9	4
4	10	27	40	0.275	178	8.8	493	2.767	$Crit_{(38)}$ +1s =	80	-0.555	-0.962	10	4
5	1	27	38	0.28	169	9.8	524	3.099	Mean =	497	0.017	0.055	1	5
5	2	27	38	0.28	169	8.5	474	2.805	Std Dev'n =	31	-0.889	-0.847	2	5
5	3	27	38	0.28	169	10.3	543	3.212	Coef. Var'n =	6.2%	0.366	0.403	3	5
5	4	27	38	0.28	169	8.1	459	2.714	Median =	497	-1.168	-1.125	4	5
5	5	27	38	0.28	169	8.0	455	2.692			-1.238	-1.194	5	5
5	6	27	38	0.28	169	9.2	501	2.963			-0.401	-0.361	6	5
5	7	27	38	0.28	169	9.1	497	2.940			-0.471	-0.431	7	5
5	8	27	38	0.28	169	nr			S_{QLCT} =	2.94			8	5
5	9	27	38	0.28	169	9.0	493	2.918	$Crit_{(38)}$ -1s =	63	-0.540	-0.500	9	5
5	10	27	38	0.28	169	9.9	528	3.121	$Crit_{(38)}$ +1s =	75	0.087	0.125	10	5
						Max	718			n =	48	48		
						Min	410			Sum =	0.000	0.000		

Plate Wgt:	0.50	kg
C Factor :	0.771	

TauSlab Data					(N/m2)
Loc	Slope	Slab	H_{Nor}	H_2O_{Nor}	TauSlab
1	27	A	0.266	37	165
2	27	A	0.285	39	174
3	26	A	0.275	38	163
4	27	A	0.275	40	178
5	27	A	0.280	38	169
Mean	26.8		0.276	38	170
Std D	0.4		0.01	1.14	6.14
CV	1.7%		2.6%	3.0%	3.6%

Plot Summary		
n =	48	
Mean TauInfin =	523	N/m2
Std Dev'n =	55	N/m2
CV TauInfin =	10.48%	
S_{QLCT} =	3.081	Mean of pooled pit S_{QLCT}
Std Dev'n =	0.325	
CV S_{QLCT} =	10.57%	
$Crit_{(38)}$ Mean =	75	mm (TauInfin mean)
$Crit_{(38)}$ -1s =	64	mm (TauInfin - 1 SD)
$Crit_{(38)}$ +1s =	87	mm (TauInfin + 1 SD)

Lionhead 30m x 30m Study Plot Stability-Sampling Trials: 1/26/02 Profile #: 12 Weak Layer: A

Location		QLCT Data Bench Mode				Pit Results *(TauInf correction term C = var)				Z Score	Z Score	Location	
Pit #	Cell #	Slope	H2OCol	Test kg	H2Otest	TauInfin (N/m2)*	S QLCT	Pit-Wise		TauInfin	S QLCT	Cell #	Pit #
1	1	26	47	14.1	0.37	970	2.328	Mean =	955	-0.601	-0.264	1	1
1	2	26	47	10.8	0.30	775	1.861	Std Dev'n =	99	-1.629	-1.448	2	1
1	3	26	47	16.7	0.43	1,123	2.696	Coef. Var'n =	10.4%	0.209	0.669	3	1
1	4	26	47	14.8	0.39	1,011	2.427	Median =	979	-0.383	-0.013	4	1
1	5	26	47	14.6	0.38	1,000	2.399			-0.445	-0.085	5	1
1	6	26	47	14.4	0.38	988	2.370			-0.507	-0.156	6	1
1	7	26	47	12.0	0.32	846	2.030			-1.255	-1.018	7	1
1	8	26	47	12.7	0.34	887	2.130	SQLCT =	2.292	-1.037	-0.766	8	1
1	9	26	47	15.0	0.39	1,023	2.455	Crit(38) -1s =	92	-0.320	0.059	9	1
1	10	26	47	13.4	0.35	929	2.229	Crit(38) +1s =	134	-0.819	-0.515	10	1
2	1	27	47.5	13.8	0.36	973	2.145	Mean =	1,234	-0.584	-0.728	1	2
2	2	27	47.5	21.6	0.53	1,442	3.179	Std Dev'n =	205	1.893	1.892	2	2
2	3	27	47.5	21.0	0.52	1,406	3.099	Coef. Var'n =	16.6%	1.703	1.690	3	2
2	4	27	47.5	20.2	0.50	1,358	2.993	Median =	1,280	1.449	1.422	4	2
2	5	27	47.5	22.6	0.56	1,503	3.311			2.211	2.228	5	2
2	6	27	47.5	13.0	0.34	925	2.039			-0.838	-0.997	6	2
2	7	27	47.5	19.1	0.48	1,292	2.847			1.099	1.052	7	2
2	8	27	47.5	16.5	0.42	1,136	2.503	SQLCT =	2.719	0.274	0.179	8	2
2	9	27	47.5	14.8	0.38	1,033	2.277	Crit(38) -1s =	121	-0.266	-0.392	9	2
2	10	27	47.5	18.7	0.47	1,268	2.794	Crit(38) +1s =	207	0.972	0.918	10	2
3	1	25	53.5	18.6	0.48	1,225	2.790	Mean =	1,066	0.745	0.908	1	3
3	2	25	53.5	17.4	0.45	1,156	2.632	Std Dev'n =	173	0.379	0.508	2	3
3	3	25	53.5	15.4	0.41	1,040	2.369	Coef. Var'n =	16.2%	-0.230	-0.159	3	3
3	4	25	53.5	12.7	0.35	884	2.014	Median =	1,086	-1.054	-1.059	4	3
3	5	25	53.5	14.1	0.38	965	2.198			-0.627	-0.592	5	3
3	6	25	53.5	18.5	0.48	1,219	2.777			0.715	0.875	6	3
3	7	25	53.5	20.4	0.52	1,329	3.027			1.294	1.508	7	3
3	8	25	53.5	17.0	0.44	1,133	2.580	SQLCT =	2.427	0.257	0.375	8	3
3	9	25	53.5	11.4	0.32	809	1.843	Crit(38) -1s =	95	-1.450	-1.492	9	3
3	10	25	53.5	12.9	0.35	896	2.041	Crit(38) +1s =	168	-0.993	-0.992	10	3
4	1	26	53	15.0	0.40	1,039	2.325	Mean =	1,019	-0.237	-0.271	1	4
4	2	26	53	21.7	0.55	1,434	3.210	Std Dev'n =	186	1.849	1.971	2	4
4	3	26	53	12.8	0.35	909	2.035	Coef. Var'n =	18.3%	-0.922	-1.007	3	4
4	4	26	53	13.1	0.35	927	2.074	Median =	1,033	-0.829	-0.906	4	4
4	5	26	53	17.0	0.44	1,157	2.589			0.386	0.399	5	4
4	6	26	53	10.5	0.29	773	1.731			-1.639	-1.776	6	4
4	7	26	53	14.8	0.39	1,027	2.299			-0.300	-0.338	7	4
4	8	26	53	11.4	0.31	826	1.850	SQLCT =	2.282	-1.359	-1.475	8	4
4	9	26	53	15.1	0.40	1,045	2.338	Crit(38) -1s =	81	-0.206	-0.237	9	4
4	10	26	53	15.3	0.40	1,057	2.365	Crit(38) +1s =	160	-0.144	-0.170	10	4
5	1	28	58	16.5	0.43	1,185	2.525	Mean =	1,145	0.533	0.235	1	5
5	2	28	58	20.2	0.51	1,411	3.007	Std Dev'n =	162	1.728	1.457	2	5
5	3	28	58	16.4	0.43	1,179	2.512	Coef. Var'n =	14.2%	0.501	0.202	3	5
5	4	28	58	11.7	0.32	891	1.899	Median =	1,179	-1.016	-1.350	4	5
5	5	28	58	18.2	0.47	1,289	2.746			1.082	0.796	5	5
5	6	28	58	17.4	0.45	1,240	2.642			0.824	0.532	6	5
5	7	28	58	16.0	0.42	1,154	2.460			0.372	0.070	7	5
5	8	28	58	16.4	0.43	1,179	2.512	SQLCT =	2.440	0.501	0.202	8	5
5	9	28	58	13.3	0.36	989	2.108	Crit(38) -1s =	108	-0.500	-0.821	9	5
5	10	28	58	12.4	0.34	934	1.991	Crit(38) +1s =	176	-0.790	-1.119	10	5
					Max	1,503			n =	50	50		
Plate Wgt:		0.25	kg		Min	773			Sum =	0.000	0.000		

TauSlab Data					(N/m2)
Loc	Slope	Slab	H Nor	H2O Nor	TauSlab
1	26	A	0.69	97	417
2	27	A	0.76	102	454
3	25	A	0.74	106	439
4	26	A	0.73	104	447
5	28	A	0.71	102	469
Mean	26.4		0.73	104	452
Std D	1.1		0.03	3	19
CV	4.3%		3.8%	3.2%	4.3%

Plot Summary		
n =	50	
Mean TauInfin =	1,084	N/m2
Std Dev'n =	189	N/m2
CV TauInfin =	17.48%	
SQLCT =	2.432	Mean of pooled cell SQLCT
Std Dev'n =	0.395	
CV SQLCT =	16.23%	
Crit(38) Mean =	133	mm (TauInfin mean)
Crit(38) -1s =	93	mm (TauInfin - 1 SD)
Crit(38) +1s =	173	mm (TauInfin + 1 SD)

APPENDIX D

t-Tests of Strength 2000/2001 Trials

Two-Sampled *t*-Test (Relaxed) of Pit Strength $\bar{\tau}_{\infty}$ to Plot Strength $\bar{\tau}_{\infty(Plot)}$

Bacon Rind Study Plot Trials, 1/3/01

Pit-to-Plot Pair	F-test: ($\alpha = .05$) s^2 ratio	F	H_o	t-test (two-sided, $\alpha = 0.05$) t	p	H_o
1 to Plot ($n_{Pit} = 10$)	$\frac{(170.653)^2}{(80.798)^2}$	4.46 (crit ≈ 2.81)	Reject	-2.065 (28.1 df, crit ≈ 1.701)	0.048	Reject
2 to Plot ($n_{Pit} = 10$)	$\frac{(170.653)^2}{(70.937)^2}$	5.79 (crit ≈ 2.81)	Reject	-3.049 (33.6 df, crit ≈ 1.692)	0.004	Reject
3 to Plot ($n_{Pit} = 10$)	$\frac{(251.496)^2}{(170.653)^2}$	2.17 (crit ≈ 2.08)	Reject	2.130 (10.7 df, crit ≈ 1.80)	0.008	Reject
4 to Plot ($n_{Pit} = 10$)	$\frac{(170.653)^2}{(72.767)^2}$	5.50 (crit ≈ 2.81)	Reject	-0.596 (32.5 df, crit ≈ 1.694)	0.556	Fail to Reject
5 to Plot ($n_{Pit} = 10$)	$\frac{(170.653)^2}{(160.759)^2}$	1.13 (crit ≈ 2.81)	Fail to Reject	0.270 (58 df, crit ≈ 1.672)	0.788	Fail to Reject

Two-Sampled *t*-Test (Relaxed) of Pit Strength $\bar{\tau}_{\infty}$ to Plot Strength $\bar{\tau}_{\infty(Plot)}$

Bradley Meadow Study Plot, 1/27/01

Pit-to-Plot Pair	F-test: ($\alpha = .05$) s^2 ratio	F	H_o	t-test (two-sided, $\alpha = 0.05$) t	p	H_o
1 to Plot ($n_{Pit} = 9$)	$\frac{(133.622)^2}{(65.313)^2}$	4.19 (crit ≈ 3.03)	Reject	4.529 (23.6 df, crit ≈ 1.712)	0.000	Reject
2 to Plot ($n_{Pit} = 10$)	$\frac{(133.622)^2}{(76.955)^2}$	3.02 (crit ≈ 2.82)	Reject	-2.341 (22.7 df, crit ≈ 1.715)	0.028	Reject
3 to Plot ($n_{Pit} = 10$)	$\frac{(133.622)^2}{(84.748)^2}$	2.49 (crit ≈ 2.82)	Fail to Reject	0.936 (54 df, crit ≈ 1.675)	0.227	Fail to Reject
4 to Plot ($n_{Pit} = 7$)	$\frac{(198.911)^2}{(133.622)^2}$	2.22 (crit ≈ 2.32)	Fail to Reject	0.236 (51 df, crit ≈ 1.677)	0.865	Fail to Reject
5 to Plot ($n_{Pit} = 10$)	$\frac{(133.622)^2}{(98.809)^2}$	1.83 (crit ≈ 2.82)	Fail to Reject	-2.173 (58 df, crit ≈ 1.672)	0.034	Reject

Two-Sampled *t*-Test (Relaxed) of Pit Strength $\bar{\tau}_{\infty}$ to Plot Strength $\bar{\tau}_{\infty(Plot)}$

Round Hill Plot, 2/18/01

Pit-to-Plot Pair	*F*-test: ($\alpha = .05$) s^2 ratio	*F*	H_o	*t*-test (two-sided, $\alpha = 0.05$) *t*	*p*	H_o
1 to Plot ($n_{Pit} = 9$)	$\frac{(416.693)^2}{(60.048)^2}$	48.15 (crit ≈ 3.06)	Reject	-6.151 (41.1 df, crit ≈ 1.683)	0.000	Reject
2 to Plot ($n_{Pit} = 10$)	$\frac{(416.693)^2}{(132.569)^2}$	9.88 (crit ≈ 2.84)	Reject	4.272 (43.6 df, crit ≈ 1.682)	0.000	Reject
3 to Plot ($n_{Pit} = 10$)	$\frac{(416.693)^2}{(63.610)^2}$	42.91 (crit ≈ 2.84)	Reject	-4.520 (41.2 df, crit ≈ 1.683)	0.000	Reject
4 to Plot ($n_{Pit} = 8$)	$\frac{(416.693)^2}{(213.732)^2}$	3.80 (crit ≈ 3.36)	Reject	4.651 (20.5 df, crit ≈ 1.723)	0.000	Reject
5 to Plot ($n_{Pit} = 0$)	No results					

Two-Sampled *t*-Test (Relaxed) of Pit Strength $\bar{\tau}_{\infty}$ to Plot Strength $\bar{\tau}_{\infty(Plot)}$

Baldy Mountain Study Plot, 2/18/01

Pit-to-Plot Pair	*F*-test: ($\alpha = .05$) s^2 ratio	*F*	H_o	*t*-test (two-sided, $\alpha = 0.05$) *t*	*p*	H_o
1 to Plot ($n_{Pit} = 0$)	No results					
2 to Plot ($n_{Pit} = 2$)	$\frac{(289.048)^2}{(60.811)^2}$	22.59 (crit ≈ 247.16)	Fail to Reject	2.118 (19 df, crit = 1.729)	0.048	Reject
3 to Plot ($n_{Pit} = 6$)	$\frac{(289.048)^2}{(170.157)^2}$	2.89 (crit ≈ 4.58)	Fail to Reject	-1.309. (23 df, crit = 1.714)	0.204	Fail to Reject
4 to Plot ($n_{Pit} = 7$)	$\frac{(289.048)^2}{(258.679)^2}$	1.25 (crit ≈ 3.90)	Fail to Reject	-0.968 (24 df, crit = 1.711)	0.343	Fail to Reject
5 to Plot ($n_{Pit} = 4$)	$\frac{(289.048)^2}{(158.831)^2}$	3.31 (crit ≈ 8.68)	Fail to Reject	1.560 (21 df, crit = 1.721)	0.134	Fail to Reject

Two-Sampled *t*-Test (Relaxed) of Pit Strength $\bar{\tau}_{\infty}$ to Plot Strength $\bar{\tau}_{\infty(Plot)}$

Saddle Peak Study Plot, 2/18/01

Pit-to-Plot Pair	*F*-test: ($\alpha = .05$) s^2 ratio	*F*	H_o	*t*-test (two-sided, $\alpha = 0.05$) *t*	*p*	H_o
1 to Plot ($n_{Pit} = 8$)	$\frac{(375.394)^2}{(298.340)^2}$	1.58 (crit ≈ 3.33)	Fail to Reject	-0.819 (53 df, crit ≈ 1.676)	0.417	Fail to Reject
2 to Plot ($n_{Pit} = 10$)	$\frac{(375.394)^2}{(288.854)^2}$	1.69 (crit ≈ 2.82)	Fail to Reject	-2.530 (55 df, crit ≈ 1.674)	0.014	Reject
3 to Plot ($n_{Pit} = 10$)	$\frac{(457.696)^2}{(375.394)^2}$	1.49 (crit ≈ 2.10)	Fail to Reject	0.293 (55 df, crit ≈ 1.674)	0.771	Fail to Reject
4 to Plot ($n_{Pit} = 10$)	$\frac{(375.394)^2}{(177.128)^2}$	4.49 (crit ≈ 2.82)	Reject	4.652 (29.2 df, crit ≈ 1.699)	0.004	Reject
5 to Plot ($n_{Pit} = 9$)	$\frac{(375.394)^2}{(242.491)^2}$	2.40 (crit ≈ 3.03)	Fail to Reject	0.060 (54 df, crit ≈ 1.675)	0.952	Fail to Reject

Two-Sampled *t*-Test (Relaxed) of Pit Strength $\bar{\tau}_{\infty}$ to Plot Strength $\bar{\tau}_{\infty(Plot)}$

Bradley Meadow Study Plot, 2/18/01

Pit-to-Plot Pair	*F*-test: ($\alpha = .05$) s^2 ratio	*F*	H_o	*t*-test (two-sided, $\alpha = 0.05$) *t*	*p*	H_o
1 to Plot ($n_{Pit} = 0$)	No results					
2 to Plot ($n_{Pit} = 8$)	$\frac{(376.178)^2}{(348.768)^2}$	1.16 (crit = 2.42)	Fail to Reject	0.627 (31 df, crit = 1.696)	0.535	Fail to Reject
3 to Plot ($n_{Pit} = 2$)	$\frac{(436.285)^2}{(348.768)^2}$	1.57 (crit = 4.26)	Fail to Reject	1.756 (25 df, crit = 1.708)	0.091	Reject
4 to Plot ($n_{Pit} = 10$)	$\frac{(348.768)^2}{(252.900)^2}$	1.90 (crit = 2.90)	Fail to Reject	-0.041 (33 df, crit = 1.692)	0.968	Fail to Reject
5 to Plot ($n_{Pit} = 5$)	$\frac{(348.768)^2}{(212.364)^2}$	2.70 (crit = 5.77)	Fail to Reject	-1.945 (28 df, crit = 1.701)	0.062	Reject

Two-Sampled *t*-Test (Relaxed) of Pit Strength $\bar{\tau}_{\infty}$ to Plot Strength $\bar{\tau}_{\infty(Plot)}$

Bradley Meadow Study Plot, 3/17/01

Pit-to-Plot Pair	*F*-test: ($\alpha = .05$) s^2 ratio	*F*	H_o	*t*-test (two-sided, $\alpha = 0.05$) *t*	*p*	H_o
1 to Plot ($n_{Pit} = 9$)	$\frac{(122.958)^2}{(116.888)^2}$	1.11 (crit ≈ 2.16)	Fail to Reject	-1.108 (53 df, crit ≈ 1.676)	0.273	Fail to Reject
2 to Plot ($n_{Pit} = 10$)	$\frac{(116.888)^2}{(93.418)^2}$	1.57 (crit ≈ 2.82)	Fail to Reject	1.590 (54 df, crit ≈ 1.658)	0.118	Fail to Reject
3 to Plot ($n_{Pit} = 8$)	$\frac{(136.174)^2}{(116.888)^2}$	1.36 (crit ≈ 2.23)	Fail to Reject	0.021 (52 df, crit ≈ 1.676)	0.983	Fail to Reject
4 to Plot ($n_{Pit} = 10$)	$\frac{(116.888)^2}{(76.940)^2}$	2.31 (crit ≈ 2.82)	Fail to Reject	-1.138 (54 df, crit ≈ 1.658)	0.260	Fail to Reject
5 to Plot ($n_{Pit} = 9$)	$\frac{(135.463)^2}{(116.888)^2}$	1.34 (crit ≈ 2.16)	Fail to Reject	0.594 (53 df, crit ≈ 1.676)	0.555	Fail to Reject

Two-Sampled *t*-Test of Plot Strength $\bar{\tau}_{\infty(Plot)}$ to Plot Strength $\bar{\tau}_{\infty(Plot)}$

Bridger Range Study Plot Trials, 2/18/01

Plot-to-Plot Pair	*F*-test: ($\alpha = .05$) s^2 ratio	*F*	H_o	*t*-test (two-sided, $\alpha = 0.05$) *t*	*p*	H_o
Baldy Mountain to Saddle Peak	$\frac{(375.394)^2}{(289.048)^2}$	1.69 (crit ≈ 2.05)	Fail to Reject	-3.710 (64 df, crit ≈ 1.670)	0.000	Reject
Baldy Mountain to Bradley Meadow	$\frac{(348.768)^2}{(289.048)^2}$	1.46 (crit = 2.15)	Fail to Reject	-5.364 (42 df, crit = 1.683)	0.000	Reject
Saddle Peak to Bradley Meadow	$\frac{(375.394)^2}{(348.768)^2}$	1.16 (crit ≈ 1.88)	Fail to Reject	1.912 (70 df, crit ≈ 1.656)	0.060	Reject

APPENDIX E

t-Tests of Strength 2001/2002 Trials

Two-Sampled *t*-Test (Relaxed) of Pit Strength $\bar{\tau}_{\infty}$ to Plot Strength $\bar{\tau}_{\infty(Plot)}$

Middle Basin Plot 12/7/01 Trials, Pooled Weak Layers A & B (no "NR" results)

Pit-to-Plot Pair	*F*-test: ($\alpha = 0.05$) s^2 ratio	*F*	H_o	*t*-test (two-sided, $\alpha = 0.05$) *t*	*p*	H_o
1 to Plot ($n_{Pit} = 10$)	$\frac{(160.417)^2}{(113.899)^2}$	4.13 (crit = 2.83)	Reject	-1.097 (18.8 df, crit ≈ 1.730)	0.286	Fail to Reject
2 to Plot ($n_{Pit} = 7$)	$\frac{(160.417)^2}{(39.147)^2}$	16.79 (crit = 3.77)	Reject	-0.121 (40.2 df, crit ≈ 1.683)	0.904	Fail to Reject
3 to Plot ($n_{Pit} = 10$)	$\frac{(176.307)^2}{(160.417)^2}$	1.21 (crit = 2.12)	Fail to Reject	1.170 (49 df, crit ≈ 1.678)	0.248	Fail to Reject
4 to Plot ($n_{Pit} = 8$)	$\frac{(261.782)^2}{(160.417)^2}$	2.66 (crit = 2.25)	Reject	0.140 (8.1 df, crit ≈ 1.857)	0.892	Fail to Reject
5 to Plot ($n_{Pit} = 6$)	$\frac{(160.417)^2}{(110.528)^2}$	2.11 (crit = 4.46)	Fail to Reject	-0.675 (45 df, crit ≈ 1.681)	0.503	Fail to Reject

Two-Sampled *t*-Test (Relaxed) of Pit Strength $\bar{\tau}_{\infty}$ to Plot Strength $\bar{\tau}_{\infty(Plot)}$

Middle Basin Plot 12/7/01Trials, Pooled Weak Layers A & B (inc. est. "NR" results)

Pit-to-Plot Pair	*F*-test: ($\alpha = 0.05$) s^2 ratio	*F*	H_o	*t*-test (two-sided, $\alpha = 0.05$) *t*	*p*	H_o
1 to Plot ($n_{Pit} = 10$)	$\frac{(231.468)^2}{(113.899)^2}$	4.13 (crit ≈ 2.81)	Reject	-2.658 (26.7 df, crit ≈ 1.704)	0.013	Reject
2 to Plot ($n_{Pit} = 10$)	$\frac{(231.468)^2}{(214.362)^2}$	1.16 (crit ≈ 2.81)	Fail to Reject	0.555 (58 df, crit ≈ 1.672)	0.581	Fail to Reject
3 to Plot ($n_{Pit} = 10$)	$\frac{(231.468)^2}{(176.307)^2}$	1.72 (crit ≈ 2.81)	Fail to Reject	-0.178 (58 df, crit ≈ 1.672)	0.859	Fail to Reject
4 to Plot ($n_{Pit} = 10$)	$\frac{(273.738)^2}{(231.468)^2}$	1.40 (crit ≈ 2.08)	Fail to Reject	0.009 (58 df, crit ≈ 1.672)	0.993	Fail to Reject
5 to Plot ($n_{Pit} = 10$)	$\frac{(308.261)^2}{(231.468)^2}$	1.77 (crit ≈ 2.08)	Fail to Reject	1.160 (58 df, crit ≈ 1.672)	0.251	Fail to Reject

Two-Sampled *t*-Test (Relaxed) of Pit Strength $\bar{\tau}_{\infty}$ to Plot Strength $\bar{\tau}_{\infty(Plot)}$

Lionhead Plot 1/9/02 Trials

Pit-to-Plot Pair	*F*-test: ($\alpha = 0.05$) s^2 ratio	F	H_o	*t*-test (two-sided, $\alpha = 0.05$) t	p	H_o
1 to Plot ($n_{Pit} = 10$)	$\frac{(39.112)^2}{(22.422)^2}$	3.04 (crit ≈ 2.81)	Reject	-0.685 (21.8 df, crit ≈ 1.718)	0.501	Fail to Reject
2 to Plot ($n_{Pit} = 10$)	$\frac{(39.112)^2}{(22.172)^2}$	3.11 (crit ≈ 2.81)	Reject	-0.746 (22.1 df, crit ≈ 1.717)	0.464	Fail to Reject
3 to Plot ($n_{Pit} = 10$)	$\frac{(57.357)^2}{(39.112)^2}$	2.15 (crit ≈ 2.08)	Reject	0.435 (10.7 df, crit ≈ 1.801)	0.672	Fail to Reject
4 to Plot ($n_{Pit} = 10$)	$\frac{(39.112)^2}{(22.659)^2}$	2.98 (crit ≈ 2.81)	Reject	2.545 (21.5 df, crit ≈ 1.719)	0.019	Reject
5 to Plot ($n_{Pit} = 10$)	$\frac{(48.945)^2}{(39.112)^2}$	1.63 (crit ≈ 2.08)	Fail to Reject	-1.306 (58 df, crit ≈ 1.672)	0.197	Fail to Reject

Two-Sampled *t*-Test (Relaxed) of Pit Strength $\bar{\tau}_{\infty}$ to Plot Strength $\bar{\tau}_{\infty(Plot)}$

Lionhead Plot 1/15/02 Trials

Pit-to-Plot Pair	*F*-test: ($\alpha = 0.05$) s^2 ratio	F	H_o	*t*-test (two-sided, $\alpha = 0.05$) t	p	H_o
1 to Plot ($n_{Pit} = 10$)	$\frac{(54.833)^2}{(43.321)^2}$	1.60 (crit ≈ 2.82)	Fail to Reject	-1.967 (56 df, crit = 1.674)	0.054	Reject
2 to Plot ($n_{Pit} = 10$)	$\frac{(56.079)^2}{(54.833)^2}$	1.05 (crit ≈ 2.09)	Fail to Reject	1.781 (56 df, crit = 1.674)	0.080	Reject
3 to Plot ($n_{Pit} = 9$)	$\frac{(73.934)^2}{(54.833)^2}$	1.82 (crit ≈ 2.15)	Fail to Reject	1.058 (55 df, crit = 1.674)	0.295	Fail to Reject
4 to Plot ($n_{Pit} = 10$)	$\frac{(54.833)^2}{(32.035)^2}$	2.93 (crit ≈ 2.82)	Reject	0.425 (21.8 df, crit ≈ 1.718)	0.675	Fail to Reject
5 to Plot ($n_{Pit} = 9$)	$\frac{(54.833)^2}{(30.771)^2}$	3.18 (crit ≈ 3.03)	Reject	-1.993 (19.2 df, crit ≈ 1.728)	0.061	Reject

Two-Sampled *t*-Test (Relaxed) of Pit Strength $\overline{\tau}_{\infty}$ to Plot Strength $\overline{\tau}_{\infty(Plot)}$

Lionhead Plot 1/26/02 Trials

Pit-to-Plot Pair	*F*-test: ($\alpha = 0.05$) s^2 ratio	*F*	H_o	*t*-test (two-sided, $\alpha = 0.05$) *t*	*p*	H_o
1 to Plot ($n_{Pit} = 10$)	$\frac{(189.426)^2}{(99.358)^2}$	3.63 (crit ≈ 2.81)	Reject	-3.113. (24.5 df, crit ≈ 1.710)	0.005	Reject
2 to Plot ($n_{Pit} = 10$)	$\frac{(205.071)^2}{(189.426)^2}$	1.17 (crit ≈ 2.08)	Fail to Reject	2.255 (58 df, crit = 1.672)	0.028	Reject
3 to Plot ($n_{Pit} = 10$)	$\frac{(189.426)^2}{(172.944)^2}$	1.20 (crit ≈ 2.81)	Fail to Reject	-0.281 (58 df, crit = 1.672)	0.779	Fail to Reject
4 to Plot ($n_{Pit} = 10$)	$\frac{(189.426)^2}{(186.155)^2}$	1.04 (crit ≈ 2.81)	Fail to Reject	-0.984 (58 df, crit = 1.672)	0.329	Fail to Reject
5 to Plot ($n_{Pit} = 10$)	$\frac{(189.426)^2}{(162.446)^2}$	1.36 (crit ≈ 2.81)	Fail to Reject	0.954 (58 df, crit = 1.672)	0.344	Fail to Reject

APPENDIX F

t-Tests of Stability 2000/2001 Trials

Two-Sampled *t*-Test (Relaxed) of Pit Stability S_{QLCT} to Plot Stability $S_{QLCT(Plot)}$
Bacon Rind Study Plot Trials, 1/3/01

Pit-to-Plot Pair	s^2 ratio	*F*-test: ($\alpha = .05$) *F* value	H_o	*t*-test (two-sided, $\alpha = 0.05$) *t*	*p*	H_o
1 to Plot ($n_{Pit} = 10$)	$\frac{(0.650)^2}{(0.317)^2}$	4.20 (crit ≈ 2.81)	Reject	-1.968 (27 df, crit = 1.703)	0.059	Reject
2 to Plot ($n_{Pit} = 10$)	$\frac{(0.650)^2}{(0.291)^2}$	4.98 (crit ≈ 2.81)	Reject	-2.329 (30.3 df, crit ≈ 1.697)	0.027	Reject
3 to Plot ($n_{Pit} = 10$)	$\frac{(0.968)^2}{(0.650)^2}$	2.22 (crit ≈ 2.08)	Reject	2.062 (10.7 df, crit ≈ 1.801)	0.064	Reject
4 to Plot ($n_{Pit} = 10$)	$\frac{(0.650)^2}{(0.270)^2}$	5.80 (crit ≈ 2.81)	Reject	-1.356 (33.6 df, crit ≈ 1.692)	0.184	Fail to Reject
5 to Plot ($n_{Pit} = 10$)	$\frac{(0.650)^2}{(0.632)^2}$	1.06 (crit ≈ 2.81)	Fail to Reject	0.364 (58 df, crit = 1.672)	0.717	Fail to Reject

Two-Sampled *t*-Test (Relaxed) of Pit Stability S_{QLCT} to Plot Stability $S_{QLCT(Plot)}$
Bradley Meadow Study Plot Trials, 1/27/01

Pit-to-Plot Pair	s^2 ratio	*F*-test: ($\alpha = .05$) *F* value	H_o	*t*-test (two-sided, $\alpha = 0.05$) *t*	*p*	H_o
1 to Plot ($n_{Pit} = 9$)	$\frac{(1.583)^2}{(0.405)^2}$	15.28 (crit ≈ 3.03)	Reject	-4.844 (49.2 df, crit ≈ 1.678)	0.000	Reject
2 to Plot ($n_{Pit} = 10$)	$\frac{(1.583)^2}{(1.152)^2}$	1.89 (crit ≈ 2.82)	Fail to Reject	3.652 (54 df, crit = 1.675)	0.001	Reject
3 to Plot ($n_{Pit} = 10$)	$\frac{(1.583)^2}{(0.812)^2}$	3.80 (crit ≈ 2.82)	Reject	0.728 (26.4 df, crit ≈ 1.705)	0.473	Fail to Reject
4 to Plot ($n_{Pit} = 7$)	$\frac{(1.901)^2}{(1.583)^2}$	1.44 (crit ≈ 2.32)	Fail to Reject	-0.024 (51 df, crit ≈ 1.677)	0.981	Fail to Reject
5 to Plot ($n_{Pit} = 10$)	$\frac{(1.583)^2}{(0.962)^2}$	2.71 (crit ≈ 2.82)	Fail to Reject	-1.919 (54 df, crit ≈ 1.675)	0.060	Reject

Two-Sampled *t*-Test (Relaxed) of Pit Stability S_{QLCT} to Plot Stability $S_{QLCT(Plot)}$
Round Hill Trials, 2/4/01

Pit-to-Plot Pair	s^2 ratio	*F*-test: ($\alpha = .05$) *F* value	H_o	*t*-test (two-sided, $\alpha = 0.05$) *t*	*p*	H_o
1 to Plot ($n_{Pit} = 9$)	$\frac{(1.134)^2}{(0.224)^2}$	25.63 (crit ≈ 3.06)	Reject	-5.680 (43.4 df, crit ≈ 1.682)	0.000	Reject
2 to Plot ($n_{Pit} = 10$)	$\frac{(1.134)^2}{(0.410)^2}$	7.65 (crit ≈ 2.84)	Reject	4.568 (40.9 df, crit ≈ 1.683)	0.000	Reject
3 to Plot ($n_{Pit} = 10$)	$\frac{(1.134)^2}{(0.210)^2}$	29.16 (crit ≈ 2.84)	Reject	-4.660 (42.9 df, crit ≈ 1.682)	0.000	Reject
4 to Plot ($n_{Pit} = 8$)	$\frac{(1.134)^2}{(0.614)^2}$	3.41 (crit ≈ 3.36)	Reject	3.978 (19.1 df, crit ≈ 1.729)	0.001	Reject
5 to Plot	No results					

Two-Sampled *t*-Test (Relaxed) of Pit Stability S_{QLCT} to Plot Stability $S_{QLCT(Plot)}$
Baldy Mountain Study Plot Trials, 2/18/01

Pit-to-Plot Pair	s^2 ratio	*F*-test: ($\alpha = .05$) *F* value	H_o	*t*-test (two-sided, $\alpha = 0.05$) *T*	*p*	H_o
1 to Plot	No results					
2 to Plot ($n_{Pit} = 2$)	$\frac{(0.358)^2}{(0.066)^2}$	29.42 (crit ≈ 247)	Fail to Reject	-0.328 (19 df, crit = 1.729)	0.746	Fail to Reject
3 to Plot ($n_{Pit} = 6$)	$\frac{(0.358)^2}{(0.306)^2}$	1.37 (crit ≈ 3.92)	Fail to Reject	-0.377 (23 df, crit = 1.714)	0.710	Fail to Reject
4 to Plot ($n_{Pit} = 7$)	$\frac{(0.498)^2}{(0.358)^2}$	1.94 (crit ≈ 3.92)	Fail to Reject	0.820 (24 df, crit = 1.711)	0.420	Fail to Reject
5 to Plot ($n_{Pit} = 4$)	$\frac{(0.358)^2}{(0.195)^2}$	3.37 (crit ≈ 8.68)	Fail to Reject	-0.630 (21 df, crit = 1.721)	0.536	Fail to Reject

Two-Sampled *t*-Test (Relaxed) of Pit Stability S_{QLCT} to Plot Stability $S_{QLCT(Plot)}$
Saddle Peak Study Plot Trials, 2/18/01

Pit-to-Plot Pair	s^2 ratio	*F*-test: ($\alpha = .05$) *F* value	H_o	*t*-test (two-sided, $\alpha = 0.05$) *t*	*p*	H_o
1 to Plot ($n_{Pit} = 8$)	$\frac{(0.487)^2}{(0.439)^2}$	1.23 (crit ≈ 3.33)	Fail to Reject	0.817 (53 df, crit ≈ 1.676)	0.418	Fail to Reject
2 to Plot ($n_{Pit} = 10$)	$\frac{(0.487)^2}{(0.391)^2}$	1.55 (crit ≈ 2.82)	Fail to Reject	-1.766 (55 df, crit ≈ 1.674)	0.083	Reject
3 to Plot ($n_{Pit} = 10$)	$\frac{(0.627)^2}{(0.487)^2}$	1.66 (crit ≈ 2.10)	Fail to Reject	1.239 (55 df, crit ≈ 1.674)	0.221	Fail to Reject
4 to Plot ($n_{Pit} = 10$)	$\frac{(0.487)^2}{(0.208)^2}$	5.48 (crit ≈ 2.81)	Reject	3.098 (33.4 df, crit ≈ 1.307)	0.004	Reject
5 to Plot ($n_{Pit} = 9$)	$\frac{(0.487)^2}{(0.240)^2}$	4.12 (crit ≈ 3.03)	Reject	-3.637 (23 df, crit = 1.714)	0.001	Reject

Two-Sampled *t*-Test (Relaxed) of Pit Stability S_{QLCT} to Plot Stability $S_{QLCT(Plot)}$
Bradley Meadow Study Plot Trials, 2/18/01

Pit-to-Plot Pair	s^2 ratio	*F*-test: ($\alpha = .05$) *F* value	H_o	*t*-test (two-sided, $\alpha = 0.05$) *t*	*p*	H_o
1 to Plot ($n_{Pit} = 0$)	No results					
2 to Plot ($n_{Pit} = 8$)	$\frac{(0.322)^2}{(0.314)^2}$	1.05 (crit ≈ 3.45)	Fail to Reject	-0.909 (26 df, crit = 1.706)	0.372	Fail to Reject
3 to Plot ($n_{Pit} = 2$)	Less than 3 valid QLCT results					
4 to Plot ($n_{Pit} = 10$)	$\frac{(0.322)^2}{(0.266)^2}$	1.47 (crit ≈ 2.96)	Fail to Reject	1.360 (28 df, crit = 1.701)	0.185	Fail to Reject
5 to Plot ($n_{Pit} = 0$)	No results					

Two-Sampled *t*-Test (Relaxed) of Pit Stability S_{QLCT} to Plot Stability $S_{QLCT(Plot)}$
Bradley Meadow Study Plot Trials, 3/17/01

Pit-to-Plot Pair	s^2 ratio	*F*-test: ($\alpha = .05$) *F* value	H_o	*t*-test (two-sided, $\alpha = 0.05$) *t*	*p*	H_o
1 to Plot ($n_{Pit} = 9$)	$\frac{(0.900)^2}{(0.828)^2}$	1.18 (crit ≈ 2.16)	Fail to Reject	-0.959 (53 df, crit ≈ 1.676)	0.342	Fail to Reject
2 to Plot ($n_{Pit} = 10$)	$\frac{(0.828)^2}{(0.664)^2}$	1.56 (crit ≈ 2.81)	Fail to Reject	1.456 (54 df, crit ≈ 1.675)	0.151	Fail to Reject
3 to Plot ($n_{Pit} = 8$)	$\frac{(0.997)^2}{(0.828)^2}$	1.45 (crit ≈ 2.23)	Fail to Reject	0.190 (52 df, crit ≈ 1.676)	0.850	Fail to Reject
4 to Plot ($n_{Pit} = 10$)	$\frac{(0.828)^2}{(0.558)^2}$	2.20 (crit ≈ 2.81)	Fail to Reject	-1.064 (54 df, crit ≈ 1.675)	0.292	Fail to Reject
5 to Plot ($n_{Pit} = 9$)	$\frac{(0.952)^2}{(0.828)^2}$	1.32 (crit ≈ 2.16)	Fail to Reject	0.358 (53 df, crit ≈ 1.676)	0.722	Fail to Reject

Two-Sampled *t*-Test of Plot Stability $S_{QLCT(Plot)}$ to Plot Stability $S_{QLCT(Plot)}$
Bridger Range Study Plot Trials, 2/18/01

Plot-to-Plot Pair	s^2 ratio	*F*-test: ($\alpha = .05$) *F*	H_o	*t*-test (two-sided, $\alpha = 0.05$) *t*	*p*	H_o
Baldy Mountain to Saddle Peak	$\frac{(0.487)^2}{(0.358)^2}$	1.85 (crit ≈ 2.05)	Fail to Reject	-0.596 (64 df, crit ≈ 1.670)	0.553	Fail to Reject
Baldy Mountain to Bradley Meadow	$\frac{(0.358)^2}{(0.322)^2}$	1.24 (crit = 2.02)	Fail to Reject	1.950 (37 df, crit = 1.688)	0.059	Reject
Saddle Peak to Bradley Meadow	$\frac{(0.487)^2}{(0.322)^2}$	2.29 (crit ≈ 2.01)	Reject	-2.829 (53.1 df, crit ≈ 1.676)	0.007	Reject

APPENDIX G

t-Tests of Stability 2001/2002 Trials

Two-Sampled *t*-Test (Relaxed) of Stability Ratio S_{QLCT}, Pit-to-Plot
Middle Basin Plot 12/7/01 Trials, Pooled Weak Layers A & B (no "NR" results)

Pit-to-Plot Pair	s^2 ratio	*F*-test: ($\alpha = .05$) *F* value	H_o	*t*-test (two-sided, $\alpha = 0.05$) *t*	*p*	H_o
1 to Plot ($n_{Pit} = 10$)	$\frac{(0.480)^2}{(0.354)^2}$	1.84 (crit = 2.83)	Fail to Reject	-0.085 (49 df, crit ≈ 1.678)	0.932	Fail to Reject
2 to Plot ($n_{Pit} = 7$)	$\frac{(0.480)^2}{(0.128)^2}$	14.06 (crit = 3.77)	Fail to Reject	1.331 (46 df, crit ≈ 1.680)	0.190	Fail to Reject
3 to Plot ($n_{Pit} = 10$)	$\frac{(0.480)^2}{(0.442)^2}$	1.18 (crit = 2.83)	Fail to Reject	-0.676 (49 df, crit ≈ 1.672)	0.502	Fail to Reject
4 to Plot ($n_{Pit} = 8$)	$\frac{(0.806)^2}{(0.480)^2}$	2.82 (crit = 2.25)	Reject	0.539 (8 df, crit = 1.856)	0.605	Fail to Reject
5 to Plot ($n_{Pit} = 6$)	$\frac{(0.480)^2}{(0.296)^2}$	2.63 (crit = 4.46)	Fail to Reject	-1.415 (45 df, crit ≈ 1.681)	0.164	Fail to Reject

Two-Sampled *t*-Test (Relaxed) of Stability Ratio S_{QLCT}, Pit-to-Plot
Middle Basin Plot 12/7/01 Trials, Pooled Weak Layers A & B (inc. est. "NR" results)

Pit-to-Plot Pair	s^2 ratio	*F*-test: ($\alpha = .05$) *F* value	H_o	*t*-test (two-sided, $\alpha = 0.05$) *t*	*p*	H_o
1 to Plot ($n_{Pit} = 10$)	$\frac{(0.697)^2}{(0.354)^2}$	3.88 (crit ≈ 2.81)	Reject	-1.740 (25.6 df, crit ≈ 1.707)	0.094	Reject
2 to Plot ($n_{Pit} = 10$)	$\frac{(0.703)^2}{(0.697)^2}$	1.02 (crit ≈ 2.08)	Fail to Reject	1.744 (58 df, crit ≈ 1.672)	0.086	Reject
3 to Plot ($n_{Pit} = 10$)	$\frac{(0.697)^2}{(0.442)^2}$	2.49 (crit ≈ 2.81)	Fail to Reject	-1.559 (58 df, crit ≈ 1.672)	0.124	Fail to Reject
4 to Plot ($n_{Pit} = 10$)	$\frac{(0.843)^2}{(0.697)^2}$	1.46 (crit ≈ 2.08)	Fail to Reject	0.498 (58 df, crit ≈ 1.672)	0.621	Fail to Reject
5 to Plot ($n_{Pit} = 10$)	$\frac{(0.825)^2}{(0.697)^2}$	1.40 (crit ≈ 2.08)	Fail to Reject	0.289 (58 df, crit ≈ 1.672)	0.773	Fail to Reject

Two-Sampled *t*-Test (Relaxed) of Stability Ratio S_{QLCT}, Pit-to-Plot
Lionhead Plot 1/9/02 Trials

Pit-to-Plot Pair	s^2 ratio	*F*-test: ($\alpha = .05$) *F* value	H_o	*t*-test (two-sided, $\alpha = 0.05$) *t*	*p*	H_o
1 to Plot	$\frac{(0.259)^2}{(0.148)^2}$	3.06 (crit = 2.81)	Reject	-1.273 (21.9 df, crit ≈ 1.717)	0.216	Fail to Reject
2 to Plot	$\frac{(0.259)^2}{(0.156)^2}$	2.76 (crit = 2.81)	Fail to Reject	1.009 (58 df, crit = 1.672)	0.317	Fail to Reject
3 to Plot	$\frac{(0.390)^2}{(0.259)^2}$	2.27 (crit = 2.08)	Reject	0.631 (10.6 df, crit ≈ 1.803)	0.542	Fail to Reject
4 to Plot	$\frac{(0.259)^2}{(0.145)^2}$	3.19 (crit = 2.81)	Reject	0.273 (22.5 df, crit ≈ 1.716)	0.788	Fail to Reject
5 to Plot	$\frac{(0.333)^2}{(0.259)^2}$	1.65 (crit = 2.08)	Fail to Reject	-1.140 (58 df, crit = 1.672)	0.259	Fail to Reject

Two-Sampled *t*-Test (Relaxed) of Stability Ratio S_{QLCT}, Pit-to-Plot
Lionhead Plot 1/15/02 Trials

Pit-to-Plot Pair	s^2 ratio	*F*-test: ($\alpha = 0.05$) *F*	H_o	*t*-test (two-sided, $\alpha = 0.05$) *t*	*p*	H_o
1 to Plot ($n_{Pit} = 10$)	$\frac{(0.325)^2}{(0.263)^2}$	1.53 (crit ≈ 2.82)	Fail to Reject	-1.142 (56 df, crit = 1.674)	0.258	Fail to Reject
2 to Plot ($n_{Pit} = 10$)	$\frac{(0.325)^2}{(0.323)^2}$	1.01 (crit ≈ 2.82)	Fail to Reject	1.151. (56 df, crit = 1.674)	0.255	Fail to Reject
3 to Plot ($n_{Pit} = 9$)	$\frac{(0.452)^2}{(0.325)^2}$	1.93 (crit ≈ 2.15)	Fail to Reject	2.055 (56 df, crit = 1.674)	0.045	Reject
4 to Plot ($n_{Pit} = 10$)	$\frac{(0.325)^2}{(0.180)^2}$	3.26 (crit ≈ 2.82)	Reject	-1.506 (23.3 df, crit ≈ 1.713)	0.146	Fail to Reject
5 to Plot ($n_{Pit} = 9$)	$\frac{(0.325)^2}{(0.182)^2}$	3.19 (crit ≈ 3.03)	Reject	-1.828 (19.3 df, crit ≈ 1.728)	0.083	Reject

Two-Sampled *t*-Test (Relaxed) of Stability Ratio S_{QLCT}, Pit-to-Plot
Lionhead Plot 1/26/02 Trials

Pit-to-Plot Pair	F-test: ($\alpha = 0.05$) s^2 ratio	F	H_o	t-test (two-sided, $\alpha = 0.05$) t	p	H_o
1 to Plot ($n_{Pit} = 10$)	$\frac{(0.395)^2}{(0.238)^2}$	2.28 (crit ≈ 2.81)	Fail to Reject	-1.075 (58 df, crit = 1.672)	0.287	Fail to Reject
2 to Plot ($n_{Pit} = 10$)	$\frac{(0.452)^2}{(0.395)^2}$	1.31 (crit ≈ 2.08)	Fail to Reject	2.048 (58 df, crit = 1.672)	0.045	Reject
3 to Plot ($n_{Pit} = 10$)	$\frac{(0.395)^2}{(0.394)^2}$	1.01 (crit ≈ 2.81)	Fail to Reject	-0.036 (58 df, crit = 1.672)	0.971	Fail to Reject
4 to Plot ($n_{Pit} = 10$)	$\frac{(0.417)^2}{(0.395)^2}$	1.11 (crit ≈ 2.08)	Fail to Reject	-1.091 (58 df, crit = 1.672)	0.280	Fail to Reject
5 to Plot ($n_{Pit} = 10$)	$\frac{(0.395)^2}{(0.346)^2}$	1.30 (crit ≈ 2.81)	Fail to Reject	0.061 (58 df, crit = 1.672)	0.952	Fail to Reject

APPENDIX H

2000/2001 Snow Profiles

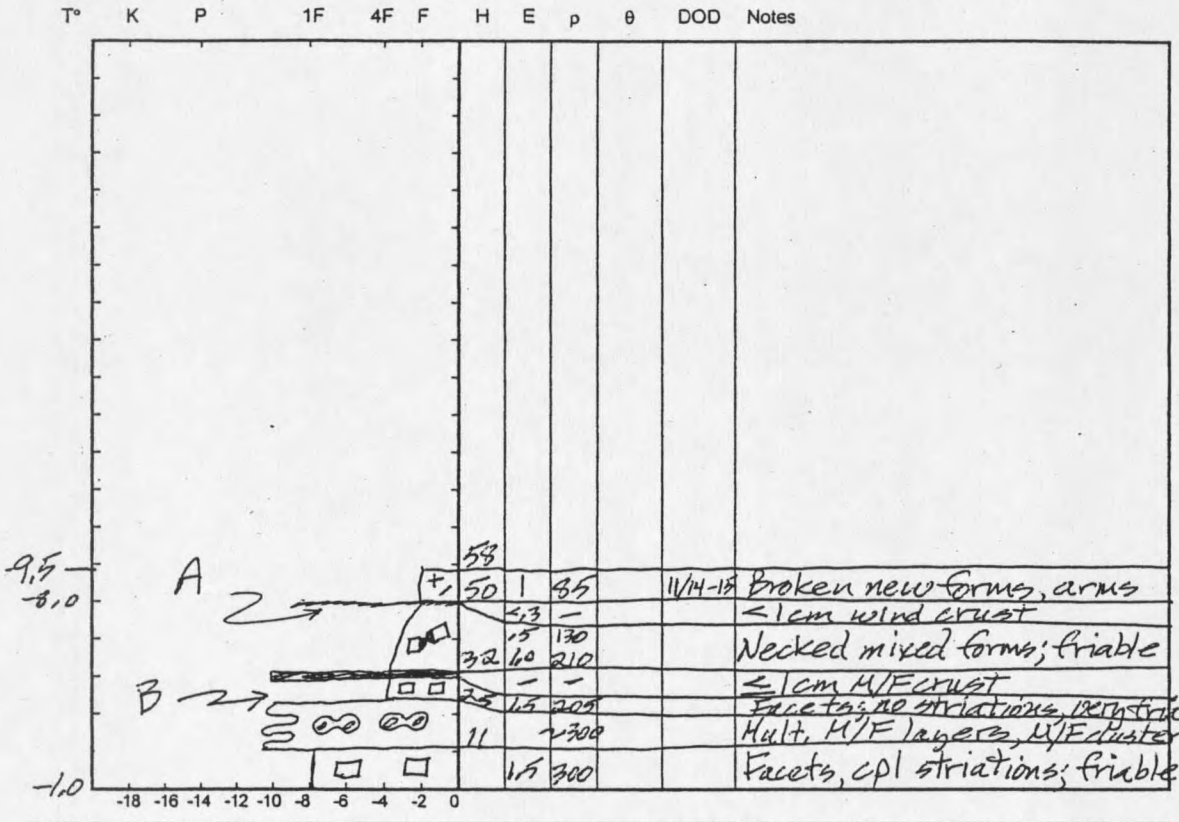
Observers: CL, KB, RS — Landry Bridger Range Research — Profile # 1

Time: 1200-1400 — **Snowpack Profile & QLCT** — Date: 11/15/00

Air T: -11 °C Sky: OVC Precip: S1 Wind: M Prior Pit: # —; —/—/—

Location: Bradley Mdw S.P. Elev. 7,600' Aspect: ENE Boot Pen: 40 cm ∠: 25°

Notes: Blustery day! Supai cold! Skinned from pipe gate.



Potential Slab				Weak Layer & Bed Surface							
Ref	$H_2O_{Nor} \div H_{Nor} = \rho_{kg}$	$\sin\angle \times H_{Nor} \times \rho \times 9.8 = \tau_{Slab}$	F	E	T_{WL}	S	C	SB	ρ_{wl}	ρ_{bed}
A	8 mm ÷ .075 m = 107	.423 x .075 x 107 x 9.8 = 33					V/3		130	130
B	41 mm ÷ .25 m = 164	.423 x .25 x 164 x 9.8 = 170					H/1.5	30/2	205	300

Slab notes:

Surface Mode QLCT w/ 0.08 m² plate

Ref	T1	T2	T3	T4	T5	T6	T7	T8	T9	T10	Avg_{Test}
A	2.3 kg	1.95 kg	2.5 kg	1.65 kg	1.6 kg	kg	kg	kg	kg	kg	2.0 kg

τ_{Test} 116 + τ_{Slab} 33 = 149 τ_{Total} x .771 C = 115 $\tau_{\infty} \div \tau_{Slab}$ 33 = 3.48 S_{QLCT}

Bench Mode QLCT w/ 0.04 m² plate

Ref	T1	T2	T3	T4	T5	T6	T7	T8	T9	T10	Avg_{Test}
B	9.0 kg	— kg	— kg	kg	kg	kg	kg	kg	kg	kg	— kg

τ_{Test} ____ = ____ τ_{Total} X ____ C = ____ $\tau_{\infty} \div \tau_{Slab}$ ____ = ____ S_{QLCT}

QLCT rig used (**check**): ☐ **0.04 m²** *or* ☐ **0.08 m²** *load plate, with* ☐ **0.5-5 kg** *or* ☐ **2-20 kg** *force gauge*

If Bench Mode: bench height (on pit face) above weak layer = 15 cm and plate setback = 10 cm for H_2O_{Col} = 16.5 mm

QLCT notes: Abandoned bench mode; column disintegrating

V. 10/15/00

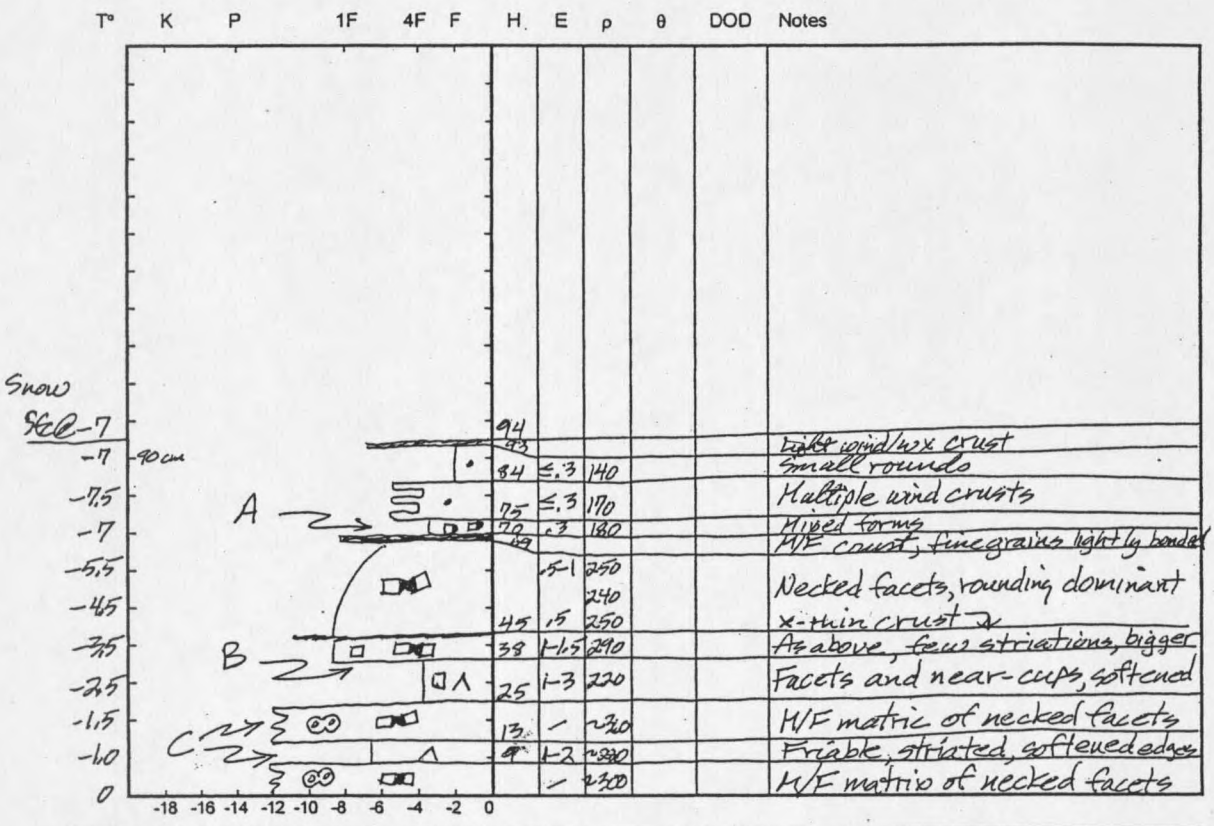
Observers: Landry+Lundy Landry Bridger Range Research Profile # 2

Time: 1100 **Snowpack Profile & QLCT** Date: 12/19/00

Air T: -4 °C Sky: OV Precip: Nil Wind: L/M, Var Prior Pit: # 1 ; 11/15/00

Location: BMSP Elev. 7,600 Aspect: ENE Boot Pen: 60 cm ∠: 24°

Notes:



Potential Slab						Weak Layer & Bed Surface							
Ref	H_2O_{Nor} ÷ H_{Nor} = ρ_{Hg}	Sin∠ x H_{Nor} x ρ x 9.8 = τ_{Slab}				F	E	T_{WL}	S	C	SB	ρ_{wl}	ρ_{bed}
A	28 mm ÷ .175m = 160	.407 x .175 x 160 x 9.8 = 112				◻	.3	-7		H/11		180	crust
B	120 mm ÷ .54 m = 222	.407 x .54 x 222 x 9.8 = 478				◻∧	1-3	-2.5		H/22		220	~360
Slab notes: C: 194mm÷.71m = 273 ...						=773 ∧	1-2	-1.5		H		~280	~360

Surface Mode QLCT

Ref	T1	T2	T3	T4	T5	T6	T7	T8	T9	T10	Avg_{Test}
A	19.6 kg	17.8 kg	19.8 kg	14.2 kg	16.2 kg	kg	kg	kg	kg	kg	17.5 kg

τ_{Test} 1616 + τ_{Slab} 112 = 1728 τ_{Total} x .667 C = 1152 τ_{∞} ÷ τ_{Slab} 112 = 10.29 S_{QLCT}

Bench Mode QLCT

Ref	T1	T2	T3	Avg B	Ref	T1	T2	T3	T4		Avg_{Test} C
B	17 kg	16.8 kg	15.5 kg	16.4 kg	C	14.4 kg	21.4 kg	23.8 kg	16.2 kg		18.95 kg

τ_{Test} 1628 = 1628 τ_{Total} x .678 C = 1103 τ_{∞} ÷ τ_{Slab} 478 = 2.31 S_{QLCT}

QLCT rig used (**check**): ☒ **0.04 m²** *or* ◻ **0.08 m²** *load plate, with* ◻ **0.5-5 kg** *or* ☒ **2-20 kg** *force gauge*

If Bench Mode: bench height (on pit face) above weak layer = 35 cm and plate setback = 13 cm for H_2O_{Col} = 67/103 mm

QLCT notes: We isolated "A" during surface mode tests, for practice. Layers B+C would alternate randomly during bench mode tests.

V. 10/15/00

C: τ_{Test} 1839 = 1839 τ_{Total} x .667 C = 1226 τ_{∞} ÷ τ_{Slab} 773 = 1.59 S_{QLCT}

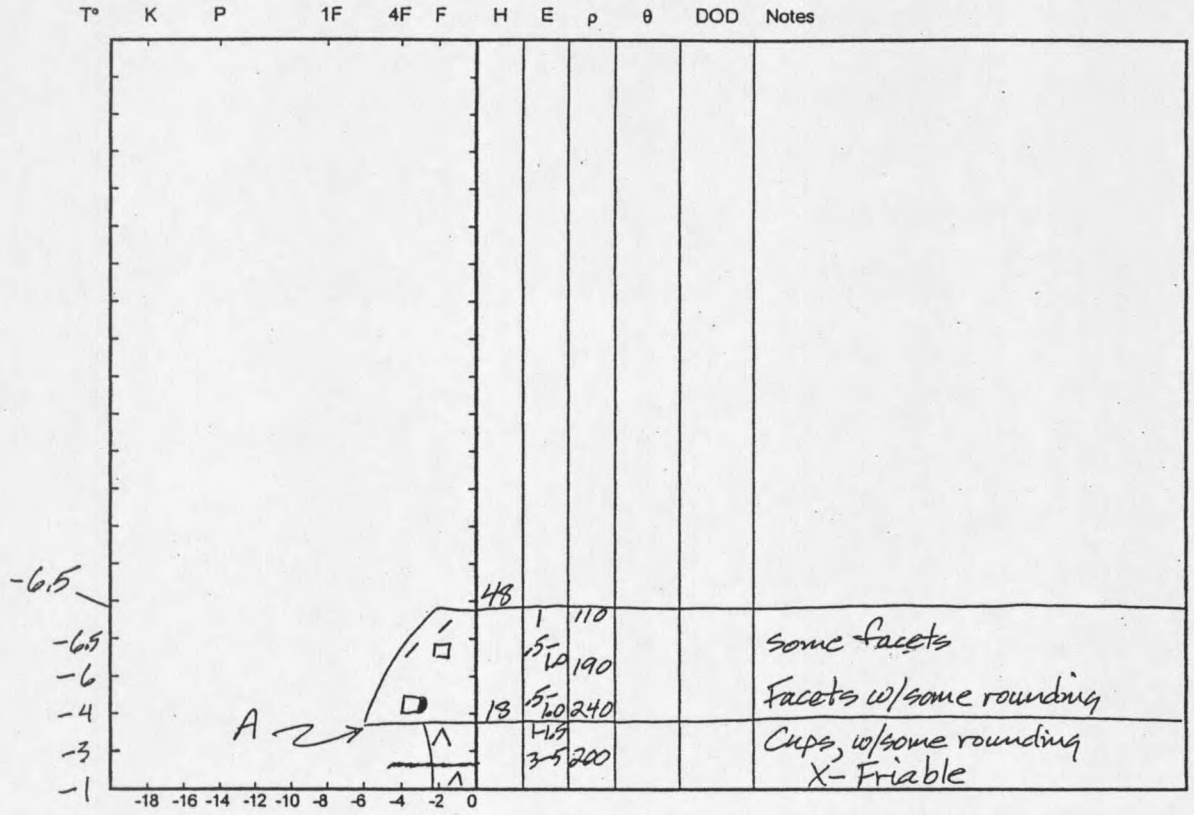
Observers: CL+KB | Landry Bridger Range Research | Profile # 4

Time: 1030 | **Snowpack Profile & QLCT** | Date: 1/3/01

Air T: 0 °C Sky: ① Precip: Nil Wind: Nil | Prior Pit: # —; —/—/—

Location: Bacon Rind Lower Glade Elev. 7,400 Aspect: ESE Boot Pen: 48 cm ∠: 32°

Notes: Location #2 of 30m x 30m layout



Potential Slab					Weak Layer & Bed Surface							
Ref	H_2O_{Nor} ÷ H_{Nor} = ρ_{kg}	Sin∠ x H_{Nor} x ρ x 9.8 = τ_{Slab}	F	E	T_{WL}	S	C	SB	ρ_{wl}	ρ_{bed}
A	47 mm ÷ .28 m = 168	0.53... x .28 x 166 x 9.8 = 244	∧	1-1.5	~3.5	E	E/9	10	200	200
B	mm ÷ m =	x x x 9.8 =								

Slab notes:

Surface Mode QLCT

Ref	T1	T2	T3	T4	T5	T6	T7	T8	T9	T10	Avg_{Test}
A	2.15 kg	5.9 kg	6.5 kg	5.85 kg	4.15 kg	8.6 kg	5.0 kg	5.1 kg	4.45 kg	4.85 kg	5.26 kg

τ_{Test} 317 + τ_{Slab} 244 = 561 τ_{Total} X 0.771 C = 433 τ_{co} ÷ τ_{Slab} 244 = 1.78 S_{QLCT}

Bench Mode QLCT

Ref	T1	T2	T3	T4	T5	T6	T7	T8	T9	T10	Avg_{Test}
	kg	kg	kg	kg	kg	kg	kg	kg	kg	kg	kg

τ_{Test} _____ = _____ τ_{Total} X _____ C = _____ τ_{co} ÷ τ_{Slab} _____ = _____ S_{QLCT}

QLCT rig used (**check**): ☐ **0.04 m²** *or* ☐ **0.08 m²** *load plate, with* ☐ **0.5-5 kg** *or* ☐ **2-20 kg** *force gauge*

If Bench Mode: bench height (on pit face) above weak layer = _____ cm and plate setback = _____ cm for H_2O_{Col} = _____ mm

QLCT notes:

V. 10/15/00

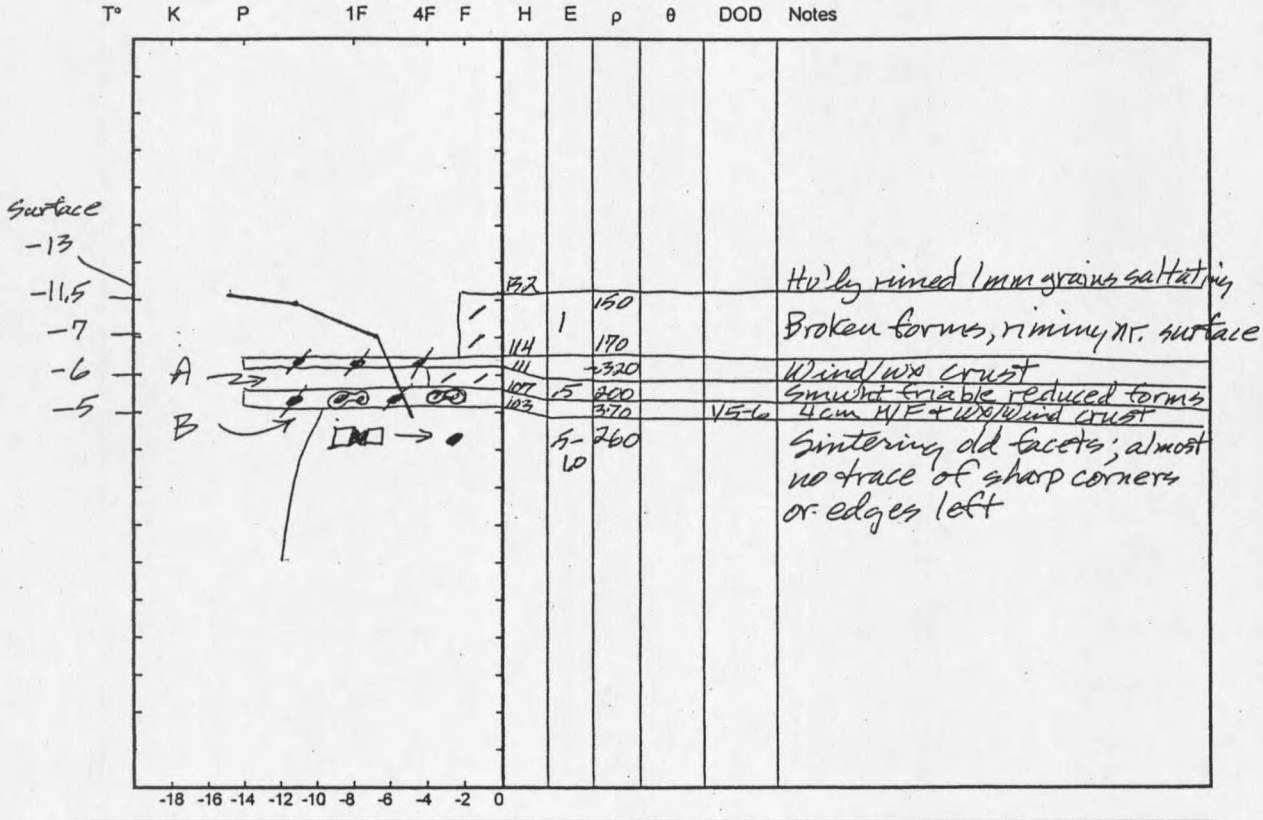
Observers: CL Bolo | Landry Bridger Range Research | Profile # 7

Time: 1430-1600 | **Snowpack Profile & QLCT** | Date: 1.20.01

Air T: -8 °C Sky: O Precip: Did Wind: M-Gusty Prior Pit: # 6; 1.17.01

Location: BMSP Elev. 7,600' Aspect: ENE Boot Pen: 45 cm ∠: 26°

Notes: Once again, BMSP getting strong gusts; significant SWE saltating



Potential Slab						Weak Layer & Bed Surface							
Ref	$H_2O_{Nor} \div H_{Nor} = \rho_{kg}$	$\sin\angle \times H_{Nor} \times \rho \times 9.8 = \tau_{Slab}$	F	E	T_{WL}	S	C	SB	ρ_{wl}	ρ_{bed}
A	37 mm ÷ .225 m = 164	.4384 x .225 x 164 x 9.8 = 158	1	.5	-6	E	PP/4		200	370
B	47 mm ÷ .26 m = 181	.4384 x .26 x 181 x 9.8 = 202	□●	.5-1	-5	E/M			260	260

Slab notes: "A" highly variable - recent during; "B" consistent, Q1 shears

Surface Mode QLCT

Ref	T1	T2	T3	T4	T5	T6	T7	T8	T9	T10	Avg_{Test}
B	18.6 kg	20.0 kg	22.0 kg	15.8 kg	23.2 kg	18.0 kg	20.6 kg	16.3 kg	17.3 kg	17.2 kg	18.9 kg

τ_{Test} 936 + τ_{Slab} 202 = 1138 τ_{Total} X .771 C = 877 $\tau_{\infty} \div \tau_{Slab}$ 202 = 4.34 S_{QLCT}

Bench Mode QLCT

Ref	T1	T2	T3	T4	T5	T6	T7	T8	T9	T10	Avg_{Test}
	kg	kg	kg	kg	kg	kg	kg	kg	kg	kg	kg

τ_{Test} _____ = _____ τ_{Total} X _____ C = _____ $\tau_{\infty} \div \tau_{Slab}$ _____ = _____ S_{QLCT}

QLCT rig used (**check**): ☐ **0.04 m²** *or* ☒ **0.08 m²** *load plate, with* ☐ **0.5-5 kg** *or* ☒ **2-20 kg** *force gauge*

If Bench Mode: bench height (on pit face) above weak layer = _____ cm and plate setback = _____ cm for H_2O_{Col} = _____ mm

QLCT notes: Substantial destruction of new slab required to get results in "B", sometimes necessitating re-positioning of plate

V. 10/15/00

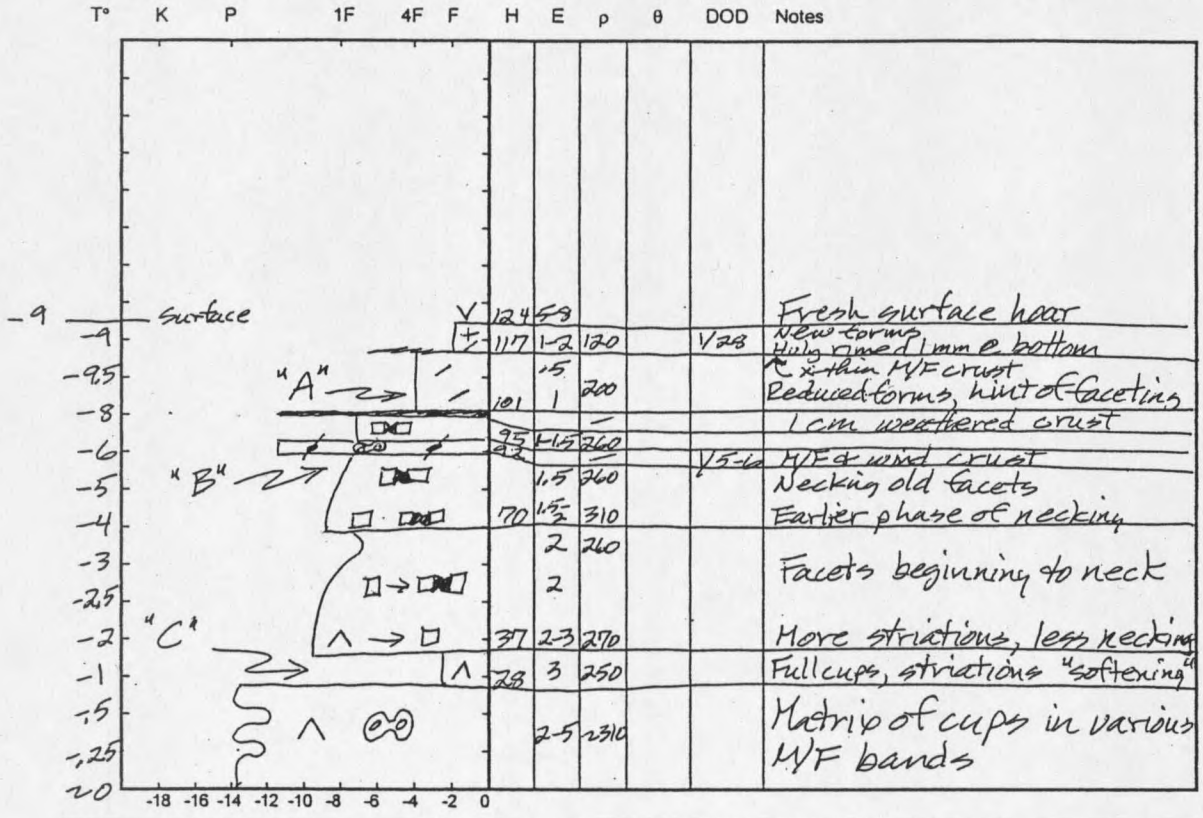
Observers: CL+JD | Landry Bridger Range Research | Profile # 9

Time: 1090 | **Snowpack Profile & QLCT** | Date: 1/27/01

Air T: -2 °C Sky: O Precip: Nil Wind: C/L | Prior Pit: # 8; 1/25/01

Location: Up+left BMSP Elev. 7640 Aspect: E Boot Pen: 45-80cm ∠: 29°

Notes: Located ~35m south and 5m west of BMSP ~~SW~~ SW corner



Potential Slab						Weak Layer & Bed Surface							
Ref	H_2O_{Nor} ÷ H_{Nor} = ρ_{kg}	Sin∠ x H_{Nor} x ρ x 9.8 = τ_{Slab}	F	E	T_{WL}	S	C	SB	ρ_{wl}	ρ_{bed}
A	34 mm ÷ .21 m = 162	.495 x .21 x 162 x 9.8 = 162	/		-8	E	M/4		200	~200
B	mm ÷ m =	x x x 9.8 =								

Slab notes: C: 202mm ÷ .81m = 249... = 956 ∧ 3 -1 2M 2M 250 ~310

Surface Mode QLCT

Ref	T1	T2	T3	T4	T5	T6	T7	T8✳	T9✳	T10✳	Avg_{Test}
A	15.2 kg	13.3 kg	11.2 kg	15.6 kg	14.8 kg	13.8 kg	14.8 kg	17.0 kg	13.8 kg	NR kg	14.4 kg

τ_{Test} 774 + τ_{Slab} 162 = 936 τ_{Total} X .771 C = 722 τ_{∞} ÷ τ_{Slab} 162 = 4.46 S_{QLCT}

Bench Mode QLCT – Rehearsal tests

Ref	T1	T2	T3	T4	T5	T6	T7	T8	T9	T10	Avg_{Test}
C	NR kg	NR kg	NR kg	kg	kg	kg	kg	kg	kg	kg	— kg

τ_{Test} ____ = ____ τ_{Total} X ____ C = ____ τ_{∞} ÷ τ_{Slab} ____ = ____ S_{QLCT}

QLCT rig used (**check**): ☐ **0.04 m²** *or* ☒ **0.08 m²** *load plate, with* ☐ **0.5-5 kg** *or* ☒ **2-20 kg** *force gauge*

If Bench Mode: bench height (on pit face) above weak layer = 60 cm and plate setback = 7 cm for H_2O_{Col} = 134.5 mm

QLCT notes: Tests 8 and 9 had simultaneous results in "A" + "C" slabs, and test 10 failed at "C" only. All "A" results Q2

V. 10/15/00

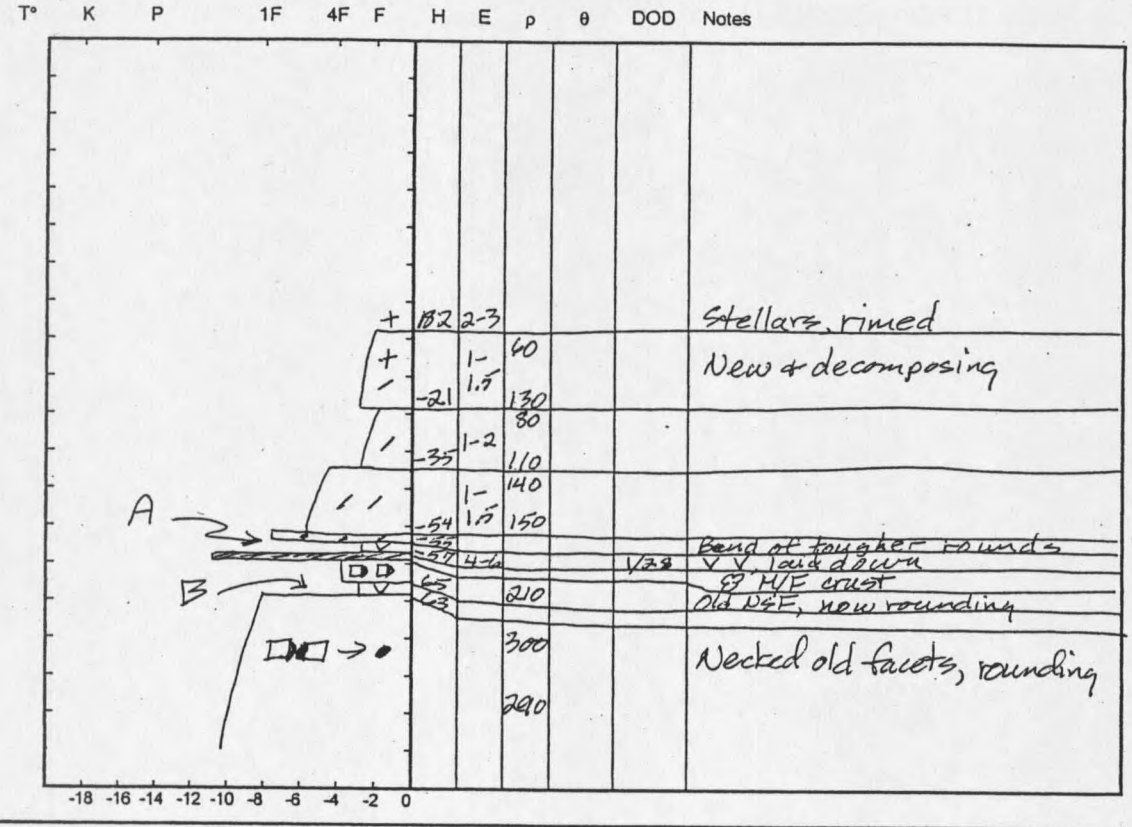
Observers: John Kelly + CL — Landry Bridger Range Research — Profile # 12

Time: 1130 — **Snowpack Profile & QLCT** — Date: 2/4/01

Air T: -8 °C Sky: ⊗ Precip: SI Wind: C/L Prior Pit: # —; —/—/—

Location: West of Round Hill Elev. 7,070' Aspect: SE Boot Pen: 40-50 cm ∠: 28°

Notes: Location #1 in 30m x 30m sampling trials



Potential Slab				Weak Layer & Bed Surface							
Ref	H_2O_{Nor} ÷ H_{Nor} = ρ_{kg}	Sin∠ x H_{Nor} x ρ x 9.8 = τ_{Slab}	F	E	T_{WL}	S	C	SB	ρ_{WL}	ρ_{bed}
A	58.5 mm ÷ 50 m = 117	.4695 x .50 x 117 x 9.8 = 269					H/11			
B	75 mm ÷ 60 m = 125	.4695 x .60 x 125 x 9.8 = 345								

Slab notes:

Surface Mode QLCT

Ref	T1	T2	T3	T4	T5	T6	T7	T8	T9	T10	Avg_{Test}
/	kg	kg	kg	kg	kg	kg	kg	kg	kg	kg	kg

τ_{Test} _____ + τ_{Slab} _____ = _____ τ_{Total} X _____ C = _____ τ_{∞} ÷ τ_{Slab} _____ = _____ S_{QLCT}

Bench Mode QLCT

Ref	T1*	T2	T3*	T4	T5	T6	T7	T8	T9	T10	Avg_{Test}
A	4.5 kg	6.5 kg	NR kg	5.2 kg	4.6 kg	4.7 kg	5.0 kg	4.5 kg	4.0 kg	2.8 kg	4.64 kg

τ_{Test} 573 = 573 τ_{Total} X .682 C = 391 τ_{∞} ÷ τ_{Slab} 269 = 1.45 S_{QLCT}

QLCT rig used (**check**): ☒ **0.04 m²** *or* ☐ **0.08 m²** *load plate, with* ☐ **0.5-5 kg** *or* ☒ **2-20 kg** *force gauge*

If Bench Mode: bench height (on pit face) above weak layer = 35 cm and plate setback = 7 cm for H_2O_{Col} = 33 mm

QLCT notes: On "B": T1, T3@4.0

V. 10/15/00

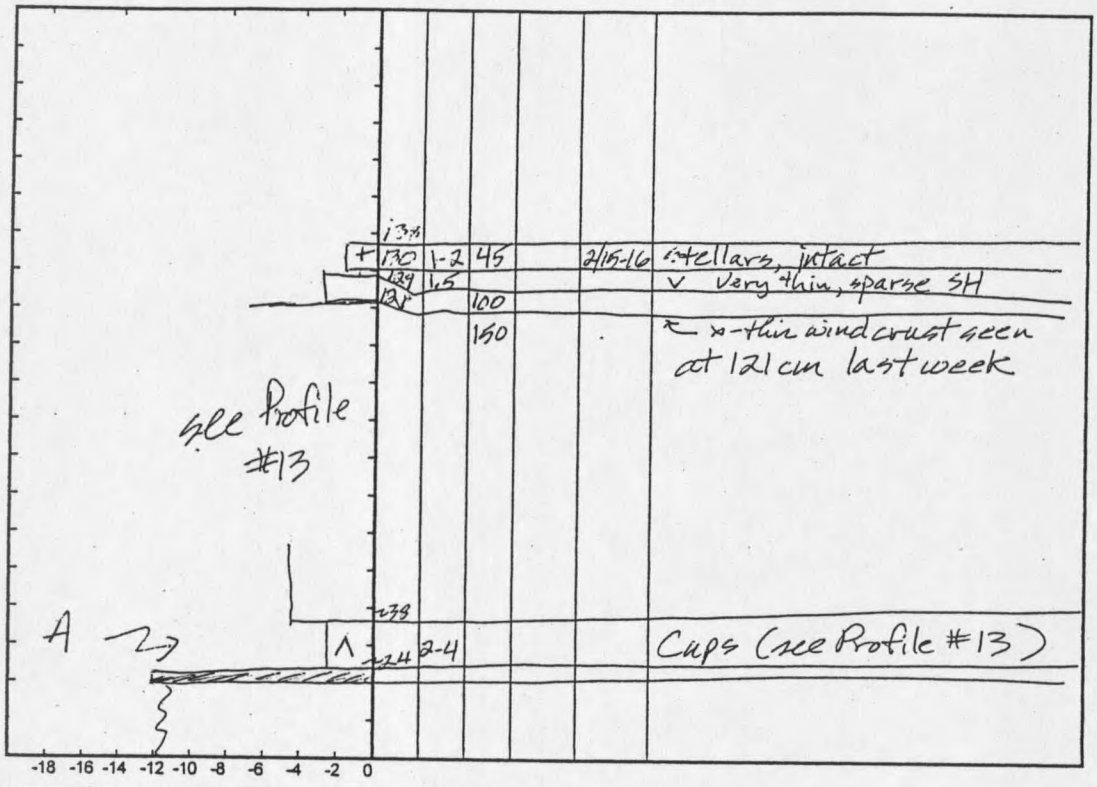
Observers: CL, CC, ZM | Landry Bridger Range Research | Profile # 14

Time: 0930-1300 | **Snowpack Profile & QLCT** | Date: 2/16/01

Air T: -5 °C Sky: ⊕ Precip: SF Wind: L Prior Pit: # 13; 1/09/01

Location: BM SP Elev. 9,600 Aspect: ENE Boot Pen: 91 cm ∠: 27°

Notes: This is a training session for Chas Day + Zach Mathews, and (*)



Potential Slab						Weak Layer & Bed Surface							
Ref	H_2O_{Nor} ÷ H_{Nor} = ρ_{kg}	Sin∠ x H_{Nor} x ρ x 9.8 = τ_{Slab}				F	E	T_{WL}	S	C	SB	ρ_{wl}	ρ_{bed}
A	190 mm ÷ .895m = 212	.454 x .895 x 212 x 9.8 = 844											
B	mm ÷ m =	x x x 9.8 =											
Slab notes:													

Surface Mode QLCT

Ref	T1	T2	T3	T4	T5	T6	T7	T8	T9	T10	Avg_{Test}
	kg	kg	kg	kg	kg	kg	kg	kg	kg	kg	kg

τ_{Test} ____ + τ_{Slab} ____ = ____ τ_{Total} X ____ C = ____ τ_{∞} ÷ τ_{Slab} ____ = ____ S_{QLCT}

Bench Mode QLCT

Ref	T1	T2	T3	T4	T5	T6	T7	T8	T9	T10	Avg_{Test}
A	13.9 kg	12.8 kg	13.3 kg	9.0 kg	15.0 kg	15.5 kg	12.5 kg	15.8 kg	12.3 kg	10.7 kg	kg

τ_{Test} 1901 = 1901 τ_{Total} X .681 C = 1295 τ_{∞} ÷ τ_{Slab} 844 = 1.53 S_{QLCT} *

QLCT rig used (**check**): ☒ **0.04 m²** *or* ☐ **0.08 m²** *load plate, with* ☐ **0.5-5 kg** *or* ☒ **2-20 kg** *force gauge*

If Bench Mode: bench height (on pit face) above weak layer = 70 cm and plate setback = 7 cm for H_2O_{Col} = 171.5 mm

QLCT notes: ~~*~~ SQLCT for Pit #13 = 1.47

V. 10/15/00

* to confirm deployment of data collection Rams Sunday

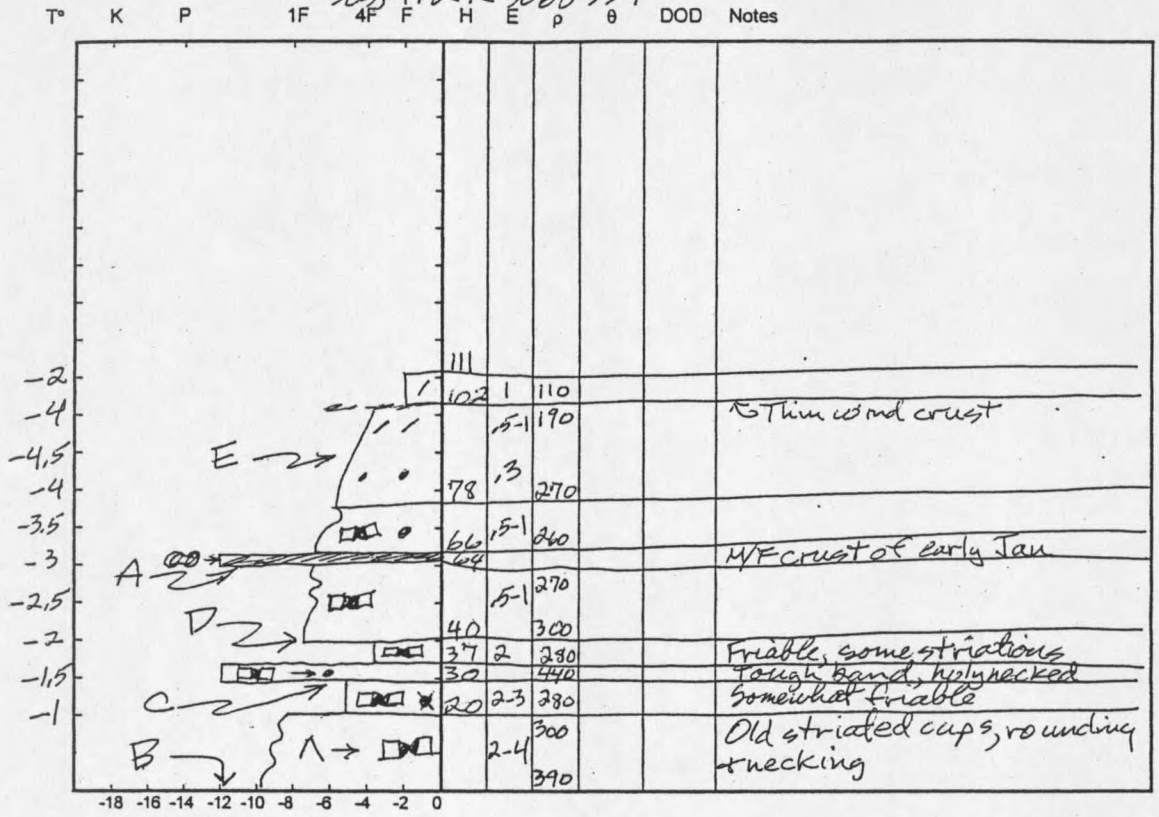
Observers: CL, SD, CL | Landry Bridger Range Research | Profile # 15

Time: 0845- | **Snowpack Profile & QLCT** | Date: 2/18/01

Air T: +1 °C Sky: ⌀ Precip: Nil Wind: L Prior Pit: # —; —/—/—

Location: Baldy Elev. 7,200 Aspect: ENE Boot Pen: 65 cm ∠: 25°

Notes: GPS: 12T 505,406 × 5065 364 at Pit (location #1)
505,412 × 5068 357



Potential Slab														Weak Layer & Bed Surface							
Ref	H_2O_{Nor} ÷ H_{Nor} = ρ_{kg}			Sin∠ x H_{Nor} x ρ x 9.8 = τ_{Slab}										F	E	T_{WL}	S	C	SB	ρ_{wl}	ρ_{bed}
A	mm ÷ m =			x x x 9.8 =																	
B	mm ÷ m =			x x x 9.8 =																	
Slab notes:																					

Surface Mode QLCT											
Ref	T1	T2	T3	T4	T5	T6	T7	T8	T9	T10	Avg_{Test}
	kg	kg	kg	kg	kg	kg	kg	kg	kg	kg	kg
τ_{Test} _____ + τ_{Slab} _____ = _____ τ_{Total} X _____ C = _____ τ_{∞} ÷ τ_{Slab} _____ = _____ S_{QLCT}											

Bench Mode QLCT											
Ref	T1	T2	T3	T4	T5	T6	T7	T8	T9	T10	Avg_{Test}
	kg	kg	kg	kg	kg	kg	kg	kg	kg	kg	kg
τ_{Test} _____ = _____ τ_{Total} X _____ C = _____ τ_{∞} ÷ τ_{Slab} _____ = _____ S_{QLCT}											

QLCT rig used (check): ☐ 0.04 m² or ☐ 0.08 m² load plate, with ☐ 0.5-5 kg or ☐ 2-20 kg force gauge

If Bench Mode: bench height (on pit face) above weak layer = _____ cm and plate setback = _____ cm for H_2O_{Col} = _____ mm

QLCT notes:

V. 10/15/00

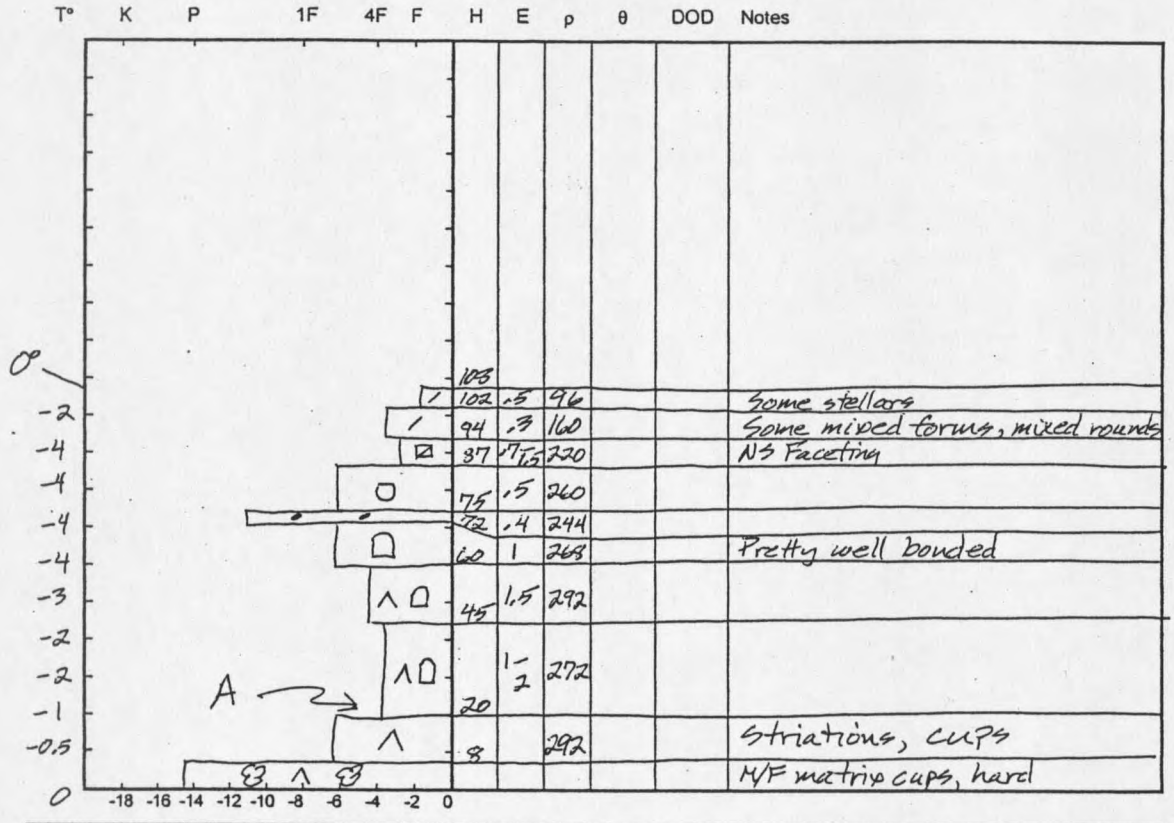
Observers: KB, DC, ZM — Landry Bridger Range Research — Profile # 16

Time: 0915 — **Snowpack Profile & QLCT** — Date: 2/18/01

Air T: 1 °C Sky: OC Precip: Nil Wind: LxS/y Prior Pit: # —; —/—/—

Location: Saddle Peak Study Plot Elev. 7,350 Aspect: E Boot Pen: 100 cm ∠: 26°

Notes:



Potential Slab									Weak Layer & Bed Surface							
Ref	H_2O_{Nor} ÷ H_{Nor} = ρ_{kg}	Sin∠ x H_{Nor} x ρ x 9.8 = τ_{Slab}							F	E	T_{WL}	S	C	SB	ρ_w	ρ_{bed}
A	159 mm ÷ 777 m = 205	.433 x .777 x 205 x 9.8 = 679							∧□	1-2	-1		H/20		272	292
B	mm ÷ m =	x x x 9.8 =											H/23			

Slab notes:

Surface Mode QLCT

Ref	T1	T2	T3	T4	T5	T6	T7	T8	T9	T10	Avg_{Test}
	kg	kg	kg	kg	kg	kg	kg	kg	kg	kg	kg

τ_{Test} _____ + τ_{Slab} _____ = _____ τ_{Total} X _____ C = _____ τ_{∞} ÷ τ_{Slab} _____ = _____ S_{QLCT}

Bench Mode QLCT

Ref	T1	T2	T3	T4	T5	T6	T7	T8	T9	T10	Avg_{Test}
	kg	kg	kg	kg	kg	kg	kg	kg	kg	kg	kg

τ_{Test} _____ = _____ τ_{Total} X _____ C = _____ τ_{∞} ÷ τ_{Slab} _____ = _____ S_{QLCT}

QLCT rig used (**check**): ☐ **0.04 m²** *or* ☐ **0.08 m²** *load plate, with* ☐ **0.5-5 kg** *or* ☐ **2-20 kg** *force gauge*

If Bench Mode: bench height (on pit face) above weak layer = _____ cm and plate setback = _____ cm for H_2O_{Col} = _____ mm

QLCT notes:

V. 10/15/00

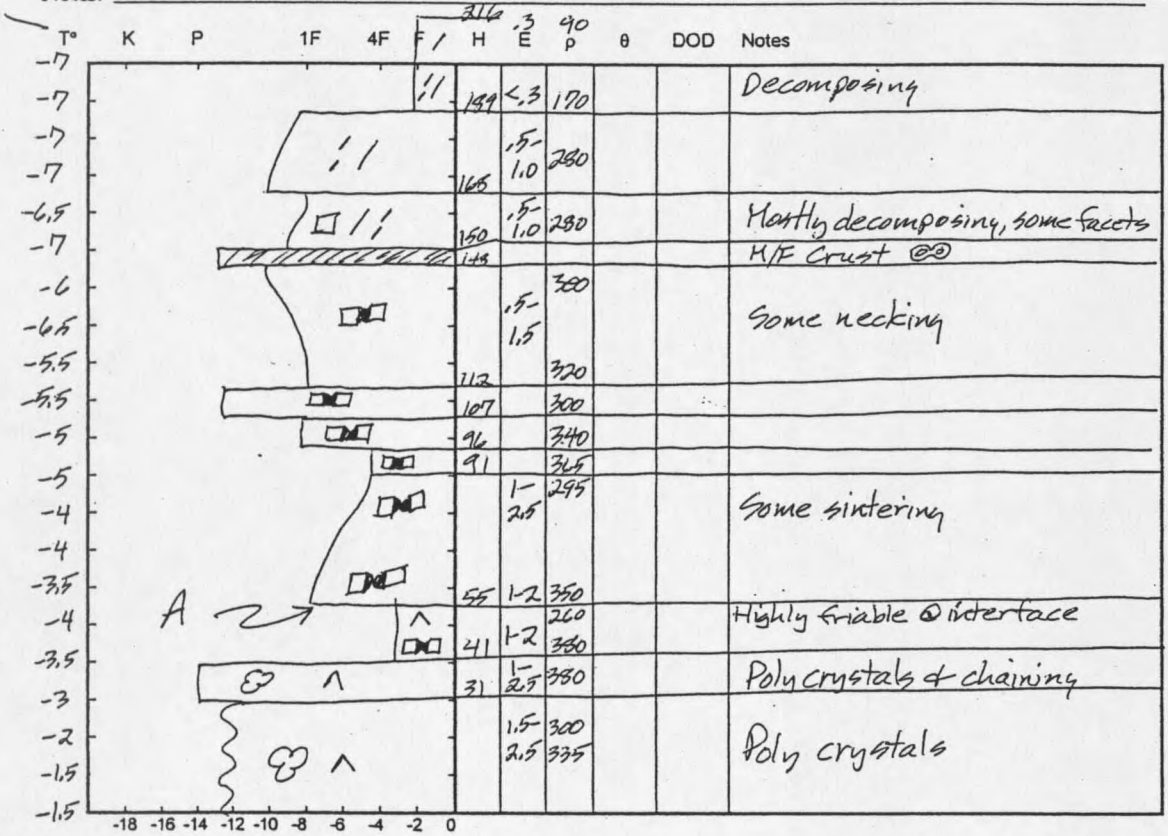
Observers: JD, JR, MS | Landry Bridger Range Research | Profile # 17

Time: 0915 | **Snowpack Profile & QLCT** | Date: 2/18/01

Air T: -3 °C | Sky: ① | Precip: Nil | Wind: L | Prior Pit: # 14 ; 2/16/01

Location: Bradley Meadow Study Plot | Elev. 7,600 | Aspect: ENE | Boot Pen: 35 cm | ∠: 30°

Notes:



Potential Slab						Weak Layer & Bed Surface							
Ref	H_2O_{Nor} ÷ H_{Nor} = ρ_{kg}	Sin∠ x H_{Nor} x ρ x 9.8 = τ_{Slab}	F	E	T_{WL}	S	C	SB	ρ_w	ρ_{bed}
A	477 mm ÷ 1.39 m = 343	.50 x 1.39 x 343 x 9.8 = 2,336	∧	1-2	-4		4/25		260	380
B	mm ÷ m =	x x x 9.8 =								

Slab notes:

Surface Mode QLCT

Ref	T1	T2	T3	T4	T5	T6	T7	T8	T9	T10	Avg_{Test}
	kg	kg	kg	kg	kg	kg	kg	kg	kg	kg	kg

τ_{Test} _____ + τ_{Slab} _____ = _____ τ_{Total} X _____ C = _____ τ_{co} ÷ τ_{Slab} _____ = _____ S_{QLCT}

Bench Mode QLCT

Ref	T1	T2	T3	T4	T5	T6	T7	T8	T9	T10	Avg_{Test}
	kg	kg	kg	kg	kg	kg	kg	kg	kg	kg	kg

τ_{Test} _____ = _____ τ_{Total} X _____ C = _____ τ_{co} ÷ τ_{Slab} _____ = _____ S_{QLCT}

QLCT rig used (**check**): ☐ **0.04 m²** *or* ☐ **0.08 m²** *load plate, with* ☐ **0.5-5 kg** *or* ☐ **2-20 kg** *force gauge*

If Bench Mode: bench height (on pit face) above weak layer = _____ cm and plate setback = _____ cm for H_2O_{Col} = _____ mm

QLCT notes:

V. 10/15/00

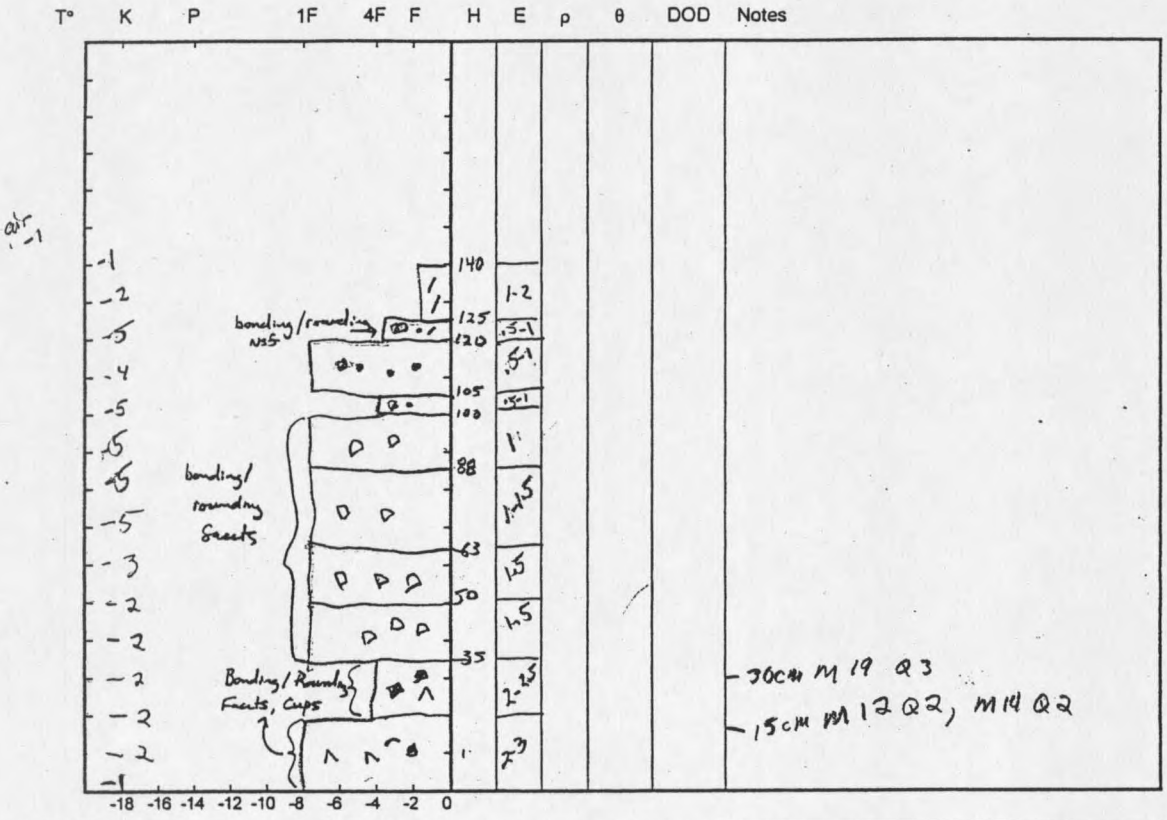
Observers: RJ, LR, CD | Landry Bridger Range Research | Profile # 18

Time: 0930 | **Snowpack Profile & QLCT** | Date: 02 / 18 / 2001

Air T: -1 °C Sky: O Precip: N/L Wind: CALM Prior Pit: # ____; ___/___/___

Location: Flt#1/ 12TWR 03426/83492 Elev. 2305 m Aspect: 62° Boot Pen: 52 cm ∠: 30°

Notes: _____



Potential Slab									Weak Layer & Bed Surface							
Ref	H_2O_{Nor} ÷ H_{Nor} = ρ_{kg}	Sin∠ x H_{Nor} x ρ x 9.8 = τ_{Slab}							F	E	T_{WL}	S	C	SB	ρ_{wl}	ρ_{bed}
A	mm ÷ m =	x x x 9.8 =														
B	mm ÷ m =	x x x 9.8 =														
Slab notes:																

Surface Mode QLCT											
Ref	T1	T2	T3	T4	T5	T6	T7	T8	T9	T10	Avg_{Test}
	kg	kg	kg	kg	kg	kg	kg	kg	kg	kg	kg
τ_{Test} _____ + τ_{Slab} _____ = _____ τ_{Total} X _____ C = _____ τ_{∞} ÷ τ_{Slab} _____ = _____ S_{QLCT}											

Bench Mode QLCT											
Ref	T1	T2	T3	T4	T5	T6	T7	T8	T9	T10	Avg_{Test}
	kg	kg	kg	kg	kg	kg	kg	kg	kg	kg	kg
τ_{Test} _____ = _____ τ_{Total} X _____ C = _____ τ_{∞} ÷ τ_{Slab} _____ = _____ S_{QLCT}											

*QLCT rig used (**check**):* ☐ **0.04 m²** *or* ☐ **0.08 m²** *load plate, with* ☐ **0.5-5 kg** *or* ☐ **2-20 kg** *force gauge*

If Bench Mode: bench height (on pit face) above weak layer = _____ cm and plate setback = _____ cm for H_2O_{Col} = _____ mm

QLCT notes:

V. 10/15/00

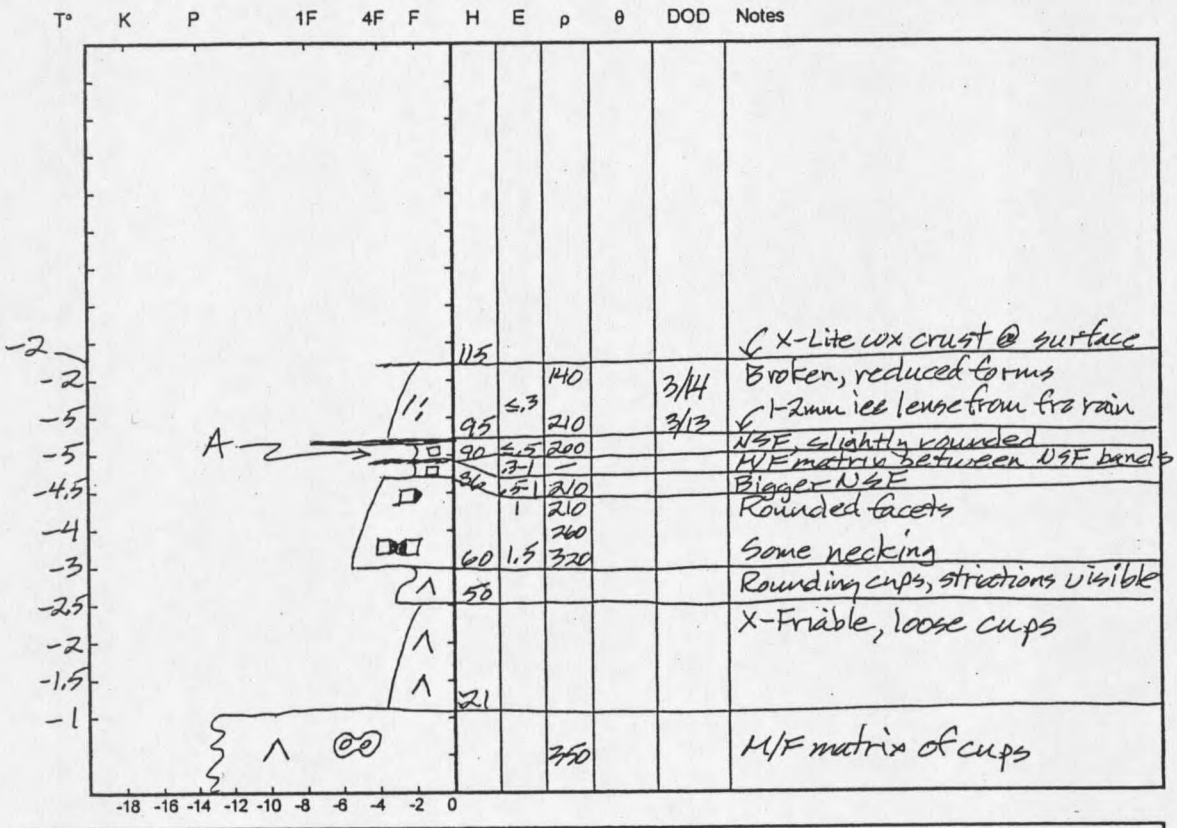
Observers: CL(RT), KB, DM Landry Bridger Range Research Profile # 19

Time: 1100 **Snowpack Profile & QLCT** Date: 3/17/01

Air T: -2 °C Sky: ⓓ Precip: Dil Wind: L/M Prior Pit: # 14; 2/16/01

Location: Bradley Meadow N Elev. 7,650 Aspect: ENE Boot Pen: ____ cm ∠: 25°

Notes: Loc #1 in 30m x 30m plot grid, located NW of NW corner of BMSP



Potential Slab						Weak Layer & Bed Surface							
Ref	H_2O_{Nor} ÷ H_{Nor} = ρ_{kg}	Sin∠ x H_{Nor} x ρ x 9.8 = τ_{Slab}				F	E	T_{WL}	S	C	SB	ρ_{wl}	ρ_{bed}
A	33 mm ÷ .20 m = 165	.423 x .20 x 165 x 9.8 = 137				□	≤.5	~.5		E/I		200	
B	mm ÷ m =	x x x 9.8 =											

Slab notes: A @ ~1cm below rain crust in subtle texture change w/in facets

Surface Mode QLCT

Ref	T1	T2	T3	T4	T5	T6	T7	T8	T9	T10	Avg_{Test}
A	4.5 kg	4.9 kg	4.5 kg	NP kg	4.3 kg	14.5 kg	9.7 kg	8.0 kg	8.3 kg	6.0 kg	7.24 kg

τ_{Test} 363 + τ_{Slab} 137 = 500 τ_{Total} X .771 C = 386 τ_{∞} ÷ τ_{Slab} 137 = 2.82 S_{QLCT}

Bench Mode QLCT

Ref	T1	T2	T3	T4	T5	T6	T7	T8	T9	T10	Avg_{Test}
	kg	kg	kg	kg	kg	kg	kg	kg	kg	kg	kg

τ_{Test} ____ = ____ τ_{Total} X ____ C = ____ τ_{∞} ÷ τ_{Slab} ____ = ____ S_{QLCT}

QLCT rig used (**check**): □ **0.04 m²** or ☒ **0.08 m²** load plate, with □ **0.5-5 kg** or ☒ **2-20 kg** force gauge

If Bench Mode: bench height (on pit face) above weak layer = ____ cm and plate setback = ____ cm for H_2O_{Col} = ____ mm

QLCT notes: Very delicate cutting required to not tear the ice lense and/or disturb the weak layer

V. 10/15/00

APPENDIX I

2001/2002 Snow Profiles

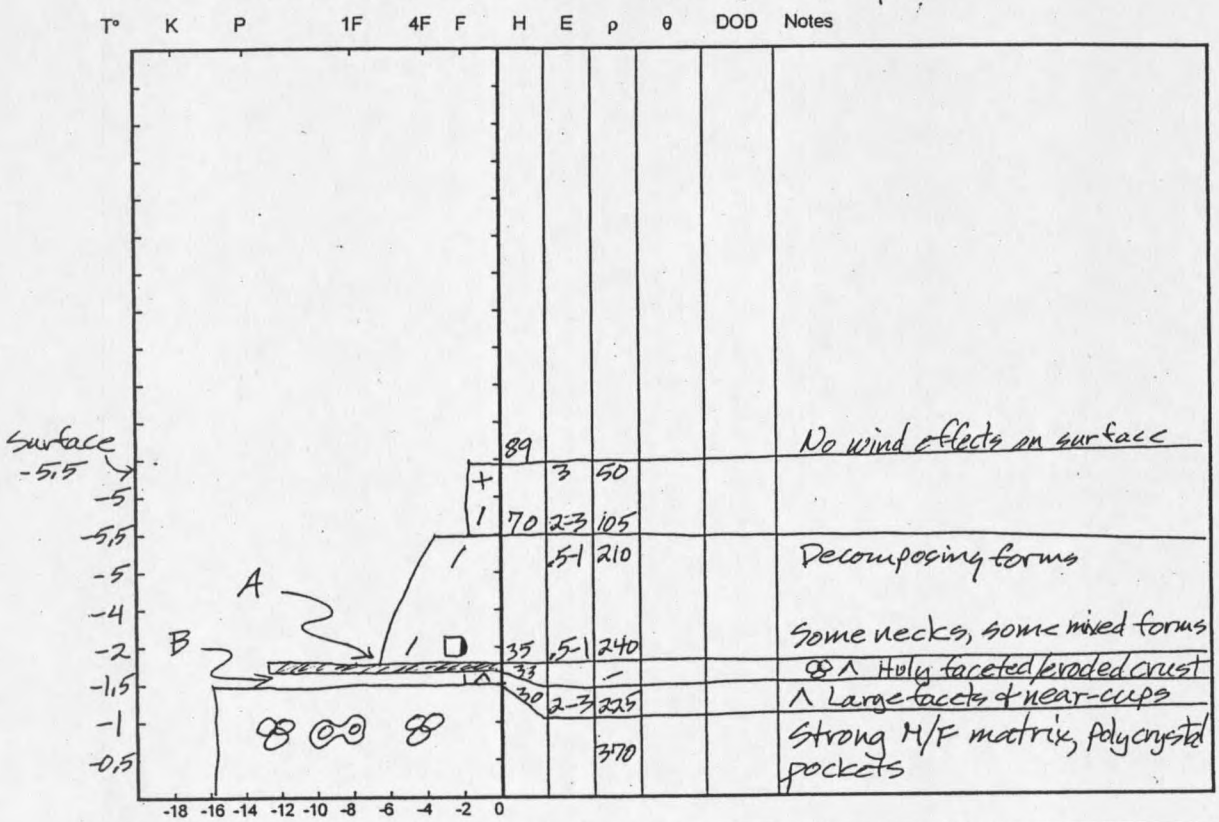
Observers: CL+KB | Landry Bridger Range Research | Profile # 2

Time: 11:15 | **Snowpack Profile & QLCT** | Date: 12/7/01

Air T: -9 °C Sky: ① Precip: S½ Wind: L Prior Pit: # —; —/—/—

Location: Spanky's - Elev. 9,000' Aspect: E Boot Pen: 51 cm ∠: 28°

Notes: Location #1 in 30m x 30m stability sampling plot



Potential Slab								Weak Layer & Bed Surface							
Ref	H_2O_{Nor} ÷ H_{Nor} = ρ_{kg}	Sin∠ x H_{Nor} x ρ x 9.8 = τ_{Slab}						F	E	T_{WL}	S	C	SB	ρ_{wl}	ρ_{bed}
A	70 mm ÷ .505m = 139	.469 x .505 x 139 x 9.8 = 323						/ □	.5-1		E	M/G		240	—
B	82 mm ÷ .535m = 153	.469 x .535 x 153 x 9.8 = 377						∧	2-3	-1.5	E			225	370
Slab notes:															

Surface Mode QLCT

Ref	T1	T2	T3	T4	T5	T6	T7	T8	T9	T10	Avg_{Test}
A	(B) kg	(B) kg	9.3 kg	9.3 kg	8.4 kg	12.3 kg	9.2 kg	6.5 kg	16.9 kg	(B) kg	10.27 kg

τ_{Test} 547 + τ_{Slab} 323 = 370 τ_{Total} x .771 C = 1.71 τ_{oo} ÷ τ_{Slab} 323 = 2.08 S_{QLCT}

Bench Mode QLCT

Ref	T1	T2	T3	T4	T5	T6	T7	T8	T9	T10	Avg_{Test}
	kg	kg	kg	kg	kg	kg	kg	kg	kg	kg	kg

τ_{Test} _____ = _____ τ_{Total} X _____ C = _____ τ_{oo} ÷ τ_{Slab} _____ = _____ S_{QLCT}

QLCT rig used (**check**): □ **0.04 m²** *or* ☒ **0.08 m²** *load plate, with* □ **0.5-5 kg** *or* ☒ **2-20 kg** *force gauge*

If Bench Mode: bench height (on pit face) above weak layer = _____ cm and plate setback = _____ cm for H_2O_{Col} = _____ mm

QLCT notes:

V. 10/15/00

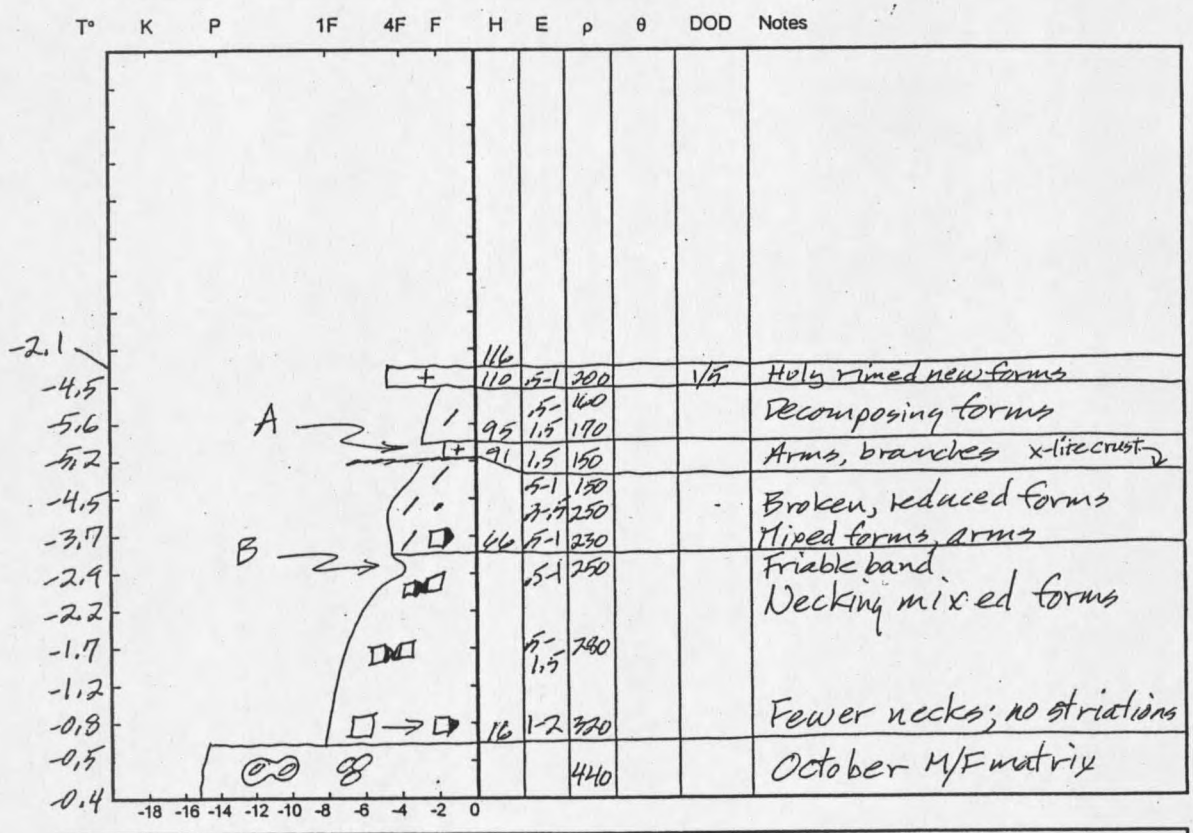
Observers: CL | Landry Bridger Range Research | Profile # 7

Time: 0930 | **Snowpack Profile & QLCT** | Date: 1/6/02

Air T: -25 °C Sky: CD Precip: Nil Wind: Lt/Gusty Prior Pit: # 3; 12/10/01

Location: Bradley Ridge Study Plot Elev. 7,650 Aspect: ENE Boot Pen: 85 cm ∠: 28°

Notes:



Potential Slab					Weak Layer & Bed Surface							
Ref	H_2O_{Nor} ÷ H_{Nor} = ρ_{Hg}	Sin∠ x H_{Nor} x ρ x 9.8 = τ_{Slab}			F	E	T_{WL}	S	C	SB	ρ_{wl}	ρ_{bed}
A	35 mm ÷ .22 m = 159	.469 x .22 x 159 x 9.8 = 161			+	1.5	-5.2	M	11/07		150	150
B	83 mm ÷ .45 m = 184	.469 x .45 x 184 x 9.8 = 381			▭	.5-1	-2.9	M	22/23		250	250

Slab notes:

Surface Mode QLCT

Ref	T1	T2	T3	T4	T5	T6	T7	T8	T9	T10	Avg_{Test}
A	NR kg	NR kg	NR kg	kg	kg	kg	kg	kg	kg	kg	kg

τ_{Test} _____ + τ_{Slab} _____ = _____ τ_{Total} X _____ C = _____ τ_{∞} ÷ τ_{Slab} _____ = _____ S_{QLCT}

Bench Mode QLCT

Ref	T1	T2	T3	T4	T5	T6	T7	T8	T9	T10	Avg_{Test}
	kg	kg	kg	kg	kg	kg	kg	kg	kg	kg	kg

τ_{Test} _____ = _____ τ_{Total} X _____ C = _____ τ_{∞} ÷ τ_{Slab} _____ = _____ S_{QLCT}

QLCT rig used (**check**): ☐ **0.04 m²** *or* ☒ **0.08 m²** *load plate, with* ☐ **0.5-5 kg** *or* ☒ **2-20 kg** *force gauge*

If Bench Mode: bench height (on pit face) above weak layer = _____ cm and plate setback = _____ cm for H_2O_{Col} = _____ mm

QLCT notes: T1: Q3@A; T2: 7.5 kg@110cm, Q3@A; T3: Q3@A@15kg

V. 10/15/00

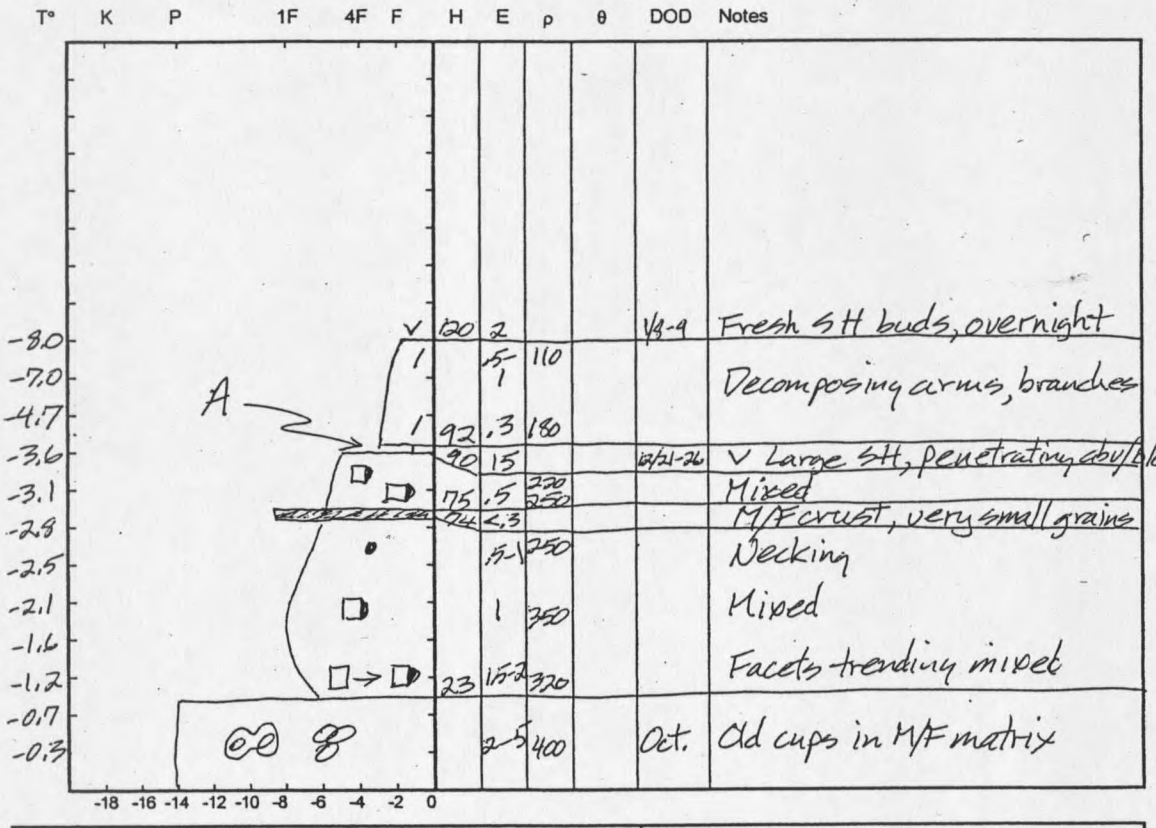
Observers: CL, ZH, RS | Landry Bridger Range Research | Profile # 9

Time: 1045 | **Snowpack Profile & QLCT** | Date: 1/9/02

Air T: -8 °C Sky: O Precip: Nil Wind: Nil | Prior Pit: # 8 ; 1/8/02

Location: Nr. "Ski Hill", Lionhead Elev. 8,000 Aspect: NE Boot Pen: 60 cm ∠: 26°

Notes: This is Location #1 in the 900 m² plot



Potential Slab						Weak Layer & Bed Surface							
Ref	H_2O_{Nor} ÷ H_{Nor} = ρ_{kg}	Sin∠ x H_{Nor} x ρ x 9.8 = τ_{Slab}	F	E	T_{WL}	S	C	SB	ρ_{wl}	ρ_{bed}
A	35 mm ÷ .25 m = 140	.4334 x .25 x 140 x 9.8 = 150	V	15	-3.6		2/21		—	220
B	mm ÷ m =	x x x 9.8 =								

Slab notes:

Surface Mode QLCT

Ref	T1	T2	T3	T4	T5	T6	T7	T8	T9	T10	Avg_{Test}
A	6.4 kg	6.6 kg	5.8 kg	7.1 kg	5.8 kg	6.7 kg	6.9 kg	6.4 kg	6.2 kg	5.1 kg	6.3 kg

τ_{Test} 328 + τ_{Slab} 150 = 478 τ_{Total} X .771 C = 369 τ_{∞} ÷ τ_{Slab} 150 = 2.46 S_{QLCT}

Bench Mode QLCT

Ref	T1	T2	T3	T4	T5	T6	T7	T8	T9	T10	Avg_{Test}
	kg	kg	kg	kg	kg	kg	kg	kg	kg	kg	kg

τ_{Test} _____ = _____ τ_{Total} X _____ C = _____ τ_{∞} ÷ τ_{Slab} _____ = _____ S_{QLCT}

QLCT rig used (**check**): ☐ **0.04 m²** *or* ☒ **0.08 m²** *load plate, with* ☐ **0.5-5 kg** *or* ☒ **2-20 kg** *force gauge*

If Bench Mode: bench height (on pit face) above weak layer = _____ cm and plate setback = _____ cm for H_2O_{Col} = _____ mm

QLCT notes: All Q1 shears.

V. 10/15/00

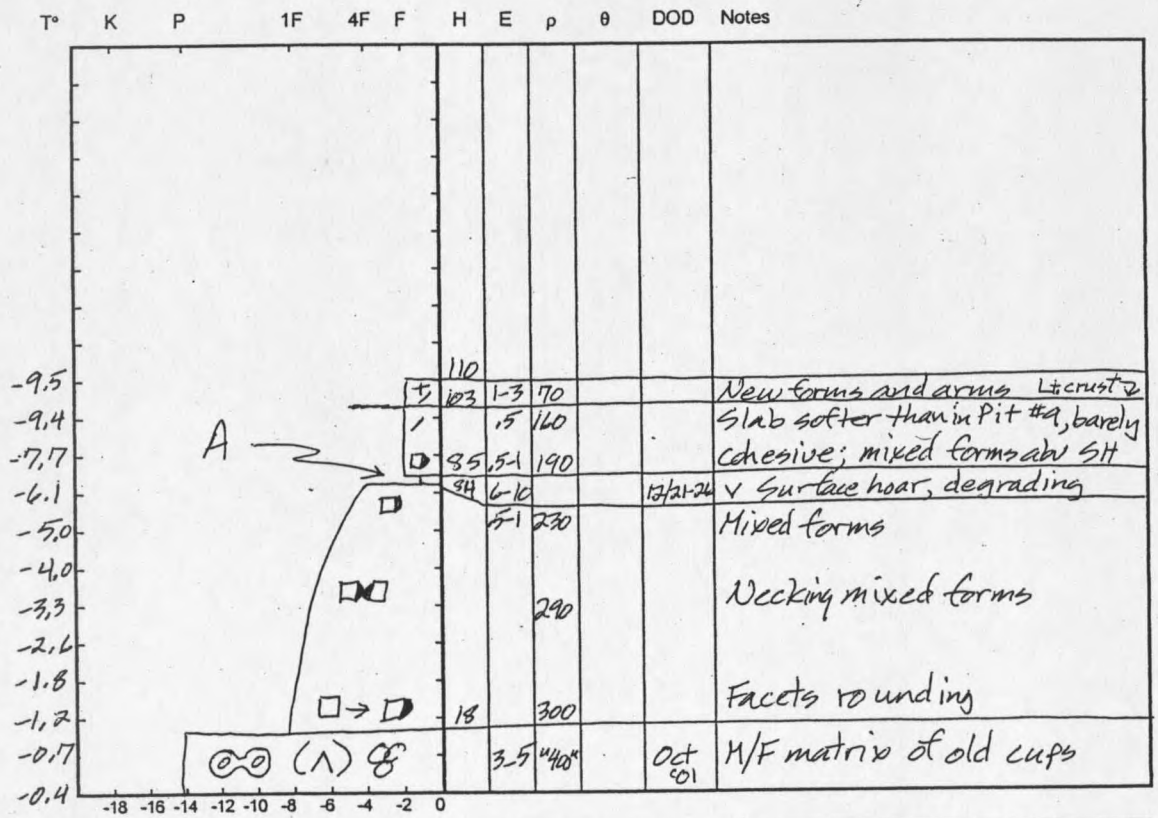
Observers: CL+JD | Landry Bridger Range Research | Profile # 10

Time: 1015 | **Snowpack Profile & QLCT** | Date: 1/15/02

Air T: -11.5°C Sky: O Precip: Nil-SI Wind: Nil-Lt | Prior Pit: # 9 ; 1/9/02

Location: Nr "Ski Hill", Lionhead Elev. 8,000 Aspect: NE Boot Pen: 55 cm ∠: 27°

Notes:



Potential Slab							Weak Layer & Bed Surface							
Ref	H_2O_{Nor} ÷ H_{Nor} = ρ_{rg}	Sin∠ x H_{Nor} x ρ x 9.8 = τ_{Slab}					F	E	T_{WL}	S	C	SB	ρ_{wl}	ρ_{bed}
A	317 mm ÷ 269 m = 138	.4540 x 268 x 138 x 9.8 = 165					V	6-10	~1.5		12/02			230
B	mm ÷ m =	x x x 9.8 =												

Slab notes:

Surface Mode QLCT

Ref	T1	T2	T3	T4	T5	T6	T7	T8	T9	T10	Avg_{Test}
A	3.9 kg	9.4 kg	7.4 kg	9.0 kg	6.9 kg	8.3 kg	9.7 kg	9.7 kg	8.5 kg	10.3 kg	8.91 kg

τ_{Test} 466 + τ_{Slab} 165 = 631 τ_{Total} X .771 C = 486.5 τ_{co} ÷ τ_{Slab} 165 = 2.95 S_{QLCT}

Bench Mode QLCT

Ref	T1	T2	T3	T4	T5	T6	T7	T8	T9	T10	Avg_{Test}
	kg	kg	kg	kg	kg	kg	kg	kg	kg	kg	kg

τ_{Test} _____ = _____ τ_{Total} X _____ C = _____ τ_{co} ÷ τ_{Slab} _____ = _____ S_{QLCT}

QLCT rig used (**check**): ☐ **0.04 m²** or ☒ **0.08 m²** *load plate, with* ☐ **0.5-5 kg** or ☒ **2-20 kg** *force gauge*

If Bench Mode: bench height (on pit face) above weak layer = _____ cm and plate setback = _____ cm for H_2O_{Col} = _____ mm

QLCT notes:

V. 10/15/00

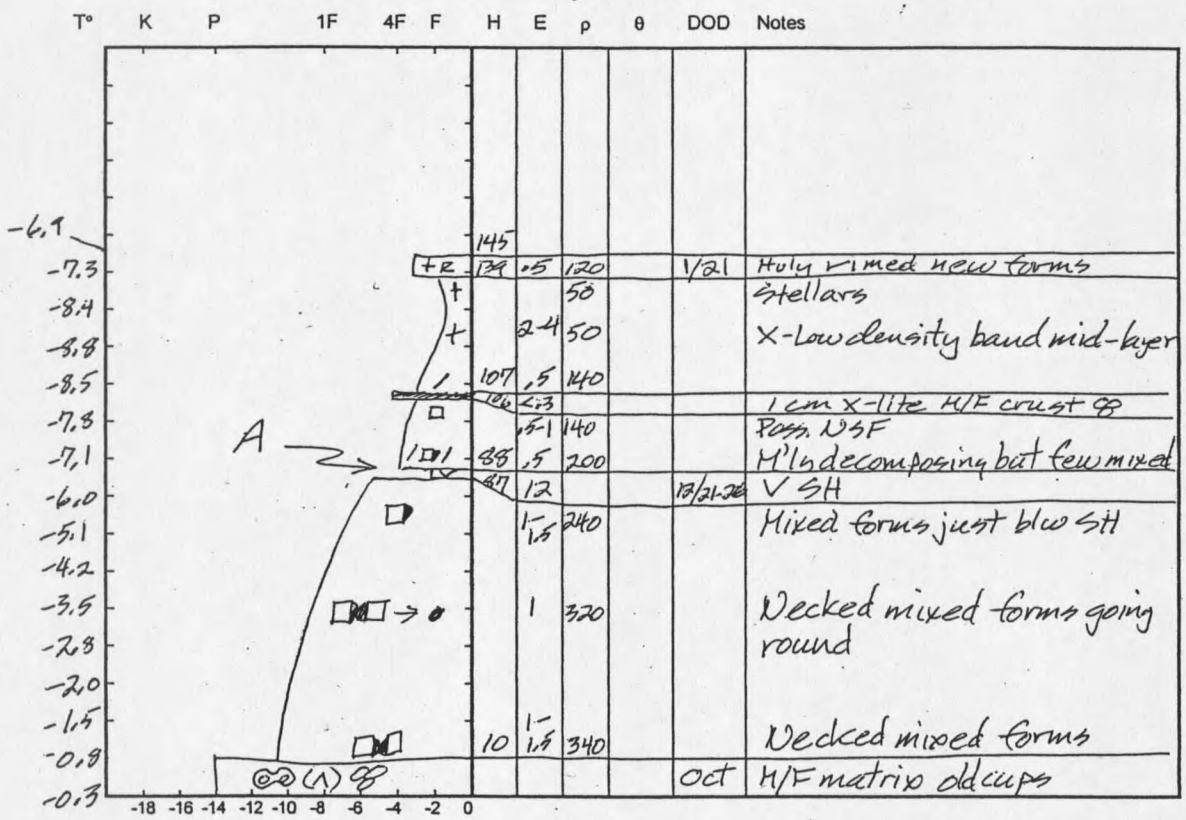
Observers: CL+MC | Landry Bridger Range Research | Profile # 11

Time: 1030 | **Snowpack Profile & QLCT** | Date: 1/21/02

Air T: -6.5 °C Sky: ⊗ Precip: SZ Wind: S | Prior Pit: # 10 ; 1/15/02

Location: Nr. "Ski Hill", Lionhead Elev. 8,000 Aspect: NE Boot Pen: 55 cm ∠: 28°

Notes: New wind slab (139-145cm) quite sensitive to ski cut



Potential Slab					Weak Layer & Bed Surface							
Ref	H_2O_{Nor} ÷ H_{Nor} = ρ_{kg}	Sin∠ x H_{Nor} x ρ x 9.8 = τ_{Slab}	F	E	T_{WL}	S	C	SB	ρ_{WL}	ρ_{bed}
A	165 mm ÷ .52m = 125	.4695 x .52 x 125 x 9.8 = 299	V	12	~63		20/21			240
B	mm ÷ m =	x x x 9.8 =								

Slab notes:

Surface Mode QLCT

Ref	T1	T2	T3	T4	T5	T6	T7	T8	T9	T10	Avg_{Test}
	kg	kg	kg	kg	kg	kg	kg	kg	kg	kg	kg

τ_{Test} ____ + τ_{Slab} ____ = ____ τ_{Total} X ____ C = ____ τ_{co} ÷ τ_{Slab} ____ = ____ S_{QLCT}

Bench Mode QLCT

Ref	T1	T2	T3	T4	T5	T6	T7	T8	T9	T10	Avg_{Test}
A	11.4 kg	11.5 kg	13.5 kg	12.6 kg	12.0 kg	kg	kg	kg	kg	kg	12.2 kg

τ_{Test} 720 = 720 τ_{Total} X .793 C = 571 τ_{co} ÷ τ_{Slab} 299 = 1.91 S_{QLCT}

QLCT rig used (**check**): ☐ **0.04 m²** *or* ☒ **0.08 m²** *load plate, with* ☐ **0.5-5 kg** *or* ☒ **2-20 kg** *force gauge*

If Bench Mode: bench height (on pit face) above weak layer = 30 cm and plate setback = 7 cm for H_2O_{Col} = 37 mm

QLCT notes: Column still quite soft; surface mode didn't work. Some column crushing (at front edge) in bench mode, but acceptable.

V. 10/15/00

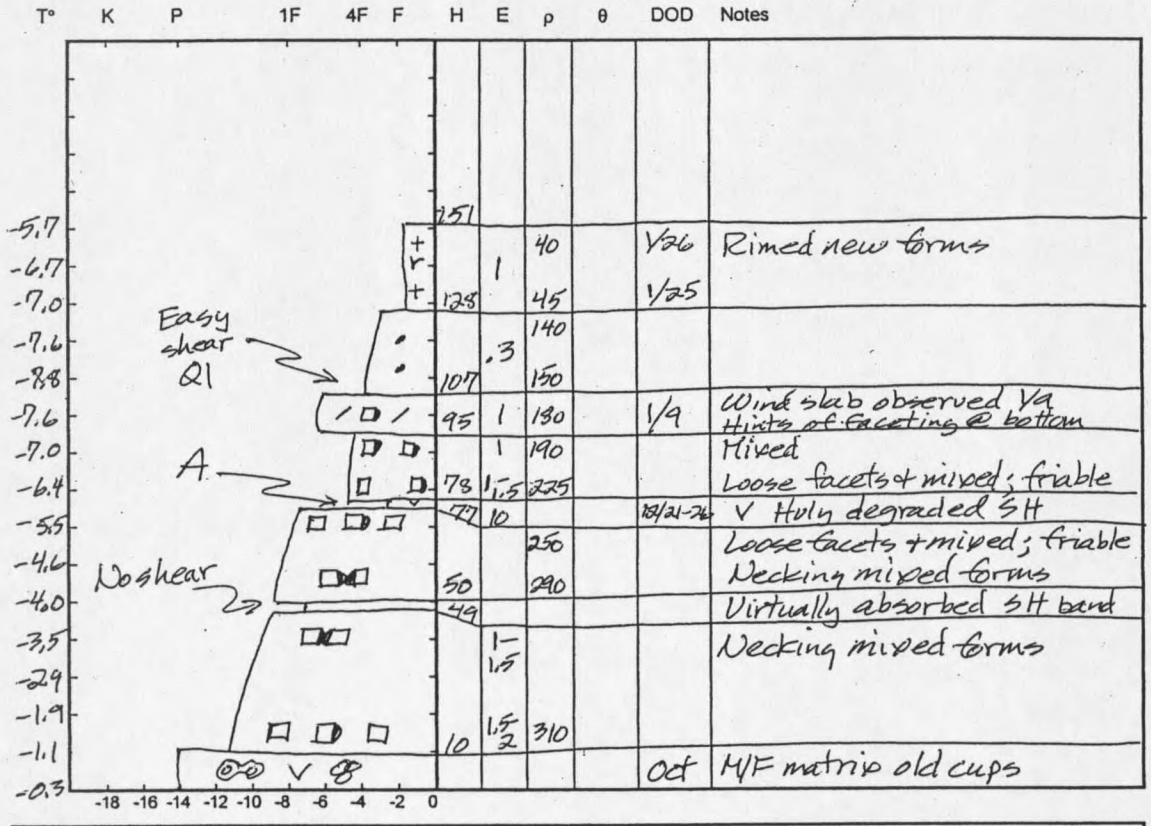
Observers: CL+RS | Landry Bridger Range Research | Profile # 12

Time: 0945 | **Snowpack Profile & QLCT** | Date: 1/26/02

Air T: -6 °C Sky: ⊗ Precip: S2-4 Wind: L/M | Prior Pit: # 11; 1/21/02

Location: "Going Home" Lionhead Elev. 8,000 Aspect: NE Boot Pen: 90 cm ∠: 26°

Notes: Location same as "Near Ski Hill"; 900 m² trial just below 1/15 trials



Potential Slab							Weak Layer & Bed Surface							
Ref	H_2O_{Nor} ÷ H_{Nor} = ρ_{kg}	Sin∠ x H_{Nor} x ρ x 9.8 = τ_{Slab}					F	E	T_{WL}	S	C	SB	ρ_{wl}	ρ_{bed}
A	97 mm ÷ 685 m = 142	.433 x .685 x 142 x 9.8 = 417					✓	10	~6	E	2½		—	250
B	mm ÷ m =	x x x 9.8 =												

Slab notes:

Surface Mode QLCT

Ref	T1	T2	T3	T4	T5	T6	T7	T8	T9	T10	Avg_{Test}
	kg	kg	kg	kg	kg	kg	kg	kg	kg	kg	kg

τ_{Test} _____ + τ_{Slab} _____ = _____ τ_{Total} X _____ C = _____ τ_{∞} ÷ τ_{Slab} _____ = _____ S_{QLCT}

Bench Mode QLCT

Ref	T1	T2	T3	T4	T5	T6	T7	T8	T9	T10	Avg_{Test}
A	14.1 kg	10.8 kg	16.7 kg	14.8 kg	14.6 kg	14.4 kg	12.0 kg	12.7 kg	15.0 kg	13.4 kg	13.35 kg

τ_{Test} 1,405 = 1,405 τ_{Total} X .680 C = 955 τ_{∞} ÷ τ_{Slab} 417 = 2.29 S_{QLCT}

QLCT rig used (**check**): ☒ **0.04 m²** or ☐ **0.08 m²** load plate, with ☐ **0.5-5 kg** or ☒ **2-20 kg** force gauge

If Bench Mode: bench height (on pit face) above weak layer = 38 cm and plate setback = 10 cm for H_2O_{Col} = 47 mm

QLCT notes: All Q1 shears; almost no column deformation

V. 10/15/00

MONTANA STATE UNIVERSITY - BOZEMAN
3 1762 10370044 7